APPENDIX 2.5L

BAJA AND CALIFORNIA - CONTINENTAL BORDERLAND FAULTS

APPENDIX 2.5L

BAJA AND CALIFORNIA - CONTINENTAL BORDERLAND FAULTS

The magnitude of the maximum earthquake for the San Onofre site is developed from analyses of fault characteristics and fault behavior in Southern California and near the site. These analyses are consistent with the present understanding of tectonics in Southern California, Baja, and the Continental Borderlands, and although based on known geology, the details of various tectonic models may not be agreed upon by the various technical investigators. Specifically, the available geologic and seismologic data do not support the connection of the hypothesized offshore zone of deformation (OZD) to faults in Baja. Further, the geomorphic characteristics of the hypothesized OZD or the San Miguel-Vallecitos trend suggest that neither zone is capable of producing earthquakes greater than M_s 7. The San Onofre Unit 2 and 3 design basis earthquake (DBE) has been shown to accommodate instrumental accelerations caused by an M_s 7 on the OZD, thus the San Onofre Units 2 and 3 design basis is unaffected by faulting in Baja.

This appendix is divided into seven parts as follows:

Section	Description
2.5L.1	Background
2.5L.2	Geologic data in the Baja-Continental Borderlands area
2.5L.3	Discussion of the hypothesized connection of the OZD to faults in Baja
2.5L.4	Comparison of degree of activity of the OZD and Baja faults
2.5L.5	Discussion of tectonic models of southern California Baja area
2.5L.6	Discussion of seismologic data
2.5L.7	Summary of conclusions

2.5L.1 BACKGROUND

The main purpose of appendix 2.5L is to clarify the role of the tectonic setting and its influence on the possible interpretations of faults in California and in Baja. In this context, the emphasis of this appendix is toward interpreting the Baja and California - Continental Borderland faults with respect to their tectonic setting and possible origins. Specific

concerns regarding fault types, surficial evidence of faulting, focal mechanisms, tectonic continuity of faulting, and the postulated Tijuana lineament are again discussed for the readers reference because of the constraints they place on interpretation of origins of the faults and their tectonic setting.

2.5L.2 GEOLOGIC DATA ON FAULTS IN THE BAJA CONTINENTAL BORDERLANDS AREA

Most of the geologic information concerning the faults onshore and offshore of Baja is presented in appendix 2.5J. That information is reproduced here and supplemented with an annotated map (figure 2.5L-1) describing each significant feature along each fault. These data include locations of mapped terminations of individual fault traces, evidence of activity, style of faulting, historical ground rupture, and evidence of offshore extensions where applicable. A discussion of the Tijuana lineament is also presented.

Onshore Faults of Northern Baja California

The major fault zones of northern Baja are the Calabasas fault zone, the Vallecitos fault zone, the San Miguel fault zone, the Tres Hermanos fault zone, and the Agua Blanca fault zone.

The following discussions of the geologic setting and the structural relationships of the area are reproduced from appendix 2.5J. Reference is made to Gastil and others (1975; 1979) for a comprehensive discussion of the geologic and structural setting of northern Baja.

Geologic Setting

The northwest corner of Baja can be divided into three physiographic and geologic provinces (as shown on figure 2.5L-2): (1) a narrow coastal margin characterized by Tertiary marine and nonmarine sedimentary rocks and Tertiary-Holocene volcanic and volcanically derived rocks, (2) the gently seaward-sloping foothills between the Pacific Coast and the central high Peninsular Ranges underlain by pre-batholithic eugeosynclinal accumulations of volcanic and sedimentary rocks that have been metamorphosed to varying degrees by intrusion of the batholith, and (3) the Peninsular Ranges of northeast Baja and southern California composed of middle Cretaceous plutonic rocks of the southern California Batholith.

Regional Structural Setting

Structurally, the western two-thirds of northern Baja consists of an uplifted and westward-tilted fault block. The high eastern edge of the block is formed by the mountain ranges of the Sierra Juarez in the north and the Sierra San Pedro Martir in the south. Uplift of the eastern edge began about 10 million years ago according to Gastil and others (1975).

Amended: April 2009 TL: E048000

The eastern escarpment was created by a series of eastward-dipping normal faults that downstep antithetic fault blocks toward the Gulf of California depression (Gastil and others, 1979) (shown schematically on figure 2.5L-3).

The main structural block has been cut by five fault zones: the San Miguel, the Vallecitos, the Calabasas, the Tres Hermanos, and the Agua Blanca. The Agua Blanca fault zone trends westerly from its eastern limit in the Sierra Juarez Mountains to the Pacific coast south of Ensenada.

The San Miguel fault zone consists of two segments. In 1956, a reported 19-kilometer length of the southern segment broke along a series of short en-echelon ruptures (Shor and Roberts, 1958) (figure 2.5L-1, No. 1). Measured fault displacements ranged from 0 to about 80 centimeters horizontally and 0 to about 90 centimeters vertically; the sense of offset was uniformly right-lateral and down to the southwest (Shor and Roberts, 1958). The southern segment is mapped as a principally dip-slip fault that dies out in the Sierra Juarez Mountains and does not connect with either the Agua Blanca fault or the dip-slip faults of the eastern escarpment (Gastil and others, 1975) (figure 2.5L-1, No. 2). Geologic mapping and geophysical exploration indicate that this fault neither offsets this escarpment nor connects with faults in the Gulf of California (Gastil and others, 1975, 1979; Henyey and Bischoff, 1973; Slyker, 1974).

The northwest end of the 1956 break lies en-echelon to the northern segment. The northern segment can be traced on aerial photos to the area northeast of the Valle San Rafael where offset streams and dikes show right-lateral separation (figure 2.5L-1, No. 3); the most clearly expressed fault trace appears to separate Mesozoic dikes only a distance of 100 meters (Gastil, 1975, 1979).

Vallecitos Fault Zone

The Vallecitos fault zone is en-echelon to the northern segment of the San Miguel fault zone but separated from it by a distance of 6 to 10 kilometers. The Vallecitos fault is a nearly continuous trace that extends 65 kilometers from the western edge of the Sierra Juarez Mountains (figure 2.5L-1, No. 4) to the northwest end of the Valle de las Palmas (about 29 kilometers southeast of Tijuana) (figure 2.5L-1, No. 5). As noted by Gastil and others (1979), the main trace of the fault is marked by erosional topographic features, and there is no evidence that the Vallecitos offsets anything younger than the Mesozoic crystalline basement rocks. An unpublished map by Raymond Elliott (cited in Gastil and others, 1979) shows 3 kilometers of right-lateral separation of a Cretaceous pluton boundary. The map prepared by Gastil and others (1975) indicates 3 kilometers of apparent right-lateral separation on the north side of a pluton but either right- or left-lateral separation on its eastern boundary. The northwest end of the fault terminates at the edge of overlying Eocene conglomerate (Gastil and others, 1979) (figure 2.5L-1, No. 5).

APPENDIX 2.5L

Calabasas Fault Zone

The Calabasas fault zone is located about 5 kilometers northeast of the Vallecitos fault zone and trends parallel to it for about 30 kilometers in a northwest-southeast direction. In the Valle de las Palmas area, the fault is marked by small sags and saddles, breaks in uplifted alluvial deposits, and relatively uneroded scarplets (Gastil and others, 1975, 1979) (figure 2.5L-1, No. 6). Detailed mapping by Frazer (1972) indicates that both northwest-southeast- and northeast-southwest-trending faults are present in the vicinity of Valle de las Palmas. The northwest-southeast-trending faults are discontinuous, with individual traces from 12 to 15 kilometers in length (figure 2.5L-1, No. 6), whereas the northeast-southwest-trending faults are shorter (Frazer, 1972). The northeastern-most segment of the Calabasas fault appears to displace Quaternary alluvium at its northwest end (figure 2.5L-1, No. 7).

Tres Hermanos Fault Zone

The Tres Hermanos fault zone is located midway between the San Miguel and Agua Blanca fault zones and essentially parallels the San Miguel fault zone. The trace, approximately 45 kilometers long, is confined to batholithic rocks and dies out east of Ensenada. The fault is marked by pronounced topographic expression and is apparent on high-altitude photos, yet recency of movement and sense of displacement are unknown (Gastil and others, 1979).

Agua Blanca Fault Zone

The Agua Blanca fault zone extends about 129 kilometers across the western two-thirds of the Baja peninsula. The Santo Tomas fault branches off to the south from the western part of the Agua Blanca fault (figure 2.5L-1, No. 8). These faults are distinctive for their west-northwest trend that is more westerly than the faults to the north. The trace of the Agua Blanca fault is indicated by abundant geomorphic evidence (Allen and others, 1960; Hamilton, 1971). Typical features are distinct scarps, offset streams, shutter ridges, fault sags and saddles, and fault-controlled valleys (figure 2.5L-1, Nos. 9, 10, 11, 12, and 13). Quaternary fan gravels in the Valle de Agua Blanca (figure 2.5L-1, No. 11) are offset about 4.8 kilometers in a right-lateral sense; between 11.3 and 22.6 kilometers of similar separation may be indicated by discontinuous igneous contacts across the fault trace in the Valle de Agua Blanca (Allen and others, 1960). Stream offsets have been documented in the area west of Valle de Agua Blanca by Allen and others (1960), but ages have not been assigned. The stream offsets range from 50 to 70 meters to as much as 300 meters. Detailed field mapping (Allen and others, 1960; Gastil and others, 1975, 1979; Slyker, 1974) indicates that the east end of the Agua Blanca fault dies out in the Sierra San Pedro Martir Mountains in Paso San Matias (figure 2.5L-1, No. 14) and does not intersect the dip-slip faults of the eastern escarpment.

APPENDIX 2.5L

Offshore Faults of Northern Baja California

The offshore faults discussed here are those that have been postulated by other works to connect to onshore faults in northern Baja. There have been numerous interpretations of the faulting in the Continental Borderlands adjacent to northern Baja (Shepard and Emery, 1941; Allen and others, 1960; Krause, 1965; Moore, 1969; Legg and Kennedy, 1979). The early interpretations of Shepard and Emery (1941), Allen and others (1960), and the work of Krause (1965) were based on bathymetry, whereas some of the more recent studies by Moore (1969) and Legg and Kennedy (1979) combined earlier studies with an interpretation of reflection profiling to locate faults.

Legg and Kennedy (1979) have suggested that there are four major fault zones in the offshore area of California and northern Baja. This division of offshore faults into four major fault zones (Legg and Kennedy, 1979) is as follows: (1) Santa Cruz-San Clemente-San Isidro (figure 2.5L-1, No. 15); (2) San Pedro-San Diego Trough-Maximinos (figure 2.5L-1, No. 16); (3) Palos Verdes Hills-Coronado Banks-Agua Blanca (figure 2.5L-1, No. 17); and (4) Newport-Inglewood-Rose Canyon-Vallecitos-San Miguel. The Applicant acknowledges these hypothesized zones but does not agree with them, as discussed below. The hypothesized Newport-Inglewood-Rose Canyon-Vallecitos-San Miguel fault zone is discussed separately in section 2.5L.3.

Santa Cruz-San Clemente-San Isidro Fault Zone

Allen and others (1960), along with Moore (1969), have suggested that the San Clemente fault zone connected to the Agua Blanca fault zone. In their more comprehensive work, Legg and Kennedy (1979) show a "gap" at Navy Bank (figure 2.5L-1, No. 18), and they interpret the San Clemente fault zone as contiguous with the San Isidro fault zone to the south. Thus, this latter interpretation of the fault zone does not indicate a connection with faults of northern Baja.

San Pedro-San Diego Trough-Maximinos Fault Zone

Studies based on reflection profiling by Legg and Kennedy (1979) suggest that these faults appear to be subparallel or en-echelon. In the vicinity of northern Baja, the connection between the San Diego Trough fault zone and the Maximinos fault zone is simply described as en-echelon because its complex structure does not allow a more detailed description (figure 2.5L-1, No. 19) (Legg and Kennedy, 1979).

Legg and Kennedy (1979) describe the Maximinos fault zone as extending offshore from a southern splay of the Agua Blanca fault zone (figure 2.5L-1, No. 20). Onshore, this fault passes through a small canyon where right-lateral offset stream channels and aligned groundwater barriers are indicated by vegetation contrasts (Legg and Kennedy, 1979). More than one subparallel fault is associated with the fault zone as it

Amended: April 2009 TL: E048000

extends northward offshore; farther north the faults splay and trend toward Navy Bank (figure 2.5L-1, No. 18) and the San Diego Trough fault zone (figure 2.5L-1, No. 19) (Legg and Kennedy, 1979).

The Maximinos fault zone is interpreted as being principally right-lateral with a small component of dip-slip; and it displaces sediments interpreted as Quaternary in age (Legg, 1979, in Legg and Kennedy, 1979). Amounts of displacement are not described in the literature.

Palos Verdes Hills - Coronado Banks - Agua Blanca Fault Zone

The Palos Verdes Hills and Coronado Banks faults were briefly discussed in appendix 2.5P. The following discussion is included to present additional data covering the fault zone where it extends into the southern Continental Borderlands adjacent to northern Baja.

Greene and others (1979) describe the Palos Verdes Hills - Coronado Banks fault zone as containing discontinuous, generally right-stepping, en-echelon faults. Individual fault traces in the zone were observed to be in relatively narrow (1 to 10 kilometers wide) zones and are thought to continue no more than 40 kilometers (Greene and others, 1979).

Legg and Kennedy (1979) describe the Coronado Banks fault zone as generally consisting of a main trace with numerous subparallel faults extending southward from the Coronado Banks area. At the Coronado Islands, the fault splays around Middle and South Coronado Islands then continues southward as a main trace to an area west of Punta Salispuedes (figure 2.5L-1, No. 21), where complex faulting and lack of data close to shore cause uncertainty to the interpretation of fault continuity. Legg (1979) suggests 11 kilometers of post-Pliocene displacement along the fault in the vicinity of the Coronado Banks (figure 2.5L-1, No. 22) by realigning the north bank with the south bank. However, there is no compelling evidence to show a relationship of the two banks to each other.

The Agua Blanca fault zone can be traced northwest from the Punta Banda area (figure 2.5L-1, No. 23) where the Punta Banda submarine canyon is reported to be right-laterally offset a distance of 4 kilometers (Legg and Kennedy, 1979). A direct connection between the Agua Blanca and Coronado fault zone has not been made because of the complex nature of the region offshore of Punta Salsipuedes (Legg and Kennedy, 1979).

In addition to the suggested right-lateral sense of displacement, high vertical relief has been observed within this zone of faulting at Palos Verdes Hills, Coronado Banks, Islas Los Coronados, Descanso Shelf-Ridge, Islas de Todos Santos, and Punta Banda (Legg and Kennedy, 1979). Vertical displacement of several hundred meters is suggested, but no data on the age of displaced materials is provided in the literature.

Amended: April 2009 TL: E048000

APPENDIX 2.5L

The Tijuana Lineament and Proposed Extension of the Rose Canyon Fault Zone

A detailed discussion of the interpretation by various authors who suggest that a southern extension of the Rose Canyon fault zone connects to faults in Mexico is provided in Appendix 2.5K. A summary of such evidence was also provided in section 2.5J.2, entitled Possible Connection between the Rose Canyon and the San Miguel and Vallecitos Fault Zones. The discussion is reproduced here and annotated where appropriate on figure 2.5L-1.

A hypothesized northwest extension of the presently mapped limits of either the Calabasas or Vallecitos faults has been inferred largely on the basis of regional alignment of discontinuous topographic, structural, and geothermal features in the southern San Diego and southeast Tijuana area. However, geologic maps by Kennedy (1975) and Gastil and others (1975) indicate a 55-kilometer distance between the mapped south end of the Rose Canyon Fault Zone (RCFZ) and the north end of the mapped Vallecitos fault. Gastil and others (1979) suggest the possibility of a northwest-trending lineament (figure 2.5L-1, No. 24) that would continue from the northwesternmost mapped trace of either the Vallecitos or the Calabasas faults, through eastern Tijuana, and across the U.S.-Mexico Border just west of San Ysidro. This suggested lineament crosses an area with a historically quiet seismic record (characterized by a single M_L 3.5 earthquake--the 1978 Canon de la Presa earthquake).

Features (Gastil and others, 1979) that comprise this lineament are:

A. The subparallel alignment of the Tijuana River Valley (figure 2.5L-1, No. 25) and the Valle de las Palmas (figure 2.5L-1, No. 6), trends of faults in the San Ysidro area, and the alignment of several thermal wells

B. The contrast between Eocene stratigraphy north and south of the lineament

C. The mapped traces of northeast-trending dip-slip faults in the southern Tijuana-Rosarito Beach area that do not continue across the lineament (figure 2.5L-1, No. 26).

If the lineament suggested by Gastil and others (1979) is a fault, it would trend northwest from the Valle de las Palmas area, cross the Eocene and pre-batholithic (figure 2.5L-1, No. 27) bedrock exposures and continue beneath the deeply alluviated Tijuana River Valley, possibly into the San Diego Bay area.

Although this lineament has been suggested by Gastil and others (1979), the lack of faulting in the well-exposed Eocene and pre-batholithic bedrock, and the lack of fault features recognized on aerial photographs of the area by Gastil (personal communication, 1979), suggest that no significant faulting has occurred in this area. Geophysical data gathered by Kennedy (1975) and Kennedy and others (1977) do not identify continuous faulting along the proposed connection of the Calabasas and Vallecitos faults and

the RCFZ in the area south of San Diego Bay and north of the International Border (figure 2.5L-1, No. 28). Therefore, the observed evidence is not supportive of a through-going fault that could connect the RCFZ with either the Vallecitos or San Miguel fault zone. Further discussion on the inferred onshore extension of the RCFZ is presented in section 2.5L.3.

2.5L.3 DISCUSSION OF HYPOTHESIZED CONNECTION OF THE OZD TO FAULTS IN BAJA

Three connections of the OZD to faults in Baja (onshore and offshore) are discussed in the subsections that follow.

Hypothesized Onshore Extension of the RCFZ

The hypothesized onshore extension of the Rose Canyon fault zone (RCFZ) through the Tijuana area is discussed in appendix 2.5J.2 under Possible Connection Between the Rose Canyon and the San Miguel or Vallecitos Fault Zones, and in appendix 2.5K. A large volume of data suggests that no connection exists and that the mapped traces of the Calabasas and Vallecitos faults terminate in the Eocene bedrock terrane in northern Valle Las Palmas.

The RCFZ cannot be traced southward into southern San Diego Bay from the north, even though Legg and Kennedy (1979) and Kennedy and others (1977) concentrated efforts to identify faulting in that area. Their work suggests that the southern extension of the RCFZ changes character in the southern part of San Diego and becomes a wide zone of faulting characterized by an extensional tectonic environment with dip-slip components. The prominent faults extend offshore to the southwest, where features from reflection profiling suggest strike-slip as well as dip-slip components. Data indicate that the faults within this wide zone die out to the south, do not trend through Tijuana Canyon, and do not connect to the Calabasas or Vallecitos faults (figure 2.5L-1, No. 29).

Hypothesized Offshore Extensions of the RCFZ

The first of two hypothesized offshore continuations of the Rose Canyon fault zone is extended from location 36 of Legg and Kennedy (1979) (figure 2.5L-1, No. 29), southward along the coast of Baja until it reaches a branch of the Agua Blanca fault zone in Bahia Todos Santos. Although the RCFZ is thought to die out south of San Diego as it curves westward, a continuation is hypothesized by Legg and Kennedy (1979) close to the shore where acoustic profiles cannot detect the fault. They also postulate connections either with the Tres Hermanos, which dies out in Baja, or with the Agua Blanca faults. The existence of these connections can not be confirmed by available data.

Amended: April 2009 TL: E048000

If such a connection truly exists between the RCFZ and the Agua Blanca fault, it would create a large, nearly S-shaped strike-slip fault bending 35° southwestward at Mt. Soledad, bending back 35° to follow the coast of Baja, and finally bending 30° eastward again in order to connect with a branch of the Agua Blanca fault. This awkward geometry would greatly hinder rupturing along a strike-slip fault and would make it atypical of southern California faults. Such sharp bends would also tend to restrain rupture propagation during earthquakes and would cause the fault to break by individual segments. Thus, the connection of the Rose Canyon fault zone to one of the proposed northward splay faults of the Agua Blanca fault has little bearing on the definition of earthquake potential on the OZD opposite the site. A comparison of evidence for surface faulting and geomorphology clearly indicates that the Agua Blanca fault is more like the San Clemente or Coronado Banks fault zones. The locations of these latter faults farther west of the Rose Canyon fault zone places them in better alignment with the Agua Blanca fault.

The other postulated offshore extension of the RCFZ implies a zone of deformation extending south from the vicinity of San Diego trending parallel to the Baja Coast. No discrete fault zone is mapped in this location and this hypothesized structural model may conceivably have no spatial limitation encompassing all of the Continental Borderlands area as a zone of deformation. Within this hypothesized zone of deformation, the closest trend of faults parallel to the OZD is near San Diego at location 33 of Legg and Kennedy (1979). Legg and Kennedy's (1979) description of this zone of faults states either that they are overlain by 5 meters of unfaulted Quaternary sediments or that fault traces are totally within older acoustic basement. This suggests a long period of inactivity. South of San Diego, Legg and Kennedy's map shows the southern end of the RCFZ trending toward the non-Quaternary parallel faults mentioned above. Because of the inactivity of those faults, inclusion of them in a zone with the RCFZ and OZD has no impact on evaluation of the DBE at the site.

In general, the connections proposed, whether onshore or offshore, are highly speculative and supported by little or no data. The Applicants do not believe that the possibility of connections of zones of deformation to the OZD will change the interpretation of earthquake potential of the faults near the site. This is supported by the comparison of the degree of activity for the faults. Under the degree-of-activity analysis, the most logical selection of a model is the Newport-Inglewood zone of deformation (NIZD), as discussed in section 2.5L.4.

2.5L.4 COMPARISON OF THE OZD AND BAJA FAULTS BY DEGREE OF ACTIVITY

In characterizing the earthquake potential of the OZD opposite the site, the Applicants applied a fault comparison or fault ranking methodology, based on known characteristics and degree of activity of strike-slip faults in southern California. These comparisons demonstrated that the OZD as a whole is far less active and is a less significant geologic structure than parallel faults east of the OZD in southern California with respect to

total displacement, evidence of Quaternary activity, fault continuity, geologic slip rate and historical seismicity. Those characteristics of faults and fault behavior, referred to as the degree of activity, were used as a comparative tool to evaluate the earthquake potential of the hypothesized OZD. The comparisons indicated that the OZD has a lower earthquake potential than faults to the east.

The area offshore from the site has been investigated with marine geophysical methods and faults have been identified in a general zone of folds and faults (South Coast Offshore Zone of Deformation or SCOZD). Definition of rupture lengths, displacement per event, and recurrence intervals are not possible in the marine environment and definition of maximum magnitude cannot be determined by analyzing only this offshore segment. Therefore, to understand the SCOZD, the projected analogous structures onshore to the north (NIZD) and to the south (RCFZ) were evaluated. Of those two, the NIZD is the closest to the SCOZD in style of faulting. The NIZD also has a higher degree of historical activity than either the RCFZ or the SCOZD. The fault characteristics along the OZD were summarized in table 2.5R-3, illustrating the lesser geologic, geomorphic, and seismologic degree of activity southward along the zone to San Diego. Thus, the NIZD is the most applicable and conservative choice as a model for the SCOZD opposite the site and for the OZD as a whole.

The Applicants now present a comparison between faults in Baja and the hypothesized OZD to further evaluate the earthquake potential and tectonic setting of the OZD. The fault data are compiled in table 2.5L-1 in a format similar to the fault ranking in southern California. The Baja faults include the Agua Blanca, the Calabasas, the Vallecitos, the San Miguel, and the Tres Hermanos fault zones. In general, the data from faults in Baja are less complete than the data from faults in southern California because: (1) offsets are not well documented, (2) ages of offsets are poorly known, (3) relationships of en-echelon segments are not defined, (4) the sense of faulting is only partially documented; and (5) data on Quaternary faulting are limited. Based on the available data, however, the San Miguel fault exhibits higher historic seismicity than the NIZD, and the Agua Blanca fault shows geomorphic evidence of a much higher degree of activity than does the San Miguel or hypothesized OZD between Santa Monica and San Diego. This interpretation is consistent with the tectonic models discussed in section 2.5L.5. In addition to tectonic setting interpretations, the fault comparison reveals valuable insights into the origins and behavior of faults in Baja and their significance to the hypothesized OZD as discussed below.

A comparison of the San Miguel, Vallecitos, and Calabasas faults provides interesting contrasts in data and in conclusions given those data. For example, based on geomorphic expression, the San Miguel fault appears to have the highest degree of activity of the three faults (Shor and Roberts, 1958; Gastil and others, 1979); it is marked by offset streams, closed depressions, and groundwater barriers. Also, the San Miguel has had six earthquakes equal to or exceeding magnitude 6.0 between 1954 and 1956 (Brune and others, 1979). However, the bedrock geology indicates that the

Amended: April 2009 TL: E048000

APPENDIX 2.5L

Table 2.5L-1
BAJA FAULTS AND OZD CHARACTERISTICS AND RANKING CRITERIA

Fault Zone Characteristics	Agua Blanca Maximinos	Calabasas Vallecitos San Miguel	Tres Hermanos	Hypothesized OZD
Dimensions and Segmentation	Total length: 200 km or more Segment length: >180 km	Total length: 160 km Vallecitos: 65 km Segment lengths: 38-48 km San Miguel: 100 km Segment lengths: 25-54 km Calabasas: 40 km Segment lengths: 12-15 km	Total length: 45 km	Total length: 200 km NIZD: 70 km Segment lengths: 6.5-36 km SCOZD: ~75 km Segment lengths: 8-27 km RCFZ: ~65 km Segment lengths: 20-48 km
Total Displacement	11-22 km (decreased eastward and dies out)	San Miguel to 3 km (Vallecitos) (crystalline basement)	Unknown	3 km (upper Miocene)
Sense of Motion	Right lateral	Nearly equal vertical to right lateral (San Miguel)	Unknown	Right lateral
Distance from Main Plate boundary	>80-90 km	>90 km (San Miguel)	>115 km	62-150 km (closest at north)
Historical Rupture Length	None Reported Numerous parallel and anastamosing fault traces	>20 km surface rupture (San Miguel) At least 3 major en-echelon segments	None Reported	30 km, subsurface (aftershock zone, 1933 NIZD) Discontinuous en-echelon segments
Continuity and Geomorphic Features	Strong linear trace in alluvium, offset streams, groundwater barrier, shutter-ridges fault sags. Evidence of activity decreases to the east	Right stepping en-echelon fault segments. Zone of springs, linear hills and valleys, displaced drainage, and closed basins extend 80 km north from 1956 surface rupture along San Miguel. No evidence of offsets younger than crystalline basement along Vallecitos. Calabasas has some scarps and evidence of Quaternary offsets	Unknown but observed on high altitude photographs	En-echelon large folds at north end with smaller and more gentle folding to the south. A few linear fault scarps at north end with persistent scarps to the south
Historical Seismicity	None Reported	Very high at south, low in central and northern areas	None Reported	High in north, low in central and southern areas
Maximum Historial Magnitude (Ms)	None Reported	6.8 (1956 San Miguel)	None Reported	6.3 (1933 NIZD)
Geologic Slip Rate	2.7 mm/yr (Quaternary)	Unknown	Unknown	0.5 mm/yr (Miocene-Pliocene)

Amended: April 2009 TL: E048000

San Miguel fault has only had 100 meters total offset. In contrast, the en-echelon Vallecitos fault has neither evidence of Quaternary activity nor significant historical seismic activity, and yet the total offset is estimated as a maximum of 3 kilometers based on offset of a pluton boundary (the other side of the pluton does not suggest comparable offset). Such data of inconsistent total offset and contrasting indicators of degree of activity between the two faults suggest a complex tectonic regime and a discontinuous seismic source.

The high seismic activity and the geomorphic evidence of activity on the San Miguel fault combined with the 100 meters of total offset are evidence for a very youthful inception of faulting, much younger than the 5-8 million year age of 3 kilometers offset indicated for the NIZD. This might suggest a more recent time of initiation of faulting for the San Miguel fault and would preclude propagation of faulting from the south to the north to form the OZD. Rather, a separate tectonic origin for the OZD and faults in Baja is indicated.

The inconsistency of fault characteristics (displacement, evidence of activity, etc.) along the faults in Baja indicate continuous, incoherent behavior of individual fault segments within the zone. This behavior suggests that this zone should not be capable of producing earthquakes of magnitudes greater than M_s 7. The discontinuous nature of this zone suggests that it should not have any effect on the earthquake potential of the OZD opposite the site.

The Agua Blanca fault appears to have the highest degree of activity of all the faults mapped in Baja, as indicated by offsets of Quaternary deposits and geomorphic features, although historical seismicity has been low. The 4.8 kilometer offset of Quaternary (~1.8 million years old) fan gravels suggests a slip rate of 2.7 mm/yr, or approximately five times that of the OZD. Other contrasts to the OZD are the oblique orientation and the relatively continuous surface fault traces and segments of the Agua Blanca fault. Total displacement and evidence of activity decrease toward the Gulf of Mexico and the plate boundary and die out completely before entering the Gulf depression (Allen and others, 1960; Gastil and others, 1975). Because of the vast difference in degree of activity of the Agua Blanca fault as compared to the hypothesized OZD (including the NIZD, SCOZD, and RCFZ), the earthquake potential of the Agua Blanca is not comparable to the OZD opposite the site. The geomorphic expression and other parameters which reflect the degree of activity of the Agua Blanca fault suggest that it is more comparable with either the Coronado Banks or San Clemente fault zones and may connect with these faults as discussed below.

It is not unexpected that faults in Baja, such as the Agua Blanca fault, have a higher degree of activity than the OZD based on its possible and apparent relationship to other Continental Borderland faults. Onshore, the Agua Blanca fault is a rather discrete zone of faults characterized by abundant geomorphic evidence for Quaternary activity (Allen and others, 1960). As the fault approaches the western coast of Baja, it splays into the Santo Tomas and Maximinos faults and then again splays into a number of faults as it turns northward into the Continental Borderlands. The most

Amended: April 2009 TL: E048000

prominent correlative structures in the borderlands that may accommodate most of the displacement transferred northward from the Agua Blanca are the San Clemente escarpment and the Coronado Banks zones. If the displacement of the Agua Blanca fault is being distributed into the Continental Borderlands faults, the OZD should not be comparable to the Agua Blanca.

In summary, the application of faults from Baja as models to characterize the OZD is considered inappropriate. To apply models of faults that are so far removed from the immediate tectonic setting of the SCOZD, with different orientations and for which very few data are available, is highly speculative. Therefore, consideration of faults in Baja has no bearing on the San Onofre DBE. This conclusion is supported by the foregoing discussion and by interpretations of the tectonic setting presented in section 2.5L.5 and summarized in section 2.5L.7.

In order to better understand the regional stresses in the Continental Borderlands and to evaluate whether a lower degree of activity is appropriate for the tectonic regime of the OZD, a discussion of the tectonic setting is presented.

2.5L.5 DISCUSSION OF TECTONIC MODELS OF THE SOUTHERN CALIFORNIA-BAJA AREA

The relative motion of the Pacific and North American plates is responsible for the presence of the San Andreas fault system and other associated parallel faults that are nearly parallel with this relative plate motion (figure 2.5L-4). The OZD is associated with this group, however, the more active faults parallel to the OZD and to the east of it, such as the San Andreas, the San Jacinto, the Elsinore, and others, relieve most of the accumulated regional shear stress. The tectonic origin of the mapped faults in Baja California and the faults in the Continental Borderlands are less well understood. Currently available data provide several tectonic models that can be used to explain the relationship of these various faults and their interaction in terms of plate tectonic theory. Three main hypotheses are summarized in the following paragraphs:

1. The parallel and subparallel faults at oblique angles to the main axis of the Baja peninsula are considered to be landward extensions of transform faults originating at the spreading ridge central to the Gulf of California (Elders and others, 1973) (figure 2.5L-5).

2. Creation of the Agua Blanca fault zone could be due to regional north-south compression similar to that of the Transverse Range resulting from interaction of the plate motions and the "Big Bend" in the San Andreas fault zone (figure 2.5L-6).

3. The Agua Blanca and other faults oblique to the main axis of the Baja Peninsula may have originated by clockwise rotation of the peninsula via the effects of variable rates of crustal spreading in the Gulf of California as the gulf opened from the south (figure 2.5L-7).

It is difficult to prove which of these models is most likely; however, of the three models presented, the third seems most plausible based on geologic data and tectonic theory. These models are evaluated in the following paragraphs.

The first hypothesis considers the parallel and subparallel faults at oblique angles to the main axis of the Baja peninsula to be landward extensions of transform faults originating at the spreading ridge central to the Gulf of California (Elders and others, 1972; Brune and others, 1979) (figure 2.5L-5). This hypothesis requires that these faults, e.g., Vallecitos, San Miguel, Agua Blanca, La Bamba, and Bahia Tortugas, etc. (figure 2.5L-4), be structurally continuous features across the Baja Peninsula to their hypothesized origin in the Gulf of California, and that the spreading rates are different between spreading centers, causing activation of fracture zones extending from the transform faults. Lomnitz and others (1970) suggest that the southern end of the Gulf is opening faster than the northern end, thus resulting in the right-lateral shear through the Baja Peninsula along such fracture zones. Generally, the fracture zones extending away from transform faults between spreading centers are inactive structures. Therefore, movement along fracture zones extending from the gulf would require differential spreading rates and would, according to plate tectonic theories, represent unique features.

In order to test whether faults crossing the Baja Peninsula are extensions of transform faults in the Gulf of California, the known geologic data are reviewed here. If present, such fracture zones should extend in both directions from ridge-ridge transforms, and fault zones equivalent to those in the Baja Peninsula might be expected in Mexico on the east side of the gulf. Brune and others (1979) indicate that no analogous faults exist east of the gulf. Further, extensive geologic studies by Gastil and others (1975, Map Sheet A) and by Allen and others (1960) indicate decreasing displacement and decreasing evidence of activity eastward along the Agua Blanca fault. Mapping also indicates that the Agua Blanca and San Miguel fault systems do not continue beyond the eastern end of their mapped traces in the San Pedro Martir Mountains and thus do not reach to the Gulf of California. In addition, work by Henyey and Bischoff (1973) indicates that there is no onshore-offshore connection on the eastern side of Baja. These findings argue against consideration of the Agua Blanca and similar faults as extensions of transform systems.

The second model draws an analogy between the Agua Blanca fault and the Transverse Ranges structures in southern California. The Agua Blanca fault cuts transversely across the Baja Peninsula, just south of Ensenada, and is nearly parallel with the Transverse Range 320 kilometers to the north (figure 2.5L-6). This parallelism suggests a tectonic origin for the Baja fault systems that is analogous to the origin of the Transverse Ranges. The Transverse Ranges in California are believed to have resulted from nearly north-south compressive stress due to great crustal shortening that is occurring along nearly east-west trending thrust faults, which exhibit a strong component of left-lateral movement. This north-south compressive stress is apparently related to the "Big Bend" in the San Andreas fault

that partially blocks the northward movement of the Pacific plate. Because of the similar orientation of the Agua Blanca fault to the Transverse Ranges structures, it could be hypothesized that both systems may be a result of similar regional compression. However, in contrast to the Transverse ranges where left-lateral distortion of the San Andreas fault and left-lateral displacements within the range are observed, the Agua Blanca fault is shown by Gastil and others (1975) and by Allen and others (1960) to have caused right-lateral displacement of the basement rocks as well as Quaternary age sediments and geomorphic features. Also, no evidence of crustal shortening is mentioned in the literature on the area. In their work, Allen and others (1960) concluded that despite its similarity in orientation to the Transverse Ranges, the Agua Blanca fault does not seem to have many of the structural features that would make it analogous to the Transverse Ranges or that would suggest a similar origin.

The third tectonic model suggests that the Agua Blanca fault and the similarly northwest-oriented faults in the Baja Peninsula arise from a different stress system than faults of the Continental Borderlands. This hypothesis concerns the combined effects of the interference of the Pacific and North American plates motions due to the bend in the San Andreas fault at the Transverse Ranges (figure 2.5L-7) and variable rates of crustal spreading in the Gulf of California. The rate of relative northward motion of the Pacific plate increases southerly along the spreading centers, and the westward-stepping, en-echelon arrangement of the spreading centers induces a right-lateral shear within the Baja Peninsula causing faults with orientations similar to the Agua Blanca fault. This increase of spreading rates to the south is supported by the fact that the faults at the Viscaino Peninsula are estimated to have as much as 50 kilometers of right-lateral displacement, whereas the Agua Blanca fault zone has only about 22 kilometers; thus, an increase in total displacement southward occurs across the peninsula (Allen and others, 1960; Robinson, 1979).

In order to accommodate the variable spreading rates, established theories of rigid plate tectonics would require that active fracture zones develop to the north of the spreading centers as direct extensions of the transform fault of the gulf. In Baja, these active extensions do not seem to be present. This conclusion is based on the studies of Gastil and others (1975) and Allen and others (1960). The oblique orientation of the Agua Blanca and similar faults in Baja may be explained by the idea that the variable spreading rates in the Gulf accompany somewhat concentrated shear loads on the Pacific plate to the northwest of the ridges. The stress field in the plate due to one of these loads would not necessarily produce shear faulting parallel to the plate edge. For example, in an elastic plate subjected to a concentrated shear load along its edge, the regions of maximum deviatoric stress will be elongated lobes oriented to 45° to the plate edge of adjoining the region where the load is applied (see page 244 of Fung, Y.C., 1965, "Foundations of Solid Mechanics," Prentice-Hall). An elastic model of this effect, while not an exact characterization of the geologic environment (for example, the crustal material is not elastic as it emerges from the spreading centers), does provide a general description of stresses resulting from loads on the plate edge. It is thus plausible

that the Agua Blanca and similar faults arise from stress perturbations near the plate edge due to spatially variable spreading rates.

The presence of the compressive Transverse Ranges system to the north and the San Clemente and Coronado Banks faults to the west of the OZD are evidence that some of the plate motion is shunted offshore in Baja and the Continental Borderlands, in order to accommodate the movement around the Transverse Ranges. The stress field resulting from that configuration is portrayed in figure 2.5L-8.

This model can accommodate the existence of a compressive stress field in the Transverse Ranges, which would block the northward motion of the crust immediately to the west of the San Andreas system and would require right-lateral shear motion to be concentrated on faults to the east and west of the OZD. This could be occurring on the San Clemente or Coronado Banks faults to the west. In this manner the OZD would be shielded from the major regional tectonic stress field by the Transverse Ranges. The lower stress field in this region would be consistent with the lower spreading rates in the northern part of the Gulf of California. This shielding effect is also consistent with the observed lower degree of activity and observed total offset on the OZD as compared to other faults to the east and probably to the west. It should be expected that the faults within the shielded block are less continuous and less significant than the bounding parallel faults.

2.5L.6 DISCUSSION OF SEISMOLOGIC DATA

Recent Regional Seismicity

Regional seismicity data covering the time period 1932 to January 1979 have been presented in the June 1979 WCC report and in appendix 2.5J. Recent seismicity since January 1979 is discussed here. Catalogues and maps of seismic activity in the study area have been updated using the southern California earthquake catalogue compiled from Caltech's SCARLET system data. This update covers all events that are routinely detected, timed, and located in the normal operation of the Caltech recording array (CEDAR). Plots of the seismic activity covered by this discussion are shown in figure 2.5L-9 (July 1, 1979 to about May 20, 1980 and events since January 1, 1980).

Observed activity is consistent with patterns previously noted from the Caltech southern California catalogue for this study region. During the second half of 1979 and the first 5 months of 1980, the largest concentration of activity was associated with the October 15, 1979 ($M = 6.6$) U.S.-Mexico Imperial Valley earthquake and its aftershocks (figure 2.5L-9). Another smaller cluster of activity also north of the U.S.-Mexico international border is noted along the San Jacinto fault, centered on the February 25, 1980, $M_L = 5.3$ Hemet earthquake. This activity is better seen in the plots of seismicity from January 1, 1980 to the present (figure 2.5L-9). Offshore and in Mexico, it can be noted that: (1) no events routinely

detected by the CEDAR system ($M_L \geq 2.5$) are located on the Agua Blanca fault; (2) there is scattered activity ($M_L \leq 5.0$) in the area of the Vallecitos and San Miguel faults, with a cluster of earthquakes occurring near where the Vallecitos and San Miguel are en-echelon; (3) offshore activity is low in that only five events with $M_L \leq 4.0$ are observed in this 11 month time period; and (4) no events are seen along the coast from Ensenada, through Tijuana and San Diego, and north to Long Beach at the level of $M_L \geq 3.0$.

Focal Mechanisms

Fault-plane solutions were obtained for 20 events associated with the NIZD, SCOZD, and RCFZ and within 10 kilometers to the east, as discussed in the report of June 1979. Limitations are imposed on data available for these studies due to the limited distribution of recording stations with respect to the locations of these earthquakes. Solutions are based on first motion data at stations in the Caltech network, which are located primarily to the east of the offshore earthquakes examined. The results obtained generally indicate a north-south maximum compressive stress, consistent with the regional stress field produced by the interaction of the North American and Pacific plates. A variety of focal mechanisms were obtained, which are suggestive of activity on faults of different orientations.

For events south of the international border, focal mechanisms are extremely difficult to obtain, even for larger events occuring in the 1930s and 1950s, because of the small number of recording stations, most of which are located north of the border.

A preliminary fault-plane solution for the El Alamo 1956 ($M_L = 6.8$) earthquake on the San Miguel fault, based only on data from Caltech stations, indicates a right-lateral strike-slip mechanism, compatible with the geologic observations of Shor and Roberts (1958).

Few fault-plane solutions for other Mexican earthquakes are available in the literature. In western Baja, first-motion data for the Canon de la Presa event located southwest of Tijuana (August 19, 1978, M_L 3.5) suggest right-lateral strike-slip movement (Brune and others, 1979). Other solutions are available for events in the Gulf of California, e.g., Canal de las Ballenas (July 8, 1975, $M_s = 6.5$), which was determined to have a right-lateral strike-slip mechanism by Munguia and others (1977), and El Golfo (August 7, 1966, $M_b = 5.3$, $M_s = 6.3$) near the mouth of the Colorado River, which was also given a right-lateral strike-slip mechanism by Ebel and others (1978). Focal plots for these two eastern Baja events are shown in figures 2.5L-10 and 2.5L-11.

APPENDIX 2.5L

Offshore Patterns of Seismicity

Offshore activity since 1932 to the present has been examined to identify possible linear patterns and to assess the validity of using data to make connections between onshore and offshore features. Only events of A or B quality epicentral location, i.e., with location errors less than 5 kilometers, are accurate enough to be useful. Legg and Kennedy (1979, in Abbott and Elliott, Figure 2, p. 39) attempt to identify a linear trend of A and B quality epicentral locations that delineate the Coronado Banks fault zone. They identify a trend that extends north at a bearing of N 45° W from the Coronado Banks, becoming more diffuse in the vicinity of Lasuen Sea Knoll. South of Coronado Banks, Legg and Kennedy (1979) interpret activity to cease at about the latitude of south San Diego Bay and then to recommence in the Salsipuedes area. Legg and Kennedy also identify a trend of epicenters farther offshore that they feel marks the San Clemente-San Isidro fault zone. If valid, this interpretation of the seismicity could be used to suggest continuity of activity along the Coronado Banks fault as far north as the Lasuen Sea Knoll and south to Salsipuedes near the Agua Blanca fault.

The Applicants have noticed a different interpretation of the same seismicity data used by Legg and Kennedy (1979) that also takes into consideration the distribution of located earthquakes. As shown in figure 2.5L-12, two potential linear patterns are indicated by the seimsic activity plotted. The pattern nearest to the shore extends from Santa Catalina Island southeast to the coastline. This trend corresponds to no mapped offshore lineament and, in fact, cuts across the Coronado Banks and the San Diego trough. This pattern is delineated by activity of $M_L = 4.0$, and it is unlikely that it indicates continuity of faulting through that area.

Another linear pattern farther offshore, that is indicated by the distribution of A and B quality locations is not as well defined. In general, this trend includes larger events than those of the nearer shore pattern. The trend of the pattern follows the San Clemente fault at its northern end, but when data are limited to A and B quality locations, it is very poorly defined to the south. The inclusion of C and D quality epicentral locations as shown on figure 2.5L-13 creates a weak pattern extending from San Clemente Island to the Mexican coast in the vicinity of the Agua Blanca fault. The epicentral location error is less than 15 kilometers for C quality events and greater than 15 kilometers for D quality events. These two epicentral patterns suggest that the majority of offshore seismic activity listed by the instrumental recordings in the Caltech catealogue is too diverse to be specifically associated with any of the connected fault zones postulated by Legg and Kennedy (1979) and thus cannot be used to support arguments of connection of these zones.

Cumulative Moment Distribution Plot

The moment of an earthquake is defined as:

$$M_o = \int_S \mu \, u \, ds$$

where:

μ is the shear modulus and u is the displacement jump across the fault and S is the fault surface. Roughly,

$M_o = \mu A < u >$, (force times length)

where:

A is the area of the fault and $< u >$ is the average dislocation on the fault. This is a quantity that is observable in far-field seismic radiation at asymptotically long periods. Assumptions regarding the time history of the displacement jump permit the estimation of M_o from shorter period data.

Kanamori and Anderson (1975) discuss an empirical moment-magnitude relationship from which the moment can be obtained from the magnitude:

$\text{Log } M_o \simeq 3/2\ M_s + \text{constant}$

A plot of spatial distribution of the cumulative moment illustrates how much seismic slip has occurred in an area, assuming that certain material parameters do not vary greatly throughout the region. It is thus a much more quantitative indicator of the long term deformation of an area than a plot in which only earthquake epicenters and magnitudes are plotted. For this reason, the cumulative moment plots are a useful tool in analysis of regional tectonics. The cumulative moment plot of southern California and northern Baja California (figure 2.5L-14) clearly shows the OZD to be a quiet region with greater activity to the east and west. The reason for this lack of activity in the OZD can be explained by the tectonic model involving the shielding effect of the Transverse Range and variable spreading rates in the Gulf of California as portrayed in figure 2.5L-8.

2.5L.7 SUMMARY OF CONCLUSIONS

The geologic and tectonic setting of the hypothesized OZD and faults in Baja are evidence for a discontinuous zone of deformation without continuity of faults. The absence of faulting and apparent difference in age of faulting between the southern end of the hypothesized OZD and the Vallecitos-San Miguel trend is evidence that tends to disassociate the two zones structurally and with respect to their earthquake potential. The historic seismicity and the geomorphic characteristics of each zone suggest that neither zone is capable of earthquakes greater than M_s 7.0. Based on those observations, the DBE for San Onofre remains unaffected.

For the connections hypothesized of the OZD to offshore faults to exist, an awkward geometry would be required--one that would not be typical of strike-slip faults in southern California. Thus, the faults offshore from Baja and the Agua Blanca fault do not directly affect the faults within the OZD. Based on the tectonic setting estimates of the maximum magnitude of the SCOZD should most appropriately be derived from evaluation of the

OZD in the vicinity of the site and not from evaluation of faults in Baja or offshore from Baja.

All three of the tectonic models applied to the southern California and northern Baja area consider that the major strain release between the North American plate and Pacific plate is occurring along the San Andreas fault and ridge transform system in the Gulf of California, including high stress in the Transverse Ranges and the Continental Borderlands. Whether the faults through Baja are related to extensions of transform faults in the Gulf, or whether they are caused by local stresses due to the relative motion of Baja, the geometry of faulting onshore and offshore is evidence for the Transverse Ranges acting as a barrier to fault propagation on the hypothesized OZD and for the ranges diverting major strain release to the offshore area of the Continental Borderlands (e.g., San Clemente and Coronado Banks faults). The fault configuration provides evidence for the shielding of the OZD from major strain and for the OZD being a minor zone of deformation responding to the regional stresses. The geologic data and the fault behavior are strongly supportive of the OZD as defined in the June 1979 WCC report and in appendix 2.5R; that is, the OZD is a discontinuous zone of deformation prone to rupture of individual fault segments or relatively short portions of the zone during earthquakes.

Amended: April 2009 TL: E048000

APPENDIX 2.5L

REFERENCES

1. Abbott, P. L., ed., 1979, Geological Excursions in the Southern California area--Prepared for the Geological Society of America Annual Meeting: San Diego State University Department of Geological Sciences, 217 p.

2. Abbott, P. L., and Elliott, W. J., eds., 1979, Earthquakes and Other Perils, San Diego region: San Diego Association of Geologists, for the Geological Society of America, Field Trip Guidebook, 227 p.

3. Allen, C. R., Silver, L. T., and Stehli, F. G., 1960, Auga Blanca Fault--a Major Transverse Structure of Northern Baja California, Mexico: Geological Society of America Bulletin, v. 71, p. 457-482.

4. Brune, J. N., Simons, R. S., Rebollar, C., and Reyes, A., 1979, Seismicity and Faulting in Northern Baja California, in Abbott, P. L., and Elliott, W. J., eds., Earthquakes and Other Perils, San Diego Region: San Diego Association of Geologists, for the Geological Society of America, Field Trip Guidebook, p. 83-100.

5. Ebel, J. E., Burdick, L. J., and Stewart, G. S., 1978, The Source Mechanism of the August 7, 1966 El Golfo Earthquake: Bulletin of the Seismological Society of America, v. 68, p. 1281-1292.

6. Elders, W. A., Rex, R. W., Meidav, T., Robinson, P. T., and Biehler, S., 1972, Crustal Spreading in Southern California: Science, Vol. 178, p. 15-24.

7. Frazer, M., 1972, Geology of Valle de las Palmas: Senior Report (unpublished), San Diego State University, 18 p.

8. Gastil, G. R., Phillips, R. P., and Allison, E. C., 1975, Reconnaissance Geology of the State of Baja California: Geological Society of America, Memoir 140, 170 p. (with map, scale 1:250,000).

9. Gastil, R. G., Kies, R., and Melius, D. J., 1979, Active and Potentially Active Faults: San Diego County and Northernmost Baja California, in Abbott, P. L., and Elliott, W. J., eds., Earthquakes and Other Perils, San Diego Region: San Diego Association of Geologists, for the Geological Society of America, Field Trip Guidebook, p. 47-60.

10. Green, H. G., Bailey, K. A., Clarke, S. H., Ziony, J. I., and Kennedy, M. P., 1979, Implications of Fault Patterns of the Inner California Continental Borderland between San Pedro and San Diego, in Abbott, P. L., and Elliott, W. J., eds., Earthquakes and Other Perils, San Diego Region: San Diego Association of Geologists for the Geological Society of America, Field Trip Guidebook, p. 21-28.

11. Hamilton, Warren, 1971, Recognition of Space Photographs of Structural Elements of Baja California: U.S. Geological Survey Professional Paper 718, 26 p.

12. Henyey, T., and Bischoff, J. L., 1973, Tectonic Elements of the Northern Part of the Gulf of California: Geological Society of American Bulletin, v. 84, p. 315-330.

13. Kanamori, H., and Anderson, D. L., 1975, Theoretical Basis of Some Empirical Relations in Seismology: Bulletin of the Seismological Society of America, v. 65, p. 1073-1095.

14. Kennedy, M. P., 1975, Geology of the Western San Diego Metropolitan Area, California, Del Mar, La Jolla, and Point Loma Quadrangles: California Division of Mines and Geology, Geology of the San Diego Metropolitan Area, California, Section A, p. 9-39.

15. Kennedy, M. P., Welday, E. E., Borchard, G., Chase, G. W., and Chapman, R. H., 1977, Studies of Surface Faulting and Liquefaction as Potential Earthquake Hazards in Urban San Diego, California: California Division of Mines and Geology Final Technical Report.

16. Krause, D. C., 1965, Tectonics, Bathymetry, and Geomagnetism of the Southern Continental Borderland West of Baja California, Mexico: Geological Society of America Bulletin, v. 76, 617-650.

17. Legg, M. R., 1979, Faulting and Earthquakes in the Inner Borderland, Offshore Southern California and Northern Baja California: Masters Thesis (unpublished), Scripps Institution of Oceanography, 75 p.

18. Legg, M. R., and Kennedy, M. P., 1979, Faulting Offshore San Diego and Northern Baja California, in Abbott, P. L., and Elliott, W. J., eds., Earthquakes and Other Perils, San Diego Region: San Diego Association of Geologists, for the Geological Society of America, Field Trip Guidebook, p. 29-46.

19. Lomnitz, C., Moser, F., Allen, C. R., Brune, J. N., and Thatcher, W., 1970, Seismicidad y Tectonica del Golfo de California; Resultados Preliminary: Geofisica Internacional 10, (2), 37. (Also in English)

20. Moore, D. G., 1969, Reflection Profiling Studies of the California Continental Borderland: Structure and Quaternary Turbidite Basins: Geological Society of America Special Paper 107, 142 p.

21. Munguia, L., Reickle, M., Reyes, A., Simons, R. S., and Brune, J. N., 1977, Aftershocks of the 8 July 1979 Canal de las Ballenas Gulf of California earthquake: Geophysical Research Letters, v. 4, no. 11, p. 507-510.

22. Robinson, J. W., 1979, Structure and Stratigraphy of the Northern Vizcaino Peninsula with a Note on a Miocene Reconstruction of the Peninsula, in Abbott, P. L., and Gastil, R. G., eds., Baja California Geology, Field Guides and Papers: Geological Society of America Annual Meeting, San Diego, Field trips 10, 12, 13, and 26, p. 77-82.

23. Rusnak, G. A., Fisher, R. L., and Shepard, F. P., 1964, Bathymetry and Faults of Gulf of California, in Van Andel, T. H., and Shor, G., eds., Marine Geology of the Gulf of California: American Association Petroleum Geologists Memoir 3, p. 59-76.

24. Shepard, F. P., and Emery, K. O., 1941, Submarine Topography off the California Coast: Canyons and Tectonic Interpretation: Geological Society of America Special Paper 31, 171, p.

25. Shor, G., and Roberts, E. E., 1958, San Miguel, Baja California Norte, Earthquakes of February, 1956--a field report: Seismological Society of America Bulletin, v. 48, p. 101-116.

26. Simons, R. S., 1979, Instrumental Seismicity of the San Diego area, in Abbott, P. L., and Elliott, W. J., eds., Earthquakes and Other Perils, San Diego region: San Diego Association of Geologists, for the Geological Society of America, Field Trip Guidebook, p. 101-106.

27. Slyker, R. G., Jr., 1974, Geophysical Survey and Reconnaissance Geology of the Valle de San Felipi Area, Baja California, Mexico, in Gastil, G. R., and Lillegraven, M., eds., Geology of Peninsular California: Pacific Section, AAPG-SEPM-SEG Guidebook, p. 107-120.

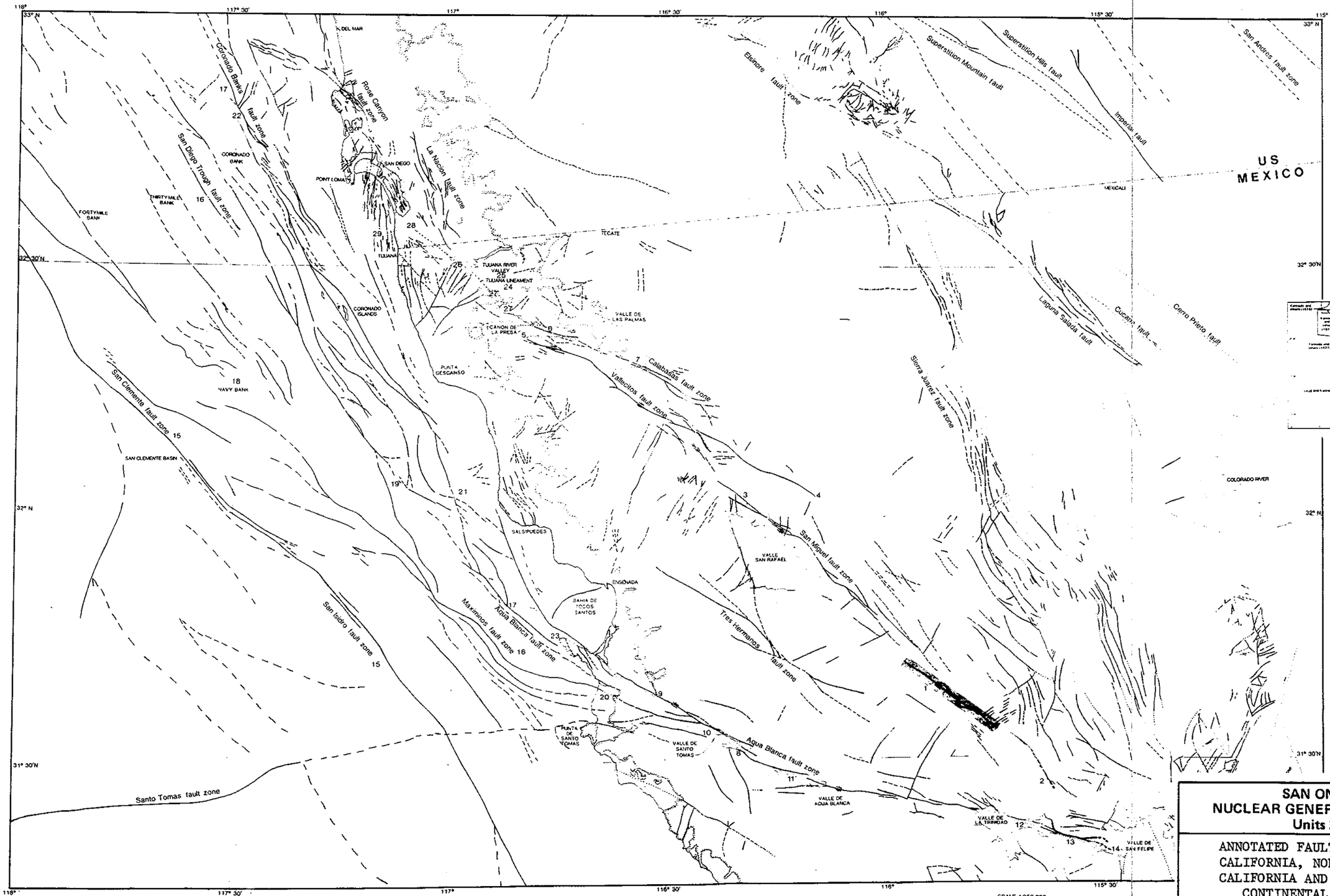

Updated

SAN ONOFRE NUCLEAR GENERATING STATION
Units 2 & 3

ANNOTATED FAULT MAP SOUTHERN CALIFORNIA, NORTHWESTERN BAJA CALIFORNIA AND THE CALIFORNIA CONTINENTAL BORDERLAND SONGS SEISMOLOGY

Figure 2.5L-1

Amended: April 2009 TL: E048000

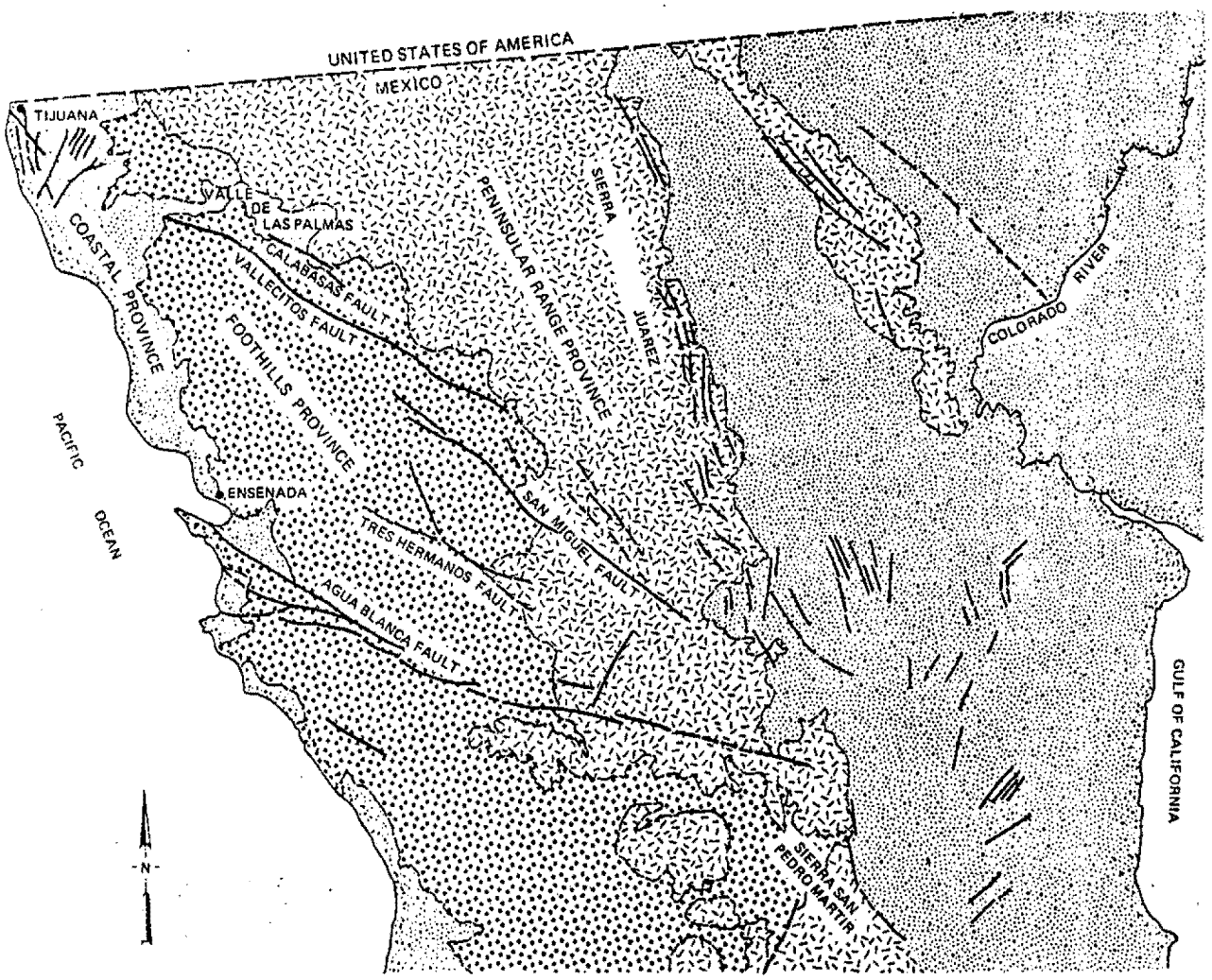

NOTE:

After Gastil and Others, 1975, Reconnaissance Geologic Map of the State of Baja California: Geological Society fo America Memoir 140.

Updated

SAN ONOFRE NUCLEAR GENERATING STATION Units 2 & 3
GENERALIZED MAP OF NORTHERN BAJA CALIFORNIA PHYSIOGRAPHIC PROVINCES AND DISTINCT GEOLOGIC TERRANES
Figure 2.5L-2

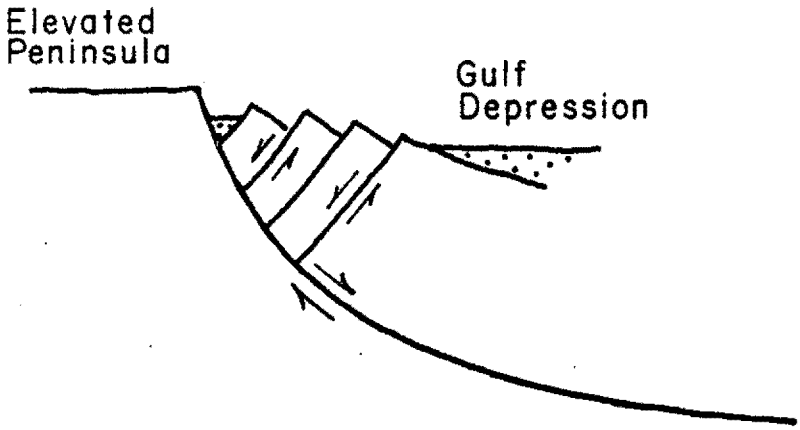

Updated

SAN ONOFRE
NUCLEAR GENERATING STATION
Units 2 & 3

ANTITHETIC FAULT BLOCKS
ALONG EASTERN ESCARPMENT
OF THE SIERRA JUAREZ

Figure 2.5L-3

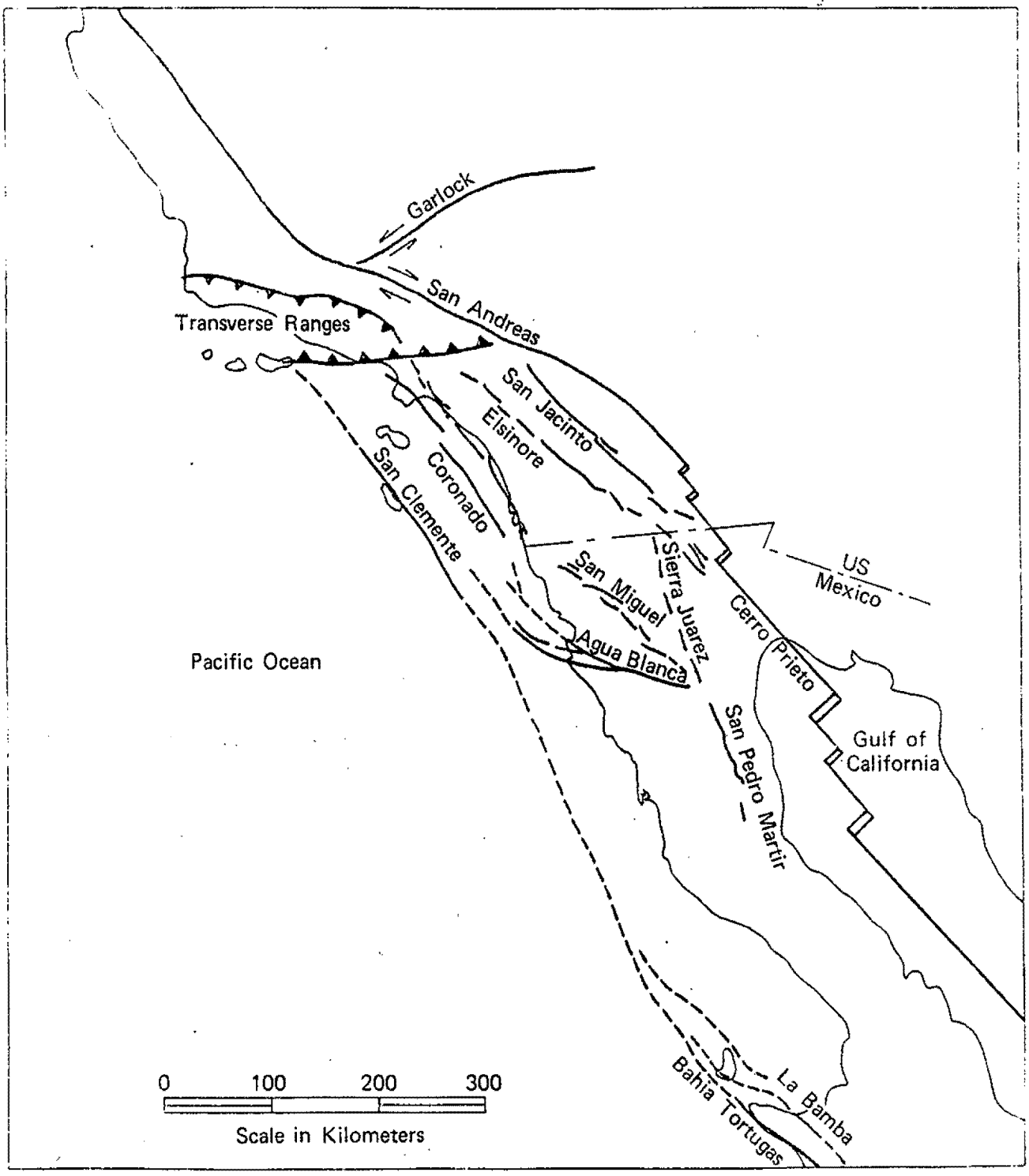

Updated

SAN ONOFRE
NUCLEAR GENERATING STATION
Units 2 & 3

LOCATION OF MAJOR TECTONIC FEATURES IN SOUTHERN CALIFORNIA AND BAJA CALIFORNIA

Figure 2.5L-4

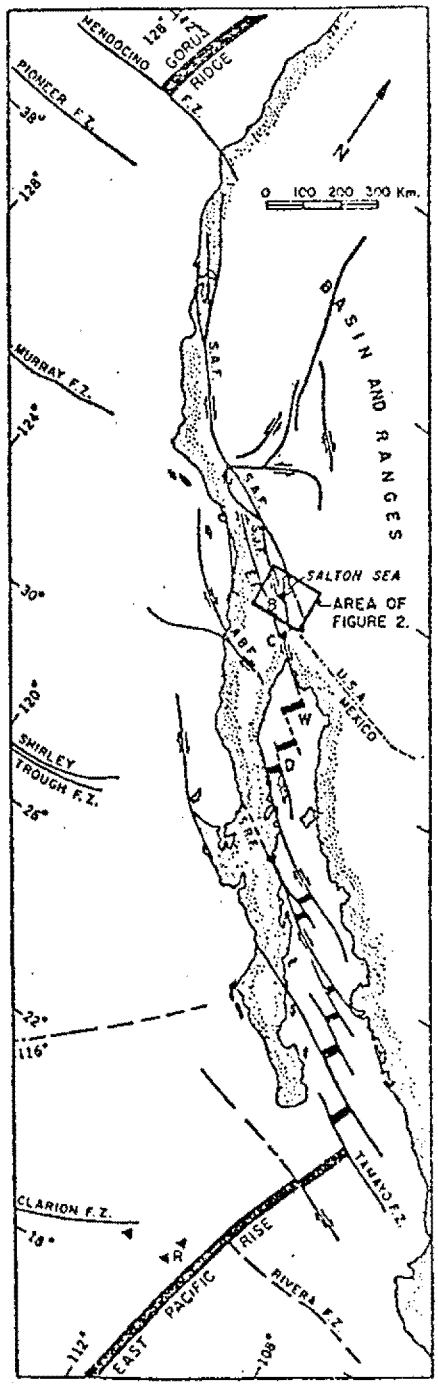

Fractures and spreading centers along part of the Pacific Coast of North America between the East Pacific Rise and the Gorda Ridge. Oceanic fracture zones (F.Z.) and continental faults (F.) are solid black lines, dashed where uncertain. S.A.F., San Andreas fault; E.F. Elsinore fault; S.J.F., San Jacinto fault; A,B.F., Agua Blanca fault; S.R.F., Santa Rosalia fault. Postulated spreading centers in the Gulf of California are shown in black: W, Wagner Basin; D, Delfin Basin.
(From Elders and others, 1972)

Updated

SAN ONOFRE
NUCLEAR GENERATING STATION
Units 2 & 3

TECTONIC MAP SHOWING
FRACTURE ZONE EXTENSIONS
FROM TRANSVERSE FAULTS

Figure 2.5L-5

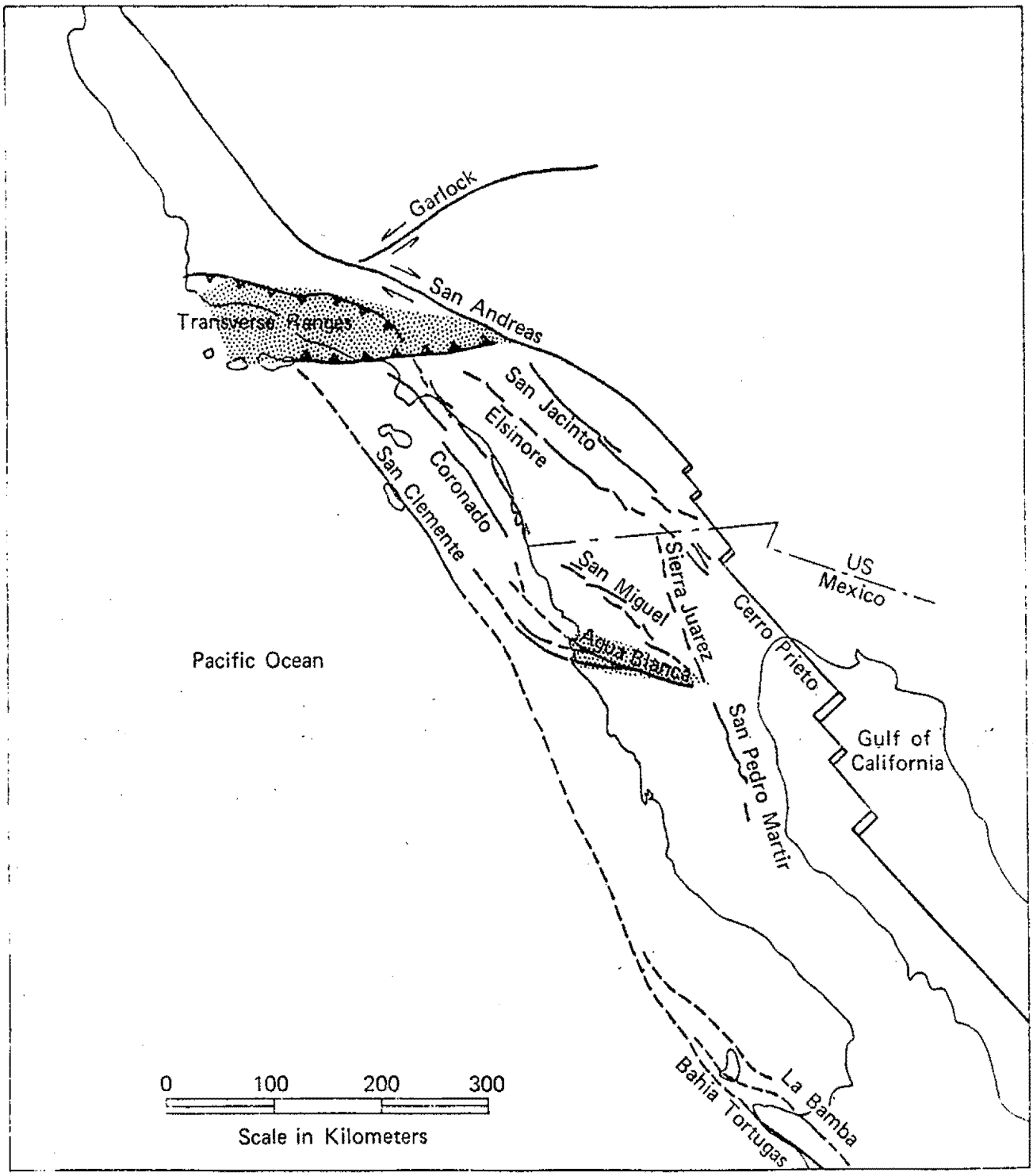

Updated

SAN ONOFRE
NUCLEAR GENERATING STATION
Units 2 & 3

TECTONIC MAP SHOWING PARALLELISM
OF AGUA BLANCA FAULT ZONE
WITH THE TRANSVERSE RANGES

Figure 2.5L-6

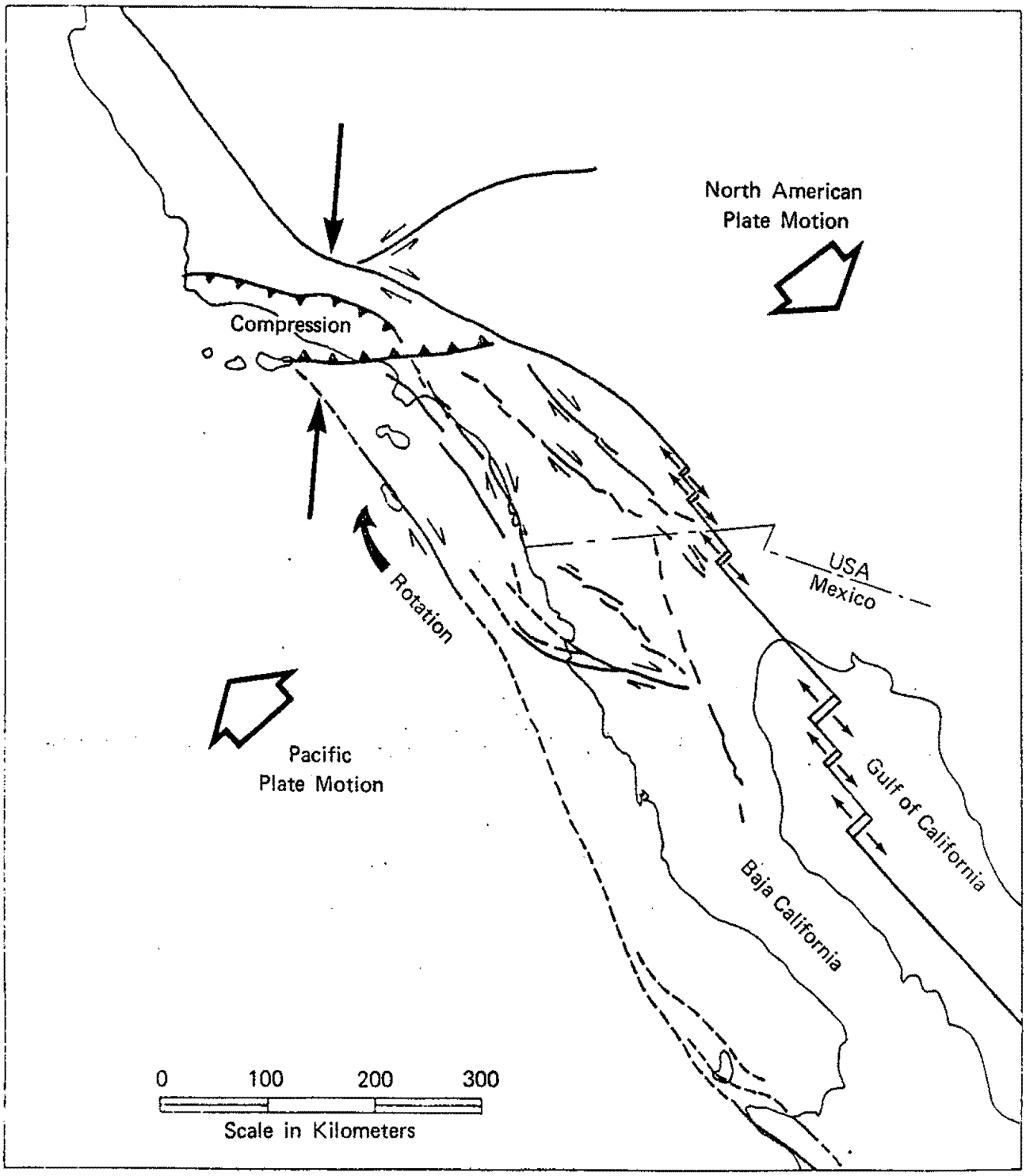

Updated

SAN ONOFRE
NUCLEAR GENERATING STATION
Units 2 & 3

TECTONIC MODEL WITH INCREASING SPREADING RATES SOUTHWARD ALONG SPREADING CENTERS IN THE GULF OF CALIFORNIA ASSOCIATED WITH RIGHT-LATERAL SHEAR IN BAJA AND COMPRESSION IN THE TRANSVERSE RANGES

Figure 2.5L-7

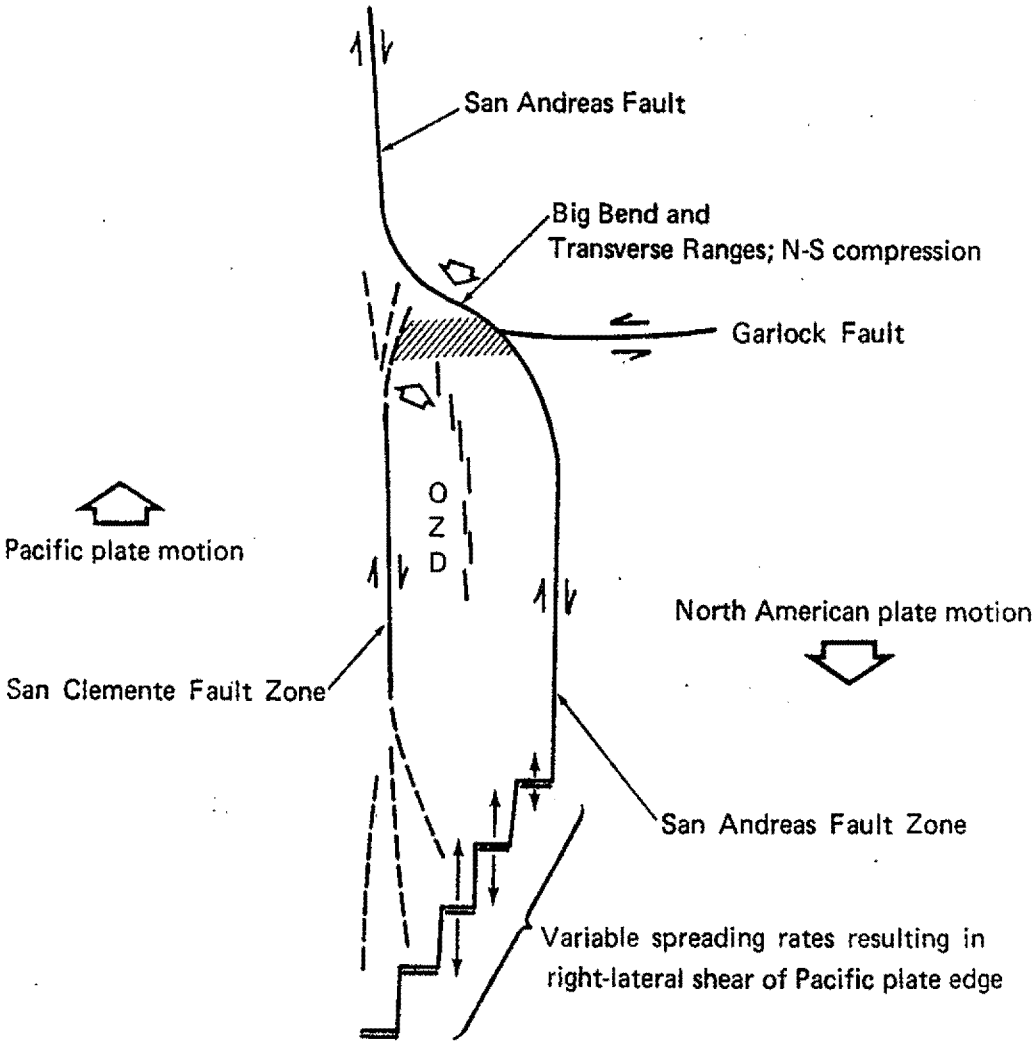

Updated

SAN ONOFRE
NUCLEAR GENERATING STATION
Units 2 & 3

SCHEMATIC DIAGRAM OF STRUCTURAL RELATIONSHIPS OF FAULTS AND SPREADING CENTERS IN SOUTHERN CALIFORNIA AND BAJA CALIFORNIA

Figure 2.5L-8

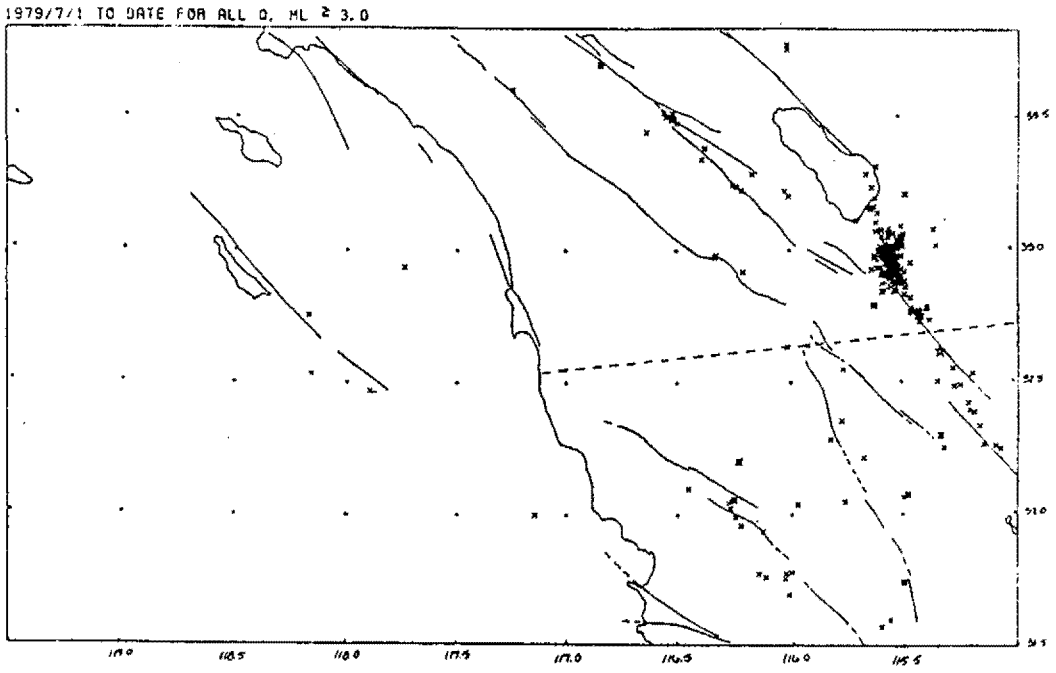

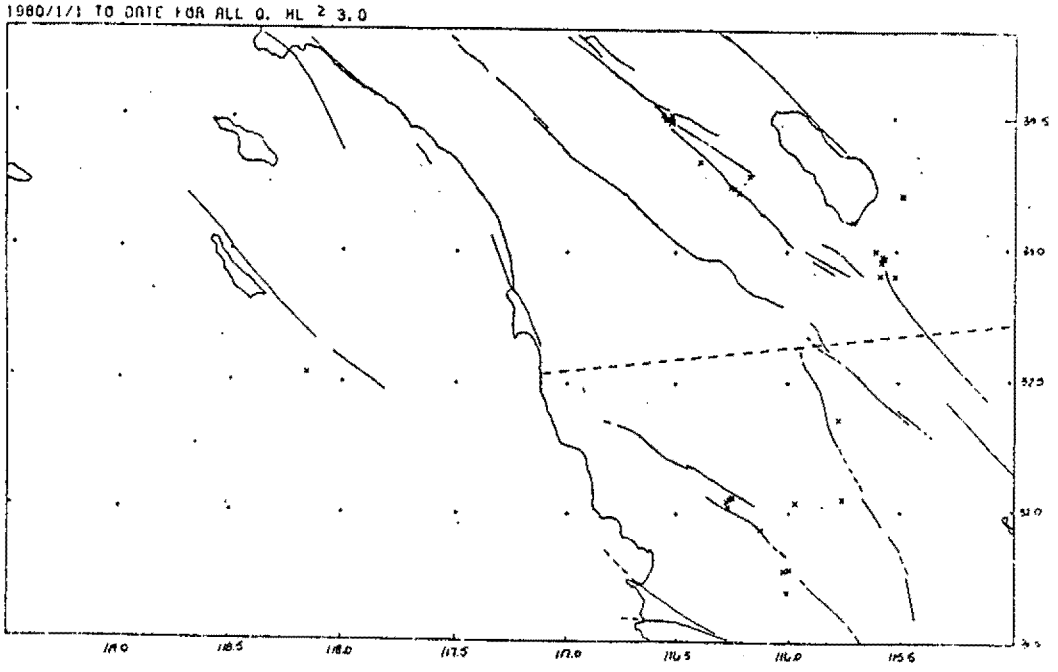

Updated

*NOTE

A. 1 JULY 1979 TO APPROXIMATELY 20 MAY 1980, AND
B. 1 JANUARY 1980 TO APPROXIMATELY 20 MAY 1980.
EVENTS OF M_L 3.0 ARE SHOWN AT ALL LEVELS OF LOCATION QUALITY INCLUDING PRELIMINARY LOCATIONS. ACTIVITY OF THE 15 OCTOBER 1979 IMPERIAL VALLEY EVENT DOMINATES 1979. EVENTS ARE OBSERVED ASSOCIATED WITH THE VALLECITOS AND SAN MIGUEL FAULTS. THERE IS NO ACTIVITY ON THE AGUA BLANCA FAULT OBSERVED DURING THIS TIME PERIOD.

SAN ONOFRE
NUCLEAR GENERATING STATION
Units 2 & 3

SEISMICITY PLOTS OF EARTHQUAKE ACTIVITY ROUTINELY LOCATED BY THE CALTECH SOUTHERN CALIFORNIA NETWORK FOR TWO TIME PERIODS*

Figure 2.5L-9

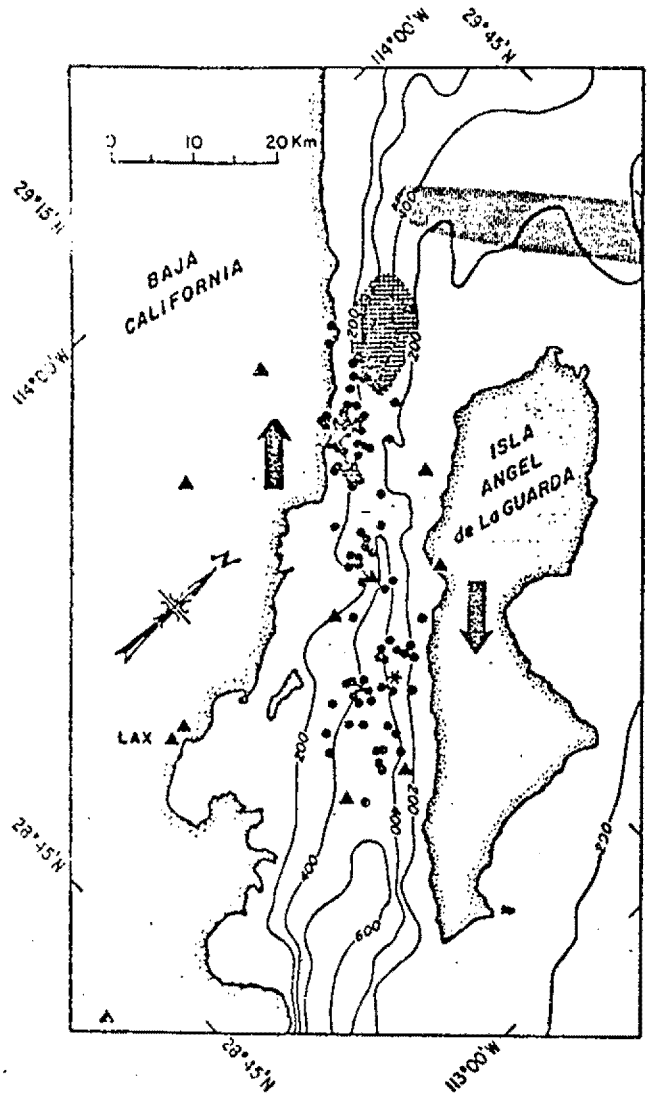

a. Aftershocks of the 8 July 1975 Canal de las Ballenas earthquake. Bathymetry after Rusnak and others (1964); contours in fathoms. Asterisk is our location of the event. Triangles are portable land-station sites and deployment sites of sonobuoys. Dots are epicenters of aftershocks located with the local array.

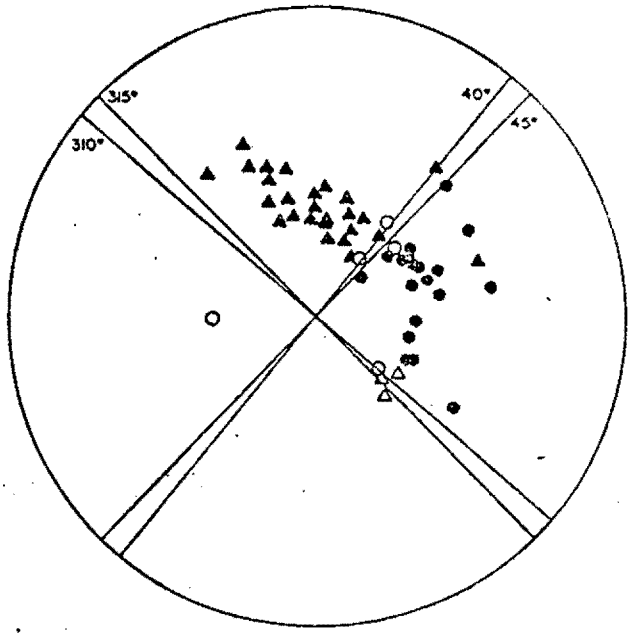

b. Fault plane solution for main event plotted on an equal area projection. Dots represent compressional first motion; triangles dilatational. Open symbols are uncertain or emergent readings. Range of solutions for a vertical fault with horizontal motion is shown.

Updated

SAN ONOFRE NUCLEAR GENERATING STATION
Units 2 & 3

LOCATION MAP AND FAULT PLANE SOLUTION FOR THE CANAL DE LAS BALLENAS EARTHQUAKE (MUNGUIA AND OTHERS, 1977)

Figure 2.5L-10

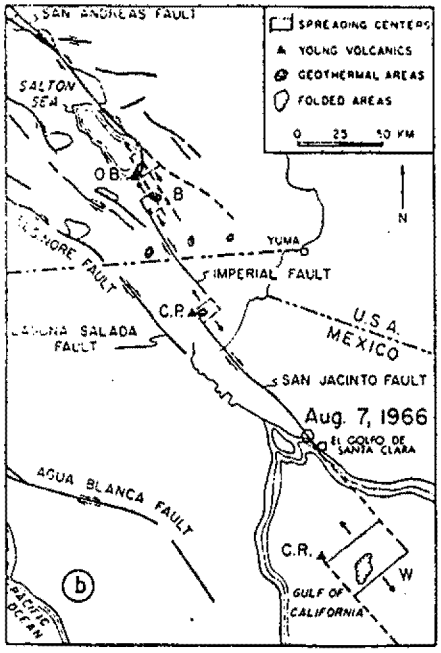

Location of El Golfo earthquake on the San Jacinto fault at the mouth of the Colorado River, The interpretation of tectonics is from Elders and others (1972).

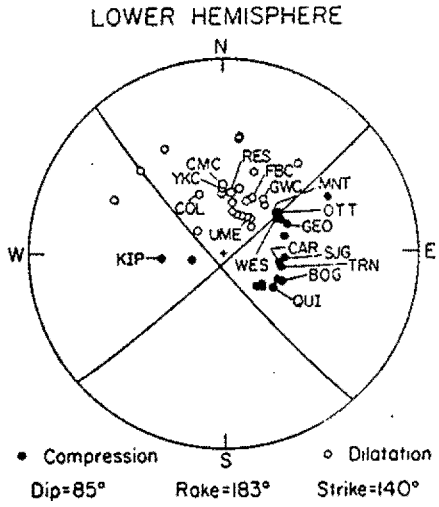

A focal plot of the *P*-wave first motions with the locations of stations for which the body waves were modeled. The nodal planes represent those found from the modeling process.

Updated

SAN ONOFRE NUCLEAR GENERATING STATION Units 2 & 3
LOCATION MAP AND FOCAL PLOT OF THE EL GOLFO EARTHQUAKE (EBEL AND OTHERS, 1978)
Figure 2.5L-11

1/1/32 TO 9/30/76

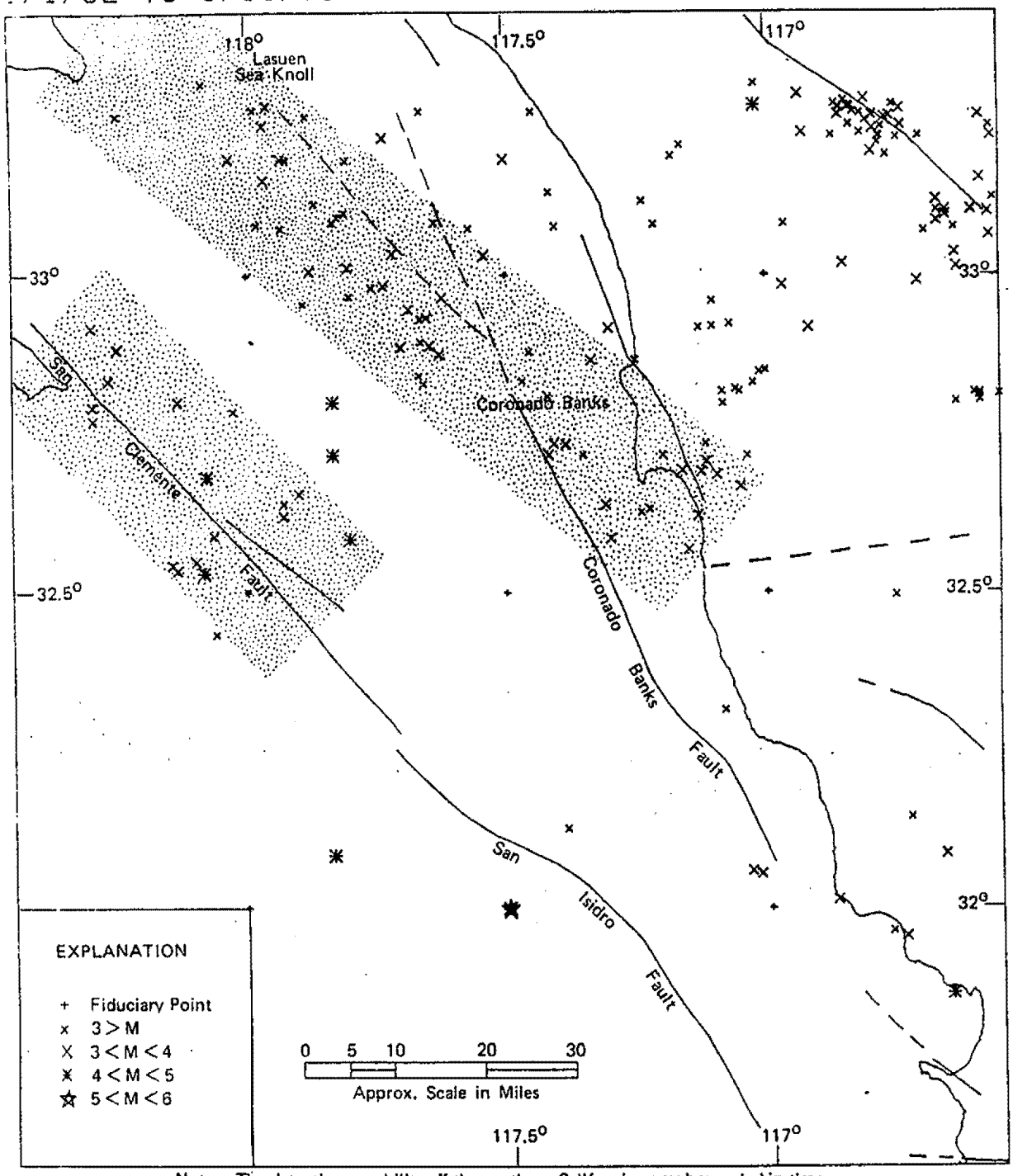

Note: The detection capability of the southern California array has varied in time, but the threshold is M_L = 3.0 or smaller for the time period shown.

Updated

SAN ONOFRE NUCLEAR GENERATING STATION Units 2 & 3

A AND B QUALITY LOCATIONS (LOCATION ERRORS 15 KM) FROM THE CALTECH SOUTHERN CALIFORNIA EARTHQUAKE CATALOGUE FOR EARTHQUAKES OFFSHORE SAN DIEGO, TIJUANA, AND ENSENADA 1932 TO 1976

Figure 2.5L-12

1/1/32 TO 9/30/76

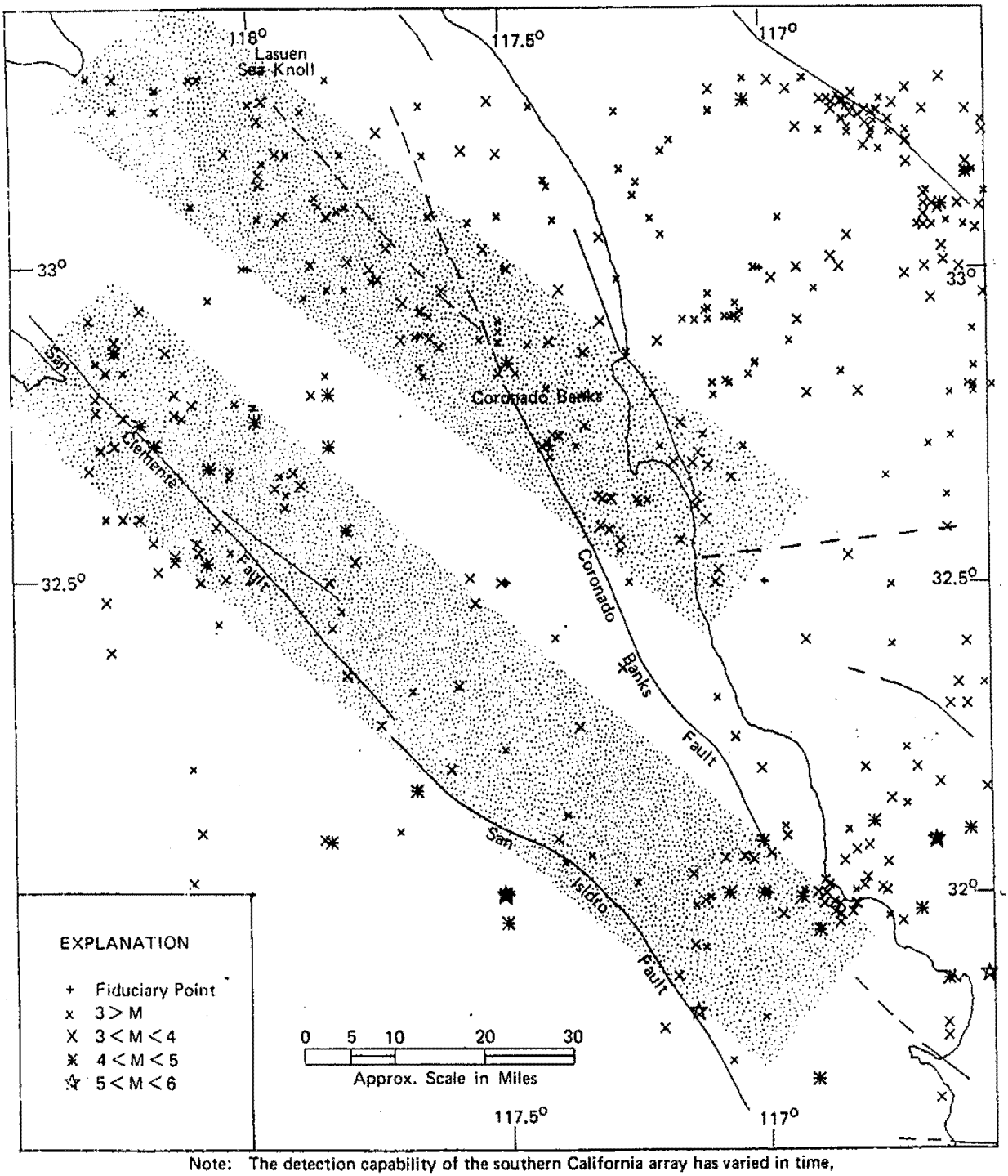

Note: The detection capability of the southern California array has varied in time, but the threshold is M_L = 3.0 or smaller for the time period shown.

Updated

SAN ONOFRE NUCLEAR GENERATING STATION
Units 2 & 3

A, B, C, AND D QUALITY LOCATIONS OF EARTHQUAKES IN THE SAME REGION AND DURING THE SAME TIME PERIOD AS FIGURE 3. D QUALITY LOCATION 15 KM IN ERROR

Figure 2.5L-13

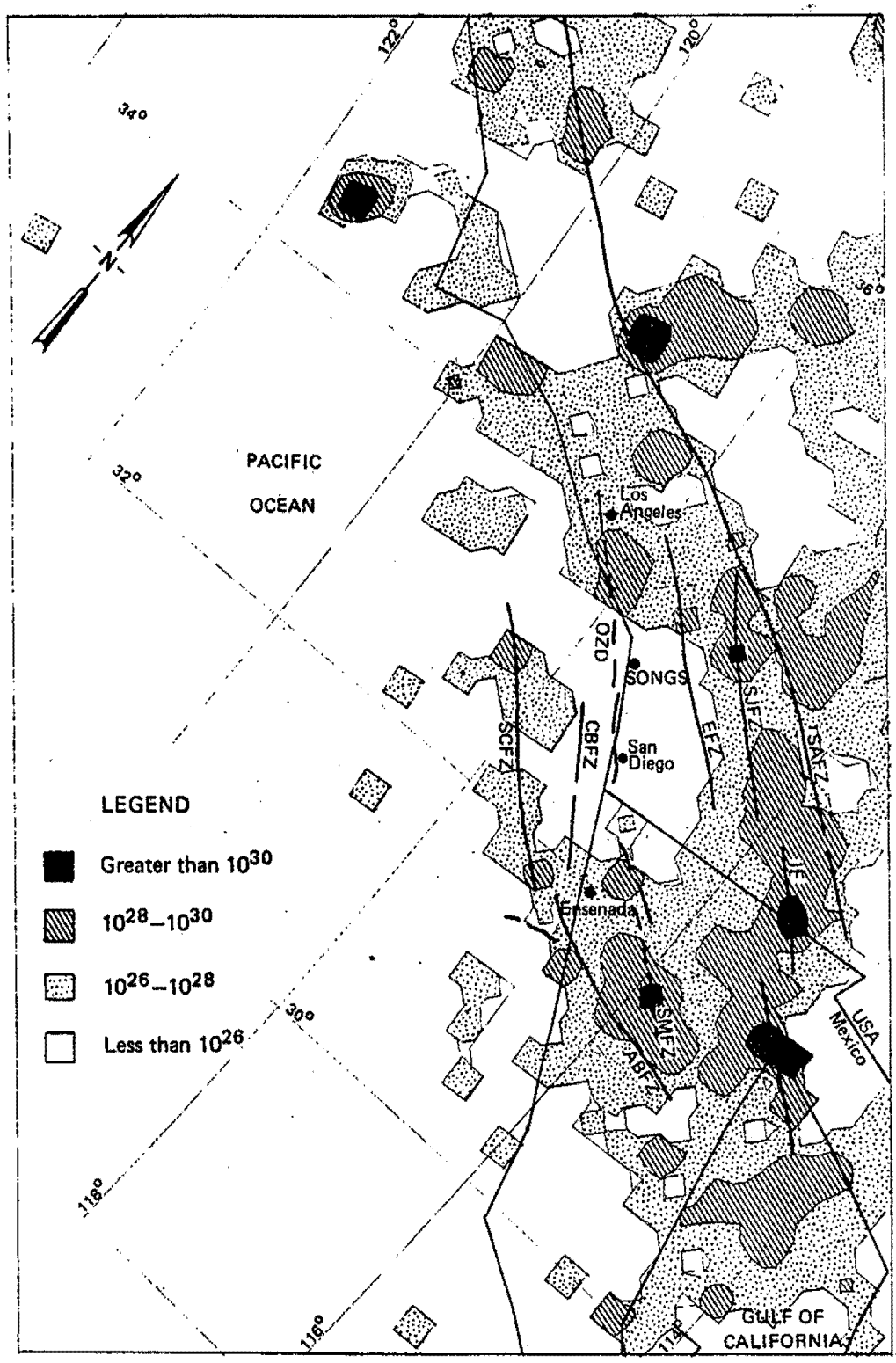

Updated

SAN ONOFRE NUCLEAR GENERATING STATION
Units 2 & 3

CUMULATIVE MOMENT RELEASE BY EARTHQUAKES 1898 TO 1979 IN SOUTHERN CALIFORNIA AND BAJA CALIFORNIA. UNITS CONTOURED ARE IN DYNE-CM/DEGREE SQUARED/YEAR

Figure 2.5L-14

APPENDIX 2.5M

HYPOTHESIZED OFFSHORE ZONE OF DEFORMATION

Site File Copy

APPENDIX 2.5M

HYPOTHESIZED OFFSHORE ZONE OF DEFORMATION

2.5M.1 FAULT CAPACITY OF OFFSHORE ZONE OF DEFORMATION

The applicants consider that the "Hypothesized Offshore Zone of Deformation" (OZD) is a northwesterly trending zone of discontinuous, folded and faulted sediments which exist as features along a zone of deformation which itself is not continuous (Marine Advisers, 1970, Western Geophysical, 1972, Vedder et al, 1974). The applicants consider that the OZD is composed of three structural entities from north to south: The Newport-Inglewood Zone of Deformation (NIZD), the South Coast Offshore Zone of Deformation (SCOZD), and the Rose Canyon fault zone (RCFZ). Interpretation of geologic data indicates that although the OZD is well expressed in several profiles obtained by Fugro, 1977, and Woodward-Clyde Consultants, 1978 (for example Fugro Track Line 6, Stations 41 and 42), it is not continuous within the Miocene and Pliocene rocks and, therefore, not capable of large earthquakes.

Since the applicants assumed the OZD to be a continuous zone during the Construction Permit proceedings, no studies based on the applicants' geologic model were performed subsequent to 1972. Accordingly, the seismic potential of the OZD relative to the applicants' geologic model has not been evaluated considering all current information.

In the interest of conservatism the OZD has been evaluated as a continuous zone of deformation capable of generating significant shaking at the site.

2.5M.2 EARTHQUAKE POTENTIAL ON OZD

The applicants assume the hypothesized Offshore Zone of Deformation to be a potential source of earthquake activity despite the geologic evidence that strongly suggests the different structural entities exhibit differing degrees of activity and, thus, differing earthquake potential.

The regional tectonics of southern California are dominated by the San Andreas fault system, consisting of the large northwest-trending, right-lateral San Andreas and San Jacinto fault zones. This system is paralleled to the west by other lesser strike-slip fault zones such as the Whittier-Elsinore fault zone, the OZD and the San Clemente fault. Although all these fault zones show evidence of predominant right slip, the faults west of the San Andreas Fault zone show an apparent progressively westward decrease in: (1) amount of total displacement, (2) continuity of surface trace, and (3) amount of seismic activity.

Although the northern part of the OZD (the NIZD) remains geologically and seismically active today, the southern part from Laguna Beach south has been relatively inactive, as evidenced by the observations that the NIZD: (1) has a higher level of historical seismicity, (2) has the

most prominent surficial anticlines, (3) is coincident with a Mesozoic basement rock discontinuity not known beneath the SCOZD or the RCFZ, and (4) is closer to the influence of the interaction between the San Andreas fault system and the Transverse Range than are the other segments of the OZD. Therefore, it is considered that OZD is responding to regional stress that is strongest in the Los Angeles basin to the north and diminishes southward. Nevertheless, in the view of the structural association among the various parts of the zone, the applicants assume any part of the OZD is a potential source of earthquake activity.

Thus, the earthquake potential of the OZD is less than that of major strike-slip faults such as the San Andreas and San Jacinto. Also, in view of the decreasing degree of activity from north to south along the zone, the potential for earthquakes (in terms of size and frequency) near the site is less than farther north in the Los Angeles basin. As is discussed in the following paragraphs, the OZD's quantitative earthquake potential is based on the conservative assumption that the maximum earthquake, which could occur anywhere along length of the OZD, occurs offshore of San Onofre.

2.5M.3 MAXIMUM EARTHQUAKE POSTULATED FOR THE OZD

Geologic, seismologic, and earthquake engineering analyses and reviews have been completed for the San Onofre site to estimate the magnitude of the maximum earthquake that could be postulated for the OZD (Woodward-Clyde Consultants, 1979, included in accordance with FSAR section 1.8).

It is recognized that a wide variation exists among faults in terms of the degree-of-fault activity; that is, slip rate, size and recurrence interval of earthquakes, and average amount of slip per event. This is true not only for faults in different tectonic environments but also for different faults within the same tectonic environment. Clearly, faults having higher degrees of activity present a greater earthquake hazard than faults having lower degrees of activity. Therefore, a method of estimating earthquake magnitude was developed that is based on comparing the degree of fault activity on the OZD with that of faults of similar style in the California region as well as in other regions of the world. By correlating this level of activity with the maximum earthquakes associated with those faults, an estimate can be made of the maximum earthquake that may be associated with the OZD. This procedure and the results of the investigation are presented in more detail in a report by Woodward-Clyde Consultants, 1979, (submitted to the NRC in accordance with section 1.8) and are summarized briefly below.

Recent investigations and analyses of the relationships between geologic and seismologic characteristics of faults and earthquakes provide a substantial basis for establishing a relationship between geologic slip rates on a fault and the size of the largest earthquake on that fault.

APPENDIX 2.5M

Empirically (Slemmons, 1977) and theoretically (Kanamori and Anderson, 1975), it has been found that earthquake magnitude is proportional to the logarithm of the associated displacement of the fault on which the earthquake occurred. The slip rate on a particular fault is the integrated effect of all earthquakes and a seismic slip and is dominated by the individual displacements associated with the largest earthquakes to occur during the selected time period. Thus, these theoretical and empirical relationships and observations suggest that the logarithmic value of the slip-rate scales linearly with the size of the largest earthquakes associated with the slipping fault. Considering these observations, figure 2.5M-1 was constructed by plotting the geologic slip-rate data and the magnitudes of the largest historical events on these faults in a semi-log format of slip rate versus magnitude.

The pattern of historic earthquake data presented on figure 2.5M-1 indicates a trend of increasing largest earthquakes with increasing geologic slip rate and suggests that an upperbound limit may exist to the right of the data points. In order to test this observation, authoritative estimates of the magnitudes of the maximum design[a] earthquakes for four of the most extensively studied of the faults (San Andreas, San Jacinto, Calaveras and Hayward) were taken from the literature. These estimates, which are based on the empirical relationships between fault length and earthquake magnitude as summarized by Slemmons (1977) indicate maximum design earthquake magnitudes for the four faults are as follows[b]: San Andreas, M8-1/2; San Jacinto, M7-1/2; Calaveras, M7; and Hayward, M6-3/4 (figure 2.5M-2). The use of these accepted design earthquakes provides a logical means to extend the short historical seismicity record to represent the substantially longer time base required for conservative seismic design purposes. An envelope of those four points defines a line that is parallel to and slightly right of the largest historic magnitudes on figure 2.5M-1: the parallelism supports an approximately log-linear relationship between maximum magnitude and geologic slip rate for strike-slip faults in the magnitude range of 6 to 8. The position of the maximum earthquake line, slightly to the right of the empirical data, suggests a degree of conservatism that is appropriate for estimating the magnitudes of the maximum design earthquakes that may be associated with the faults represented on figure 2.5M-2.

This outer bounding line or limit was used to estimate the maximum earthquake magnitude for the Newport-Inglewood portion of the OZD. The slip rate of 0.5 mm/yr, previously calculated for the Newport-Inglewood portion, when entered into the graph, figure 2.5M-2, results in a maximum earthquake magnitude of about M6-1/2. The Newport-Inglewood portion is considered to conservatively represent the earthquake potential of the OZD. Therefore, the maximum earthquake magnitude that may be conservatively associated with OZD is M6-1/2.

a. The maximum earthquake considered likely to be generated by future displacement on a particular fault.
b. In order not to leave the impression of high accuracy, these estimates have been rounded to the nearest 1/4 magnitude unit.

APPENDIX 2.5M

2.5M.4 POSTULATED GROUND MOTION FOR MAXIMUM EARTHQUAKE ON OZD

Based on the estimated maximum earthquake magnitude of M6-1/2 as given in section 2.5M.3 above, the known local soil conditions at the San Onofre site and the regional tectonic setting, 56 earthquake records were selected to correspond closely to the conditions of the estimated maximum earthquake and analyzed to develop instrumental mean (average) and 84th percentile response spectra as shown in figure 2.5M-3. A response spectrum appropriate for design would of course be significantly below the 84th percentile instrumental spectrum which in turn is enveloped by the DBE response spectrum as shown in figure 2.5M-4. Therefore, the DBE response spectrum is an extremely conservative representation of the appropriate design response spectrum for the site.

The high level of conservatism of these results is further demonstratd by a comparison of the 84th percentile instrumental spectrum with the site specific results obtained by TERA (May 1978). These TERA results are based on modeling of a major earthquake postulated on the OZD, taking into account the crustal properties of the San Onofre site, and yield a response spectrum substantially lower than the 84th percentile response spectrum at all frequencies.

As indicated in the Woodward-Clyde (1979) report, the procedure used above to develop the maximum earthquake for the OZD makes use of the high quality data set available for the Newport-Inglewood portion of the OZD. For purposes of comparison and completeness, other characteristics of faulting were considered to develop an estimate of maximum earthquake including fault rupture length and maximum seismicity as discussed below. Although it is not intended to depend on such characteristics to determine maximum magnitude, because the data are of lesser quality, it is important to note that this type of consideration would lead to compatible results.

Of the entire 70-km length of the Newport-Inglewood portion of the OZD, the largest potentially connected fault segments extend about 36 km from Newport Beach to Signal Hill having a maximum single segment length of about 18 km. Considering that the rupture associated with the 1933 Long Beach earthquake (M6.3) extended to about 30 km in length (based on aftershock zone data, Woodward-Clyde Consultants, 1979), it appears reasonable that a full rupture of the 36 km zone (Newport Beach to Signal Hill) would yield a maximum earthquake of about M6-1/2.

A review of the seismicity of the area indicates a maximum historic magnitude of 6.3 (Long Beach, 1933). Considering the estimated slip for that event (Woodward-Clyde Consultants, 1979) of 31 to 46 cm, and the 1/2 mm per year slip rate, a recurrence interval of about 600 to 900 years can be calculated. Considering the total length of the OZD of about 240 km and the 30 km rupture length, it can be estimated that an earthquake in the range of M6.3 could occur every 70 to 100 years somewhere along the zone. Thus, it is reasonable that an earthquake has been observed along the OZD during historical time.

APPENDIX 2.5M

BIBLIOGRAPHY

1. Fugro, 1977, published Seismic Reflection Profiles

2. Kanamori, H. and Anderson, D. L., 1975, "Theoretical Basis of Some Empirical Relations in Seismology", Bulletin of the Seismological Society of America, v 65, pp. 1073-1095.

3. Marine Advisers, Inc., 1970, "Continuous Seismic Profiling Investigation of the Continental Slip Off San Onofre, California."

4. Slemmons, D. B., 1977 , "State-of-the-art for Assessing Earthquake Hazards in the United States, Report 6: Faults and Earthquake Magnitude," U.S. Army Corps of Engineers Miscellaneous Paper S-73-1, 129 pp.,

5. Tera, 1978, "Simulation of Earthquake Ground Motions"

6. Vedder, J. G., et al., "Preliminary Report on the Geology of the Continental Borderlands of Southern California," USGS MF-624.

7. Western Geophysical Co., 1972, "Fivac Report: San Onfore Offshore Investigation."

8. Woodward-Clyde Consultants, 1979, "Report of the Evaluation of Maximum Earthquake and Site Ground Motion Parameters Associated with the Offshore Zone of Deformation, San Onofre Nuclear Generating Station: prepared for Southern California Edison Company.

9. Woodward-Clyde Consultants, 1978, Unpublished Seismic Reflection Profiles developed for California Control Commission LNG Terminal Sites.

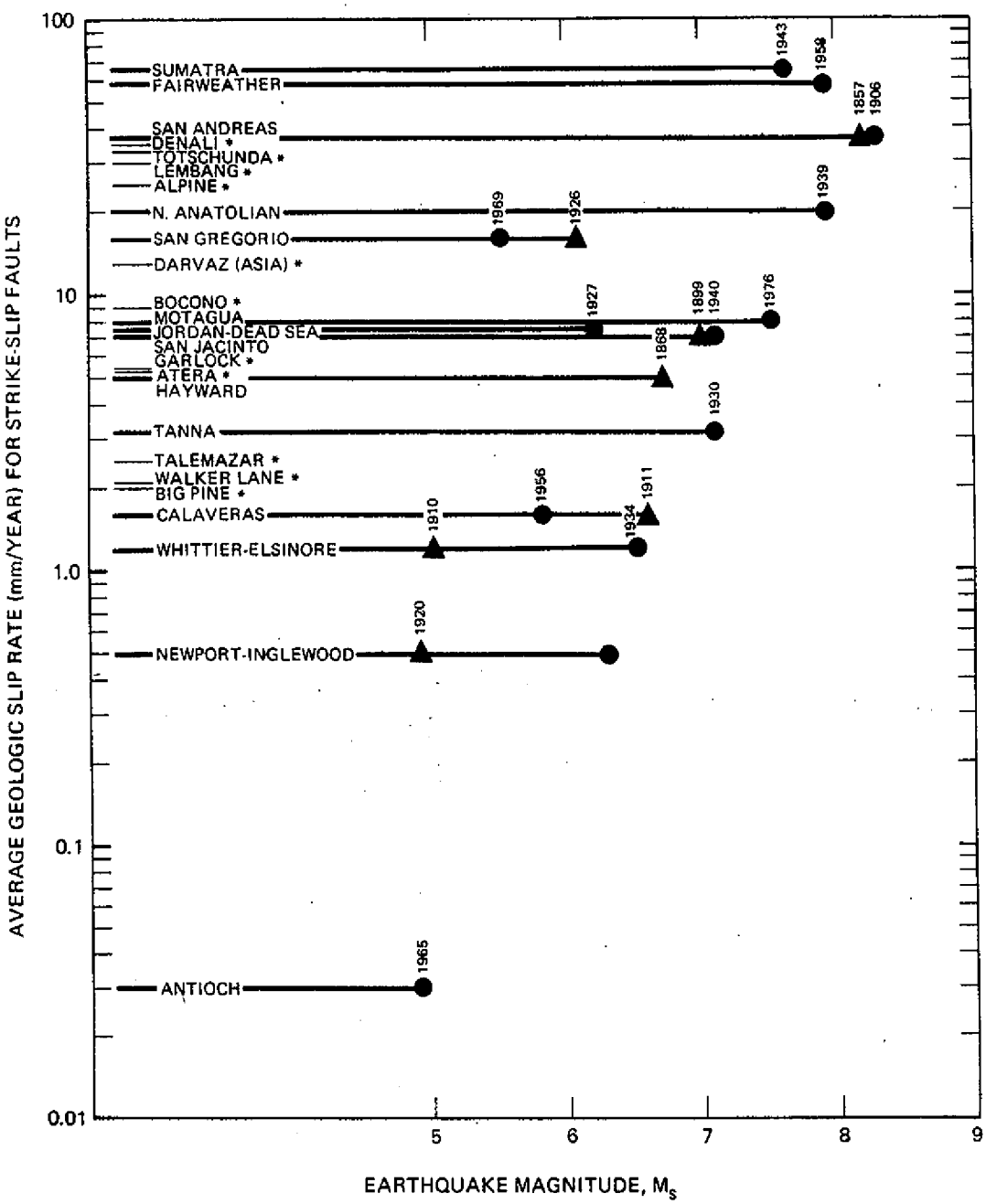

EXPLANATION

- ● Maximum instrumental recordings
- ▲ Maximum pre-instrumental estimates
- — Range over which smaller earthquakes occur
- * No associated large earthquake

Updated

SAN ONOFRE NUCLEAR GENERATING STATION Units 2 & 3
GEOLOGIC SLIP RATE vs HISTORIC MAGNITUDE FOR STRIKE-SLIP FAULTS
Figure 2.5M-1

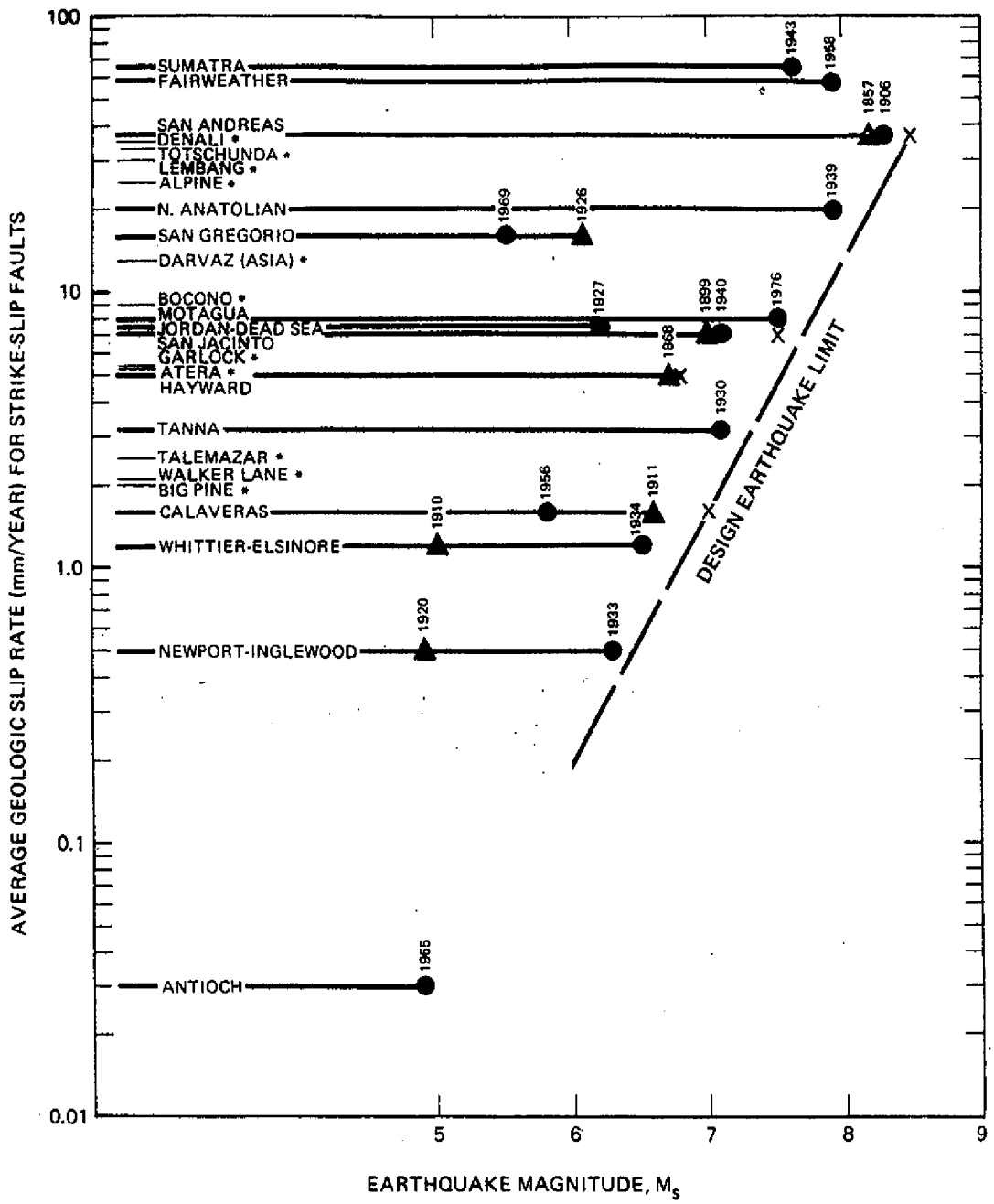

EXPLANATION

- ● Maximum instrumental recordings
- ▲ Maximum pre-instrumental estimates
- — Range over which smaller earthquakes occur
- • No associated large earthquake
- X Maximum design earthquake

Updated

SAN ONOFRE NUCLEAR GENERATING STATION Units 2 & 3

GEOLOGIC SLIP RATE vs MAGNITUDE SHOWING DESIGN EARTHQUAKE LIMIT FOR STRIKE-SLIP FAULTS

Figure 2.5M-2

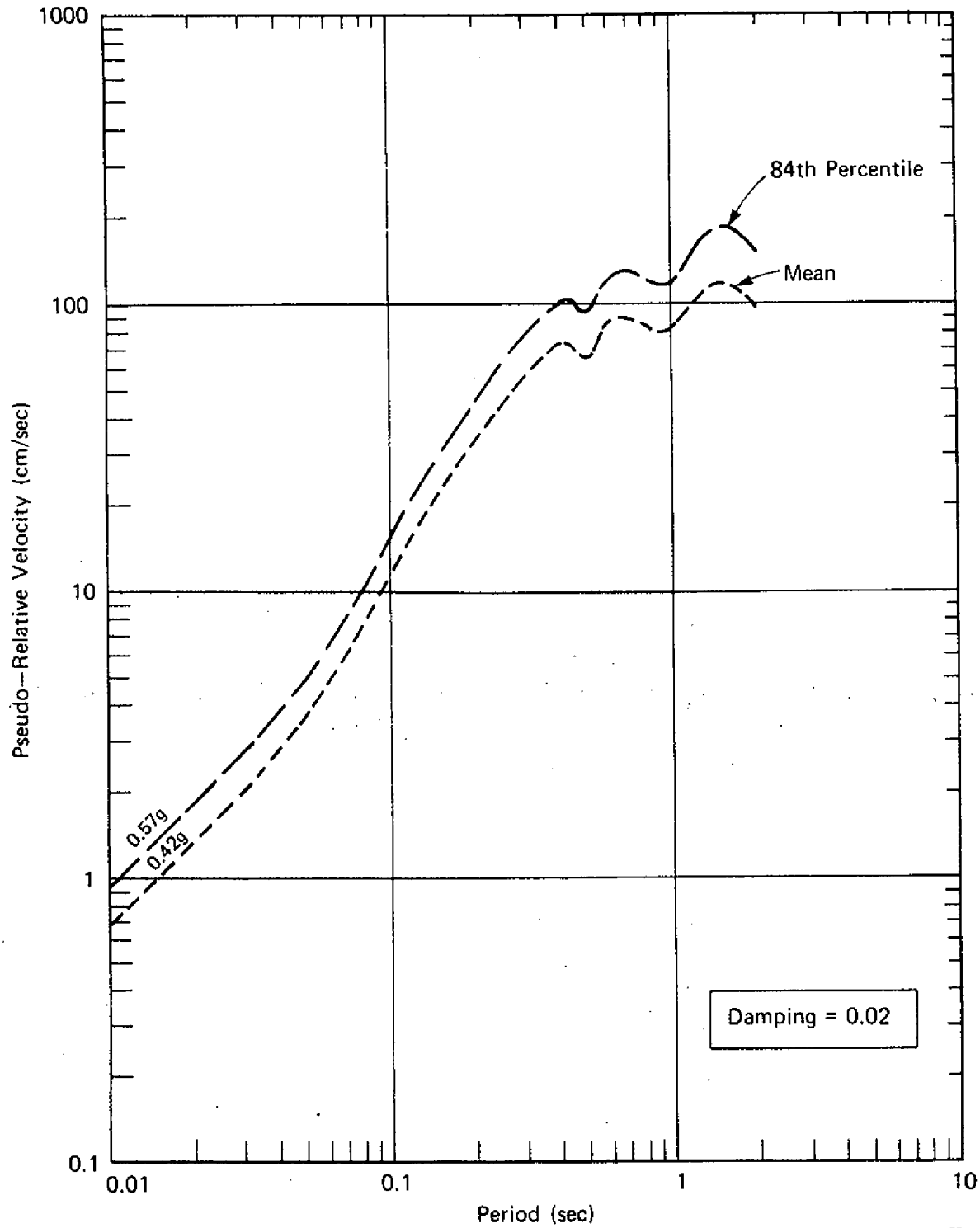

Updated

SAN ONOFRE NUCLEAR GENERATING STATION Units 2 & 3
EMPIRICALLY DERIVED MEAN AND 84TH PERCENTILE SPECTRA, MAGNITUDE ≈ 6.5, DISTANCE = 10 km
Figure 2.5M-3

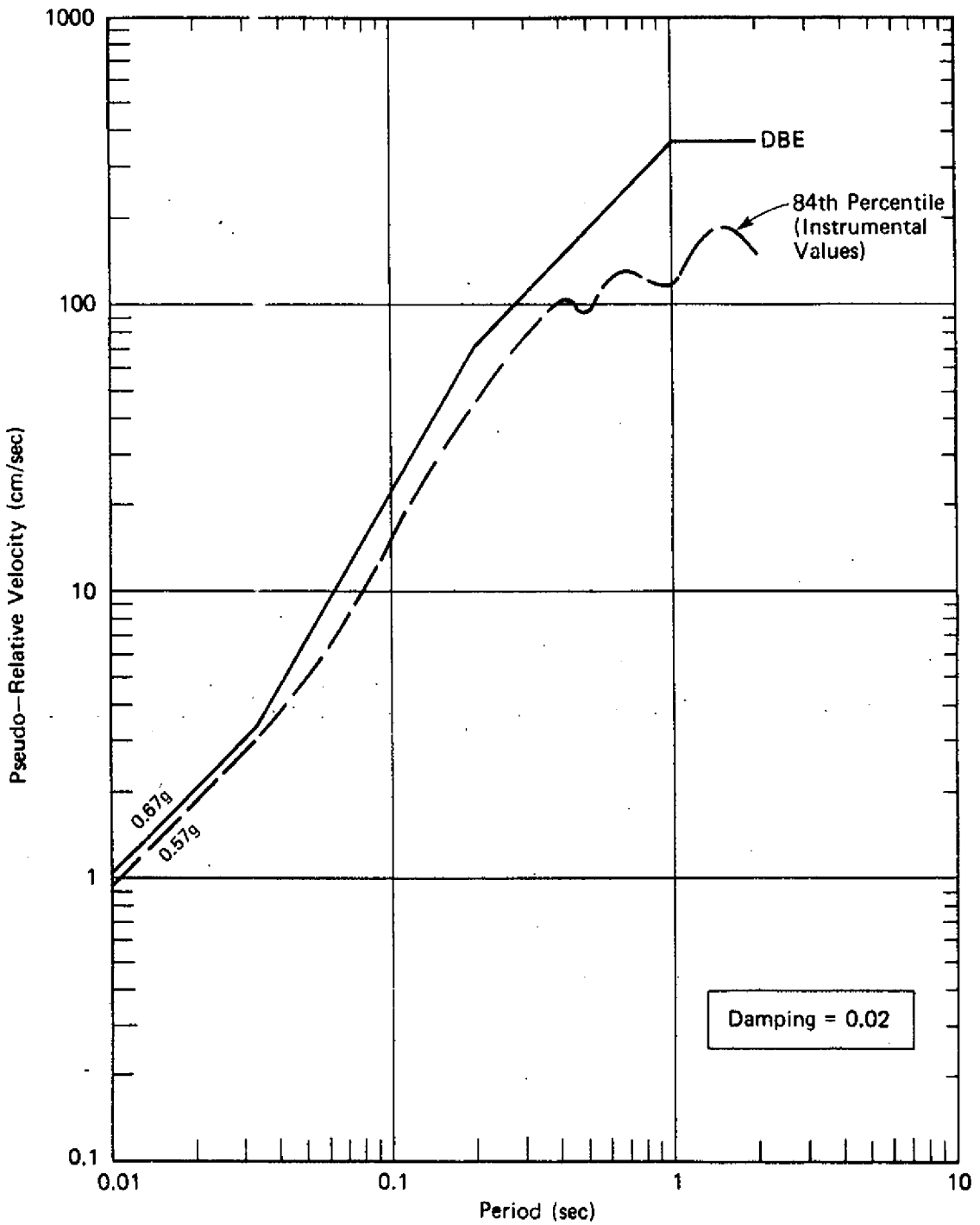

Updated

SAN ONOFRE NUCLEAR GENERATING STATION Units 2 & 3
COMPARISON OF 84TH PERCENTILE INSTRUMENTAL SPECTRUM WITH SAN ONOFRE DBE SPECTRUM
Figure 2.5M-4

APPENDIX 2.5N

Site File Copy

APPENDIX 2.5N

2.5N.1

Ben-Menahem and others (1976, p 21) state: "The estimates of the average rate of slip vary from 0.65 cm/year (Freund, et al., 1970) to 1.0 cm/yr for the past 3 to 4 million years (Girdler, 1958)." Neither the 1.0 cm/yr rate nor any other rate of slip can be found in Girdler (1958). It appears that the citation of Girdler (1958) by Ben-Menahem and others is either incorrect or unfounded, or that the authors are inferring something from Girdler's paper that is not inherently obvious to the reader. The 1.0 cm/yr rate is not substantiated by the available data. The 0.65 cm/yr rate of slip for the Jordan-Dead Sea fault can be found in Freund and others (1970).

For the empirical plot of slip rate versus magnitude (Woodward-Clyde Consultants, June 1979, Figures 6 and 7), the selected rate value was chosen as 7.5 mm/yr; this value was based on Quaternary displacements along the Jordan-Dead Sea fault (Zak and Freund, 1966). In 1970, Freund and others (1970) presented a range of slip rate values from 3.5 mm/yr to 6.0 mm/yr for the 40 to 45-km displacements during the past 7 to 12 million years. In the same paper, the Quaternary rate of 6.5 mm/yr is given, revising the age given in the Zak and Freund (1966) paper. This range of 3.5 to 6.5 mm/yr from Freund and others (1970) is the selected data range and is used in the revised slip rate/maximum-magnitude data base documented in appendix 2.5M, section 2.5M.5. The range of values provided by Ben-Menahem and others (1976) is not considered because confirmation of the higher rate of slip cited in the paper is lacking.

The pre-instrument earthquakes associated with the Jordan-Dead Sea fault are listed in Ben-Menahem and others (1976, p 46). During a 2000-year time span from 117 BC to 1956 AD, 40 earthquakes occurred in the estimated range of 5 to 7 magnitude. Of those earthquakes only the ones which occurred in 1546 and 1927 have specific magnitude assignments. The 1927 earthquake was assigned magnitude 6.2 (Ben-Menahem and others, 1976, Table III, p 8); the 1546 earthquake was assigned magnitude 6.5 on the basis of a comparison of it with the 1927 earthquake. Because the event of 1546 and other early events occurred so long ago, assignment of Richter magnitude is purely speculative and the confidence in these data is low enough to exclude them from comparison with more readily verifiable earthquake magnitudes on other faults of the world. Therefore, to maintain the quality and integrity of the data being used in the slip rate/maximum-magnitude data base, magnitude estimates of the early events on the Jordan-Dead Sea fault have not been included. The 1927 magnitude 6.2 earthquake on the Jordan-Dead Sea fault is included in the data base, as documented in appendix 2.5S, section 2.5S.5.

Amended: April 2009 TL: E048000

2.5N.2

The Bocono fault was first discussed in the literature by Rod (1956), who recognized it as one of the most important structural features of the Venezuelan Andes and the only major Venezuelan strike-slip fault for which the relative horizontal displacement could be directly measured. Mencher (1963) has suggested that the Bocono fault may have originated as a series of normal faults that later coalesced into a right-lateral system. Dewey (1972) has suggested that the Bocono fault represents a portion of the plate boundary between the Carribean plate and the South American plate and that, because of the northeast-trend of the fault, the net slip on the fault could be right-reverse oblique slip. However, displaced Pleistocene glacial moraines in the Paramo de Muchuchies clearly show that the dominant displacement over the past 10,000 years has been right-slip (Rod, 1956; Schubert and Sifontes, 1970; Woodward-Clyde and Associates, 1969). A review of the data presented by these authors indicates a slip rate of 8 to 10 mm/yr for the past 10,000 years, with an estimate of 9.75 mm/yr based on a measured displacement of glacial moraine of 320 ft (97.5 m).

Woodward-Clyde and Associates (1969) also provide an estimate of the magnitude of the 1812 earthquake, which they believe is the largest event on the Bocono fault in historical time. They estimate a Richter magnitude of from 7-3/4 to 8-1/4 and use 8 as an average. This estimate has been used in conjunction with the estimated slip rate to provide an additional data point for the slip rate/maximum-magnitude data base as documented in section 2.5S.5. However, the magnitude is only an estimate of an event that occurred approximately 168 years ago and is therefore speculative.

2.5N.3

The West Wairarapa fault in New Zealand has been added to the slip rate/ maximum-magnitude data base, as documented in section 2.5S.5 and discussed below.

The slip rate for the West Wairarapa fault was developed from the cumulative displacements of the offset Waiohine River Terrace Sequence. The faulting of these terrace sequences has been discussed by Lensen (1973) and by Lensen and Vella (1971) and is summarized in Figures 14 and 21 of Lensen's Guidebook (1973). The units of measure for the displacements listed in Figure 14 of Lensen's Guidebook (1973) are not clearly labeled. However, a close comparison of the units used for displacement of the Waiohine Terraces in Figure 11, in the graph of Figure 21, and in the text of the guidebook reveals that the values listed for cumulative displacements in Figure 14 are in feet. The range of total cumulative displacements reported by Lensen (1973) for the Waiohine River Terrraces is 329 to 389 feet (100 to 118 meters). This wide range results from uncertainties in the amount of the initial displacement of the oldest displaced terrace (Waiohine surface).

The age of Waiohine surface has not been definitely established. The problems in the age estimates result from uncertainties in the correlation of the Waiohine surface either with an earlier glacial advance in the Otira Glacial stage (35,000 years before Pleistocene) or with the latest principal glacial advance in the Otira Glacial stage (20,000 years before Pleistocene). The ages of these glacial advances are supported by radiocarbon dates obtained in other regions of New Zealand (Lensen, 1973; Suggate, 1963; Vella, 1963).

Calculated slip rates from the data in Table 14 of Lensen's Guidebook (1973) range from 2.9 to 6 mm/yr. The slip rate range was extended to 6.6 mm/yr because Suggate and Lensen (1973) have suggested 18,000 years before Pleistocene may be the youngest age for the latest principal glacial advance in the Otira Glacial stage in New Zealand. An average slip rate of 4.8 mm/yr is considered the best selected value. However, the processes of lateral erosion during the time of formation of the Waiohine River terraces most likely resulted in apparent terrace displacements smaller than the displacement values that actually occurred; thus, the displacement values and the calculated slip rates should be considered as minimum values.

The largest earthquake known to have occurred on the West Wairarapa fault was in 1855. Slemmons (1977) estimated a magnitude 8 for this earthquake; however, there is no direct evidence available for establishing a magnitude. No New Zealand literature publishes a magnitude estimate for this earthquake. Although surface rupture of the West Wairarapa fault was reported, no measurements of the amount of displacement that occurred during the earthquake were obtained. The comparison of isoseismals of the 1855 event and the 1929 event is made in figure 2.5N.1. Clark and others (1965) provided estimated isoseismal contours, using both Modified Mercalli and Rossi-Forel scales, for the 1855 earthquake (figure 2.5N-1). Modified Mercalli isoseismals contours were also presented by Clark and others (1965) for the 1929 West Nelson (magnitude 7.6) earthquake, the first large instrument-recorded earthquake in New Zealand (Richter, 1958). However, caution must be exercised when comparing equivalent Modified Mercalli isoseismals of these two earthquakes because (1) the delineation of intensity isoseismal contours is based on subjective judgments and (2) the earthquakes occurred in two separate regions of New Zealand on two different faults.

A comparison of areas covered by the Modified Mercalli isoseismals presented by Clark and others (1965) for the 1855 earthquake and the 1929 earthquake shows they are very similar. It should be noted here that the Rossi-Forel scale isoseismals for the 1855 earthquake are much larger than the Modified Mercalli isoseismals and that different scales should not be compared to one another. Thus a reasonable assessment of Clark's data would be that the 1855 earthquake was similar in size to the 1929 earthquake (magnitude 7.6). For this reason a value of M_S 7.6 was used in the slip rate/maximum-magnitude data base as documented in section 2.5S.5.

2.5N.4

Subsequent to the publication of Schwartz and others (1979), new field data (Schwartz, personal communication, 1979) suggest that the low slip rate value of 1.5 mm/yr presented in the publication is not valid and therefore it is not presented in the slip rate versus maximum-magnitude analysis. Thus, the 6 mm/yr rate on the Motagua fault is the only value presented to represent the fault. The 10 mm/yr rate presented in the June 1979 report was based on preliminary data and is supported by recent data.

2.5N.5

The 3.2 mm/yr value of slip rate on the Tanna fault reported in the WCC June 1979 report was subsequently revised to 1.5 to 2.5 mm/yr on the basis of a review of Matsuda (1977) and a recent personal communication with Matsuda (December 1979). Though this revised data point is accommodated by the slip rate/maximum-magnitude relationship shown in figure 2.5R-7, the Japanese data have been deleted from the data base.

2.5N.6

The Kopet-Dagh fault zone is included in the slip rate/maxium-magnitude data base as documented in section 2.5S.5. Data provided by Trifonov (1971 and 1978), and Krymus and Lykov (1969) indicate a possible range of slip rate values for the Kopet-Dagh fault zone between 3.6 mm/yr and 8 mm/yr. The Quaternary data were reviewed for slip rate values and, on the basis of the criteria in section 2.5S.5, the 3.6 mm/yr value has been selected as a representative slip rate (Trifonov, 1978).

The 1948 Ashkhabad earthquake is attributed to the Kopet-Dagh fault. Various station estimates of magnitude for the earthquake range from 6.5 to 7.5 (Louderback, 1949). Gutenberg and Richter (1954) cited a magnitude of 7.3. In general, most magnitudes are in the 7.0 to 7.3 range. The 7.3 magnitude is an average of several stations and is thus representative.

2.5N.7

Herd (1978) estimates that the present slip rate on the Calaveras-Paicines fault (the southern section of the Calaveras fault, south of the junction with the Hayward fault) is from 12 to 15 mm/yr based on the difference in apparent long-term slip rate on the San Andreas fault north and south of the Calaveras branch. This rate appears to be consistent with modern-day creep but is not based on direct geologic data. Prowell (1974) estimates a rate of 5 mm/yr from mid-Pliocene to the present based on tentative correlations of volcanic rock terrains. Thus, a range from 5 mm/yr to 15 mm/yr seems reasonable for this southern segment of the fault. Herd states that the slip rate is at least 12 mm/yr.

To the north, the slip of 12 to 15 mm/yr is apportioned between the Hayward and Calaveras-Sunol faults. Herd (1978) suggests that this apportionment should be about equally divided considering the similar creep measurements of 6 mm/yr on both faults. These slip rates, though not based on geologic correlations, appear reasonable. Prowell (1974) displaced volcanic rocks of approximately 8 mm/yr. Based on similar volcanic rock displacements, he calculates a slip rate of 5 to 5.5 mm/yr for the Hayward fault. Both sets of data are considered together and are included in the slip rate/maximum-magnitude data base, as documented in section 2.5S.5.

2.5N.8

New data on possible slip rates along the San Jacinto fault have been discussed with Robert V. Sharp (December 1979) and are presented in the most recent U.S. Geological Survey volume of Summaries of Technical Reports (Sharp, 1980). Sharp gives estimates of strike-slip displacements of strata and possible slip rates for three areas along the fault, one on the main trace or Casa Loma-Clark segment and two on the Coyote Creek segment. This recent work is summarized below.

Sharp (1980) reports minimum horizontal offsets of Pleistocene gravels of between 5.7 and 8.6 km on the Casa Loma-Clark segment. He states that these units have been offset since 730,000 years before Pleistocene and calculates a slip rate of 8-12 mm/yr. This is a slight increase from the minimum rate of 7.1 mm/yr quoted earlier by Sharp (1978).

Sharp presents two estimates of Holocene displacements based on trenching studies of stratigraphic offsets on the Coyote Creek fault. For one of these estimates, Sharp (1980) uses data from Clark and others (1972) to develop a horizontal slip of 1.7 meters; this value is based on measured vertical offsets and on a vertical to horizontal offset ratio derived from measurements taken following the 1968 Borrego Mountain earthquake. Sharp (1980) uses this estimate of displacement for the "youngest sediment" of Lake Cahuilla since its deposition 283 to 478 years before Pleistocene. The corresponding slip rate is between 3 and 5 mm/yr but is suspect because it is not based on actual measurement of strike-slip offset.

At another trench site on the Coyote Creek fault, Sharp (1980) cites 10.9 meters of right-slip of buried stream channel older than 5000 years before Pleistocene but younger than 6800 years before Pleistocene. He states that using an intermediate time period of 5400± to 6000± years before Pleistocene gives an estimated slip rate of 1 to 2 mm/yr (however, calculations based on the quoted numbers actually give 1.8 to 2.0 mm/yr).

Sharp (1980) goes on to conclude that the average rates of slip for these three time intervals indicate a major relatively quiescent period for the San Jacinto fault zone from about 4000 BC to about 1600 AD. The applicants find this conclusion hard to support because Sharp's analysis looks at only

two segments of the fault zone. The variations in slip rates due to low rates for the Coyote Creek fault could well be explained by apportionment of the total zone slip to adjacent known and suspected segments of the San Jacinto fault zone, whereas Sharp's data presented above the Casa Loma-Clark fault appear to represent movement on a major segment of the zone and have been considered as representative of the total fault zone potential. The lower slip rate, calculated for the Coyote Creek fault segment alone, has been used in conjunction with the magnitude 6.7 Borrego Mountain earthquake of 1968 in preparing the slip rate/maximum-magnitude relationship. Both of these data sets are included in the slip rate/maximum-magnitude data base, as documented in section 2.5S.5.

2.5N.9

The central section of the San Andreas fault from Cholame to Cajon Pass has been considered separately for the slip rate/maximum-magnitude comparison; this separate consideration was considered appropriate because abundant data are available to estimate the late Holocene slip rate and maximum historical earthquake. Sieh's (1978) data are reasonable and are the best available (i.e., a slip rate of 34 to 41 mm/yr with the best estimate being 37 mm/yr and M_s approximately equal to 8.25 for the 1857, Fort Tejon earthquake). These figures are used in the slip rate/maximum-magnitude data base documented in section 2.5S.3.

2.5N.10

The northern section of the San Andreas fault from Hollister to Cape Mendocino has also been considered separately for comparison purposes. The most recent and perhaps best summary of the slip rate on this section of the fault is presented by Herd (1978) in which he selects 20 mm/yr as the most reasonable rate. This figure has been used in the slip rate/maximum-magnitude data base, as documented in section 2.5S.3.

2.5N.11

The strike-slip displacement and resulting slip rate reported for the Rose Canyon fault in California Division of Mines and Geology (CDMG) Special Report 123 are based on the distribution of the San Diego Formation along the fault and on the Z-shaped bend in the coastline where the fault crosses it at La Jolla Bay. The observational data needed to evaluate the validity of these proposed offsets are not provided in Special Report 123, but they have been published by Kennedy (1975) in CDMG Bulletin 200 and by Moore and Kennedy (1975) in the USGS Journal of Research (vol. 3, pp 589-595). In addition, Kern (1977) has published data on the displacement and slip rate of the Rose Canyon fault based on his correlation and projection of Late Pleistocene marine terraces in the La Jolla area.

Each of the proposed offsets and resulting slip rates is discussed below and is shown to be based on speculative assumptions which are either incorrect or unsupportable. Although the available data provide no unique geologic line which can be used as piercing points for the precise determination of net slip along the Rose Canyon fault, geologic relationships discussed below indicate that the displacement is dominantly dip-slip with little or no strike-slip displacement.

Data pertaining to the published displacements and slip rates cited are discussed in order from the largest to the smallest proposed displacements. Figure 2.5N-2 is a generalized geologic map of the San Diego area and the Rose Canyon fault showing the published displacements.

2.5N.11.1

Moore and Kennedy (1975, p 593) state that: "The north edge of the San Diego basin has been offset 6 km right laterally as marked by the Eocene-Pliocene unconformity at Mission Bay" (Kennedy and Moore, 1971), figure 2.5N-2. Referring to the same feature, Kennedy (1975, p 36) states that: "The distribution of the San Diego Formation along the Rose Canyon fault zone between Pacific Beach and Tecolote Canyon is interpreted as resulting from 4 km of right-lateral strike-slip motion on the Rose Canyon fault."

The above proposed offsets of 6 and 4 km are based on the assumption that the line formed by the pinching out of the Late Pliocene San Diego Formation beneath the Pleistocene Lindavista Formation was originally east-west trending and that the pinch-out line on Mount Soledad west of the fault originated opposite the pinch-out line located east of the fault, near the San Diego River, figure 2.5N-2 (Kennedy and Moore, 1971). The cited offsets have different magnitudes because Moore and Kennedy (1975) obtained theirs from a generalized geologic map which shows the San Diego Formation as pinching out on the southside of the San Diego River, whereas Kennedy (1975) based his offset on an occurrence of the San Diego Formation on the ridge along the north side of the San Diego River.

Both of the proposed offsets have questionable validity because the basic premise of an east-west pinch-out line on each side of the fault is incorrect. As mapped by Kennedy (1975), the San Diego Formation pinches out toward the east and thickens toward the west in the vicinity of the San Diego River east of the Rose Canyon fault and pinches out toward the north and thickens toward the south on Mt. Soledad, west of the fault. If on the east side of the fault, a straight line were extended from the pinch-out point south of the river through the pinch-out line north of the river, the line would project about N25W, that is, subparallel to the Rose Canyon fault, thus nullifying its use as a piercing point for offset determination. The actual pinch-out line probably followed a curved path which crossed the Rose Canyon fault near the mouth of the Rose Canyon fault and lapped onto Mount Soledad (see figure 2.5N-2). The observed relationship can be explained without any lateral displacement on the Rose Canyon fault as pointed out by Threet (1979).

The offset correlation is also questioned because the San Diego Formation resets on different formations at the presumed "match points" for the pinch-out line on opposite sides of the fault. West of the fault on Mount Soledad it overlies the Eocene Ardath Shale, whereas east of the fault at the "match points" it overlies the Eocene Scripps Formation on the ridge north of the San Diego River and the Eocene Mission Valley Formation on the ridge south of the river; thus the correlation cannot be reconciled.

Therefore, the published right-lateral displacements of 6 and 4 km are invalid and do not represent a reasonable interpretation of the available data.

2.5N.11.2

Moore and Kennedy (1975, p 593) state that: "The 200-meter depth contour has been offset about 4 km right laterally where the fault zone passes out to sea near Point La Jolla."

This refers to the fact that the continental shelf offshore from La Jolla is broader and extends farther seaward west of the Rose Canyon fault than east of the fault. Differential vertical uplift provides a more logical explanation for the observed relationship than does right slip on the Rose Canyon fault.

The west side of the Rose Canyon fault has been uplifted relative to the east side as demonstrated by the exposure of Late Cretaceous formations on Mount Soledad and along the coast west of the fault, whereas the oldest formations exposed east of the fault are of Eocene age. The amount of uplift west of the fault increases in a westward direction as shown by the eastward dip of Cretaceous strata exposed along the coast. Thus, the broad continental shelf west of the fault was probably formed by the combined effects of tectonic uplift and marine planation during low stands of sea level. To explain it by strike-slip displacement on the Rose Canyon fault is an unreasonable interpretation of available data, as pointed out by Threet (1979).

2.5N.11.3

"The coast on opposite sides of the fault zone where it passes out to sea near Point La Jolla has rocks of similar resistance to erosion and a similar structural elevation of the Lindavista Formation. The southwestward coast has been moved seaward right laterally 1 km to form the point." (Moore and Kennedy, 1975, p 593).

This statement and a similar but less explicit statement by Kennedy and others (1975, p 8) are based on the same reasoning as the one dealing with the 200-meter subsea contour. In essence, Moore and Kennedy (1975) believe that the coast juts out along the south side of La Jolla Bay because of right slip on the Rose Canyon fault. It is more reasonable

to explain the bend in the coast by greater uplift on the south side of the bay. This uplift is indicated by exposures of Cretaceous strata there, whereas only Eocene strata are exposed on the north side of the bay.

Moore and Kennedy (1975) seem to rule out vertical uplift by inferring that the base of the Pleistocene Lindavista Formation is at the same altitude on either side of the fault in this area. Although the base of the Lindavista Formation east of the fault is broadly planar and nearly horizontal, it is not so on Mt. Soledad. On Mt. Soledad the base occurs instead as a series of wave-cut terraces, and, consequently, it is not a reliable reference for measuring deformation.

2.5N.11.4

In reference to relationships across the projection of the Rose Canyon fault in the vicinity of La Jolla Bay, Kern (1977, p 1, 563) interprets the Nestor terrace shoreline angle to be offset approximately 150 meters right laterally and 55 meters vertically (with the east side up) within the past 120,000 years. This yields an average displacement rate of 1.25 mm/yr right slip and 0.46 mm/yr vertical slip.

The vertical component of the above offset depends upon correlation of the same shoreline angle on opposite sides of the fault. The lateral component not only depends on the proper correlation of shoreline angles but also requires the proper projection of the shoreline angle to the fault trace.

There is a gap of about 2 km on the east side of the fault where the shoreline angle is concealed. A field examination of exposures in this area suggests that Kern (1977) has erred in his correlation of terraces. As mapped and correlated by Kern (1977, Figures 2, 5, and 7), the shoreline angles of the Bird Rock and Nestor terraces rise in altitude as they aproach the Rose Canyon fault from the south. An examination of exposures in this area leads to the alternate conclusion that the terraces do not experience significant uplift as they approach the Rose Canyon fault. Instead, there appear to be several discrete wave-cut benches arranged in stair-step fashion.

Along the coast extending eastward from Point La Jolla, the lowest benches have been removed by subsequent erosional undercutting along the present beach. Extending for a distance of several kilometers southward from Point La Jolla, there are numerous remnants of a wave-cut bench at an elevation of about 10 meters above sea level. Kern correlates this bench with the Bird Rock terrace along the southern part of the coast, but he maps the Bird Rock terrace as rising along the northern part of the coast. However, exposures are poor in this area because the ground is covered by roads and buildings of the La Jolla metropolitan area and by Quaternary sediments concealing the erosion surface at the base of this terrace. In this location, Kern (1977) appears to consider the entire terrace to be underlain by a single wave-cut bench of the Nestor terrace;

however, a field examination suggests that the terrace includes at least two, and probably more, discrete wave-cut benches as suggested by breaks in slopes along the streets within the area and by exposures in the sea cliffs east of Point La Jolla. As interpreted here, the Bird Rock terrace and its shoreline angle extend about 300 meters east from Point La Jolla but have been removed by coastal erosion farther to the east. Furthermore, a terrace exposed on Goldfish Point appears to be the Nestor terrace, not the Bird Rock terrace as mapped by Kern (1977). Its shoreline angle is exposed at an estimated elevation of 15 to 20 meters above sea level in the cliff east of Goldfish Point. Farther east is a higher terrace; the shoreline angle of this terrace does not appear to be exposed. It is on this higher terrace that Kern (1977, Figure 2) located a shoreline angle at 60 meters above sea level which he correlates with the Nestor terrace.

In the area northeast of the Rose Canyon fault only one terrace is exposed below the elevation of the Lindavista terrace. The shoreline angle of this terrace crops out about 5 meters above sea level in the sea cliff, a short distance north of the Scripps Institute pier. The shoreline angle trends southward into the cliff and the wave-cut platform dips westward. The platform has a relatively steep dip adjacent to the shoreline angle where it is armored by sandstone blocks from the adjacent bluff. The dip of the platform flattens and the armor diminishes in exposures toward the south. Kern (1977, Figure 2, pp 1563) tentatively correlates this terrace with the Nestor terrace but considers that it might instead be the Bird Rock terrace. He projects the shoreline angle inland toward the Rose Canyon fault essentially along the contact between the Pleistocene Bay Point Formation and the Eocene bedrock, as mapped by Kennedy (1975). This forms the basis for his estimate of the amount of displacement on the Rose Canyon fault during the past 120,000 years (the age of the Nestor terrace). However, Kern's correlation of the terraces and his projection of the shoreline angle appear to be incorrect.

In order for the 5-meter terrace exposed near the Scripps Institute pier to be the Nestor terrace, it would have to have been downwarped about 15 meters along the east side of the Rose Canyon fault; however, there is no evidence for downwarping in either the Eocene bedrock or the base of the Lindavista terrace. The Eocene bedrock dips toward the northeast away from the fault. This suggests uplift near the fault rather than downwarping. The platform at the base of the Lindavista Formation is at an altitude of about 100 meters where it is exposed in the bluffs inland from La Jolla Bay to the east of Rose Canyon fault. The base of the Lindavista Formation remains at a nearly constant altitude for at least 14 km northwestward along the coast. This indicates that no significant warping has occurred in this area since the formation of the Lindavista platform. In this area, the Lindavista platform is at essentially the same elevation as at Point Loma where terrace relationships are well-known and where the Nestor shoreline angle is at 20 meters and the Bird Rock shoreline angle is at 8 meters. Consequently, the 5-meter terrace at Scripps Institute is more likely to correlate with the Bird Rock terrace; however, there is no compelling reason to correlate it with either the Bird Rock or Nestor terraces.

The 5-meter terrace at Scripps Institute has a different origin than most of the terraces elsewhere along the coast. It was formed in a coastal embayment, the La Jolla embayment, rather than along a straight coastline. The embayment appears to result from the erosion of a canyon along the north side of the Mount Soledad uplift and is probably a landward extension of the La Jolla submarine canyon. It may have been eroded in a submarine environment during early or middle Pleistocene by sluicing of sand banked against the Mt. Soledad headland, or it may be a product of normal stream erosion. In either case, its configuration suggests that it was formed by processes other than wave erosion. It has an analogous origin to estuaries which occur elsewhere along the present coast. During early stages of submergence associated with a rise in sea level, the shoreline would conform to an altitude contour along the side of the partially submerged canyon without regard to the shape of the contours. With time, longshore drift would build a smoothly curving bar across the mouth of the canyon and leave a lagoon behind the bar. Carter (1957, pp 217-254) presents evidence documenting such an origin for the La Jolla embayment. Kern (1977) seems to assume implicitly that the embayment was cut exclusively by wave erosion simultaneous with a gradual offsetting of the coastline by right slip along the Rose Canyon fault. Kern's projection of the 5-meter shoreline angle is at best an indication of the degree to which the coast was embayed during its formation. It is not a measure of fault offset.

In summary, there is no compelling evidence for strike-slip displacement on the Rose Canyon fault. None of the published data on the magnitude and rate of horizontal displacement are valid. Efforts to establish valid measures of slip have been frustrated by the inability to locate points at which unique geologic lines cross the fault. It is clear that dip-slip displacement has occurred along the fault with the amount varying along the trace because formations east of the fault are essentially horizontal whereas those to the west are folded. Accordingly, the slip rate developed in CDMG 123 has not been included in the slip rate/maximum-magnitude analysis.

BIBLIOGRAPHY

1. Ben-Menahem, A., Nur, A. and Vered, M., 1976, Tectonics, seismicity and structure of the Afro-Eurasian junction--The breaking of an incoherent plate: Physics of the Earth and Planetary Interiors, v. 12, p. 1-50.

2. Carter, G. F., 1957, Pleistocene Man at San Diego: Baltimore, John Hopkins Press, 400 p.

3. Clark, M. M., Grantz, A., and Rubin, M., 1972, Holocene activity of the Coyote Creek Fault as recorded in sediments of Lake Cahuilla, in The Borrego Mountain Earthquake of April 9, 1968: U.S. Geological Survey Professional Paper 787, pp. 112-130.

4. Clark, R. H. Dibble, R. R., Fyfe, H. E., Lensen, G. J., and Suggate, R. P., 1965, Tectonic and earthquake risk zoning: Royal Society of New Zealand, Transactions, general, v. I, no. 10, p. 113-126.

5. Dewey, J. W., 1972, Seismicity and tectonics of Western Venezuela: Seismological Society of American Bulletin, v. 62, no. 6, p. 1711-1751.

6. Euge, K. M. and Miller, D. S., 1973, Evidence for a possible onshore Extension of the Rose Canyon fault in the vicinity of Oceanside, California: Geological Society of America, Abstracts with Programs, v. 5, no. 1, 39 p.

7. Freund, R., Garfunkel, Z., Zak, I., Goldberg, M., Weissbrod, T., and Derin, B., 1970, The shear along the Dead Sea rift: Philosophical Transactions, Royal Society of London, Series A, v. 267, p. 107-130.

8. Gastil, R. G., Phillips, R. P., and Allison, E. C., 1975, Reconnaissance geology of the state of Baja California: Geological Society of America Memoir 140, 170 p.

9. Gastil, R. G., Kies, R., and Melins, D. J., 1979, Active and potentially active faults--San Diego County and northernmost Baja California in Abbott, P. L., and Elliott, W. J., eds., Earthquakes and other perils, San Diego region, p. 47-60.

10. Girdler, R. W., 1958, The relationship of the Red Sea to the East Africa rift system: Quarterly Journal of the Geological Society of London, v. 114, p. 79-115.

11. Gutenberg, B. and Richter, C. F., 1954, Seismicity of the Earth and Associated Phenomena: Hafner Publishing Company, New York and London, reprinted 1965, 310 p.

12. Herd, D. G., 1978, Neotectonic framework of central coastal California and its implications to microzonation of the San Francisco Bay region, in Second International Conference on Microzonation for Safer Construction--Research and Application, Proceedings, v. 1, p. 231-240.

13. Kennedy, M. P., 1975, Del Mar, La Jolla, and Point Loma Quadrangles, western San Diego metropolitan area, California: California Division of Mines and Geology Bulletin 200A, p. 9-39.

14. Kennedy, M. P., Bailey, K. A., Greene, H. G., and Clark, S. H., 1978, Recency and character of faulting offshore from metropolitan San Diego, California: California Division of Mines and Geology Final Technical report.

15. Kennedy, M. P. and Moore, G. W., 1971, Stratigraphic relationship of upper Cretaceous Eocene formations, San Diego coastal area, California: American Association of Petroleum Geologists Bulletin, v. 55, no. 5, p. 709-722.

16. Kennedy, M. P., Tan, S. S., Chapman, R. R., and Chase, G. W., 1975, Character and recency of faulting, San Diego metropolitan area, California: California Division of Mines and Geology Special Report 123.

17. Kern, J. P., 1977, Origin and history of upper Pleistocene marine terraces, San Diego, California: Geological Society of America Bulletin, v. 88, p. 1553-1566.

18. Krymus, V. N. and Lykov, V. I., 1969, The character of the junction of the Epi-Hercynian platform and the Alpine folded belt, south Turkmenia; Geotectonics, Academy of Science, U.S.S.R., translated by the American Geophysical Union, v. 6, p. 391-396.

19. Legg, M. R. and Kennedy, M. P., 1979, Faulting offshore San Diego and northern Baja California, in Abbott, P. L., and Elliott, W. J., eds., Earthquakes and Other Perils, San Diego region: San Diego Association of Geologists for Geological Society of America, Field Trip Guidebook, p. 29-46.

20. Lensen, G. J., 1970, Elastic and non-elastic surface deformation in New Zealand: New Zealand Society of Earthquake Engineering Bulletin, v. 3, no. 4, p. 131-142.

21. Lensen, G. J., 1973, Guidebook for excursion A-10, Tour Guide for International Association of Quaternary Research Conference, Christchurch, New Zealand, 76 p.

22. Lensen, G. J., and Vella, P., 1971, The Waiohine faulted terrace sequence recent crustal movements: Royal Society of New Zealand, Bulletin 9, p. 117-119.

23. Louderback, C. D., ed., 1949, Seismological notes: Seismological Society of America Bulletin V. 39, no. 1, p. 61.

24. Matsuda, T., 1977, Empirical rules on sense and rate of recent crustal movement: Journal of Geodetic Society of Japan, v. 22, no. 4, p. 252-263.

25. Mencher, E., 1963, Tectonic history of Venezuela in Backbone of the Americas: American Association of Petroleum Geologists Memoir 2, p. 73-89.

26. Moore, G. W., 1972, Offshore extension of the Rose Canyon fault, San Diego, California: U.S. Geological Survey Professional Paper 800-C, p. 113-116.

27. Moore, G. W. and Kennedy, M. P., 1975, Quaternary faults at San Diego Bay, California: Journal of Research of the U.S. Geological Survey, v. 3, no. 5, p. 589-595.

28. Prowell, D. C., 1974, Geology of selected Tertiary volcanics in the central coast range mountains of California and their bearing on the Calaveras and Hayward fault problems: University of California Santa Cruz, unpublished Ph.D. thesis, 182 p.

29. Richter, C. F., 1958, Elementary seismology: W. H. Freeman, San Francisco and London, 768 p.

30. Rod, E., 1956, Strike-slip faults of northern Venezuela: American Association of Petroleum Geologists, v. 40, no. 3, p. 457-476.

31. Schubert, C. and Sifontes, R. S., 1970, Bocono fault, Venezuelan Andes, evidence of postglacial movement: Science, v. 170, p. 66-69.

32. Schwartz, D., Cluff, L. S., and Donnelly, T., 1979, Quaternary faulting along the Caribbean and North American plate boundary: Tectonophysics, v. 52 (in press).

33. Sharp, R. V., 1978, Salton trough tectonics: U.S. Geological Survey, National Earthquake Hazards Reduction, Summaries of Technical Reports, v. 7, p. 34-35.

34. Sharp, R. V., 1980, Salton trough tectonics: U.S. Geological Survey, National Earthquake Hazards Reduction Program, Summaries of Technical Reports, v. 9, Open-File Report 80-6.

35. Sieh, K. E., 1978, Prehistoric large earthquakes produced by slip on the San Andreas fault at Pallett Creek, California: Journal of Geophysical Research, v. 83, no. B8, p. 3907-3939.

36. Sieh, K. E., 1979, Late Holocene behavior of the San Andreas fault--U.S. Geological Survey Contract No. 14-08-0001-16774: U.S. Geological Survey, National Earthquake Hazard Reduction Program, Summaries of Technical Reports, v. 8, June, p. 50.

37. Slemmons, D. B., 1977, State-of-the-art for assessing earthquake hazards in the United States--Reports 6, Faults and Earthquake Magnitude: U.S. Army Corps. of Engineers, Waterways Experiment Station, Soils and pavements Laboratory, Miscellaneous Paper S-73-I, 129 p.

38. Suggate, R. P., 1963, The Alpine fault: Transactions of the Royal Society of New Zealand, v. 2., no. 7, p. 105-129.

39. Suggate, R. P. and Lensen, G. J., 1973, Rate of horizontal fault displacement in New Zealand: Nature, v. 242, p. 815.

40. Threet, R. L., 1979, Rose Canyon fault--An alternative interpretation, in Abbott, P. L., and Elliott, W. J., eds., Earthquakes and Other Perils, San Diego region: Geological Society of America, Field Trip Guidebook, November, p. 61-71.

41. Trifonov, V. G., 1971, The pulse-like character of tectonic movements in regions of most recent mountain-building (Kopec Dagh and southeast Caucasus): Geotectonics, U.S.S.R., Academy of Sciences, Geological Institute, no. I, p. 234-235.

42. Trifonov, V. G., 1978, Late Quaternary tectonic movements of western and central Asia: Geological Society of America Bulletin, v. 89, no. 7, p. 1059-1072.

43. Vella, P., 1963, Upper Pleistocene succession in the inland part of Wairarapa Valley, New Zealand: Royal Society of New Zealand (Geology) Transactions, v. 2, no. 4, p. 63-78.

44. Woodward, Clyde and Associates, 1969, Seismicity and seismic geology of northwestern Venezuela: Report to Shell Oil Company of Venezuela, v. 2, 77 p.

45. Woodward-Clyde Consultants, 1979, Report of the evaluation of maximum earthquake and site ground motion parameters associated with the offshore zone of deformation, San Onofre Nuclear Generating Station: Report for Southern California Edison Company, June, 241 p.

46. Zak, I. and Freund, R., 1966, Recent strike slip movements along the Dead Sea rift: Israel Journal of Earth Sciences, v. 15, p. 33-37.

47. Ziony, J. I., 1973, Recency of faulting in the greater San Diego area, California, in Ross, A. and Dowlen, R. J., eds., Studies on the geology and geologic hazards of the greater San Diego area, California: San Diego Association of Geologists and Association of Engineering Geologists, 1973 Guidebook, p. 68-75.

PERSONAL COMMUNICATIONS

1. Matsuda, T., 1979, Earthquake Research Institute, University of Tokyo, Japan.

2. Schwartz, D., 1979, Woodward-Clyde Consultants, San Francisco.

3. Sharp, R., 1979, U.S. Geological Survey.

Isoseismal Maps of 1929 and 1855 Earthquakes

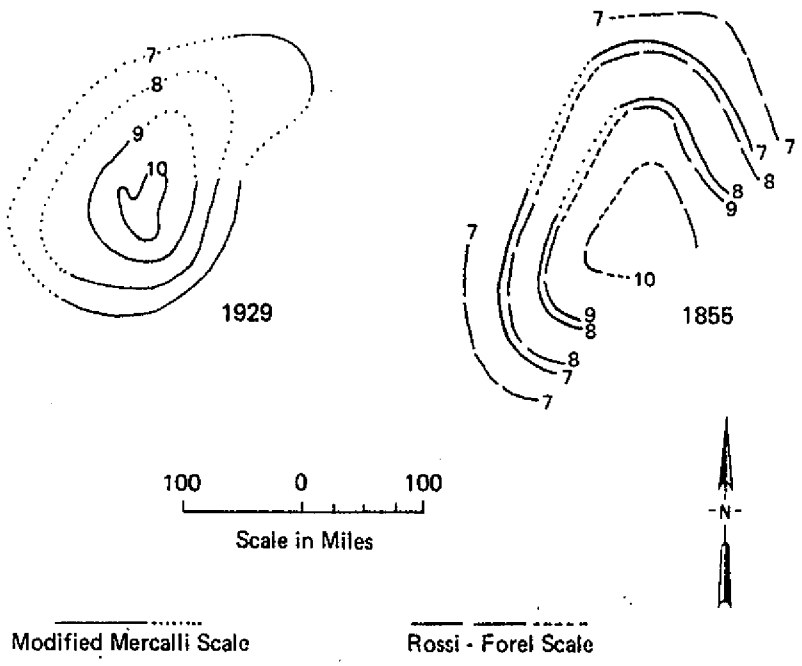

Isoseismal Comparisons

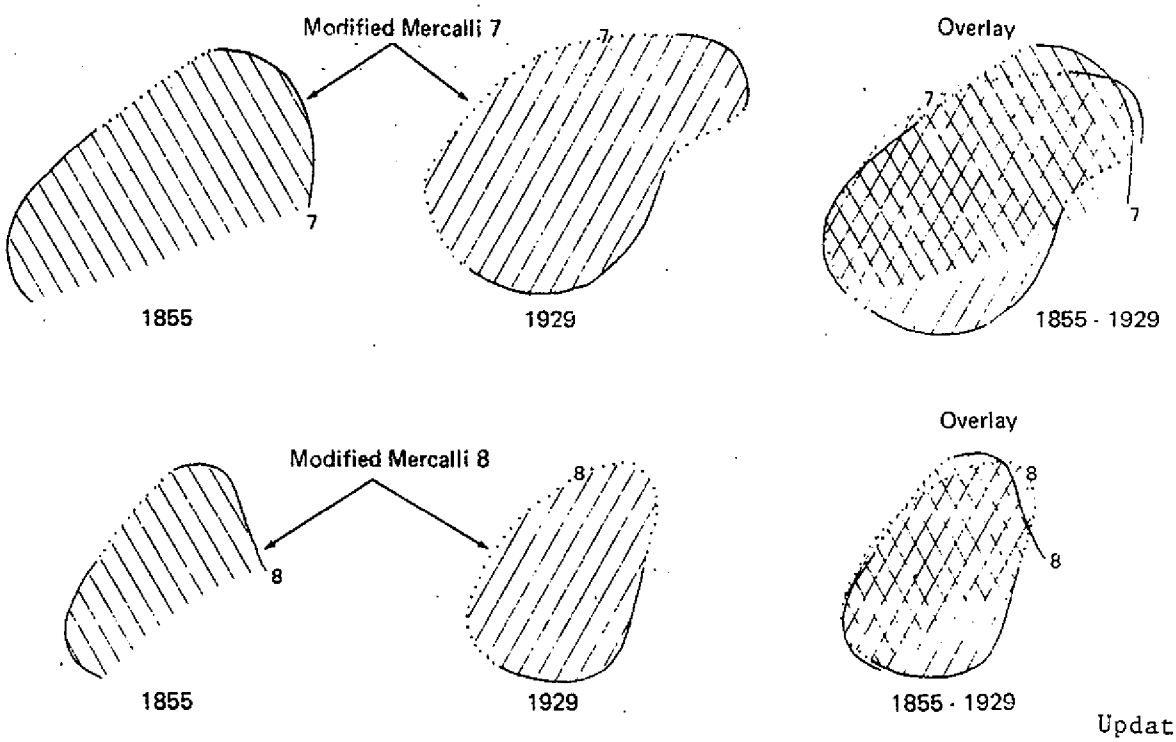

Updated

Note: Data from Clark and others, 1965

SAN ONOFRE NUCLEAR GENERATING STATION Units 2 & 3
COMPARISON OF 1855 and 1929 (M7.6) NEW ZEALAND EARTHQUAKES
Figure 2.5N-1

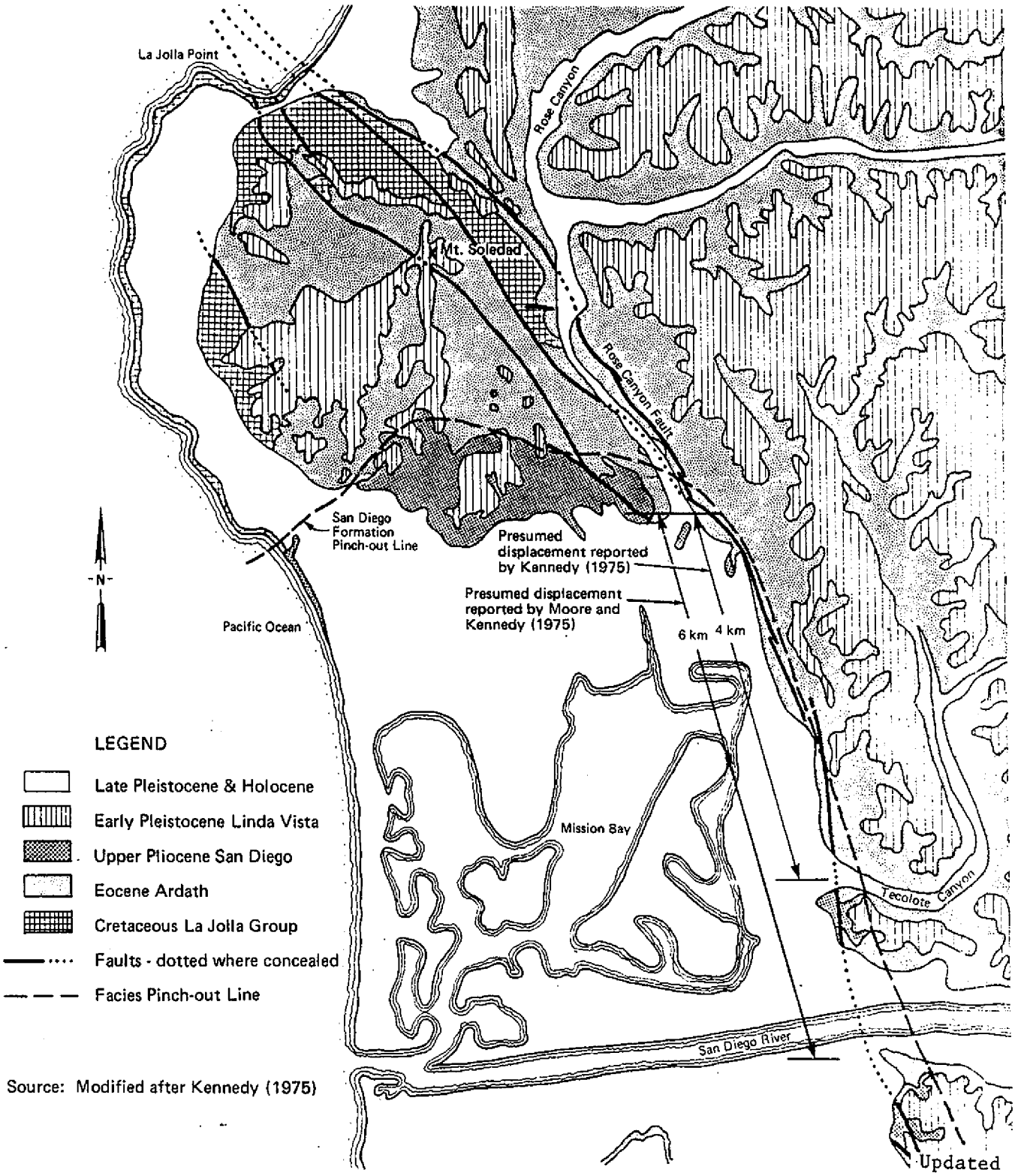

SAN ONOFRE NUCLEAR GENERATING STATION
Units 2 & 3

GENERALIZED GEOLOGIC MAP OF SAN DIEGO AREA SHOWING ROSE CANYON FAULT AND PINCH-OUT LINE OF SAN DIEGO FORMATION

Figure 2.5N-2

APPENDIX 2.50

FAULTS WITH QUARTERNARY MOVEMENT

WITHIN 25 MILES OF SAN ONOFRE

Site File Copy

APPENDIX 2.50

FAULTS WITH QUATERNARY MOVEMENT WITHIN 25 MILES OF SAN ONOFRE

The only faults (or zones of deformation) that have Quaternary movement and occur within 25 miles of the site are the Whittier-Elsinore fault zone, the Palos Verdes fault and the hypothesized Offshore Zone of Deformation. The hypothesized Offshore Zone of Deformation is the controlling feature for seismic design at San Onofre Units 2 and 3, as discussed in the Safety Evaluation Report. The Whittier-Elsinore fault zone and the Palos Verdes fault are discussed below.

The Palos Verdes fault lies 11 miles from the site at its closest point. In order to cause 0.67g at the site, a magnitude greater than 8-1/2 would have to occur. This would require a rupture length of more than 250 miles. The Palos Verdes fault is 60 miles long, which is a great deal less than that required to cause a magnitude 8-1/2.

The Whittier-Elsinore fault zone is a series of fault segments lying 23 miles from the site at its closest point. In order to cause 0.67g at the site, a magnitude greater than 8-1/2 would have to occur. This would require a rupture length of more than 250 miles. The Whittier-Elsinore fault zone is 145 miles long, which is a great deal less than that required to cause a magnitude 8-1/2.

Amended: April 2009 TL: E048000

APPENDIX 2.5P

CORONADO BANKS AND PALOS VERDES FAULTS

APPENDIX 2.5P

CORONADO BANKS AND PALOS VERDES FAULTS

The Coronado Banks and Palos Verdes faults were not considered in this or in earlier earthquake analyses for San Onofre because of their greater distance (35 km) from the site than the hypothesized Offshore Zone of Deformation (OZD) (8 km) as shown on figure 2.5P-1. The Applicants' study of slip-rate/maximum-magnitude relationships used strike-slip faults. The strike-slip nature of these two faults is conjectural and both faults display abundant evidence of vertical movement.

The rate of strike slip of either the Palos Verdes or Coronado Banks faults is poorly known and the lack of conclusive evidence for strike slip precluded their consideration in the Applicants' analysis. The intent with respect to decreasing activity west of the San Andreas was to characterize the structures between the San Andreas and the hypothesized OZD in a relative ranking comparison. There was no intent to claim that faults farther west were similarly less active. Indeed, the San Clemente fault zone is one of those that may be more active than the hypothesized OZD.

Amended: April 2009 TL: E048000

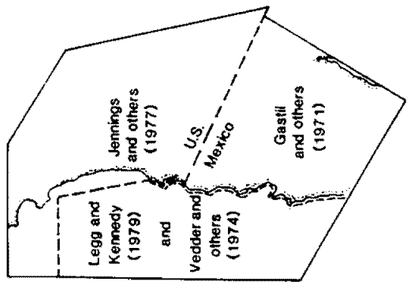

INDEX TO GEOLOGIC MAPPING

LEGEND:

——— SOLID WHERE KNOWN

– – – – – DASHED WHERE INFERRED

Tijuana GEOGRAPHIC NAME IN BOLD TYPE

N I Z D NEWPORT - INGLEWOOD ZONE OF DEFORMATION

S C O Z D SOUTH COAST OFFSHORE ZONE OF DEFORMATION

COMPILED FROM:

GASTIL, R.G., AND OTHERS, 1971, RECONNAISSANCE GEOLOGIC MAP OF THE STATE OF BAJA CALIFORNIA: GEOLOGICAL SOCIETY OF AMERICA MEMOIR 140. SCALE: 1:120,000

JENNINGS, C.W., AND OTHERS, 1977, GEOLOGIC MAP OF CALIFORNIA: CALIFORNIA DIVISION OF MINES AND GEOLOGY, SCALE: 1:250,000

LEGG, M.R., AND KENNEDY, M.P., 1979, FAULTING OFFSHORE SAN DIEGO AND NORTHERN BAJA CALIFORNIA IN EARTHQUAKE AND OTHER PERILS, SAN DIEGO REGION (ABBOTT, P.L., AND ELLIOT, W.J., EDITORS)

VEDDER, J.G., AND OTHERS, 1974, PRELIMINARY REPORT ON THE GEOLOGY OF THE CONTINENTAL BORDERLAND OF SOUTHERN CALIFORNIA. U.S.G.S. MAP MF-624

SCALE 1 : 750,000

0 10 20 30 40 50 KILOMETERS

0 10 20 30 40 50 MILES

Updated

SAN ONOFRE NUCLEAR GENERATING STATION Units 2 & 3

REGIONAL FAULT MAP
SOUTHERN CALIFORNIA,
NORTHWESTERN BAJA CALIFORNIA,
AND THE
CALIFORNIA CONTINENTAL BORDERLAND

Figure 2.5P-1

Amended: April 2009 TL: E048000

APPENDIX 2.5Q

ROSE CANYON AND CRISTIANITOS FAULT ZONES

APPENDIX 2.5Q

CONTENTS

TABLES

FIGURES

APPENDIX 2.5Q

ROSE CANYON AND CRISTIANITOS FAULT ZONES

Numerous and extensive seismic reflection profiling surveys have been performed offshore in the vicinity of San Onofre. Several of these have been performed for the Applicants over a 10-year period to investigate the Cristianitos fault and other structural features offshore. The remaining surveys were done by other investigators for other purposes. The seismic reflection data that are relevant for evaluating geologic structures offshore San Onofre are those along and landward of the Offshore Zone of Deformation (OZD)[a] which is approximately 8 km offshore of the site. Particularly relevant to evaluating the offshore extension of the Cristianitos fault and its postulated connection with the OZD is the data in the first 10 km southeast of the site. However, this appendix addresses the data in a larger area extending 25 km up and down the coast from San Onofre and out to 10 km from the shore (figure 2.5Q-1). The profile data available to the Applicants at the time were transmitted to the NRC under separate cover on April 18, 1980.

This appendix has six parts. The first is a description and inventory of seismic reflection profiles in the offshore vicinity of San Onofre, which are located on figure 2.5Q-1 and characterized in tables 2.5Q-1 and 2.5Q-2. The second part summarizes the offshore geophysical investigations performed for San Onofre and the interpretations that provided the basis of the Applicants' position on the Cristianitos fault during the construction permit phase of this proceeding. The third part summarizes more recent geophysical investigations and interpretations.

The fourth part describes the sources and nature of available data on (a) the offshore Miocene bedrock stratigraphy, and (b) the age of submerged Quaternary sediments. The fifth part represents the interpretation of the data described in the fourth part by way of description of the tectonic and stratographic evolution of the Cristianitos fault and the Capistrano Embayment. The Applicants' conclusion on the hypothesized Cristianitos - OZD connection is presented in the sixth part.

2.5Q.1 SEISMIC REFLECTION PROFILES IN THE OFFSHORE VICINITY OF SAN ONOFRE

For ease in describing the distribution and density of seismic data, the subject area has been divided into blocks approximately 10 km square corresponding to the general orientation of the tracklines. Each block is

a. Green et al's identification of the "Newport-Inglewood Rose Canyon Fault Zone" is approximately equivalent to the Offshore Zone of Deformation (OZD) designation used by the Applicants. For consistency of nomenclature used in this proceeding, the term OZD will be used in this Appendix.

outlined in figure 2.5Q-1 and identified with a Roman numeral from I to VI. Inasmuch as most of the individual surveys cover the entire vicinity, each survey is described first and is followed by a description of the distribution and density of seismic data in the blocks within distances of 10 to 25 km from San Onofre. Table 2.5Q-3 presents sources of offshore stratigraphic data. Summary logs of borings by Dames & Moore, 1970, are presented in table 2.5.Q-4.

2.5Q.1.1 LIST OF SEISMIC REFLECTION SURVEYS

2.5Q.1.1.1 Marine Advisers Sparker

These surveys, performed in 1970 specifically for the Applicants, follow the coastline from north of the subject area to about 15 km southeast of San Onofre (figure 2.5Q-1). Tracklines are arranged with legs parallel and perpendicular to the coastline, forming a "square wave" pattern with spacing of 1.0 to 4.5 km between the northeast-trending legs. These extend as much as about 15 km offshore. The tracklines also include east-west legs across the southern projection of the Cristianitos fault, south of San Onofre. The Marine Advisers' survey totals 200.1 line-km within the subject area.

2.5Q.1.1.2 General Oceanographics, Inc.

In 1970, General Oceanographics performed for the Applicants both sparker and high-resolution surveys extending to as much as 10 km offshore in the area from San Onofre northward (figure 2.5Q-1). Tracklines trend generally north-south and east-west, forming a stepped pattern along the coastline. In addition, six intersecting tracklines with various orientations were about 10 km due south of San Onofre. The General Oceanographics surveys total 63.1 line-km in the subject area.

2.5Q.1.1.3 U.S. Geological Survey (USGS)

Five UNIBOOM and sparker tracklines were run by the USGS in 1970 for USGS research purposes. The lines are within the southern part of the subject area (figure 2.5Q-1). These lines trend northeast, northwest, and generally east-west, intersecting and forming stepped patterns. These are 55.5 line-km of this survey in the subject area.

2.5Q.1.1.4 Western Geophysical Company

Offshore "Aquapulse (common-depth-point, or CDP) surveys for the Applicants were run by Western Geophysical Company in 1970-1971 covering the vicinity of San Onofre and extending well beyond. Tracklines were on a generally rectangular grid with northeasterly lines at spacings of 1.2 to 4.3 km and northwesterly lines spaced at 5 to 8 km. The grid is crossed by an additional east-west line south of San Onofre. A total of 160.6 line-km of this survey are within the subject area (figure 2.5Q-1).

APPENDIX 2.5Q

Table 2.5Q-1
SEISMIC REFLECTION PROFILES IN THE VICINITY OF SAN ONOFRE

Survey	Block No. I (47 km^2) Description	Length (km)	Block No. II (98 km^2) Description	Length (km)	Block No. III (96 km^2) Description	Length (km)	Block No. IV (96 km^2) Description	Length (km)	Block No. V (79 km^2) Description	Length (km)	Block No. VI (30 km^2) Description	Length (km)	Total (446 km^2) Line-km	Submittal Status
Marine Advisers Sparker 1970	2 NE-SW legs 2.7 km apart; 2 NW-SE legs 0.2-0.8 km apart	15.3	5 NE-SW legs 1.2-2.4 km apart; tied with 5 NW-SE legs	31.7	4 NE-SW legs 1.5-4.5 km apart; 4 NW-SE & 1 E-W leg	35.2	4 NE-SW legs 1-2.4 km apart; 8 E-W legs 0.5-2 km apart; 5 NW-SE tie lines	101.2	2 NE-SW legs 2.1-3.0 km apart 1 cross line	16.7	None		200.1	Reported in PSAR, App. 2B, Data submitted April 18, 1980
General Oceanographics Sparker and High Resolution 1970	1 N-S line, 1 E-W line, 1.5 km apart at closest approach	5.3	2 E-W lines 4.6 km apart, intersected by 1 E-W & 1 NE-SW line	20.1	1 E-W line and 1 N-S line crossing	13.2	6 Intersecting lines of various orientation; 10.8 km Sparker, 13.7 km Hi Res	24.5	None	---	None	---	63.1	Reported in PSAR, App. 2B. Data no longer available
U.S.G.S. 1970 UNIBOOM & Sparker	None	---	None	---	None	---	1 E-W line & 1 NE-SW line, 0.2 km apart @ closest appraoch	17.5	1 WNW & 1 ENE line crossing 1 EW line	17.9	5 lines in radiating fan Patterm	20.1	55.5	Reported in PSAR, App. 2C. Data not available to applicant
Oceanographic Services 1974 Boomer	None	---	None	---	1 ENE line	4.2	2 NE-SW lines, 0.2 to 0.5 km apart, 1 E-W tie line	9.3	None	---	None	---	13.5	Reported in PSAR, App. 2.5.A.3. Data submitted with this response
Western Geophysical 1970-71 CDP	1 NE-SW line, 2 NW-SE lines, 5.3-5.9 km apart	16.4	2 NE-SW lines 4.3 km apart; 2 NW-SE lines 5.8-7.6 km apart	36.0	3 NE-SW lines @ 4 km spacing; 2 NW-SE lines 8 km apart; 1 E-W line	39.3	3 NE-SW lines 1.2-4.3 km apart; 1 E-W line; 1 NW-SE line	30.6	2 NE-SW lines 3.2-3.5 km apart; 1 cross line	26.7	1 NE-SW line & 2 NW-SE lines 0.6-1.0 km apart	11.6	160.6	Reported in PSAR, App. 2E. Data submitted by letter dated April 18, 1980
Fugro Inc. 3.0 kHz Sonia 1978	None		1 NW-SE line	4.5	2 NE-SW lines 1.6 km apart; 1 cross line	24.5	1 NE-SW line (1.6 km from line in adj. block); 1 NW-SE line	7.7	None	---	None	---	36.7	Reported to NRC March 16, 1979 and April 18, 1980
Woodward-Clyde 1978 UNIBOOM & Sparker	None	---	None	---	None	---	30 NE-SW lines @ 0.1-0.3 km spacing; 1 tie line	126.3	None	---	None	---	126.3	Reported to NRC March 16, 1979 and included in FSAR section 1.8 on December 24, 1979
CSUN/CSUSD 3.5 kHz High Resolution 1979	6 NE-SW lines @ 0.3-1.5 km spacing; 6 NW-SE @ 0.2 to 1.3 km spacing; 1 E-W; 1 NS	52.3	8 NE-SW lines @ 0.6-1.7 km spacing 5 NW-SE lines @ 0.1-2.4 km spacing	78.8	8 NE-SW lines @ 0.8-2.0 km spacing 2 cross lines	53.9	7 NE-SW lines @ 0.3-2.1 km spacing; 1 partial tie line	42.2	6 NE-SW lines @ 1.2-3.2 km spacing 1 cross line	33.8	3 NE-SW lines 1.4-2.1 km apart; 1 cross line	14.3	275.3	Referenced on P.S. Fischer track line maps, submitted by letter dated May 12, 1980
Total line-km		89.3		171.1		170.3		359.3		95.1		46.0	931.1	
Density (line-km/km^2)		1.90		1.75		1.77		3.74		1.20		1.53	2.09	
Equivalent average spacing (km)		0.53		0.57		0.56		0.27		0.83		0.65	0.48	

2.5Q-3/2.5Q-4 (Blank)

APPENDIX 2.5Q

Table 2.5Q-2
QUANTITATIVE SUMMARY OF OFFSHORE SEISMIC
REFLECTION PROFILING IN THE VICINITY OF SAN ONOFRE

	Line-km	Density (line-km/km^2)	Equivalent Average Spacing
Blocks 0-10 km from San Onofre:			
Block III	170.3	1.77	0.56
Block IV	359.3	3.74	0.27
Combined	529.6	2.76	0.36
Blocks 10-25 km from San Onofre:			
Blocks I & II	260.4	1.80	0.56
Blocks V & VI	141.1	1.29	0.77
Combined	401.5	1.58	0.63
All Blocks	931.1 (total)	2.09 (average)	0.48 (average)

Amended: April 2009 TL: E048000

Table 2.5Q-3
SOURCES OF OFFSHORE STRATIGRAPHIC DATA

Investigation	Date	Type	Submittal Status
Dames & Moore, seismic and foundation studies onshore	1970	4 bucket-auger and rotary-wash borings, 55-987 feet deep	Reported in PSAR, Appendix 2B
Marine Advisers, Inc., offshore conduit study	1970	4 jet probes, 10-21 feet deep	Reported in PSAR, Appendix 2B
General Oceanographics, Inc., offshore stratigraphic study	1970	22 dart-core samples less than 2 feet deep	Reported in PSAR, Appendix 2C. Data summarized in this report.
Woodward-McNeill & Assoc., offshore liquefaction study for conduit	1974	3 rotary-wash borings 41-61 feet deep; seven Vibra-Core holes 3-14.5 feet deep	Reported in FSAR, appendix 2.5A, section 2.5A.3.
Woodward-Clyde Consultants, offshore conduit study	1978	9 rotary-wash borings, 28-338 feet deep	Performed for construction purposes only. Summarized in this report.

Amended: April 2009 TL: E048000

APPENDIX 2.5Q

Table 2.5Q-4
SUMMARY LOGS OF BORINGS BY DAMES & MOORE, 1970

Boring No.	Depth (ft)	Description	Stratigraphic Interpretation
1.	0-45 45-936 936-987	Brown sand, silt, clay Light brown to gray sand Gray siltstone	Terrace deposits San Mateo Fm. Capistrano (?) Formation
2.	0-51 51-252	Brown sand, silt clay Light brown to white sand	Terrace deposits San Mateo Formation
3.	0-45 45-55	Brown sand, gravel, cobbles Light brown sand	Terrace deposits San Mateo Formation
4.	0-45 45-55	Brown sand, silty sand Light brown sand	Terrace deposits San Mateo Formation

Table 2.5Q-5
SUMMARY LOGS OF JET PROBES BY
MARINE ADVISERS, 1970

Probe No.	Depth (ft)	Description
1.	0-1 1-10	Sand cobbles, boulders Sand
2.	0-22	Sand
3.	0-1 1-5 5-14 14-21	Sand Sand, cobbles Fine sand Coarse sand (dense)
4.	0-1 1-4 4-12 12-21	Sand Cobbles, sand, clay, shells Medium sand Coarse sand

2.5Q.1.1.5 Oceanographic Services

In 1974 and under subcontract to Woodward-Clyde Consultants for the Applicants, Oceanographic Services performed a 170-joule Boomer survey in the vicinity of the San Onofre 2 and 3 cooling water conduits. The purpose of the survey was to evaluate the material properties of the sediments with respect to excavation and construction of the conduits. The tracklines closely follow the conduit alignment along the boundary between Blocks III and IV (figure 2.5Q-1), with one line located about 2000-7000 feet farther northwest. This survey totals 13.5 line-km.

2.5Q.1.1.6 Fugro, Inc. 3.0 kHz

Fugro performed this high resolution SONIA (3.0 kHz) survey for purposes of equipment testing and calibration in 1978. The largest part of this survey, 36.7 line-km, is within the subject area (figure 2.5Q-1) and one line extends offshore behond the boundary used herein. The survey involved three northeasterly lines, spaced about 1.6 km apart, in the area just offshore of San Onofre, and one northwesterly line crossing these and continuing to about 15 km northwest of San Onofre.

2.5Q.1.1.7 Woodward-Clyde Consultants

Woodward-Clyde Consultants ran a survey, consisting of closely-spaced UNIBOOM and sparker lines, in 1978 for the California Coastal Commission as part of an LNG Plant siting study. Tracklines trend northeasterly at spacings of 0.1 to 0.3 km and are crossed by a northwesterly tie line. This survey totals 126.3 line-km and is entirely within Block IV (figure 2.5Q-1).

2.5Q.1.1.8 California State Universities at Northridge and San Diego 3.5 kHz

This high-resolution survey was performed in 1979 for academic research purposes by the California State Universities at Northridge and San Diego. The survey covers the San Onofre vicinity to about 8 to 10 km offshore. A total of 275.3 line-km of this survey are within the subject area (figure 2.5Q-1). Tracklines within this area trend generally northeast and are at spacings of 0.3 to 3.2 km. These are crossed by a single northeast-trending line in part of the area south of San Onofre. To the north, as many as five cross-lines are recorded and intersect at low angles. Supplemental lines at various orientations also were run, mainly in the northern part of the area. The data from these lines have not been received by the Applicants, but are in the process of being obtained.

2.5Q.1.2 DENSITY OF SURVEYS

In general, the area within 10 km offshore of San Onofre 25 km along the coastline to the northwest and southeast has been subjected to intensive seismic exploration. The average density of tracklines in this area is 2.09 line-km/km^2, equivalent to an average spacing between lines of 480 meters over the entire area. The distribution of tracklines with this area is summarized on tables 2.5Q-1 and 2.5Q-2, and is discussed briefly in the following paragraphs.

2.5Q.1.2.1 Blocks III and IV (0 to 10 km from San Onofre)

As would be expected, the greatest density of seismic survey lines is in the area closest to the site. Data is particularly abundant and most significant from Block IV because of the general north-south orientation of onshore geologic structures. Here additional detail was obtained and used to evaluate possible structural relationships between the offshore and onshore faults. In this block, the equivalent average spacing between tracklines is 270 meters. The combined average for the two blocks within 10 km of San Onofre is 360 meters. The density of lines in Blocks III and IV are 1.77 and 3.74 line-km/km^2, respectively, for a combined average of 2.76 line-km/km^2.

2.5Q.1.2.2 Blocks I, II, V and VI (10 to 27 km from San Onofre)

Although data here are not as dense as in the blocks closer to the site, these blocks also have good coverage. Block II has a higher density of 1.75 line-km/km^2, equivalent to an average spacing of 570 meters between lines. Block V is beyond the area investigated in great detail for San Onofre and has an equivalent line spacing of 830 meters and a density of 1.2 km/km^2. The equivalent line spacing over Blocks I, II, V and VI combined is 630 meters. The average density of these blocks combined is 1.58 line-km/km^2.

2.5Q.2 DESCRIPTION AND INTERPRETATION OF SEISMIC REFLECTION PROFILING PERFORMED FOR SAN ONOFRE

2.5Q.2.1 INVESTIGATION BY MARINE ADVISERS, INC.

During 1970, seismic reflection profiling was undertaken by Marine Advisers, Inc., for the Applicants. The results of this work, reported in Appendix 2B of the PSAR, drew on data from sparker, high resolution boomer, and 7-kHz high resolution systems, side-scan sonar, and jet probing by diving geologists. The objectives of the investigation were to:

- Accumulate data relative to possible faulting of the ocean floor along the shelf and upper slope directly offshore from the proposed plant site.

- Search for a possible offshore extension of the Cristianitos fault.

- Determine the bottom sediment type and distribution along the offshore cooling water conduit.

The most significant relevant interpretations of the investigation are summarized as follows:

1. No faults were found to project toward or through the proposed site;

2. A northwest-trending fault, Fault A (renamed later the South Coast Offshore Zone of Deformation, an element of the OZD), lies along the edge of the continental shelf;

3. All shelf structures have been truncated by marine and subaerial erosion during lower stands of sea level, and no sea floor expression of faults was discernible on sparker records or side scan sonar;

4. The seaward extension of the Cristianitos fault turns to the southeast and subparallels the coast. (The data for this interpretation was reviewed by the Applicants' Board of Technical Review, with the conclusion reached that the "disturbance" observed in profiles suggestive of a southeast extension of the Cristianitos fault was not due to faulting, but to spurious reflections that occur when tracklines are parallel to the strike of bedding.) Table 2.5Q-5 presents the summary log of jet probes by Marine Advisers in 1970.

2.5Q.2.2 INVESTIGATION BY THE BOARD OF TECHNICAL REVIEW (BTR)

During 1970, the Applicants convened a group of authorities in the fields of geology and seismology to make an independent review of offshore geologic structure, regional tectonics, and site response to earthquakes. The results of this review, reported in Appendix 2C of the PSAR, were based in part on additional offshore date from Navy and oil company archives, and from seismic reflection profiling and dart-coring for the Applicants by General Oceanographics, Inc. The objectives of the investigation by the BTR were to:

- Identify and characterize structural features of the Continental Shelf offshore from San Onofre.

- Evaluate the Newport-Inglewood zone of deformation.

- Determine ground motion to be used for design at San Onofre.

The interpretations of the BTR, in summary regarding structural features offshore San Onofre, were:

1. The structure near the edge of the Continental Shelf off San Onofre consists of a gentle anticline and a syncline with discontinuous

minor faults. The strata on both sides of the anticline are upper to lower Mohnian (Upper Miocene) shale, making them approximately stratigraphic equivalents of the shale found in the San Onofre bluffs excavation. These folds offshore of San Onofre are not related to onshore structural features.

2. Offshore subbottom profiling data indicate that the Cristianitos fault extends less than 10,000 feet offshore, supporting the conclusions in Appendix 2A of the PSAR that the Cristianitos fault dies out toward the south.

3. Some of the faults interpreted by Marine Advisers, Inc., and much of the "disturbance of beds" apparent on seismic profiles of this area, actually represent geomorphic and structural features other than faulting. Such features include sea gullies, erosional terraces, and tightly-folded or steeply-dipping strata, and spurious up-dip and down-dip reflections seen in profiles run along the strike of bedding.

During March 1971, the BTR reviewed seismic reflection profiles collected by the U.S. Geological Survey, during December 1970, which were not previously available to the Board for inspection. While the additional data confirmed the BTR's earlier views on the offshore geology, the main focus of the review was on the structure along the shelf edge.

To supplement existing data, which chiefly represented sediments and their structure to depths of hundred of feet, the Applicants subsequently undertook to provide additional definition of the offshore area to depths of 10,000 feet or more. This investigation was conducted by the Western Geophysical Company (Western) of a region much larger than the immediate vicinity of the San Onofre site.

2.5Q.2.3 INVESTIGATIONS BY WESTERN GEOPHYSICAL COMPANY

During the period September 1971 to March 1972, Western conducted a geophysical survey of the offshore region opposite San Onofre. The scope of the survey included seismic reflection (Western's aquapulse technique of common-depth-point profiling), refraction and magnetic surveys. In the surveyed region between Long Beach and San Diego and extending about 30 miles off-shore from the coastline, 350 miles of new reflection data were collected for the Applicants and combined with 650 miles of proprietary data acquired for other purposes by Western during 1969-1970. Ninety-six miles of these data lie within Blocks I-VI. Seven refraction profiles and 450 miles of seaborne magnetometer data were also acquired by Western for the Applicants. The results of this work were reported in Amendment 11, Appendix 2E (Attachment A1) of the PSAR.

The purpose of the Western investigation was to determine the structural configuration of the subsurface rocks, with special emphasis on the location of faults, and to define the age of cessation of their movement. Major products of the survey were maps of the sea floor (Horizon A), a subsea floor horizon in Upper Miocene rocks at depths varying between 1000 and 3000 feet (Horizon B), and of the acoustic basement (Horizon C) representing the base of coherent reflection horizons penetrated by the aquapulse system (depths generally 10,000 or more feet below the sea floor).

A summary of interpretations relevant to the postulated connection between the Cristianitos fault and OZD is as follows:

1. The South Coast Offshore Zone of Deformation strikes northwest-southeast about 8 km offshore. For most of its length (26 km) it has only one major fault trace, across which rocks are down-thrown seaward. It is continuous on Horizon C, but dies out rapidly upward and it is not continuous on Horizon B or shallower horizons.

2. North-south trending faults on Horizon C that are parallel or in approximate alignment with the Cristianitos fault are, in general, not present on Horizon B.

3. Seismic data suggest that the Cristianitos fault extends seaward and dies out into the South Coast Offshore Zone of Deformation on Horizon C, but does not extend upward very far into the section and does not cut Horizon B.

Western's interpretation that north-south faults in Horizon C correspond with the Cristianitos fault was based on fault position and orientation. At that time Western did not have an in-depth knowledge of the age and origin of the Cristianitos fault. Subsequently, the evolution and tectonic setting of the Cristianitos fault and of the Capistrano Embayment were investigated in detail by the Applicants during the period 1977-1979, as described in section 2.5Q.5 of this appendix.

2.5Q.2.4 INVESTIGATION BY OCEANOGRAPHIC SERVICES

The boomer data[(b)] of this survey (presented in appendix 2.5A of the FSAR) were collected in 1974 for Woodward-Clyde Consultants to investigate the thickness of Holocene sediments overlying the Miocene bedrock of the San Onofre shelf at this locality. Penetration into bedrock was minimal, and little information on bedrock structure can be gained through interpretation of the data. The data do not define any faulting and, in general, they confirm a gentle seaward dip of bedrock strata as indicated in earlier sparker data from this locality off of the San Onofre site.

b. Listed in table 1.8-7.

Amended: April 2009 TL: E048000

APPENDIX 2.5Q

2.5Q.3 REVIEW OF INVESTIGATIONS BY FUGRO, INC., WOODWARD-CLYDE CONSULTANTS, AND CALIFORNIA STATE UNIVERSITIES AT NORTHRIDGE AND SAN DIEGO

For its own in-house research purposes in 1978 Fugro, Inc. ran four seismic reflection profiles offshore of San Onofre to test and calibrate its high-resolution SONIA equipment. The data were acquired by the Applicants and reviewed. However, the profiles lie too far west to cross the seaward extension of the Cristianitos fault.

Also in 1978, Woodward-Clyde Consultants performed a seismic reflection survey of about 10 square kilometers offshore and south of San Onofre. Their survey was part of a siting study for a proposed LNG facility and was done for the California Coastal Commission. The data were acquired from Woodward-Clyde Consultants by the Applicants and reviewed. These data were collected at closer line-spacings than those of earlier investigations, and allow better definition of faulting. The Applicants' review of the data supports the conclusion that no seaward extension of the Cristianitos fault can be found farther than about 6000 feet along a projected strike of the fault. A reflection profile (S-26 between shot points 327 and 328) across the projection at this distance displays some evidence suggestive of faulting that may represent the Cristianitos.

A structural zone that crosses the seaward projection of the Cristianitos fault, but which is clearly unrelated to that fault, lies between 6000 feet and 16,000 feet from the shoreline. It comprises a series of gentle en-echelon anticlines and synclines with associated short discontinuous en-echelon faults in the section above basement. The zone as a whole is about 5 miles in length and its trend is approximately north 30 degrees west.

These folds and associated short faults are not connected with the Cristianitos fault and they, furthermore, required compression for their development rather than the extension that resulted in the growth of the Cristianitos fault. The faulted anticlinal and synclinal structures are clearly truncated by Pleistocene erosional surfaces. These surfaces are well displayed on the high resolution records. The erosional unconformity is overlain by about 25 to 40 feet of apparently undisturbed Late Pleistocene or Holocene sediments.

The acoustic basement, presumed here to be San Onofre breccia, is faulted in several lines (S-22, WC-839, and WC-841) that cross an approximate seaward projection of the Cristianitos fault 8500 to 9500 feet offshore of the seacliff exposure. This basement faulting does not extend far into overlying sedimentary rock. Faulting in acoustic basement occurs at depths of about 1400 to 1750 feet in the section and is down-thrown to the east in the opposite sense to that of the Cristianitos. The apparent trend of this basement faulting is about north 10-15 degrees east. These basement faults are unrelated to the Cristianitos fault.

Amended: April 2009 TL: E048000

APPENDIX 2.5Q

During 1979, the California State Universities at Northridge and San Diego compiled a series of maps of the offshore region as part of their Southern California Inner Margin Project under the direction of Peter J. Fischer. These maps portray: the location of seismic reflection tracklines by a number of investigators, bathymetry, interpreted structure, and the distribution of Holocene deposits. The Applicants have acquired some of these maps (tracklines, bathymetry, Holocene deposits) and are attempting to obtain the structural interpretation maps and the data on which they are based. Figure 2.5Q-1 is modified from the trackline maps (sheets 11 and 12) of this series.

As part of the offshore geophysical investigation described in section 2.5Q.1 of this appendix, General Oceanographics, Inc. sampled the sea floor at 22 locations along seismic reflection lines 5-6 miles south of San Onofre (figure 2.5Q-2). The purpose of the sampling was to determine the lithology and age of rock exposed along the crest and flanks of a large anticline. As reported by the Board of Technical Review (Appendix 2C, Amendment No. 6 of the San Onofre 2 and 3 PSAR, pp 4, 8, 9), bedrock samples were gray shale of upper to lower Mohnian (Late Miocene) age, and had steep dips where folds are indicated by the seismic-profiling data. Samples that were not of bedrock were not stratigraphically correlated by the Board of Technical Review, but the general age of their fossil content was determined and is given together with the age of bedrock samples in table 2.5Q-6. The age of the bedrock in these samples indicates either upper Monterey or lower Capistrano Formation.

To evaluate the liquefaction potential of soil beneath the cooling water conduits of San Onofre 2 and 3, Woodward-McNeil & Associates conducted an investigation in 1974 that included three rotary-wash borings on the beach and seven Vibra-Core holes 2500-10,000 feet offshore (figure 2.5Q-2). The exploration was designed exclusively to measure the thickness of unconsolidated sea floor sediments, and to determine the extent and configuration of the underlying San Mateo Formation. To these ends the investigation also utilized shallow-penetration Boomer profiling performed by Oceanographic Services (see section 2.5Q.1 of this appendix). The conclusions of the investigation, as reported in the Woodward-McNeill report of December 19, 1974, and presented in appendix 2.5A of the FSAR, were that bottom sediments generally 3-5 feet thick, but locally up to 8 feet thick, overlie the San Mateo Formation in the area surveyed. Summarized logs from this investigation are presented in table 2.5Q-7.

Following some unanticipated excavation difficulties during construction of the cooling water conduits, Woodward-Clyde Consultants drilled eight rotary-wash borings in 1978 from the drillship CALDRILL-1 along the conduit alignment (figure 2.5Q-2). The results of this work were reported to the Applicants on December 19, 1978, "Offshore Soil Investigation, Cooling Water Discharge Conduits, San Onofre Units 2 and 3, San Onofre, California" by Woodward-Clyde Consultants. Upon completion of the conduit exploration, but before demobilization of the drillship, an additional boring was drilled farther offshore (approximately 10,000 feet along projection of the conduit alignment, figure 2.5Q-2) to obtain bedrock samples at depth for microfossil analysis. Drilling was halted at a depth of 338 feet below

APPENDIX 2.5Q

Table 2.5Q-6
AGE OF FAUNAL ASSEMBLAGES FROM DART-CORE
SAMPLES BY GENERAL OCEANOGRAPHICS, INC., 1970

Sample No.	Age
#4	Probable Mohnian, Upper Miocene
#4 O.B.	Pleistocene-Recent
#5	Pleistocene-Recent
#6	Pleistocene-Recent
#7	Upper Mohnian, Upper Miocene
#8	Pleistocene-Recent
#9	Mixed Mohnian and Pleistocene-Recent
#1	Lower Mohnian, Upper Miocene
#2	Upper Mohnian, Upper Miocene
#3a	Pleistocene-Recent
#4+	Pleistocene-Recent
#10	Pleistocene-Recent
#11 O.B.	Probable Mohnian, Mixed with Pleistocene-Recent
#11	Upper Mohnian, Upper Miocene
#12	Lower Mohnian, Upper Miocene
#12 O.B.	Pleistocene-Recent
#13A	Pleistocene-Recent Forams (Brown limestone nodules)
#13A O.B.	Pleistocene-Recent
#14	Pleistocene-Recent
#15 O.B.	Pleistocene-Recent
#15	Probable Mohnian, Upper Miocene
#16	Pleistocene-Recent
#17	Pleistocene-Recent
#17 O.B.	Pleistocene-Recent
#18	Pleistocene-Recent Forams (Brown limestone nodules)
#19	Upper Mohnian, Upper Miocene
#20	Probable Mohnian, Upper Miocene
#21	Upper Mohnian, Upper Miocene
#22	Mixed Upper Miocene and Pleistocene-Recent

Amended: April 2009 TL: E048000

Table 2.5Q-7
SUMMARY LOGS OF BORINGS AND VIBRA-CORE HOLES BY WOODWARD-MC NEILL & ASSOCIATES

Boring No.	Depth (ft)	Description	Interpretation
1	0-1'	Loose, tan-gray sand	
	1-8'	Dense, gray gravel and cobbles	
	8-16'	Dense, gray-green silty sand	
	16-24'	Dense, gray-green clayey silt	
	24'-61'	Dense, yellow sand	San Mateo Formation
2	0-1'	Loose, tan-gray sand	
	1-8'	Dense, yellow sand	San Mateo Formation
3	0-1'	Loose, tan-gray sand	
	1-8'	Gray sandy gravel and boulders	
	8-40'	Dense, yellow sand	San Mateo Formation

Vibra-Core	Depth to San Mateo Formation
3	2.5 ft
4	5 ft (overlain by cobbles)
8	3 ft
14	4 ft (overlain by cobbles and sand)
15	4+ ft (San Mateo not encountered)
19	2 ft (overlain by cobbles; 7 ft total penetration)
24	1.5 ft (5 ft total penetration)

the sea floor because of rough sea conditions and continued storm-weather forced abandonment of the hole. Summarized boring logs from this investigation and the Applicants' stratigraphic interpretation are presented in table 2.5Q-8. Results of the microfossil analysis are presented in table 2.5Q-9.

2.5Q.4 INTERPRETATION OF STRATIGRAPHIC DATA

The stratigraphy of the offshore vicinity of San Onofre should be interpreted in the context of the evolution of the Capistrano Embayment and the Cristianitos fault.

In response to NRC questions the Applicants performed investigations during 1977 to clarify the stratigraphic relationship of the Capistrano Formation and the San Mateo Formation. Toward this end the Applicants retained Dr. Perry Ehlig, Professor of Geology at the California State University at Los Angeles. Dr. Ehlig's investigation consisted of detailed geologic mapping of the Camp Pendleton-San Onofre coastal area, extending inland approximately 3 miles. This mapping, plus regional reconnaissance northwesterly to the San Joaquin Hills and northerly to the Santa Ana Mountains, led to a more comprehensive analysis of the Capistrano Embayment, its tectonic evolution and stratigraphy, and the tectonic setting of the Cristianitos fault. The results of these studies have been published (Ehlig, 1979a & b) and have been incorporated into the FSAR. A summary of the findings relative to the postulated connection between the Cristianitos fault and the OZD, and on the stratigraphy offshore San Onofre follows.

The Cristianitos fault is a north-trending west-dipping normal fault located along the eastern margin of the Capistrano Embayment. The west side of the fault was down-thrown in association with the development and deepening of the embayment during the Late Miocene and Early Pliocene. Both the fault and the embayment were caused by east-west crustal extension. Numerous other basins developed within the California Continental Borderland during this same time span, probably as a result of a slightly divergent motion between the Pacific and North American plates (Blake and others, 1978). In mid-Pliocene the tectonic setting changed from east-west extension to north-south crustal shortening, probably as a result of interplate convergence near the bend in the San Andreas fault. Since early Pliocene the Capistrano Embayment has been uplifted at least 1000 meters relative to sea level (Ehlig, 1979a), an amount of uplift equal to or greater than the amount of uplift in the Peninsular Ranges east of the embayment. The Cristianitos fault does not have the proper orientation to be involved in the uplift and appears to have been inactive since mid-Pliocene. In any event, the fault has not moved in at least the last 125,000 years since it was overlapped by terrace deposits exposed in the sea cliff at San Onofre State Beach.

APPENDIX 2.5Q

Table 2.5Q-8
SUMMARY LOGS OF BORINGS
BY WOODWARD-CLYDE CONSULTANTS (Sheet 1)

Boring No.	Depth (ft)	Description	Interpretation[a]
1	0-4	Olive gray silty sand with some gravel	Qs
	4-6.5	Olive gray gravelly sand with some silt	Tsm
	6.5-32	Dark gray silty clay with fine sand	Tca
2	0-4	Olive gray silty sand with some shells	Qs
	4-10.5	Olive gray gravelly sand	Tsm
	10.5-31.5	Olive gray silty sand with dark gray clay layers	Tsm
	31.5-34	Dark gray sand	Tsm
3	0-8	Gray sand with some silt	Tsm
	8-27.5	Dark gray silty sand	Tsm
4	0-6	Gray silty sand with fine gravel	Qs
	6-15	Olive yellow silty sand	Tsm
	15-17	Gray sand	Tsm
	17-31	Dark gray silty sand with some gravel	Tsm
5	0-6	Olive gray silty sand with some gravel	Qs
	6-23	Olive yellow silty sand with some gravel	Tsm
	23-30	Olive gray sand with gravel to 3/4 in.	Tsm
	30-85	Olive gray sand	
6		(not drilled)	
7	0-3	Olive gray silty sand	Qs
	3-13	Yellow brown sand	Tsm
	13-32	Yellow brown gravelly sand	Tsm
8	0-1.5	Olive yellow sandy silt	Qs
	1.5-12	Light brown gravelly sand with some silt and shells, becoming gray with clay pockets at 6 ft	Qs
	12-17	Yellow brown sand	Tsm
	17-33	Yellowish gravelly sand with some silt	Tsm

a. Qs = Quaternary Sediments
Tca = Capistrano Formation
Tsm = San Mateo Formation

APPENDIX 2.5Q

Table 2.5Q-8
SUMMARY LOGS OF BORINGS
BY WOODWARD-CLYDE CONSULTANTS (Sheet 2 of 2)

Boring No.	Depth (ft)	Description	Interpretation[a]
9	0-3	Gray silty sand with sandy silt	Qs
	3-16	Light gray sand with shells	Qs
	16-27	Light gray gravelly sand with some silt	Tsm
	27-33	Dark gray silty sand with gravel and clay pockets	Tsm
10	0-13	Dark gray sandy silt	Qs
	13-20.5	Light gray silty sand with shells	Qs
	20.5-33.5	Dark gray silty clay	Qs
	33.5-58	Gray gravel and cobbles with shells	Qs
	58-130	Dark gray to black silty clay (stiff to hard) with foraminifera at 122-133 ft: Delmontian (Late Miocene)	Tca
	130-152	Very dense olive green sandy silt	Tca
	152-170	Gravel	Tsm
	170-338	Very dense olive green silty sand	Tsm

Table 2.5Q-9
MICROFOSSIL ANALYSIS BY ANDERSON-WARREN & ASSOCIATES OF
SAMPLES FROM BORING 10 OF WOODWARD-CLYDE CONSULTANTS, 1978

San Onofre B-10 (Core) (122-123 ft)

Bolivana sinuata var. (C), B. spissa (C), Bulminella curta (R), Cassidulina californica (R), C. cushmani (F), C. translucens var. (CA), Cibicides mckannai var. (C), Gyroidina roundimargo (VR), Nodogenerina sp. (VR), Nodosaria sp. (VR), Planulina ariminensis (R), Pulvinulinella pacifica (RF), Uvigerina peregrina (C), U. subperegrina (C), Valvulineria araucana (R), Cancris sp. (R).

AGE: Provincial Late Mocene, Delmontian Stage

ENVIRONMENT: Upper Bathyal

REMARKS: The presence of Bolivina sinuata var., Cassidulina translucens var., Cibicides mckannai var., and Uvigerina subperegrina indicate that this core is Late Miocene, Delmontian in age.

The timing of displacement on the Cristianitos fault has been established by its relationship with sedimentary formations. The Monterey and older formations show no evidence that the fault was present during their deposition. In the case of the Monterey Formation there are several areas where thinly bedded strata, including laminated diatomite, are exposed adjacent to the fault with no evidence of a topographic break in the sea floor during deposition. The initiation of displacement on the Cristianitos fault created a west-facing submarine scarp and caused a change in depositional environment marked by the contact between the Monterey Formation and overlying Capistrano Formation. The Capistrano and San Mateo Formations occur only west of the Cristianitos fault. In exposures close to the fault, the San Mateo Formation (actually a member of the Capistrano Formation) consists of coarse-grained sandstone which grades westward into siltstone and mudstone within the interior of the Capistrano Embayment. The sandstone was deposited as submarine fans along the fault. The submarine fan features exposed in the cliffs along San Clemente State Beach are described by Walker (1975) and Hess (1979). Similar sandstone of submarine fan origin mark the west side of the Capistrano Embayment. Their features in the Dana Point area are described by Bartow (1966, 1971) Normark and Piper (1969), Piper and Normark (1979) and Normark (1979). The change from the depositional environment of the Monterey Formation to that of the Capistrano Formation, which marks the start of displacement on the Cristianitos fault and development of the Capistrano Embayment, occurred during the Late Miocene about 10 million years ago based on the dating of microfossil assemblages (Ehlig, 1979a).

The subsidence of the Capistrano Embayment relative to the Peninsular Ranges to the east was controlled primarily by normal faulting on the Cristianitos fault. The relative subsidence ceased by mid-Pliocene (Ehlig, 1979a), from which we infer that movement on the Cristianitos fault stopped about mid-Pliocene time. The ocean regressed from the Capistrano Embayment during the Late Pliocene as shown by the transition from shallow marine deposits to nonmarine deposits in the Niguel Formation. Since late Pliocene, north-south compression has caused broad warping of the embayment with the southern part uplifted more than the northern part.

Displacement on the Cristianitos fault varies along its trace as determined from the stratigraphic separation of formations exposed along it and from structure contour maps and cross-sections prepared from subsurface data by West (1979). The maximum stratigraphic separation is about 4000 feet near the center of the embayment northeast of San Juan Capistrano. The separation diminishes both to the north and to the south of this area. The separation is less than 1000 feet in the north part of the embayment northeast of El Toro and decreases to zero where the Cristianitos fault dies out in the Santa Rosa Mountains. Displacement along the southern half of the fault decreases southward to about 1000 feet in the vicinity of San Onofre (West, 1979, cross-section K-J). The decrease in stratigraphic separation continues in a seaward direction as indicated by the fact that strata on the eastern upthrown side of the fault are downwarped in a seaward direction in exposures along the coast whereas those to the west on the downthrown side of the fault are nearly flat lying. Offshore profiles (S-22, WC-839 and WC-841) suggest that the Cristianitos fault dies out within 6000 feet of the coast.

APPENDIX 2.5Q

The stratigraphy seaward of San Onofre is best understood by examining the logs of borings and samplings at the site and offshore. Comparison of that data with selected high-resoluton seismic profiles leads us to the following interpretations:

1. The San Mateo Formation west of the Cristianitos fault extends offshore from the site more than 10,000 feet. It interfingers with siltstone and claystone of the Capistrano Formation, as indicated by Woodward-Clyde Consultants' 1978 Boring Nos. 1 and 10.

2. Quaternary sediments overlying the San Mateo Formation are only a few feet thick within 7000 to 8000 feet of the coast, and are essentially absent over much of the sea floor in that interval.

3. In the vicinity of Woodward-Clyde Consultants' 1978 Boring No. 10, and seaward of Fugro's line SNO-3, the Quaternary sediments are approximately 60 feet thick and represent three generations of marine-terrace erosion and deposition. These sediments are probably younger than 125,000 years, but some of them may be significantly older than 11,000 years.

4. The Monterey Formation underlies the San Mateo Formation in the San Onofre site at a depth of about 900 feet. Offshore the top of the Monterey Formation (Horizon B approximately) reaches depths on the order of 3000 feet.

5. The Monterey Formation and the San Onofre breccia are exposed at the ground surface east of the Cristianitos fault just inland of San Onofre State Beach. East of the fault the Monterey extends seaward several thousand feet with a thin cover of Quaternary sediments. Farther offshore, the Monterey Formation is probably overlain by strata that are laterally equivalent to the San Mateo and Capistrano Formations.

2.5Q.5 CONCLUSION

Based on an integrated interpretation of onshore and offshore geologic and geophysical data, it is concluded that no connection exists between the Cristianitos fault and the OZD.

The reasons for this are as follows:

1. Although the Cristianitos fault projects offshore from its seacliff exposure, it cannot be identified in nearshore seismic reflection profiles farther than about 6000 feet seaward along the strike of the fault. In view of the onshore evidence for southerly-decreasing displacement on the Cristianitos fault, the fault is interpreted to die out along the strike within a few thousand feet of the coast, and it does not connect with the OZD.

2. The only faults that might be considered as candidates for seaward extension of the Cristianitos fault are those that are in approximate alignment with the Cristianitos but which are identified only in seismic reflection profiles approximately 8500 to 9500 feet south-east to south of the seacliff exposure. However, the offsets on these faults are opposite in sense of displacement to those on the Cristianitos fault, and they are apparent only in the acoustic basement. They do not offset significantly higher horizons, and their trend is about north 10 to 15 degrees east. They are unrelated to the Cristianitos fault.

This conclusion that no connection exists between the Cristianitos fault and the OZD has persisted from the earliest offshore investigation for San Onofre, despite somewhat different interpretations by several investigators utilizing various types and generations of data.

REFERENCES

1. Bartow, A. J., "Deep submarine channel in upper Miocene, Orange County, California," Journal Sed. Petrology, Vol. 36, pp 700-705, 1966.

2. Blake, M. C.; et al., "Neogene Basin Formation in Relation to Plate Tectonic Evolution of the San Andreas Fault System, California," American Association Petroleum Geologists Bulletin, Vol. 62, pp 344-372, 1978.

3. Ehlig, P. L. "The Late Cenozoic evolution of the Capistrano Embayment," cited in Fife, D. L. (ed), Geologic Guide of San Onofre Nuclear Generating Station and Adjacent Regions of Southern California, Pacific Section AAPG, pp A-38 - A-44, 1979.

4. Hess, G.R., "Miocene and Pliocene inner suprafan channel complex, San Clemente, California," cited in Stuart, C. J. (ed), A Guidebook to Miocene Lithofacies and Depositional Environments, Coastal Southern California and Northwestern Baja California, Pacific Section SEPM, pp 43-51, 1979.

5. "Miocene Stratigraphy and Depositional Environments of San Onofre Area and Their Tectonic Significance," cited in Stuart, C. J. (ed), A Guidebook to Miocene Lithofacies and Depositional Environments, Coastal Southern California and Northwestern Baja California, Pacific Section SEPM, pp 43-51, 1979.

6. Normark, W. R. and Piper, D. J., "Deep-Sea Fan-Valleys, Past and Present," Geological Society of America Bulletin, Vol 80, pp 1859-1866, 1969.

7. Normark, W. R. "Doheny Channel and the Neogene Capistrano Submarine Fan," cited in Stuart, C. F. (ed), A Guidebook to Miocene Lithofacies and Depositional Environments, Coastal Southern California and Northwestern Baja California," Pacific Section SEPM, pp 43-51, 1979.

8. Piper, J. W., and Normark, W. R., "Reexamination of a Miocene Deep-Sea Fan and Fan-Valley, Southern California," Geological Society of America Bulletin., Vol 82, pp 1823-1830, 1971.

9. "The Doheny Channel, A Miocene Deep-Sea Fan-Valley Deposit, Dana Point, California," cited in Bergen, F. W., et al., (eds), Geologic Guidebook, Newport Lagoon to San Clemente, California, Soc. Econ. Paleontologists and Mineralogists, Pacific Section, pp 43-49, 1971.

10. Walker, "Nested Submarine-Fan Channels in the Capistrano Formation, San Clemente, California," Geological Society of America Bulletin, Vol 86, pp 915-924, 1979.

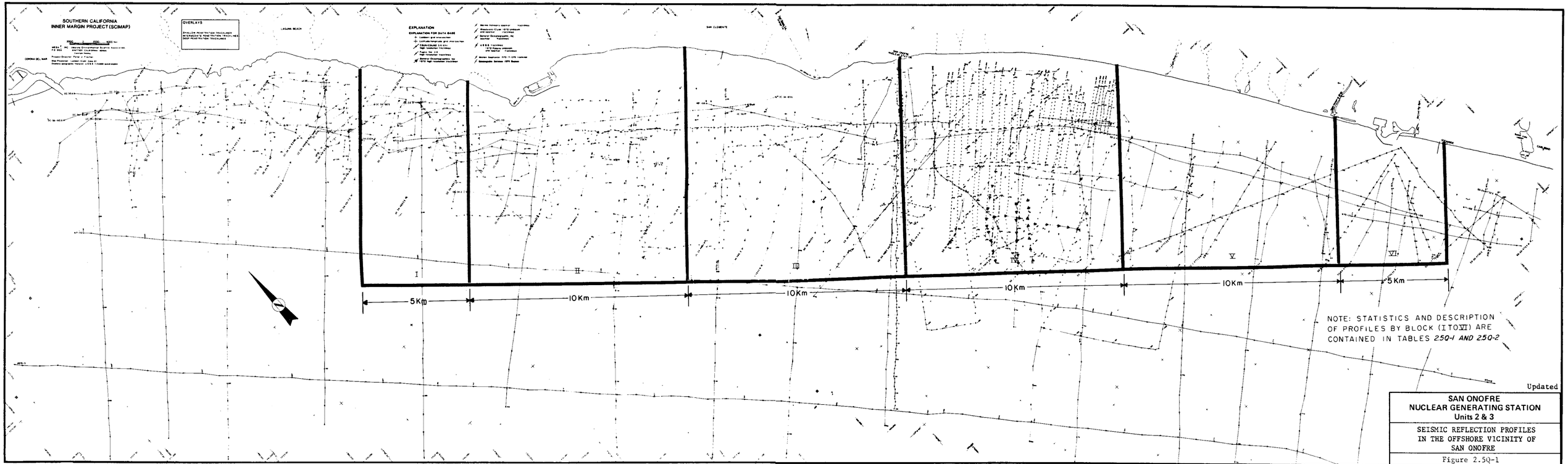

Updated

SAN ONOFRE NUCLEAR GENERATING STATION
Units 2 & 3

SEISMIC REFLECTION PROFILES IN THE OFFSHORE VICINITY OF SAN ONOFRE

Figure 2.5Q-1

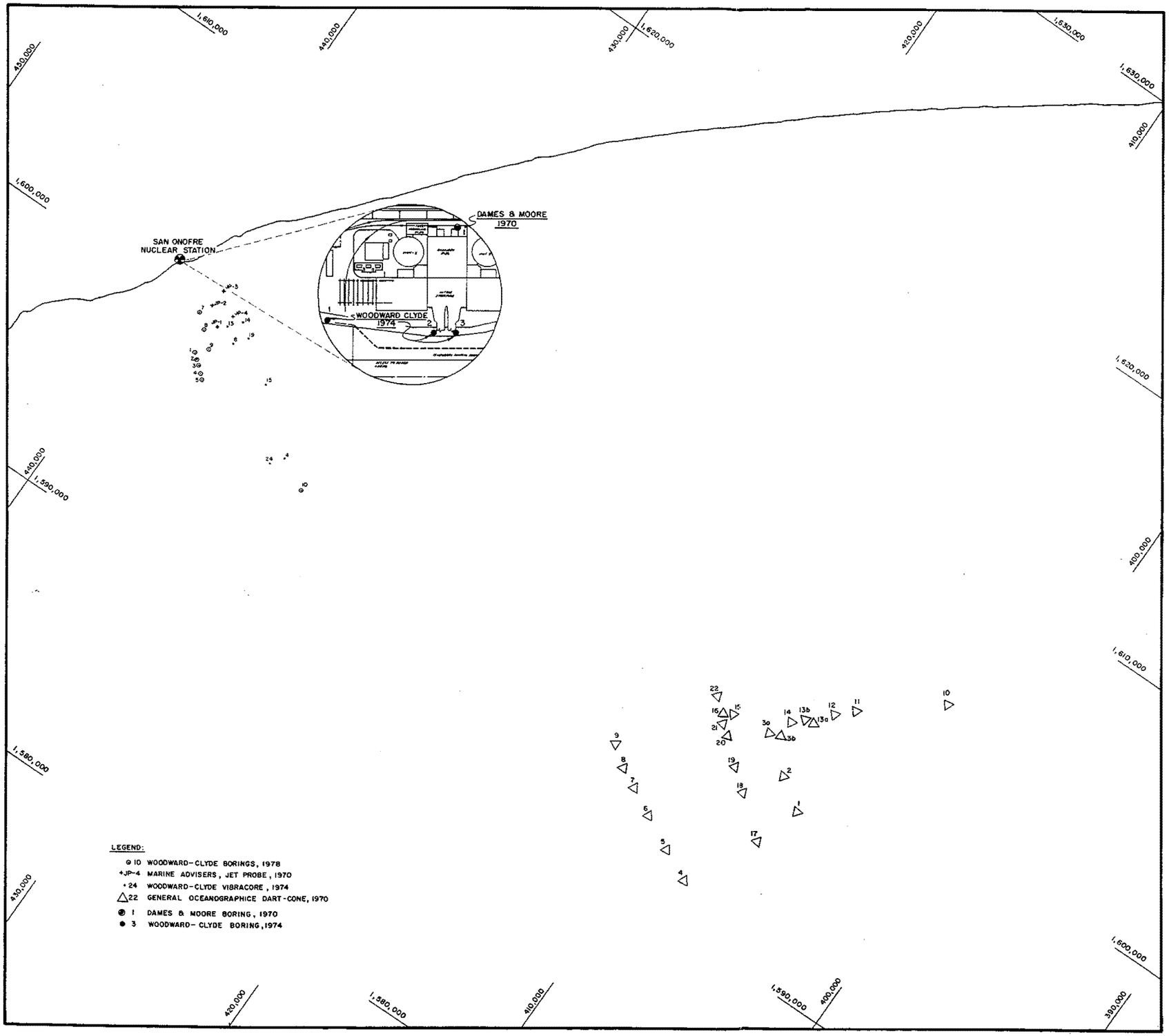

Updated

SAN ONOFRE
NUCLEAR GENERATING STATION
Units 2 & 3

BORINGS, DART-CORES AND VIBRACORES
IN THE VICINITY OF SAN ONOFRE

Figure 2.5Q-2

APPENDIX 2.5R

EVALUATION OF MAXIMUM EARTHQUAKE ON HYPOTHESIZED OFFSHORE ZONE OF DEFORMATION

Site File Copy

APPENDIX 2.5R

CONTENTS

TABLES

FIGURES

APPENDIX 2.5R

EVALUATION OF MAXIMUM EARTHQUAKE ON HYPOTHESIZED OFFSHORE ZONE OF DEFORMATION

Several methodologies were considered in evaluating the maximum earthquake applicable to the hypothesized Offshore Zone of Deformation (OZD). The specific approach of the Woodward-Clyde Consultants (WCC) June 1979 report uses both a qualitative comparison of features, such as maximum historic earthquake, fault rupture length, total displacement, and degree of deformation, as well as a quantitative comparison of slip rate on faults as a means of differentiating and ranking faults and evaluating the earthquake potential of the hypothesized OZD. The applicants also evaluated rupture-length versus magnitude, and displacement-per-event versus magnitude relationships; however, use of either of those methodologies alone is not appropriate based upon the uncertainties in the data base available for the hypothesized OZD. The degree-of-fault-activity approach as presented in June 1979 and as supplemented in this appendix and appendix 2.5S, section 2.5S.5, is neither a new nor unconventional methodology and is neither independent of, nor is it meant to replace other methods of estimating maximum magnitude. The approach extends existing knowledge and provides a viable alternative to other methods when absence or sparsity of data limits the usefulness of other methods, especially for en-echelon systems.

Section 2.5R.1 includes additional information concerning the basis for selection of degree-of-fault-activity methodology and the applicability of other methodologies to the hypothesized OZD. In addition, section 2.5R.1 places in perspective the role of the slip rate-maximum magnitude relationship in comparison with other fault parameter relationships used in the degree-of-fault-activity methodology.

In response to the NRC's request for comparison of the results of the applicants' methodology with the results from conventional methods, it is worthy of note that the Construction Permit stage assessment of the hypothesized OZD was partially based on ranking of faults (Atomic Safety and Licensing Board Initial Decision in the matter of San Onofre Nuclear Generating Station Units 2 and 3, Construction Permit Stage, Docket Nos. 50-361 and 50-362, October 15, 1973, pp 75-81). As noted in section 2.5R.1 and the June 1979 WCC report, ranking of faults is the basis for the subject methodology. The fact that the site design parameters determined at the PSAR stage are consistent with the results of the current fault ranking approach (degree-of-faults-activity approach) provides a measure of comparison between the two studies. A comparison between magnitudes predicted using the degree-of-fault-activity approach and magnitudes assigned to other faults based on the fault length-magnitude methodology is provided in section 2.5R.2.

Section 2.5R.3 provides a comparison of probabilistic risk on the hypothesized OZD with the San Andreas and San Jacinto fault zones and provides further demonstration of the conservatism of the applicants' assessment of

Amended: April 2009 TL: E048000

the hypothesized OZD. Section 2.5R.4 compares the expected geologic effects for several hypothetical maximum magnitudes with the observed geologic evidence along the hypothesized OZD.

Applicants consider magnitude 6.5 to be a conservative maximum magnitude based on consideration of degree-of-fault-activity, maximum realistic rupture length, fault ordering, and historic seismicity. However, the applicants recognize that some of those responsible for review of the project geology/seismology would value presentation of assessment of the site geoseismic setting in terms of a magnitude 7 event on the hypothesized Offshore Zone of Deformation.

2.5R.1 DEGREE OF FAULT ACTIVITY METHODOLOGY

The general approach used in the WCC June 1979 report for the assessment of the maximum earthquake is to consider a fault-ranking in terms of degree-of-activity of the hypothesized OZD relative to other faults in the southern California tectonic province and in similar tectonic settings throughout the world. Generally, a degree-of-activity approach considers: relative behavior of faults, particularly in terms of strain or slip rates; the size, periodicity, and energy release of seismic events; the mechanical and compositional properties of the faults; and the tectonic setting. This approach for a specific fault considers evidence of fault behavior in the following steps:

A. The tectonic setting and style of the fault is defined.

B. Fault activity parameters are compiled for faults within the tectonic province, including the fault of interest. For this purpose, all faults which have experienced displacement during the currently active tectonic stress regime should be considered "active." The fault activity factors most accessible and germane to characterize the difference in degree-of-fault-activity include: slip rate, stress drop, recurrence for large slip events, slip per event, fault rupture length, and tectonic setting.

C. The degree-of-activity parameters are compared so that the fault of interest is placed in context relative to other faults. From this context, a limit for the maximum magnitude can be estimated for each fault.

Techniques such as using fault-length versus magnitude or amount-of-surface-displacement versus magnitude incorporate the range of values for active faults in estimating a maximum earthquake. Typically, however, only one or two aspects of fault behavior are considered in these conventional methods. Such singular approaches fail to describe the complexities of fault behavior; for example, the effect of differing rates of slip on the maximum earthquake associated with faults of similar length is not taken into consideration. Therefore, the degree-of-fault-activity methodology evaluates characteristics of the hypothesized OZD and presents an approach comparing those characteristics to other faults.

Amended: April 2009 TL: E048000

APPENDIX 2.5R

The specific approach of the WCC June 1979 report uses both a qualitative comparison of features, such as maximum historic earthquake, fault rupture length, total displacement, and degree of deformation, as well as a quantitative comparison of slip rate on faults as a means of differentiating and ranking faults and evaluating the earthquake potential of the OZD. The type of tectonic regime considered is limited to a strike-slip environment. The result of this analysis is shown in Figure 7 of the WCC June 1979 report and indicates that the maximum historic earthquake of magnitude M_s 6.3 is very close to the maximum earthquake possible for the Newport-Inglewood Zone of Deformation. Further refinements and additional data points have been incorporated in the data base originally used for Figure 7, and a revised slip rate versus magnitude graph has been prepared as discussed in appendix 2.5S, section 2.5S.5.

The method used in this approach is an extension of existing techniques in the seismic hazards literature. Slemmons (1977) has described interrelationships among fault-slip rates, recurrence intervals, and earthquake magnitude.

Matsuda (1975, 1977) uses geologic slip rates to classify faults and to evaluate recurrence intervals of large magnitude earthquakes. Cluff (1978) and Packer and Cluff (1977) have described differences in relative degree of activity in terms of slip rate, recurrence interval, and slip per event. Brune (1968) has used seismic moments of earthquakes to obtain average rates of slip on major fault zones. Anderson (1979) extends this analysis to estimate recurrence using geologic slip rate. Molnar (1979) relates these seismic slip rates to geologic and geodetic slip rates and establishes a procedure for estimating return periods for earthquakes with certain moment values. Smith (1976) uses the geologic slip rate to obtain the average rate of seismic activity and to limit the maximum earthquake that can be expected to occur along the fault. In reviewing known methods of estimating maximum magnitude, Chinnery (1978) suggests that the use of slip rate in the context of Smith (1976) is one of the most reasonable. Each of these authors utilizes relationships among various measures of fault activity in a manner similar to that used in the WCC June 1979 report.

Various methods for evaluating maximum magnitude are employed in the state-of-the-practice of seismic hazards analyses (Slemmons, 1977). These methods include several empirical relationships such as historic rupture length versus magnitude, maximum displacement during a single historic event versus magnitude, and maximum magnitude estimates based on tectonic setting and simple ranking of faults. These "conventional" techniques and their applicability to estimating maximum earthquakes are discussed in subsections 2.5R.1.1 through 2.5R.1.3. Subsection 2.5R.1.4 discusses the application of these methods to the OZD.

2.5R.1.1 RUPTURE LENGTH VERSUS MAGNITUDE CORRELATION

The rupture length versus magnitude method consists of correlating the empirical relationship between the fault rupture lengths for various historical earthquakes and the magnitudes of these events. The length is

measured either by the observed surface rupture length or (in some analyses) by the aftershock zone. Attempts to refine the method have included adding more rupture-length data to the data set. These additional data are interpreted from:

- Rupture lengths calculated from tsunami generation, (Abe, 1973; Acharya, 1979)
- Geodetic data
- The rupture area of the fault surface based on assumed depth and length of an aftershock zone

Although considerable effort has been put into refining the data base, several difficulties persist. First, the regression lines used to estimate earthquake magnitudes for a given rupture length are averages based on least-squares regressions, so about half of the data points lie below the regression line and half above (Marck, 1977). The conservatism in the analysis is usually introduced by combining as many fault segments as possible to provide a maximum length for the analysis, as in the case of long en-echelon fault systems. This is often arbitrary and leads to arbitrary results. Second, the fault length versus magnitude realtionship varies significantly with tectonic province (Acharya, 1979) and style of faulting (Bonilla and Buchanon, 1970; Slemmons, 1977) (figure 2.5R-1), yet no attempt has been made to account for combinations of these variations in general applications of the rupture length versus magnitude technique. Third, there is always a major uncertainty in estimating the maximum potential rupture length of a fault being investigated, as will now be discussed.

Most conventional rupture length versus magnitude applications assume that half the total mapped fault-length is a conservative rupture length for estimation of maximum earthquakes. This half-length approach was proposed many years ago by Albee and Smith (1966) and Wentworth and others (1969) who argue that rupture of half the length of a fault, or less, is more likely than rupture of the entire fault; this belief is based on historic surface ruptures in southern California. However, in North America historic ruptures have broken from 2% to more than 75% of the total fault length (Wentworth and others, 1969). In addition, some Japanese earthquakes appear to have been accompanied by rupture of the entire mapped fault lengths and, in one case (Tottori earthquake, Japan, 1943) the rupture was longer than the mapped fault (Bonilla, 1979). Thus, a uniform application of half-length (or one-third length, or any other fault length) fails to account for the wide range in fault behavior.

Although advances have been made in the understanding of fault behavior since the formulation of the rupture length method, it is still difficult to estimate the maximum rupture length that can be reasonably expected on a fault. Despite these difficulties and without other information, the choice of half or a third the fault length is still, in practice, presumed to be a reasonable and conservative method for estimating a maximum earthquake.

When using a half-length, third-length, or any other length-defined method of estimating maximum magnitude, it is often difficult to estimate the full length of the fault to which the method is applied. The details of fault rupture processes are not sufficiently understood to assess how readily fault systems with relatively short, discontinuous surface traces can produce lengthy ruptures and large-magnitude earthquakes; and it is not known how effective en-echelon breaks in fault zones are in creating barriers to propagation of fault ruptures. For example, several major en-echelon fault segments comprise the San Jacinto fault zone, which has ruptured essentially over its entire length in historic time, although the individual historic earthquakes have not approached rupturing half or even one-third the entire length. In fact, one of the segments, the Coyote Creek fault, appears to rupture as an independent segment with frequent lower-magnitude earthquakes rather than as a part of the entire zone during one large earthquake (Slemmons, 1977). This type of behavior for en-echelon systems may be very typical for other en-echelon faults in California, such as in the hypothesized OZD.

2.5R.1.2 DISPLACEMENT-PER-EVENT VERSUS MAGNITUDE CORRELATION

The displacement/magnitude relationship method compares the empirical correlation of maximum observed surface displacement for a single earthquake to the corresponding earthquake magnitude. To apply this technique to a given fault, either observations of displacements during historic events or geologic data on prehistoric events are required for the fault in question. Typically, this requires data from numerous locations along the fault because amounts of surface displacement during earthquakes are often highly variable along the fault trace. Such data are available for only a few faults.

Several difficulties exist in applying the displacement versus magnitude relationship. First, ideal geologic conditions must exist to preserve displacement per event occurrences. Second, the maximum surface displacement measured for any particular earthquake may not be the characteristic displacement, or may represent an exaggeration of net tectonic displacement. Examples include: (1) the 1976 Guatemala earthquake, with an average surface displacement of 1.0 meters, but with a maximum displacement in one location of about 3.4 meters (Bucknam and others, 1976); and (2) the 1954 Dixie Valley earthquake where the maximum surface displacement was approximately 20% greater than the maximum tectonic displacement because of graben formation and deformation of the down-thrown block (Slemmons, 1957). Because definitive data on displacement per event cannot be obtained for the hypothesized OZD, this approach is not directly applicable to estimate a maximum magnitude for the zone.

2.5R.1.3 RANKING OF FAULTS

Ranking of faults covers a broad range of possible systems for differentiating faults. Among conventional ranking systems are:

- Relative geomorphic expression of the faults being ranked
- The relative importance of a fault in its structural-tectonic setting
- Relative rates of deformation

Typically, such techniques do not provide a unique maximum earthquake magnitude but often provide ranges of probable earthquake magnitudes for different categories or rankings of faults. Such ranking, however, serves to help evaluate maximum earthquake estimates from the length and displacement methods. In general, ranking of faults is a comprehensive approach which does not rely on a single characteristic of a fault for evaluation of earthquake potential.

One method of ranking faults is by geologic slip rate; this method is particularly useful because it describes quantitatively the relative degree of activity of faults in their present tectonic setting, and it incorporates properties of the mechanics and behavior of faults, including strain accumulation, strain release in earthquakes, and recurrence intervals of earthquakes. Because geologic slip rates average fault displacement during a relatively long time interval, the behavior of faults in the past can be evaluated and projected into the future.

2.5R.1.4 APPLICABILITY OF METHODOLOGIES TO THE OZD

The nature of the OZD is reviewed below to evaluate the application of the fault-length methodology to the zone. The Newport-Inglewood Zone of Deformation (NIZD), South Coast Offshore Zone of Deformation, and the Rose Canyon Fault Zone are collectively known as the hypothesized Offshore Zone of Deformation which is collectively about 200 km in length extending from the Santa Monica Mountains to offshore near the international border. It is best described as a zone of deformation because it is characterized onshore and offshore by a series of en-echelon faults and folds, rather than by a continuous zone of faulting. Greene (1980) states that a through-going fault has not been defined and continuity of the en-echelon traces is not demonstrated; this is similar to many other California faults composed of short en-echelon faults. The longest single uninterrupted faults in the OZD extend no more than 40 km (Greene, 1980). The en-echelon nature of the hypothesized OZD raises valid questions regarding the ability of the rupture to propagate from fault trace to fault trace. The difficulty in interpreting a magnitude based on fault-length methodologies for the hypothesized OZD is the uncertainty of the maximum length of potential rupture during a maximum earthquake on the zone.

Amended: April 2009 TL: E048000

Therefore, the length methodology cannot rationally be applied to the hypothesized OZD. However, the reasonableness of the maximum magnitude for the hypothesized OZD can be evaluated by comparing rupture length associated with that magnitude with the physical characteristics of the OZD as discussed in section 2.5R.4.

The displacement-per-event versus maximum magnitude relationship cannot be applied to the hypothesized OZD because surface traces of the fault are poorly developed along most of the onshore portions of the zone and estimates of past displacements are unavailable. Furthermore, the lack of continuous dramatic surface expression can be used to imply that large displacements, and accompanying large earthquakes, either do not occur on or have not occurred recently on the Newport-Inglewood Zone of Deformation and Rose Canyon Fault Zone.

Because of the difficulties in applying the fault length and displacement correlation methods to evaluating the maximum earthquake on the hypothesized OZD, the Applicants evaluated the earthquake potential by using a quantitative fault-ranking criterion, slip rate. The slip rate ranking method uses maximum, rather than average, values to estimate magnitude. Furthermore, it deals more directly with the earthquake process than other methods by relating and analyzing measures of strain accumulation and release. This method provides an alternative to the length and displacement methods when available data limit or prevent their use.

2.5R.2 SLIP RATE COMPARED TO HALF-LENGTH METHOD

The slip rate versus maximum-magnitude method of the degree-of-activity approach has been specifically applied to a comparison of strike-slip faults in Southern California. The empirical relationship between slip rate and magnitude defined by Southern California faults appears to hold for strike-slip faults in similar tectonic environments in other parts of the world. Some variations appear to occur when different tectonic environments are considered. As a test of the slip rate versus maximum-magnitude relationship, the results of the slip-rate method are compared to the half-length maximum-magnitude method in the following paragraphs. The result is a synthesis plot of slip rate versus maximum-magnitude based on half lengths using the Slemmons (1977) rupture-length versus magnitude correlation (figure 2.5R-1) for strike-slip faults. The synthesis is based on half-length rupture because half the total fault length is often considered to be a conservative estimate (for that portion of the fault that may rupture during the largest earthquake a fault can generate) when applying the rupture length-magnitude relationship. This synthesis plot is closely comparable to empirical bounding limit shown in figure 7 of the WCC June 1979 report, as discussed below.

The slip rate approach to estimating magnitude can be compared to the half-length method if a relationship between slip rate and half-length can be established. Menard (1962) and Renalli (1977) have shown that a

positive correlation exists between total displacement on a fault and its total length. Since slip rate is related to displacement by time (Rs = D/T), a possible correlation between slip rate and length is suggested.

To investigate this possibility, a log-log plot of selected slip rate versus length (in this case, half-length) has been constructed (figure 2.5R-2). A least-squares regression analysis of half-length as a function of slip rate (both expressed as logarithms) was calculated to produce a "best fit" line through the data and to evaluate the correlation of the variables. For the 31 pairs of data, for which both slip rate and length are relatively well known, a correlation coefficient of 0.730 was calculated. Thus, the data suggest a positive correlation between slip rate and fault-length.

Slemmons (1977) used the same regression technique to establish a widely accepted relationship between rupture length and magnitude. The correlation coefficient for slip rate versus half-fault length is comparable to the 0.775 correlation coefficient resulting from the Slemmons (1977) plot of rupture-length versus magnitude for strike-slip faults (figure 2.5R-1). It seems reasonable to synthesize the slip rate-length relationship and the rupture length-magnitude relationship of Slemmons (1977) in order to develop a slip rate-magnitude comparison for strike-slip faults.

Slemmons' (1977) relationship can be expressed:

$$M = 4.651 + 0.587 \ln L_R$$

where:

M = magnitude

L_R = rupture length

The relationship of half-length to slip rate shown on figure 2.5R-2 can be expressed:

$$L/_2 = 48.1\ R_s\ 0.620$$

where:

$L/_2$ = half length

R_s = slip rate

If half length of the fault is taken as the potential rupture length, then $L_{1/2} = L_R$.

Amended: April 2009 TL: E048000

Combining the two relations,

$$M = 4.651 + 0.587 \ln (48.1 R_s^{0.620})$$

This line represents a slip rate versus maximum-magnitude curve synthesized through consideration of the half-length method. The line is shown as the synthetic earthquake line (SEL) in figure 2.5R-3.

The degree-of-fault-activity approach, as described in section 2.5R.1, is an alternative method for evaluating maximum magnitude using available slip rate data to derive an estimated upper bound limit for possible earthquakes on the hypothesized OZD consistent with behavior on other faults. As discussed in the WCC June 1979 report, these data support a maximum magnitude of 6.5. The approach shown in 1979 represents one interpretation of the data set in order to derive a conservative estimate of maximum magnitude. Since preparation of the WCC June 1979 report, the Applicants have continued the data review and have augmented the data base, as described in section 2.5S.5. The most representative slip rate values and their associated maximum historical earthquake magnitude for selected faults are plotted in figure 2.5R-4. Also shown are several faults with no large historical earthquakes. The selection criteria for these data are discussed in section 2.5S.5.

A line can be drawn bounding these empirical observations as shown in figure 2.5S-3 and defined as the maximum historic earthquake limit (HEL). This line suggests that there is a consistent limit to the size of an earthquake associated with the geologic slip rate of a strike-slip fault. This assumes that some of the strike-slip faults in the world have had maximum or close-to-maximum earthquakes and that when their maximum data points are enveloped they form a maximum earthquake limit related to slip rate.

The empirical data line (HEL) is compared to the line derived from half-length ruptures related to slip rate (SEL, figure 2.5R-4). The synthesis line based on half-length ruptures has a slightly steeper slope than the empirical line and indicates that slightly larger magnitudes may occur in the lower slip rate range. However, the lines are generally compatible and their comparison suggests that the empirical plot is reasonably conservative when compared to the results of half-length.

The conservatism of the slip rate versus magnitude data set is further investigated by considering the ranges of slip rate and magnitude data obtained from published and unpublished sources. These data, presented in section 2.5S.5 provide for assessment of uncertainty in the data interpretation.

Based on the evaluation of uncertainty of slip rate and magnitude data as described in section 2.5S.5, a maximum earthquake line (MEL) was obtained (figure 2.5S-4). In order to demonstrate the consistency of the results of fault length versus magnitude methodology with degree-of-fault-activity results, figure 2.5R-4 compares these three lines, the SEL, MEL and HEL.

APPENDIX 2.5R

2.5R.3 EARTHQUAKE RECURRENCE

In a collective sense, seismic activity on a group of faults is well described by the magnitude-frequency relationships

$$\text{Log } N = a - bM$$

where:

N is the number of earthquakes of magnitude M and larger occurring within a defined time interval for the group of faults or portion of the earth's surface containing a group of faults. Using this relationship leads directly to numerical estimates for return period as a function of magnitude for the zone.

Significant uncertainties exist in how this relationship should be applied to a single fault. Detailed geologic evidence for earthquake recurrence has only recently been developed for a few faults: for example, Sieh (1978) suggests that, for the central San Andreas fault, episodes of major displacement occur about every 160 to 240 years. The actual magnitudes of earthquakes producing these episodes are not known. Historical seismicity data appear to be generally inadequate and unreliable in constraining the parameters of the magnitude-frequency relationship for large magnitude earthquakes on a single fault. The frequency of occurrence of earthquakes of a specific magnitude on a fault appears to be highly variable and may be related to cyclic periods of activity and inactivity lasting many tens to hundreds of years. Thus, the geologic and historical data available in California for the past 50 to 180 years primarily provide evidence for consistency with a recurrence model, but do not provide the basis for constructing the model.

An alternative approach to estimating earthquake recurrence is to assume a form of the magnitude-frequency relationship and to distribute the total amount of seismic moment on the fault within the range of possible earthquakes. The assumptions made for this analysis are the following:

A. The total moment rate on a fault is given by the product of the length of the fault zone and the geologic slip rate. The lengths and moment rates for several southern California faults are listed in table 2.5R-1.

B. All of the displacement is considered to occur seismically.

C. The magnitude-frequency relationship is considered to be linear with an assumed slope of - 0.85 up to the maximum magnitude assigned to the fault. This slope is selected to be typical for the southern California tectonic setting and seismicity.

D. Several possible values for maximum magnitude are considered and are shown in table 2.5R-2.

Amended: April 2009 TL: E048000

Table 2.5R-1
FAULT AND SEISMICITY PARAMETERS

Fault	Slip Rate (mm/yr)	Maximum Historic Magnitude (m_s)	Historic Observation Period	Total Fault Length	Total Fault Width	Moment Rate (dyne-cm/yr) $x10^{23}$	
Sumatra	67.	7.6	81	1650	15	49747.50	
Fairweather	58.	7.9	80	1150	15	30015.00	
Central San Andreas	37.	8.2	200	330	15	5494.50	Group
Denali	35.	(a)	100	2150	15	33862.50	1
Totschunda	33.	(a)	100	150	15	2227.50	
South San Andreas	25.	6.5	200	225	15	2531.25	
North San Andreas	20.	8.3	200	435	15	3915.00	
San Gregorio-Hosari	16.	6.1	138	375	15	2700.00	
Darvaz	13.	(a)	100	700	15	4095.00	
Calaveras-Paicines	12.	6.6	130	171	15	923.40	
Bocono	9.75	8.0	167	500	15	2193.75	
Garlock	8.	(a)	200		15	954.00	
San Jacinto	8.	7.1	130	260	15	936.00	
Jordan-Dead Sea	6.5	7.5	142	800	15	2340.00	Group
North Anatolia	7.	7.9	200	1180	15	3717.00	2
Hayward-Healdsburg	6.	6.7	200	205	15	553.50	
Motagua	6.	7.5	206	700	15	1890.00	
Clarence-W. Wairarapa	4.8	7.6	141	430	15	928.80	1710
Awatare-Wellington	4.	7.1	141	547	15	984.60	(mean)
Hope-E. Wairarapa	4.	6.7	141	418	15	752.40	
Kopet-Dagh	3.6	7.3	84	600	15	972.00	
Calico	3.4	(a)	130	129	15	197.37	
Sheep Hole-Ludlow	3.4	(a)	130	106	15	162.18	
Helendale	3.	(a)	130	105	15	141.75	
Pinto Mountain	3.	(a)	130	85	15	114.75	
Talemazar	2.5	(a)	100	300	15	337.50	
Dasht-e Bayas	2.4	7.2	100	80	15	86.40	Group
Big Pine	2.4	(a)	130	80	15	86.40	3
Elsinore-Laguna Sal.	2.3	6.	130	297	15	307.39	
Blue Cut	1.8	(a)	130	83	15	67.23	1520
Whittier	1.2	(a)	130	42	15	22.68	(total)
Collayami	1.	(a)	130	35	15	15.79	
OZD	0.50	6.3	167	200	15	45.00	
Antioch	0.10	4.9	130	58	15	2.61	

a. Maximum observed magnitude is less than 6.0.

APPENDIX 2.5R

Table 2.5R-2
RECURRENCE INTERVALS OF EARTHQUAKES ON
SOUTHERN CALIFORNIA FAULTS CALCULATED FROM MOMENT RATES

Faults (a)	Maximum Magnitude (b)	Recurrence Interval (c) (yr)				
		6.0	6.5	7.0	7.5	8.0
San Andreas (central segment)	8.0	5	13	30	80	200
	8.5 (MEL)	11	30	70	180	450
San Jacinto	7.5	16	40	100	260	
	8.0 (HEL)	36	90	230	570	1440
	8.3 (MEL)	60	150	370	930	2340
OZD	6.5 (DEL)	60	150			
	7.0 (MEL)	130	340	840		
	7.5 (hypothesized)	270	720	1910	5060	

a. Fault parameters are listed in table 2.5R-1.

b. Used only for calculation of 'a' value assuming b = 0.85; MEL and HEL defined on figure 2.5R-4 and figure 2.5S-4, DEL defined on Figure 7 of WCC June 1979 report.

c. For events within 0.25 units of the magnitude value listed.

Using these assumptions, the recurrence intervals (return periods) for possible earthquakes on the San Andreas fault, San Jacinto fault, and the hypothesized OZD are calculated and listed in table 2.5R-2. The method of Anderson (1979) was used to calculate the 'a' values. Using the 'a' and 'b' values, the numbers of earthquakes expected annually in the adjoining magnitude ranges 6.25 to 6.75, 6.75 to 7.25, and 7.25 to 7.75, are calculated. The inverses of these numbers are the recurrence intervals of earthquakes within the respective magnitude ranges. For simplicity, the ranges are denoted by their mean values (6.5, 7.0, and 7.5) in the table.

Several observations can be made about the consistency of the recurrence values in table 2.5R-2 with the geologic and historical data:

A. The value of maximum magnitude used in each calculation has an important impact on the recurrence. As illustrated in figure 2.5R-5, increasing the maximum magnitude by 0.5 magnitude units reduces the 'a' value by a factor of more than 2.0, assuming constant 'b' value. This effect is produced by the constant slip rate producing a constant average rate of release of seismic moment. Allowing the occurrence of larger earthquakes with large slip reduces the frequency of occurrence of all earthquakes on the fault.

Amended: April 2009 TL: E048000

B. The maximum value of 8.0 for the central San Andreas fault gives a recurrence time (200 years) that is reasonably consistent with the geologic data discussed above. The calculated recurrences of large earthquakes (M_s 6.0 to 7.5) are not reflected in the historical data, suggesting that the magnitude-frequency relationship for the San Andreas may not be correct in its parameters or functional form over the magnitude range 6 to 8.

C. For the San Jacinto fault, the predicted recurrence intervals using a maximum earthquake value of 7.5 are more consistent with the seismicity of the past 100 to 180 years than the longer recurrence times produced by maximum earthquakes in the range 8.0 to 8.3.

D. The occurrence of the 1933 earthquake (and possibly the 1800 and 1812 earthquakes) on the hypothesized OZD is consistent with recurrence intervals calculated for the maximum magnitude of 6.5. The low instrumental and historical seismicity of the offshore portions of the hypothesized OZD suggest that the slip rate value applied to these portions is possibly too high.

E. If the maximum magnitude for the OZD is hypothesized to be M_s 7.5, the recurrence times for smaller earthquakes are longer than the historical data would suggest. The lack of Holocene geologic evidence along the OZD for such large earthquakes is not consistent with the recurrence intervals tabulated for the hypothesized M_s 7-1/2 earthquake in table 2.5R-2.

In summary, the recurrence calculations presented above are consistent with maximum magnitude values less than the MEL values obtained from figure 2.5S-4 and listed in table 2.5R-2.

2.4R.4 EVALUATION OF PHYSICAL CONSERVATISM OF THE MAXIMUM EARTHQUAKE

This section evaluates the physical conservatism of hypothetical maximum earthquake magnitudes of M_s 6.5, M_s 7.0, and M_s 7.5 for the hypothesized OZD by considering how consistent the occurrence of such earthquakes is on the zone with the geologic, geophysical, and seismological environment of the zone. This examination uses the qualitative and quantitative factors included within the more general evaluation of degree of fault activity. For reference purposes, the table summarizing fault ranking of the San Andreas, San Jacinto, and Whittier-Elsinor faults, and the hypothesized OZD, presented in the September 13, 1979 meeting, is included in table 2.5R-3. More detailed information on the hypothesized OZD from north to south is summarized in table 2.5R-4.

Table 2.5R-3
SOUTHERN CALIFORNIA STRIKE-SLIP FAULT ZONES CHARACTERISTICS AND RANKING CRITERIA (Sheet 1)

Fault Zone Characteristics	San Andreas	San Jacinto	Whittier-Elsinore-Laguna Salada	Hypothesized OZD
Dimensions and Segmentation	Total length - 1300 km Imperial-Cerro Prieto segment - 180 km (Imperial Valley to Gulf of California) Southern segment - 225 km (Cajon Pass to Imperial Valley) Central segment - 330 km (Parkfield to Cajon Pass) Creep segment - 135 km (Hollister to Parkfield) Northern segment - 435 km (Cape Mendocino to Hollister)	Total length - 260 km Loma Linda-Claremont - 97 km Casa Loma-Clark - 126 km Coyote Creek - 60 km Superstition Mountain - 50 km Superstition Hills - 53 km	Total length - 339 km Whittier - 42 km Chino - 32 km Eagle-Glen Ivy - 43 km Wildomar-Elsinore - 160 km Laguna Salada - 80 km	Total length - 200 km NIZD - 70 km Segment lengths - 6.5-36 km SCOZD - 75 ± km Segment lengths - 8-27 km (Horizon B) RCFZ - 65 ± km Segment lengths - 20-48 km
Total Displacement	300 km (Miocene-Cretaceous)	24 km (Pliocene)	8-13 km (Tertiary)	3 km (Upper Miocene-NIZD)
Distance from San Andreas Fault (Plate Boundary)	0 km	0-48 km	40-80 km	62-150 km
Historic Rupture Length	435 km (Northern Segment)	33 km (Coyote Creek)	N/A	30 km (Aftershock zone - NIZD)
Historic Displacement	6.1 m	.38 m (Coyote Creek)	N/A	31 - .46 m (Seismic moment - NIZD)

Table 2.5R-3
SOUTHERN CALIFORNIA STRIKE-SLIP FAULT ZONES CHARACTERISTICS AND RANKING CRITERIA (Sheet 2 of 2)

Fault Zone Characteristics	San Andreas	San Jacinto	Whittier-Elsinore-Laguna Salada	Hypothesized OZD
Continuity and Geomorphic Features	Great continuity Long linear surface scarps, numerous traces; traces suggest great continuity; sag pods, offset streams and topography	En-echelon segments Strong linear trends in young alluvium, water barriers; sag depressions, offset streams and topography, linearity and continuity not as pronounced as San Andreas	En-enchelon Segments Linear scarps, offset alluvial fans and streams but fault trace vanishes frequently in younger sediments sag depressions	Discontinuous en-echelon segments En-enchelon large folds at north end with smaller and more gentle folding to the south. Occasional linear fault scarps at north end with no persistant scarps to the south.
Historic Seismicity	Very high	Very high	Moderate	High in the north, low in central and southern areas
Maximum Historic Magnitude, M_s	8.2 (1857)	6.7 (1968 Coyote Creek) 7.1 (1940 Imperial)	5.5-6 (1910)	6.3 (1933 - NIZD)
Geologic Slip Rate	37 mm/yr	8 mm/yr	2.3 mm/yr (Elsinore) 1.2 mm/yr (Whittier)	0.5 mm/yr (NIZD)

Table 2.5R-4
COMPARISON OF ZONE CHARACTERISTICS NORTH TO SOUTH ALONG
THE HYPOTHESIZED OFFSHORE ZONE OF DEFORMATION

Fault-Related Characteristics	North	Central	South
	Newport-Inglewood Zone of Deformation	South Coast Offshore Zone of Deformation	Rose Canyon Fault Zone
Total length	70 km	75 ± km	65 ± km
Maximum segment length	18 km (36 km combined)	48 ± km (Horizon "B")	35 ± km (offshore)
Structural features	Large en-echelon folds, en-echelon faults, north trending branch faults near basement	Smaller en-echelon folds, en-echelon faults, north trending branch faults near basement	Gentle folds on opposite sides of fault zone. En-echelon faults
Continuity of geomorphic features	Low en-echelon folds, short fault scarps	Little to none. Fault scarps up to 1/2 meter	Main fault segments tend to follow Rose Canyon, no persistent fault scarps
Distance from San Andreas Fault (plate boundary)	62 - 80 km	85 - 130 km	110 - 150 km
Historic seismicity	High	Very low	Low
Maximum historic earthquake - M_s	6.3 (1933)	4.5 (1969)	3.7 (1958)
Historic rupture Length	30 km (aftershock zone)	U.K.	U.K.
Geologic slip rate	0.5 mm/yr	U.K.	Indeterminant

Amended: April 2009 TL: E048000

If a large enough shallow earthquake is generated on a fault, it will be accompanied by surface rupture and other ground deformation. These surface disturbances may be ephemeral or may be preserved in the topography depending on the size and periodicity of surface rupture events. In all but the most active geomorphic environments, large earthquakes on faults express their occurrence in the geomorphic features along those faults. Thus, evaluation of the geomorphic features allows the reconstruction of earthquake histories and the estimation of earthquake magnitudes based on the degree of surface disturbance during individual events. This method can be an important tool in the evaluation of maximum earthquakes.

If a fault generates small displacements during earthquakes, those earthquakes are probably not large in magnitude. If geomorphic expression of past displacements are poorly preserved along a fault, then the fault probably has not produced large earthquakes since the landscape formed. In California, most earthquakes with M_s 6 or greater are accompanied by surface rupture (Tocher, 1958), and smaller earthquakes are sometimes accompanied by surface faulting. Thus, the geomorphic expression of a fault can be used to check the size of earthquakes that have occurred in the past.

A lack of dramatic surface morphologic expression of faulting is noted along the hypothesized OZD where late Pleistocene deposits overlie the fault along much of the NIZD. Locally, evidence of Quaternary surface faulting exists, but neither continuous, large scarps nor abundant offset geomorphic features are present. The low degree of geomorphic expression is more apparent within the morphology of the hypothesized OZD as compared to the Elsinor, San Jacinto, or San Andreas faults to the east. The geomorphic processes in southern California have been sufficiently slow to preserve evidence of late Pleistocene displacements on these other faults. The lack of well-developed surface expression along the hypothesized OZD suggests that very large earthquakes have not occurred on the fault at least since Pleistocene.

In the following paragraphs, the geomorphic expression and geologic relationships of the hypothesized OZD are used to test how reasonable is the occurrence of earthquakes of various magnitudes on the zone. Mark (1977) points out that the regression lines of Slemmons (1977) can be used to estimate magnitude from displacement or rupture length, but new equations must be used for the reverse process. For the following analyses, new regressions of rupture length versus magnitude and displacement versus magnitude based on Slemmons (1977) data on historic strike-slip faulting are used in order to apply the correct statistical procedure. Those regressions are plotted on figures 2.5R-7 and 2.5R-8.

According to the empirical relationships of length and displacement, a magnitude 6.5 earthquake should result in approximately 30 kilometers of surface rupture and about 0.95 meter of surface displacement. Of the entire 70 km length of the Newport-Inglewood portion of the hypothesized OZD, the largest potentially connected fault segments (based on subsurface oil field and groundwater interpretation (Yeats, 1973) extend about 36 km from Newport Beach to Signal Hill and have a maximum single segment length

of about 18 km. Considering that the rupture associated with the 1933 Long Beach earthquake (M_s 6.3) extended to about 30 km in length along this portion of the NIZD (based on aftershock zone data in the WCC June 1979 report), it appears reasonable that a full rupture of the 36 km zone (Newport Beach to Signal Hill) would be consistent with an earthquake of about M_s 6-1/2. No surface rupture due to faulting was documented in 1933, although much ground disturbance was attributed to liquefaction. The magnitude 6.3 was below, but possibly near, the threshold of causing surface rupture of the NIZD portion of the OZD.

If M_s 7 is considered, the corresponding surface rupture length and surface displacement should approximate 50 km of surface rupture and 1.7 meters of displacement. No surface ruptures are evident along the zone in the geomorphology for this great a distance. In fact, the longest single faults/within the zone do not exceed 40 km (Greene, 1980), and a 50 km rupture must, therefore, involve two or more en-echelon segments. The 1.7-meter displacement should be observable in the geomorphology along the zone if a magnitude 7 earthquake were typical of the zone. Considering that the recurrence of a magnitude 7 is about 900 years (see section 2.5R.3) on the hypothesized OZD as a whole, or approximately 3600 years at a particular point, such as the NIZD, we should see approximately 5 meters of surface displacement in Holocene age sediments and approximately 47 meters of surface displacement in the Pleistocene marine terrace deposits. Certainly, those magnitude displacements should be preserved in the uplifted marine terraces along the NIZD if magnitude 7 earthquakes are the maximum events. The geomorphic evidence does not support such large earthquakes and suggests something smaller.

If a hypothetical M_s 7.5 is considered for the NIZD and for the hypothesized OZD, individual events of that magnitude would be expected to result in about 83 kilometers of surface rupture and about 3.2 meters of surface displacement. These figures are again unreasonably large compared to the geomorphic evidence along the hypothesized OZD. The nature of the hypothesized OZD and the faulting along it indicate that no large surface ruptures have occurred. This is supported by the fact that the faults, both onshore and offshore, become shorter and less continuous from deeper horizons to shallower horizons. This relationship is clearly indicated for the faults directly offshore from San Onofre where interpretation of the geophysical data shows the individual faults to be most continuous on the acoustic basement (Horizon C) and less continuous and shorter in the younger rocks, such as those represented by Horizon B (probably upper Miocene in age).

If the continuity at depth is incomplete, becoming less upward in section, then the surface ruptures cannot be long. In other words, the surface ruptures cannot be longer than the faults at these relatively shallow depths. This limitation suggests that large earthquakes equal to M_s 7 or larger have not occurred offshore from San Onofre.

REFERENCES

1. Abe, K., 1973, Tsunami and mechanism of great earthquakes: Physics of the Earth and Planetary Interiors, v. 7, p. 143-153.

2. Acharya, H. K., 1979, Regional variations in the rupture-length magnitude relationships and their dynamical significance: Seismological Society of America Bulletin, v. 69, no. 6, p. 2063-2084.

3. Albee, A. L., and Smith, J. L., 1966, Earthquake characteristics and fault activity in southern California, in Lung, R., and Proctor, R., eds., Engineering Geology in Southern California: Association of Engineering Geologists, Glendale, California, p. 9-33.

4. Anderson, J. G., 1979, Estimating the seismicity from geologic structure for seismic-risk studies: Seismological Society of America Bulletin, v. 69, no. 1, p. 135-158.

5. Bonilla, M. G., 1979, Historic surface faulting--map patterns, relation of subsurface faulting, and relation to pre-existing faults: U.S. Geological Survey Open-File Report 79-1239, p. 36-65.

6. Bonilla, M. G., and Buchanan, J. M., 1970, Interim report on world-wide historic surface faulting: U.S. Geological Survey Open-File Report.

7. Brune, J. N., 1968, Seismic Moment, seismicity and rate of slip along major fault zones: Journal of Geophysical Research, v. 73, no. 2, p. 777-784.

8. Bucknam, R. C., Plasker G., Sharp R. V., and Bonis, S. B., 1976, Surface Displacement in the Motagua Fault Zone during the February 1976 Guatemala Earthquake (Abstract), EOS. 57:946.

9. Chinnery, M., 1978, Investigations of the seismological input to the safety design of nuclear power reactors in New England: U.S. Nuclear Regulatory Commission, NUREG CR-0563.

10. Cluff, L. S., 1978, Geologic considerations for seismic microzonation: Second International Conference on Microzonation, San Francisco, November 26 to December 1, 1978 proceedings, v. 1, p. 135-152.

11. Greene, H. G., 1980, Quaternary tectonics, offshore Los Angeles-San Diego area: U.S. Geological Survey, National Earthquake Hazards Reduction Program, Summaries of Technical Reports, v. 9, p. 11-12.

12. Mark, R. K., 1977, Application of linear statistical models of earthquake magnitude versus fault length in estimating maximum expectable earthquakes: Geology, v. 5, p. 464-466.

13. Matsuda, T., 1975, Magnitude and recurrence interval of earthquakes from a fault (in Japanese): Earthquake, Series 2, v. 28, p. 269-283.

14. Matsuda, T., 1977, Estimation of future destructive earthquakes from active faults on land in Japan: Journal of Geophysics of the Earth, v. 25, supplement, p. S251-S260.

15. Menard, H. W., 1962, Correlation between length and offset on very large wrench faults: Journal of Geophysical Research, v. 67, no. 10, p. 4096-4098.

16. Molnar, P., 1979, Earthquake recurrence intervals and plate tectonics: Seismological Society of America Bulletin, v. 69, no. 1, p. 115-133.

17. Packer, D. R. and Cluff, L. S., 1977, Comparison of activity of late Cenozoic faults in the western Sierra foothills, California, with other active faults (abs.): Earthquake Notes, v. 49, no. 1, p. 89-90.

18. Ranali, G., 1977, Correlation between length and offset in strike-slip faults: Tectonophysics, v. 37, p. T1-T7.

19. Richter, C. F., 1958, Elementary Seismology: W. H. Freeman and Company, San Francisco.

20. Sieh, K. E., 1978, Prehistoric large earthquakes produced by slip on the San Andreas fault at Pallett Creek, California: Journal of Geophysical Research, v. 83, no. B8, p. 3907-3939.

21. Shimazaki, D. and Somerville, P., 1979, Static and Dynamic Parameters of the Izu-Oshima, Japan Earthquake of January 14, 1978: Seismological Society of America Bulletin, v. 69, p. 1343-1378.

22. Slemmons, D. B., 1957, Geological effects of the Dixie Valley-Fairview Peak, Nevada, earthquakes of December 16, 1954: Seismological Society of America Bulletin, v. 47, no. 4, p. 353-375.

23. Slemmons, D. B., 1977, State-of-the-art for assessing earthquake hazards in the United States--Report 6, Faults and Earthquake Magnitude: U.S. Corps of Army Engineers, Waterways Experiment Station, Soils and Pavements Laboratory, Miscellaneous Papers S-73-1, 129 p.

24. Smith, W. S., 1976, Determination of maximum earthquake magnitude: Geophysical Research Letters, v. 3, p. 351-354.

25. Toucher, D., 1958, Earthquake energy and ground breakage: Seismological Society of America Bulletin, v. 48, no. 2, p. 147-153.

26. Wentworth, C. M., Bonilla, M. G., and Buchanan, J. M., 1969, Burro Flats site seismic environment of the Ventura, California: U.S. Geological Survey Open-File Report 1973.

27. Woodward-Clyde Consultants, 1979, Report of the evaluation of maximum earthquake and site ground motion parameters associated with the offshore zone of deformation, San Onofre Nuclear Generating Station: report for Southern California Edison Company, June, 241 p.

28. Wyss, M., 1979, Estimating maximum expectable magnitude of earthquakes from fault dimensions: Geology, v. 7, p. 336-340.

29. Yeats, R. S., 1973, Newport-Inglewood Fault Zone, Los Angeles basin, California: American Association of Petroleum Geologists Bulletin, v. 57, no. 1, p. 117-135.

Personal Communications

Schwartz, D., 1979, Woodward-Clyde Consultants, San Francisco.

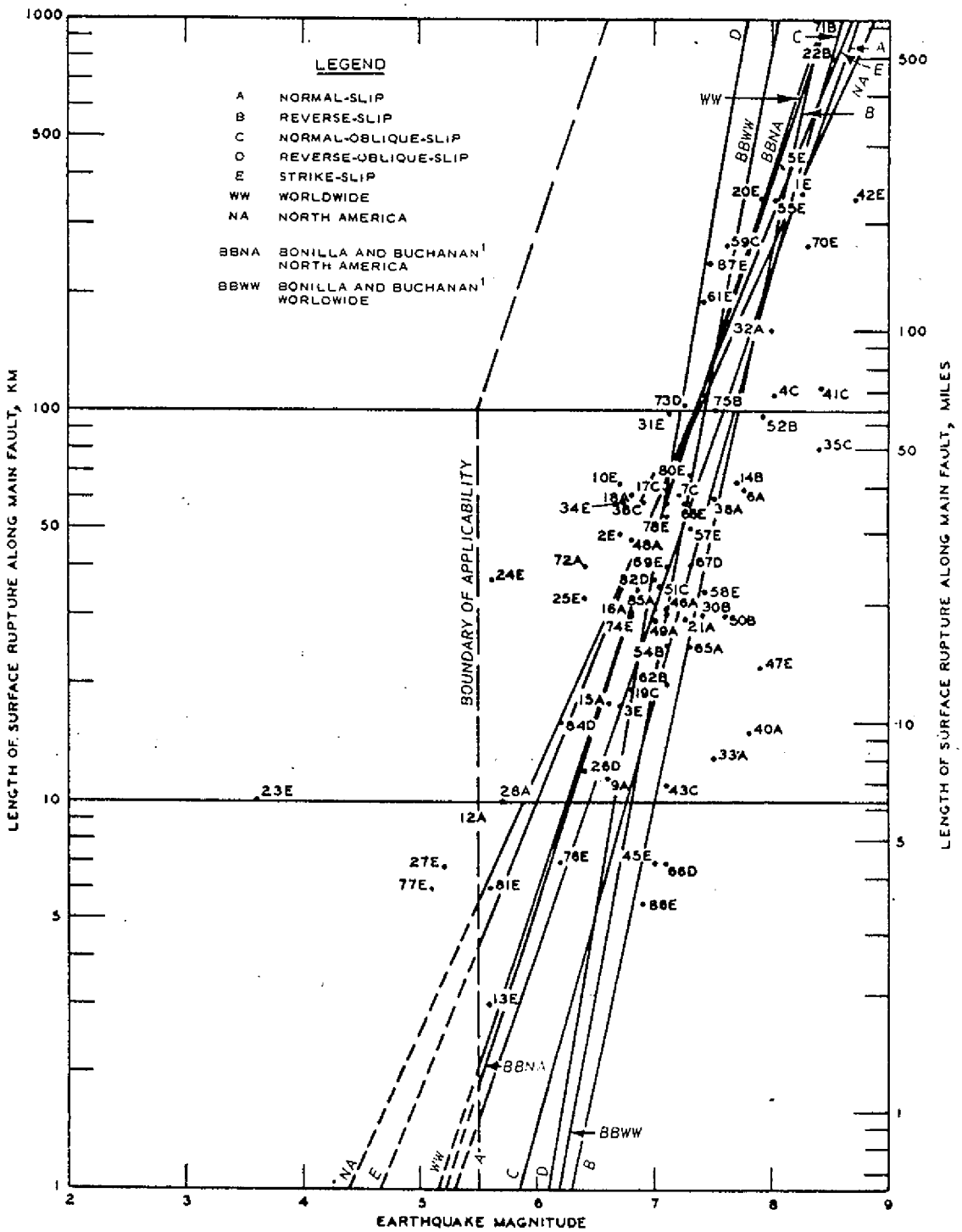

Reprinted from Slemmons, 1977.

[1] Bonilla and Buchanan, 1970.

Updated

SAN ONOFRE NUCLEAR GENERATING STATION
Units 2 & 3

RELATION OF EARTHQUAKE MAGNITUDE TO LENGTH OF ZONE OF SURFACE RUPTURE ALONG THE MAIN FAULT ZONE

Figure 2.5R-1

Amended: April 2009 TL: E048000

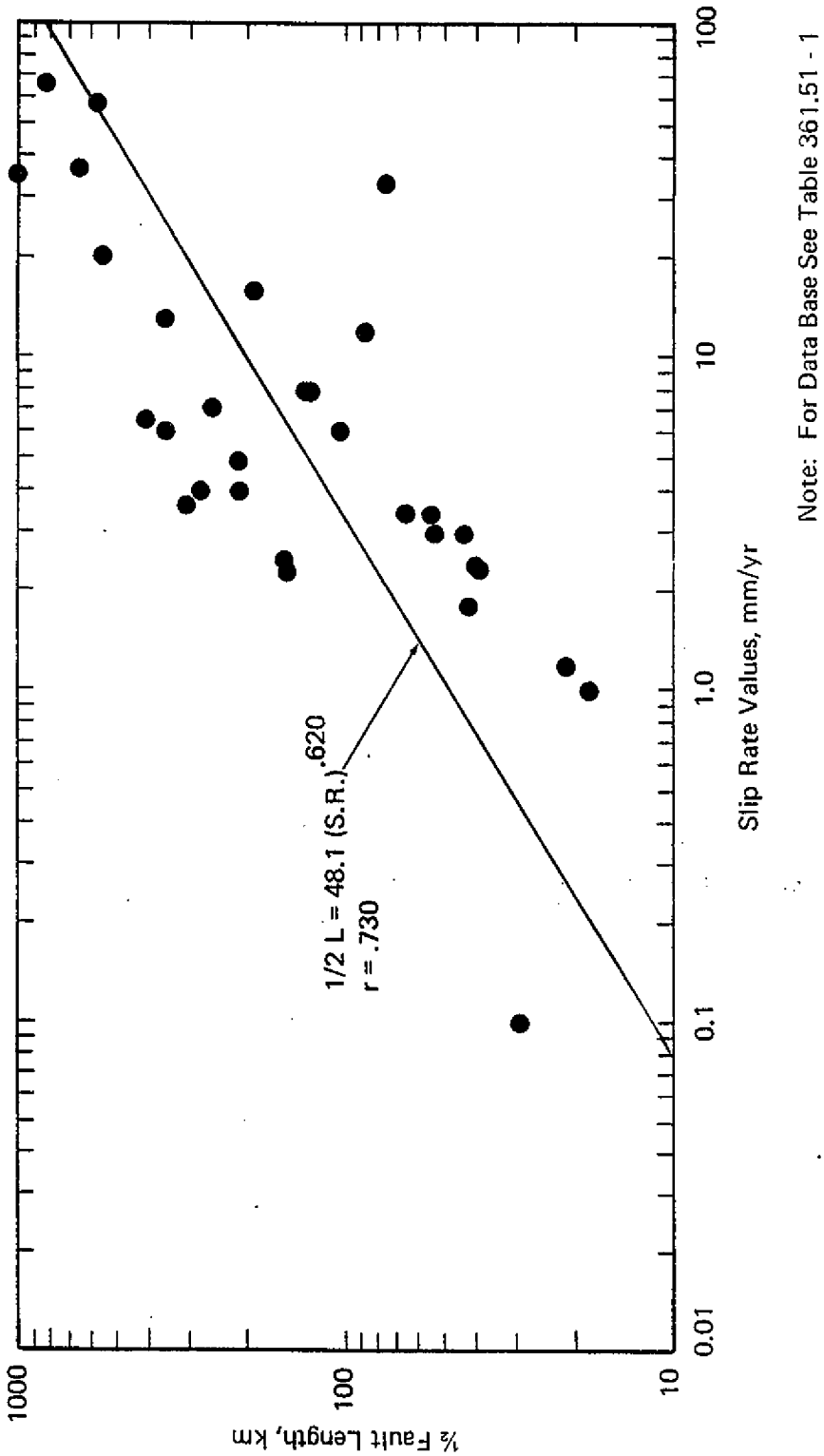

Updated

SAN ONOFRE NUCLEAR GENERATING STATION Units 2 & 3
LEAST SQUARES LINEAR REGRESSION, 1/2 FAULT LENGTH AS A FUNCTION OF SELECTED SLIP RATE
Figure 2.5R-2

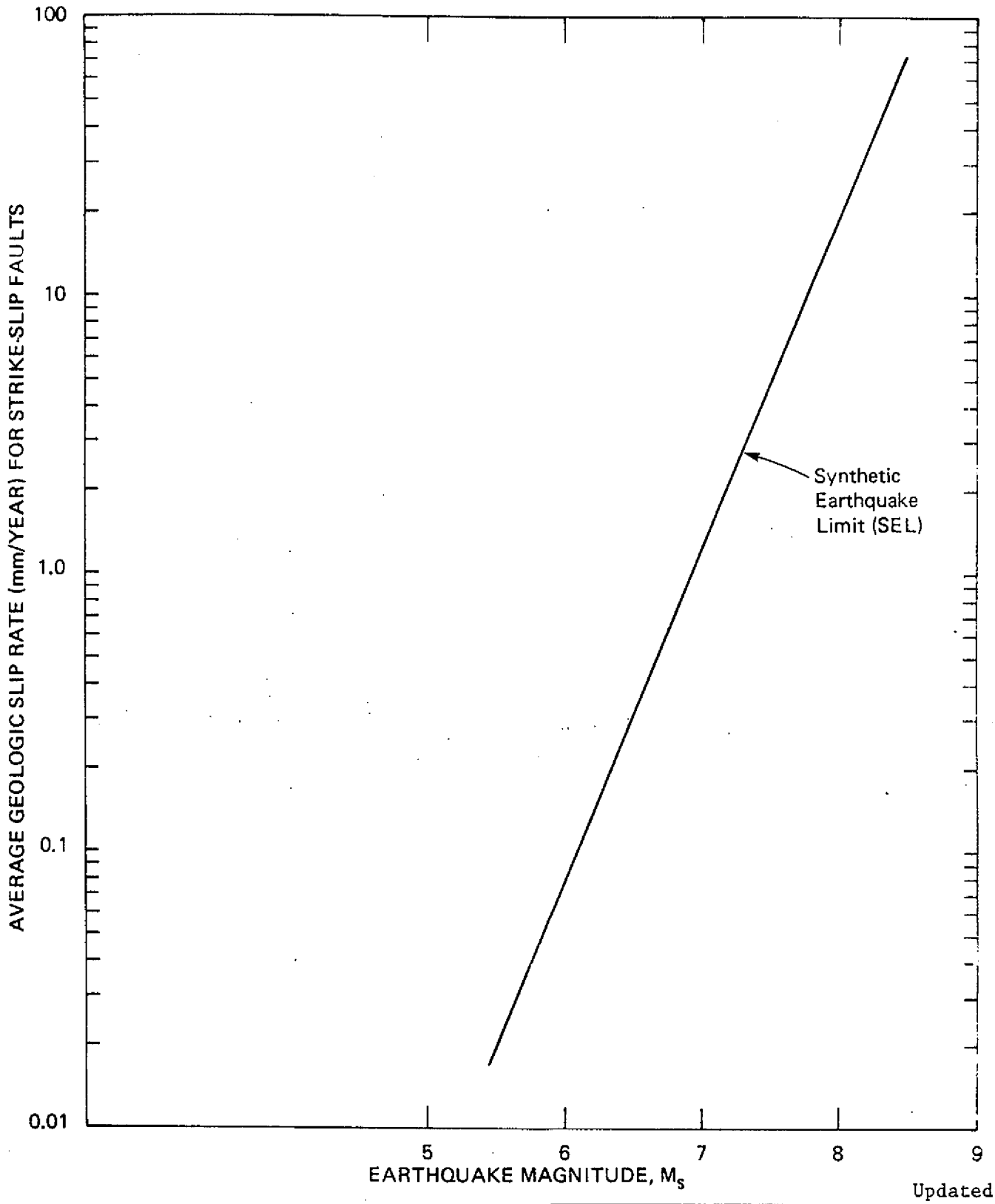

Updated

SAN ONOFRE
NUCLEAR GENERATING STATION
Units 2 & 3

SYNTHETIC PLOT BASED ON SLIP RATE VS 1/2 FAULT LENGTH AND SLEMMONS (1977), RUPTURE LENGTH VS MAGNITUDE FOR STRIKE-SLIP FAULTS

Figure 2.5R-3

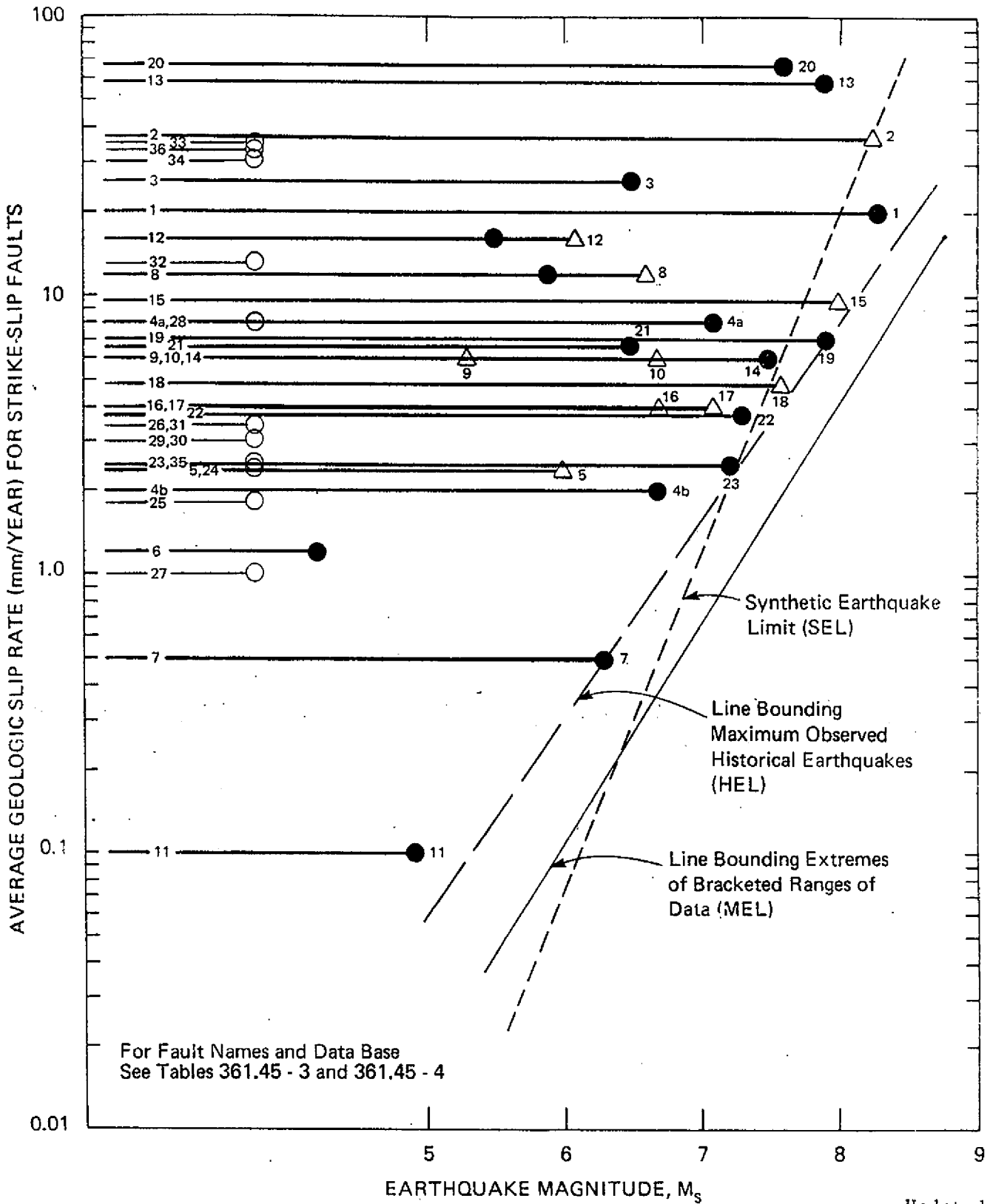

EXPLANATION

- ● Maximum instrumental recording
- △ Maximum pre-instrumental estimates
- — Range over which smaller earthquakes occur
- ○ No maximum magnitude from instrumental or pre-instrumental data.

Updated

SAN ONOFRE NUCLEAR GENERATING STATION Units 2 & 3

SEL, MEL, HEL COMPARISON
GEOLOGIC SLIP RATE VS HISTORICAL MAGNITUDE FOR STRIKE-SLIP FAULTS

Figure 2.5R-4

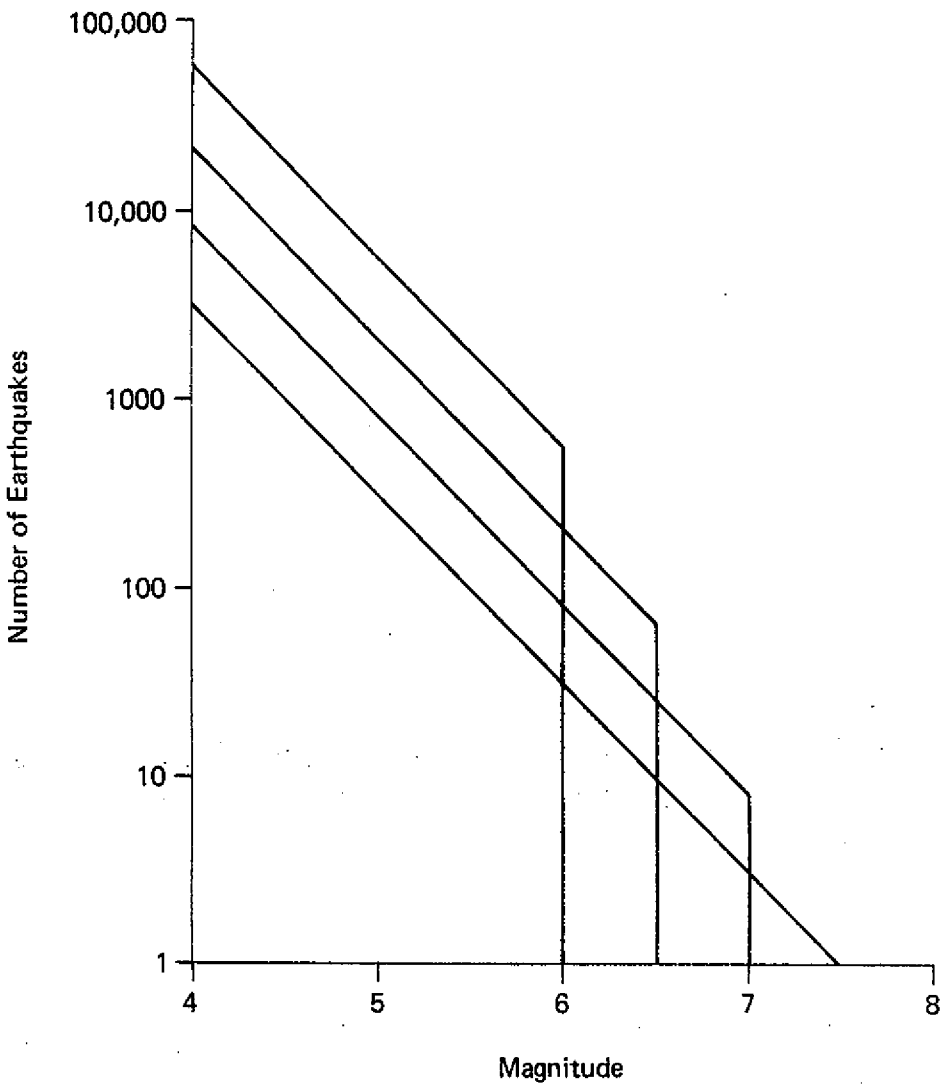

b = 0.85

Constant Slip Rate (Moment Rate)

Updated

SAN ONOFRE NUCLEAR GENERATING STATION Units 2 & 3
EFFECT OF MAXIMUM MAGNITUDE ON RECURRENCE
Figure 2.5R-5

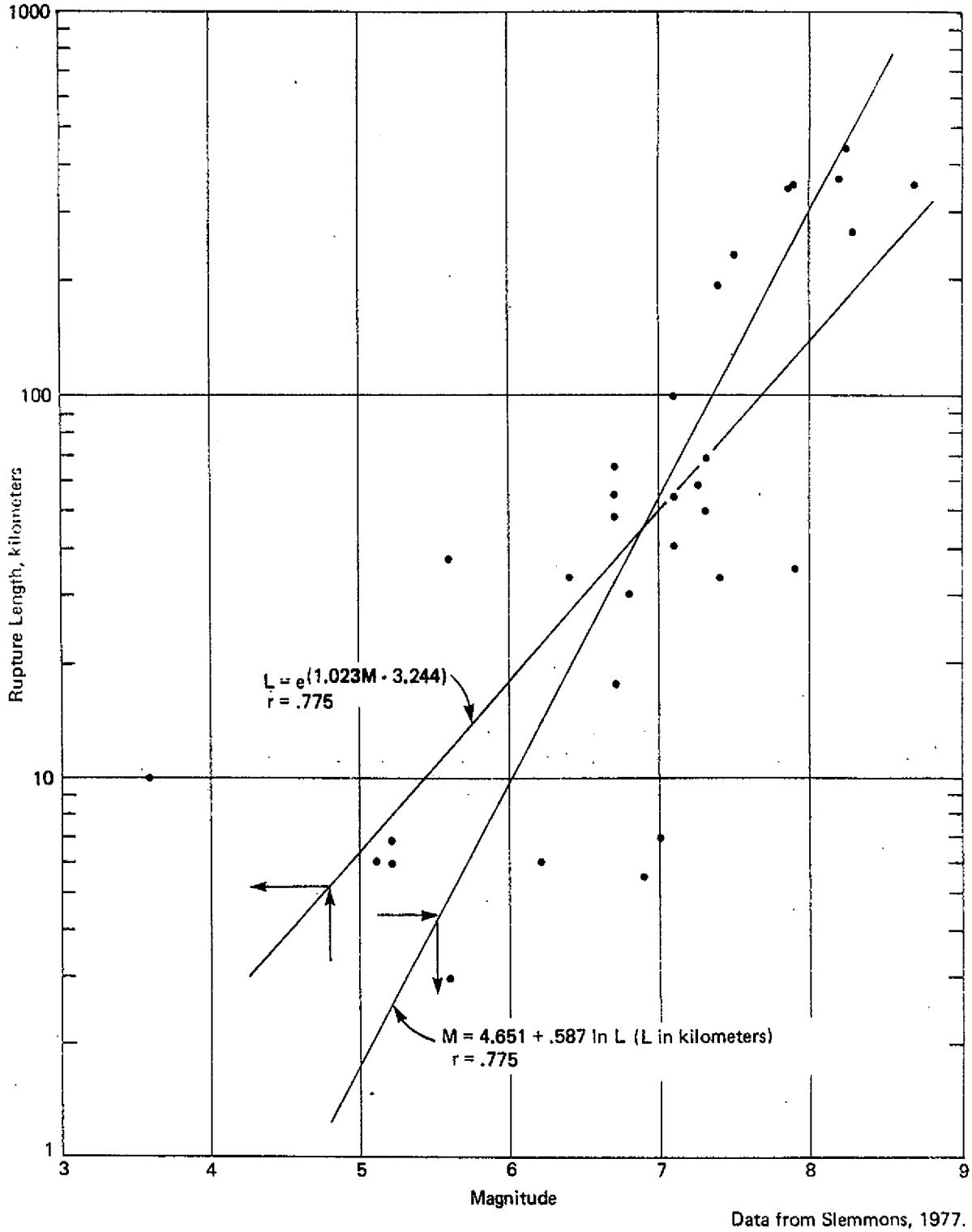

Data from Slemmons, 1977.

Updated

SAN ONOFRE NUCLEAR GENERATING STATION Units 2 & 3

LEAST SQUARES LINEAR REGRESSION, STRIKE-SLIP FAULTS RUPTURE LENGTH VS. MAGNITUDE

Figure 2.5R-6

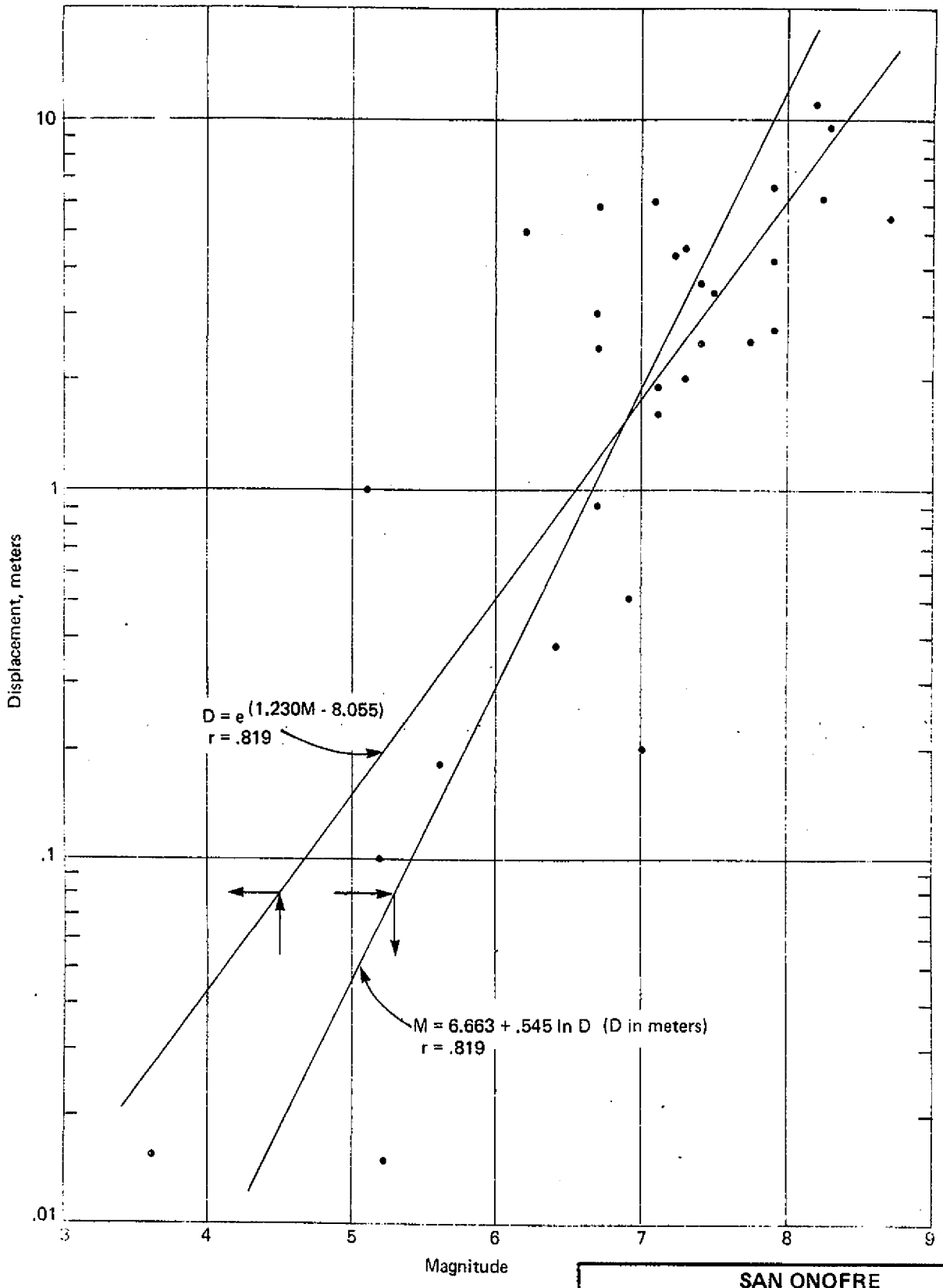

Data from Slemmons, 1977.

Updated

SAN ONOFRE NUCLEAR GENERATING STATION
Units 2 & 3

LEAST SQUARES LINEAR REGRESSION, STRIKE-SLIP FAULTS DISPLACEMENT VS. MAGNITUDE

Figure 2.5R-7

APPENDIX 2.5S

Site File Copy

APPENDIX 2.5S

2.5S.1

The data base for Figure 7 of the Woodward-Clyde Consultants (WCC) June 1979 report, which was used in part to establish the maximum earthquake for the hypothesized Offshore Zone of Deformation (OZD), has been reviewed and revised as discussed in section 2.5S.5. The results of these studies are incorporated in appendix 2.5R. The historical earthquake limit (HEL) shown in figure 2.5S-3 was modified from figure 2.5R-7. The maximum earthquake limit (MEL) defined in section 2.5S.5 is shown in figure 2.5S-4. The maximum magnitude estimates for the hypothesized OZD are based on various lines of evidence which are summarized in appendix 2.5R. These values are conservative with respect to the limits of the historic data as shown in figures 2.5R-4 and 2.5S-4. Because of this conservative interpretation, the Applicants do not consider it credible to have higher magnitudes on low slip rate strike-slip faults (in southern California or in similar tectonic environments) that would fall to the right of the MEL (figures 2.5R-4 and 2.5S-4). There would thus be no effect on the San Onofre design basis earthquake.

2.5S.2

The predicted maximum earthquakes, marked by x's in WCC figures 6 and 7 were presented for comparison and as a reference framework, but, are not used in the derivation of the maximum earthquake line discussed in 2.5S.5. The maximum magnitude values for the San Andreas, San Jacinto, Hayward, and Calaveras faults, as shown in Figure 7 of the WCC June 1979 report, were taken from or based upon the rupture-length versus magnitude relationship discussed by Selmmons (1977). However, on the basis of a review of numerous professional publications and consulting reports, a wide variation was found to exist in the approaches used for various earthquake hazard investigations to establish conservative maximum earthquake values. For example, table 2.5S-1 lists the range of maximum earthquake values that have been used for several more intensively studied faults. These values were generally based upon half-fault-length/magnitude relationships coupled with judged levels of conservatism. The wide range in values reflect the many different bases of evaluation used.

In many cases, the maximum magnitude estimates for other purposes were based on a limited investigation or were based on very conservative assumptions. The conditions leading to the use of high maximum values include the following:

A. The fault for which the maximum magnitude was selected may have been at sufficient distance from the project under investigation to render the project design insensitive to highly conservative maximum magnitude estimates for the fault.

APPENDIX 2.5S

Table 2.5S-1
REPORTED MAXIMUM EARTHQUAKE VALUES

Fault	Magnitude Range	Number of Reports Cited (a)
San Andreas	8+ - 8.5	49
Hayward	6.7 - 8.4	16
Calaveras	7.0 - 8.4	16
San Jacinto	7.25 - 8.25	28

a. Many different reports may use the same sources for maximum earthquake values.

B. The type of structure or development may not have been sensitive to large earthquake motions.

C. The time required to investigate the fault more fully may have been of greater impact to the project than the cost of additional conservatism in design and construction.

For the above reasons and because of the differences in the scale and scope of work among the many investigators, inconsistencies should be expected among reports on maximum magnitude for a given fault.

In order to circumvent these variations, the data base for the selection of a maximum magnitude for the hypothesized OZD has been expanded from that of the WCC June 1979 report and ranges of both magnitude and slip rate data have been addressed. This is discussed in appendix 2.5R. The degree-of-fault-activity approach, incorporating slip rate in conjunction with all other geologic data, is a comprehensive procedure for the selection of maximum magnitude on the hyposthesized OZD. Uncertainties in the data base for the slip rate/maximum-magnitude relationship and analysis of the physical constraints on earthquake magnitude provide the basis for constraining the maximum magnitude earthquake for the hypothesized OZD.

2.5S.3

The definitions set forth by the California Division of Mines and Geology (CDMG, 1977) for Maximum Credible and Maximum Probable earthquakes are:

Maximum Credible Earthquake - The maximum credible earthquake is the maximum earthquake that appears capable of occurring under the presently known tectonic framework.

Maximum Probable Earthquake - The maximum probable earthquake is the maximum earthquake that is likely to occur during a 100-year interval.

Though the limit line (MEL, figure 2.5R-5) has not been established according to these specific definitions, it is most compatible with that of the maximum credible earthquake. That is, for the OZD, it represents the largest earthquake that is physcially realizable as constrained by the level of fault activity and by the other specific physical characteristics of the OZD (section 2.5R.4). For the maximum probable earthquake, a consistent criterion with the above definition is a 50% chance of occurrence in a period of 100 years. This is consistent with an average recurrence interval of about 130 to 150 years (Mortgat and others, 1977). Using the recurrence results tabulated in table 2.5R-2, a recurrence interval of 130 to 150 years corresponds to a maximum on the order of M_S 6.0+ for the hypothesized OZD. Therefore, for the hypothesized OZD, the maximum probable earthquake as defined above would lie on, or to the left of, the historical earthquake limit (HEL).

The maximum possible earthquake has not been explicitly defined and, therefore, has not been addressed in this appendix.

2.5S.4

The relationship of maximum or limiting values to fault half-length, fault third-length, or other types of calculated limits was evaluated and compared to the geologic slip rate/maximum-magnitude relationship. These comparisons and relationships are discussed in appendix 2.5R and section 2.5S.5.

2.5S.5

Data Selection Process

Table G-1 was presented by the Applicants in the WCC June 1979 report as a data base representing the displacement and slip rate data from as many authors as possible for strike-slip faults; according to the criteria set forth on pages G-1 and G-2. The table presents the possible range of data and the possible interpretations of slip rates for faults described in the literature but it includes no attempt to appraise the quality or validity of the data. The 24 faults shown in Table G-1 are those that provided any slip rate data identified during a review of approximately 100 strike-slip faults identified in various literature sources. In preparation of Figures 6 and 7, the data in Table G-1 were not used directly but were subjected to a discriminating evaluation of the quality of the data. The most reliable data were selected in preparation of table H-1 and in subsequent preparation of Figures 6 and 7.

In response to a NRC request, and to clarify this selection process, a more detailed description of data used or rejected in the construction of Figures 6 and 7 is given and all of the data presented in Table G-1 of

the WCC June 1979 report have been reviewed and tabulated on a revised Table G-1 (table 2.5S-2). The revised table also contains additional data obtained since the publication of the WCC June 1979 report; thus, several modifications to the slip rates presented in Table G-1 are presented and several faults have been added. The new table is reorganized to clarify better which data are from literature sources and which are based on the assumptions or interpretations, if any, made by the Applicants. Data determined to be extraneous and unverifiable which were included in June 1979 have been eliminated in the revised table. The following screening criteria apply to the fault data presented in table 2.5S-2.

A. Only faults with tectonic settings and styles of faulting similar to the Southern California strike-slip faults are presented. For example, more detailed examination of the tectonic setting in Japan indicates that the strike-slip faults there cannot be equated to the California faults and they have thus been excluded from the slip rate comparison.

B. Geologic data are used for estimating rates of slip. Total plate motion, geodetic slip, and fault creep are not necessarily representative of long term geologic slip. Generally, these data are not considered unless supported by geologic data.

C. Quaternary offsets are preferred for slip rate calculations because they probably most accurately reflect the present tectonic setting and current rate of slip. However, when Quaternary offsets are not available, longer term offsets are accepted when they are believed to reflect the present day tectonic setting. Generally these longer term offsets are not greater than 10 to 15 million years.

D. Strike-slip faults with large dip-slip components are eliminated in order to keep the data set as similar as possible to the strike-slip style of the Southern California faulting. In general, the cut-off is approximately five to one (horizontal to vertical ratio).

E. The data range encompasses the data that are based on sound geologic fact as judged in the literature or through personal communications. Rough estimates of ages or of offsets are excluded so that unsubstantiated estimates of data are not equated to more detailed, factual data.

Table 2.5S-3 summarizes the data presented in table 2.5S-2 providing the slip rate range as well as a selected slip rate value, which best represents the fault. The following criteria were used to select those values for each fault plotted on the revised slip rate versus magnitude graphs (figures 2.5S-1 and 2.5S-2). One of the three categories of selection criteria were used for each fault.

Table 2.5S-2
SELECTED GEOLOGIC SLIP RATE INFORMATION FOR STRIKE-SLIP FAULTS
IN CALIFORNIA AND SIMILAR TECTONIC REGIONS (Sheet 1)

Fault Reference Number	Fault Name/ Locality	Reference	Displacement Data from Reference					Slip-Rate Evaluations		Comments
			Offset Feature	Age of Feature	Amount of Offset	Age of Offset	Slip Rate (mm/yr)	Assumptions	Slip Rate (mm/yr)	
1	San Andreas (northern section)	Herd, 1978	Rocks	Pliocene	-	1.8-5 m.y.	6-22	-	-	Cites Addicot, 1968. No estimate of time of initiation of faulting given.
			Deposits	1-3 m.y.	-	1-3 m.y.	10-30	-	-	Cites Cummings, 1968. Questionable time constraints.
			-	-	-	-	20	-	-	Generalized rate based on data of Addicot, 1968, and Cummings, 1968, also generally accepted rate in northern California.
		Cummings, 1968	Source of Corte Modera facies	Early Pleistocene 1-3 m.y.	28 km	1-3 m.y.	10-30	Author's offset and range of Early Pleistocene of 0.7 to 1.8 m.y.	15-40	Questionable time constraints; not used.
2	San Andreas (central section)	Huffman, 1972	Source areas of clastic units	Mohnian 8-12 m.y.	224-256 km	-	-	Author's offset; Mohnian at 6-12 m.y.	19-43	Best data for Late Miocene north of Big Bend.
		Clark and Neilson, 1973	Point of Rocks Sandstone and Butano Sandstone; Kreyenhagen Shale-Twobar Shale	Eocene 44-49 m.y. (K-Ar date)	305-330 km	44-49 m.y.	-	-	-	Ages are too old to be representative of present rates. Not used.
		Huffman, and others, 1973	Pinnacles volcanics-Neenach volcanics and associated sedimentary rocks	Oligocene-Miocene boundary 22-23.5 m.y. (K-Ar date)	295 km	22-23.5 m.y.	-	-	-	Ages are too old to be representative of present rates. Not used.

Table 2.5S-2
SELECTED GEOLOGIC SLIP RATE INFORMATION FOR STRIKE-SLIP FAULTS IN CALIFORNIA AND SIMILAR TECTONIC REGIONS (Sheet 2)

Fault Reference Number	Fault Name/ Locality	Reference	Displacement Data from Reference					Slip-Rate Evaluations		Comments
			Offset Feature	Age of Feature	Amount of Offset	Age of Offset	Slip Rate (mm/yr)	Assumptions	Slip Rate (mm/yr)	
	San Andreas (central section) continued	Vedder, 1975	Source areas of lithologic units	Middle Miocene	300 km	Middle Miocene	-	12-15 m.y. for Middle Miocene; author's offset	20-25	Vedder bases data on previous studies. Time constraits are assumed.
			Source areas of marine mudstones and sandstones	Early Pliocene	80 km	Early Pliocene	-	3.1-5 m.y. for Early Pliocene; author's offset	16-25	Time constraints are assumed.
		Sieh, 1977	Wallace Creek channel	3430±160 yr (C^{14} date)	118-138 m	3430±160 yr	34-41	-	-	Sieh indicates 37 mm/yr is most likely. Best data available for this section of the fault.
		Sieh, 1978	Marsh deposits at Pallett Creek	Holocene 500-1857 A.D.	4.5 m/ event	-	30	-	-	Assumes 4.5 meters per major event and 160 year recurrence. Speculative, not used.
		Barrows and others, 1979	Harold Fm.	Post Rancho La Brea 600,000 yrs	15 km	600,000 yr or younger	-	Author's age and offset	25	Rate represents a minimum.
	San Andreas (south and central sections)	Crowell, 1973	Sedimentary units and Pelona-Orocopia Schist	Paleocene to Miocene	260+ km	Late Miocene 8-12 m.y.	22-32	Late Miocene at 6-12 m.y.	22-43	Includes San Gabriel fault in Big Bend area.
		Ehlig and others, 1975	Source of Solodad and Mint Canyon formations	Middle to Late Miocene	297-307 km	12 m.y.	-	Author's age and offset	25-26	Good constraint on amount of offset but not on time of initiation of faulting.
3	San Andreas (southern section)	Peterson, 1975	Source of Coachella Fanglo-merate	Miocene 10±1.2 m.y. (K-Ar Date)	215 km	10±1.2 m.y.	-	Author's age and offset	19-25	

Table 2.5S-2
SELECTED GEOLOGIC SLIP RATE INFORMATION FOR STRIKE-SLIP FAULTS
IN CALIFORNIA AND SIMILAR TECTONIC REGIONS (Sheet 3)

Fault Reference Number	Fault Name/ Locality	Reference	Displacement Data from Reference					Slip-Rate Evaluations		Comments
			Offset Feature	Age of Feature	Amount of Offset	Age of Offset	Slip Rate (mm/yr)	Assumptions	Slip Rate (mm/yr)	
	San Andreas (southern section) continued	Weldon, Ray and Seih, 1979 (personal communication)	Terrace riser	Holocene 9400 - 12500 yr	Approx. 250 m	9400-12500 yr	20-25	-	-	Age based on well constrained extrapolation of sedimentation rates from C^{13}/C^{12} dates. Good estimate for southern section.
		Norris and others, 1979	Pediment-alluvial fan	Late Pleistocene	900 m	17000-70000 yr	10-50 (40-50 preferred)	Author's age and offset	13-53	Ages not well controlled; range too wide for present use.
4	San Jacinto/ Southern California	Sharp, 1967	Source of Bautista gravel beds	Pleistocene	5.2 km	as old as 2 m.y.	2.6	-	-	Age uncertain; superceded by Sharp, 1980. Not used.
			Basement rocks	Middle to Late Cretaceous	24 km	-	-	Initiation of faulting at opening of Gulf of California, 4-5 m.y.	4.8-6	Offsets differ from later study (Morton, 1979). Rates appear reasonable.
			Sedimentary rocks	Cenozoic	29-32 km	-	-	as above	5.8-8	as above
		Sharp, 1978	Source of Boutista gravel beds	Pleistocene, less than 0.73 m.y.	5.2 km	less than 0.73 m.y.	greater than 7.1	-	-	Date based on chemical correlation of underlying Ash bed with K-Ar dated Bishop Ash elsewhere. Displacement considered minimum; age maximum.
		Morton, 1979	Igneous rocks correlated by K-Ar dates	Cretaceous	22 km	-	-	Initiation of faulting at opening of Gulf of California, 4-5 m.y.	4.4-5.5	Author states Pliocene units offset same amount; sets lower slip rate limit.
		Sharp, 1980	Source of Boutista gravel beds	Pleistocene, less than 0-73 m.y.	5.7-8.6 km	less than 0.73 m.y.	greater than 8-12	-	-	Most recent and best data on one of the main traces of the fault zone, Claremont-Clark segment.

Table 2.5S-2
SELECTED GEOLOGIC SLIP RATE INFORMATION FOR STRIKE-SLIP FAULTS IN CALIFORNIA AND SIMILAR TECTONIC REGIONS (Sheet 4)

Fault Reference Number	Fault Name/ Locality	Reference	Displacement Data from Reference					Slip-Rate Evaluations		Comments
			Offset Feature	Age of Feature	Amount of Offset	Age of Offset	Slip Rate (mm/yr)	Assumptions	Slip Rate (mm/yr)	
4b	San Jacinto (Coyote Creek segment)/ Southern California	Clark and others, 1972	Lake Cahuilla sediments	Several up to 3080±600 yr (C^{14} date)	Up to 1.7 m vertical	Up to 3080±600 yr	.1.4-4 (3 preferred)	-	-	Based on vertical to horizontal ratio of 1:2.7 and offset to drag ratios of 0:1 to 2:1 from 1968 Borrego Mtn. earthquake; speculative; not used.
			Lake Cahuilla sediments	200 yr recurrence interval	.3 to .38 m horizontal + drag at 1:1	1968 Borrego Mtn. earthquake	3-3.8	-	-	Recurrence interval based on C^{14} dated offsets up to 3000 yr old; speculative, not used.
		Sharp, 1980	Lake Cahuilla sediments	Holocene 283-478 yr (C^{14} dates)	1.70 m	283-478 yr	3-5	Author's offset and age range	3.5-6	Offset based on vertical data, vertical to horizontal ratio and recurrence intervals after Clark and others, 1972, for Borrego Mtn. earthquake. May not be valid.
			Stream channel	Holocene 5000 yr (C^{14} date)	10.9 m	5400-6000 yr	1-2	Author's age and offset recalculated	1.8-2.0	Lower bound on Coyote Creek segment as timing of fault could be later.
5	Elsinore/ Southern California	Weber, 1977a, 1977b	Bedford Canyon Fm; pegmatite dikes; contact of basement and Santigo Peak Volcanics	Late Cretaceous	9-11 km	-	-	Initiation of strike-slip faulting at opening of Gulf of California, 4-5 m.y.	1.8-2.75	Faulting style may have changed to strike-slip at opening of the Gulf.
			Sespe-Vaqueros contact	Lake Eocene	10-13 km	-	-	Initiation of strike-slip faulting at opening of Gulf of California, 4-5 m.y.	2-3.25	Faulting style may have changed to strike-slip at opening of the Gulf.

Table 2.5S-2
SELECTED GEOLOGIC SLIP RATE INFORMATION FOR STRIKE-SLIP FAULTS
IN CALIFORNIA AND SIMILAR TECTONIC REGIONS (Sheet 5)

Fault Reference Number	Fault Name/ Locality	Reference	Displacement Data from Reference					Slip-Rate Evaluations		Comments
			Offset Feature	Age of Feature	Amount of Offset	Age of Offset	Slip Rate (mm/yr)	Assumptions	Slip Rate (mm/yr)	
	Elsinore/ Southern California continued	Weber, 1977a	Fault contact	Paleocene	9.5 km	-	-	Initiation of strike-slip faulting at opening of Gulf of California, 4-5 m.y.	1.9-2.4	Faulting style may have changed to strike-slip opening of the Gulf.
		Lamar and others, 1973	Sediments	Post Late Miocene	32 km	Post late Miocene	-	-	-	Correlation not well supported. Not used.
		Kennedy, 1977	Facies change	Lower Pleistocene	5 km	-	-	Author's offset and .7 to 1.8 m.y.	2.8-7.1	Age not well constrained; seems to be an upper value.
		Sage, 1973	Paleogeography of similar lithologic terrane	Paleocene rocks	40 km	Post Miocene	-	-	-	Offset and age are speculative. Not used.
6	Whittier/ Southern California	Heath, 1954	Fault contact	Late Miocene units faulted	3.7 km	Late Miocene or Post Miocene	-	Author's offset and 3-6 m.y.	.6-1.2	Age of faulting not well defined; probably yields minimum slip-rate value. Not used.
			Stream channels	Pleistocene	2.5 km	Pleistocene	-	Author's offset and 1.0-1.8 m.y. age at beginning of Pleistocene	1.4-2.5	Age of stream channels poorly defined; probably yields maximum slip-rate value; not used.
		Lamar and others, 1973	Sediments	Upper Miocene and Pliocene	4.7-4.8 km	6 m.y.	0.8	Author's offset and 3-6 m.y.	0.8-1.6	Age of offset poorly defined.
			Stream channels	Pleistocene	2.4 km	Pleistocene	-	Author's offset and assume 1.0-1.8 m.y. at beginning of Pleistocene	1.3-2.4	Age of stream channels poorly defined. Not used.

Table 2.5S-2
SELECTED GEOLOGIC SLIP RATE INFORMATION FOR STRIKE-SLIP FAULTS IN CALIFORNIA AND SIMILAR TECTONIC REGIONS (Sheet 6)

Fault Reference Number	Fault Name/ Locality	Reference	Displacement Data from Reference					Slip-Rate Evaluations		Comments
			Offset Feature	Age of Feature	Amount of Offset	Age of Offset	Slip Rate (mm/yr)	Assumptions	Slip Rate (mm/yr)	
	Whittier/ Southern California continued	Yerkes, 1972, Durham and Yerkes, 1964 and Yerkes and others, 1965	Fault contact	Upper Mohnian	4.6 km	Upper Mohnian	-	Author's offset; Upper Mohnian to Early Pliocene, 4-6 m.y.	0.8-1.2	Offset is based on projection of fault contact. Faulting of contact could be younger.
7	Newport-Inglewood Zone of Deformation/ Southern California	Castle and Yerkes, 1976	"Gyroidina" zone; Inglewood oil field	Mid to Late Pliocene	3000 to 4000 ft. (915-1220 m)	-	-	Absolute ages based on Hardin & Henyey (1978), 1.8-3.0 m.y.	0.3-0.68	Generalized displacement and age but gives good overall range. Poor age control.
			Stream channel	Late Quarternary	100 to 150 ft (30-45 m)	-	-	-	-	Stream channel not dated.
		Wright and others, 1973	Anticlinal axis, Inglewood oil field	Latest Pliocene	4000 ft (1220 m)	Post Latest Pliocene	-	Absolute ages based on Hardin and Henyey, (1978), 1.8-2.5 m.y.	0.5-0.68	Good data, may indicate slightly higher rates at north end of NIZD.
		Yerkes and others, 1965	Oil Bearing sediments	Lower Pliocene	3000 to 5000 ft (915-1525 m)	-	-	-	-	Age of offset not stated; poorly defined offset; not used.
		Hill, M.L., 1971	Sediments with E-log correlations	Miocene	10000 ft (3050 m)	-	-	Age of offset 5 to 8 m.y.	0.38-0.61	Age of offset not defined but believed to be good range for maximum reported offset.
		Dudley, 1954	Top of brown zone structure Long Beach field	Lower Pliocene	3000 ft (915 m)	-	-	-	-	Poor age and displacement control.

Table 2.5S-2
SELECTED GEOLOGIC SLIP RATE INFORMATION FOR STRIKE-SLIP FAULTS IN CALIFORNIA AND SIMILAR TECTONIC REGIONS (Sheet 7)

Fault Reference Number	Fault Name/ Locality	Reference	Displacement Data from Reference					Slip-Rate Evaluations		Comments
			Offset Feature	Age of Feature	Amount of Offset	Age of Offset	Slip Rate (mm/yr)	Assumptions	Slip Rate (mm/yr)	
	Newport-Inglewood continued	Woodward-Clyde Consultants 1979	Sediments with E-Log correlations Huntington Beach oil field	Late Miocene	12000 ft (3660 m)	Late Miocene	0.52 (ave.)	-	-	Detailed offset and age data presented in Appendix B of referenced report.
			Sediments with E-log correlations, Seal Beach oil field	Pliocene	4000 to 8000 ft (1220-2440 m)	Pliocene	0.49 (ave.)	-	-	Detailed offset and age data presented in Appendix B of referenced report.
			Sediments with E-log correlations, Long Beach oil field	Late Miocene and Pliocene	2000 to 10000 ft (610-3050 m)	Late Miocene to Pliocene	0.5 (ave.)	-	-	Detailed offset and age data presented in Appendix B of referenced report.
8	Calaveras-Paicines (South of Hayward branch)/ Central California	Prowell, 1974	Quien Sabe-Coyote Lake volcanics	Pliocene 3.5 m.y. (K-Ar date)	11-27 km	3.5 m.y.	5 mm/yr	-	-	Author gives two correlations and an average slip rate of 5 mm/yr.
			San Filipe-Coyote Lake volcanics	Pliocene 3.5 m.y. (K-Ar date)	7-21 km	3.5 m.y.	as above	-	-	as above
		Herd, 1978	Anderson-Coyote Lake volcanic rocks	Pliocene	unstated	Pliocene	1.4-7.1	-	-	Considered as a minimum rate by Herd.
			-	-	-	-	12-15	-	-	Based on difference in apparent slip rate on the San Andreas north and south of the Calaveras-Paicines fault. Limited geologic data. Consistent with creep rates.

Table 2.5S-2
SELECTED GEOLOGIC SLIP RATE INFORMATION FOR STRIKE-SLIP FAULTS
IN CALIFORNIA AND SIMILAR TECTONIC REGIONS (Sheet 8)

Fault Reference Number	Fault Name/ Locality	Reference	Displacement Data from Reference					Slip-Rate Evaluations		Comments
			Offset Feature	Age of Feature	Amount of Offset	Age of Offset	Slip Rate (mm/yr)	Assumptions	Slip Rate (mm/yr)	
9	Calaveras-Sunol (North of Hayward Branch)/ Central California	Crittenden, 1951	Tularcitos syncline	Plio-Miocene (Blancan)	3 mi (4.8 km)	-	-	-	-	Long term geologic rate without control of recency of offset; not used.
		Prowell, 1974	Quien Sabe area - Mt. Hamilton volcanics	Late Miocene 8.2 m.y. (K-Ar date)	66-73 km	8.2 m.y.	8	-	-	Probably upper bound for slip rate.
		Herd, 1978	-	-	-	-	6-7.5	-	-	Author apportions 50% of Calaveras-Paicines slip rate to the Calaveras-Sunol branch. Indirect geologic data.
10	Hayward/ Central California	Prowell, 1974	Grisley Peak volcanics	Late Miocene 8.2 m.y. (K-AR dating)	42-45 km	8.2 m.y.	-	Author's age and offset	5-5.5	Only known correlation across the Hayward fault.
		Herd, 1978	-	-	-	-	6-7.5	-	-	Author apportions 50% of Calaveras-Paicines slip rate to the Hayward fault. Indirect geologic data.
11	Antioch-Vaca and Davis/ Central California	Burke and Halley, 1973	Nortonville Shale	Eocene	1.2 km (map)	-	-	-	-	Horizontal separation could be affected by vertical offset of shallowly dipping beds. Not used.
			Ciebro Sandstone	Upper Miocene	.18 km (map)	-	-	Post Middle Miocene initiation 4-8 m.y.	.022-.045	At base of unit across Antioch fault.
			Ciebro Sandstone	Upper Miocene	.38 km (map)	-	-	Post Middle Miocene initiation 4-8 m.y.	.047-.095	At base of unit across Davis fault.

Table 2.5S-2
SELECTED GEOLOGIC SLIP RATE INFORMATION FOR STRIKE-SLIP FAULTS IN CALIFORNIA AND SIMILAR TECTONIC REGIONS (Sheet 9)

Fault Reference Number	Fault Name/ Locality	Reference	Displacement Data from Reference					Slip-Rate Evaluations		Comments
			Offset Feature	Age of Feature	Amount of Offset	Age of Offset	Slip Rate (mm/yr)	Assumptions	Slip Rate (mm/yr)	
	Antioch-Vaca and Davis/ Central California continued	Burke and Halley, 1973	Ciebro Sandstone	Upper Miocene	.56 km (map)	-	-	Post Middle Miocene initiation 4-8 m.y.	.07-.14	At base of unit across Antioch-Davis zone.
		Knuepfer, 1977	Volcanic tuff	Middle Miocene	.18 to .66 km	-	-	Middle Miocene from 8 m.y.; initiation of faulting may be 4 m.y.	022-.16	Tuff is near base of unit across Antioch fault.
		Kneupfer, 1979 (personal communication)	Streams in alluvium	Streams same age as Quaternary alluvium	35 m	Since 120,000 to 500,000 yr	-	Author's age range	.07-.29	On Vaca fault (continuation of Antioch fault to north).
12	San Gregorio/ Central California	Silver, 1977	unstated	Miocene	100 km	80-90% in Miocene	-	-	-	Applies to the Miocene and not present tectonics.
				Post Miocene	10-20 km	Post Miocene	-	Maximum of 5 m.y.	2-4	Offset cited from Hamilton and Willingham, 1978; data not well defined. Not used.
		Graham, and Dickinson, 1977	Lithologic units	Post Early Miocene and probably post Late Miocene	115 km	-	-	5-15 m.y. for post Early through Late Miocene	7.7-23	Age not well defined. Not used.
		Greene, 1977	Pioneer and Ascension faults	Middle Miocene 20 m.y.	110 km	20 m.y.	none	Author's offset and age	5.5	Correlation and age seem speculative. Not used.
		Weber and La Joie, 1979	Shoreline angles	Late Pleistocene (amino acid dates; unspecified)	unstated	Late Pleistocene	16 (ave.)	From author's graph; minimum and average values	9-16	Authors present slip rate graphs across 3 faults within zone.

Table 2.5S-2
SELECTED GEOLOGIC SLIP RATE INFORMATION FOR STRIKE-SLIP FAULTS
IN CALIFORNIA AND SIMILAR TECTONIC REGIONS (Sheet 10)

Fault Reference Number	Fault Name/ Locality	Reference	Displacement Data from Reference					Slip-Rate Evaluations		Comments
			Offset Feature	Age of Feature	Amount of Offset	Age of Offset	Slip Rate (mm/yr)	Assumptions	Slip Rate (mm/yr)	
13	Fair-weather/ Alaska	Page, 1969	Vertical offset of ground surface	1000 yr	6 m vertical 36 - 42 m horizontal)	1000 yr	40	-	-	Page assumes 6:1 to 7:1 horizontal to vertical ratios to derive horizontal slip rate.
		Plafker, and others 1978	Three streams	940 ± 200 yr (C_{14} date)	55 m	940 ± 200 yr	48-58 (58 preferred)	Author's offset and age	58	Streams post-date the latest glacial advance.
			Lateral moraine	1300 ± 200 yr (C_{14} date)	50 m	1300 ± 200 yr	-	Author's offset and age	38	-
14	Motagua/ Guatemala	Schwartz and others, 1979	Stream terrace	10000 to 40000 yr	58.3 m	10000 to 40000 yr	1.5-6.0 (6.0 is most representative)	-	-	40000 year age of offset is not valid (Personnel Communication Schwartz 1979)
		Schwartz, 1979 (personal communication)	Stream terrace	10000 yr	58.3 m	10000 yr	6	-	-	Lower terrace yields date of 1300 years, suggests offset terrace is "quite young".
15	Bocono/ South America	Schubert and Sifontes, 1970	Glacial moraines	10,070 yr	66 m	10,070 yrs	6.6	-	-	Not maximum offset of moraines; not used.
		Dewey, 1972	unstated	5 m.y.	50 km	5 m.y.	10	-	-	Suggests plate motions are more E-W than 1140°E parallel to the Bocono fault, thus motion may be right-reverse-oblique.
		Rod, 1956	Glacial moraines	Late Pleistocene	80-100 m	Late Pleistocene	-	Faulting continuous since end of Pleistocene 10,000 yr	8-10	-
		Woodward, Clyde and Associates, 1969	Glacial moraines	Late Pleistocene 10,000 yr	320 ft (97.5 m)	10,000 yr	9.75	-	-	Most accurate measurements of offsets; best estimate of rate. Authors measured numerous offsets.
16	Hope/ New Zealand	Scholz and others, 1973	unstated	-	20 km	Since Miocene	-	5 m.y. since Miocene	4	Author quotes Freund, 1971 and Clayton, 1966.

Table 2.5S-2
SELECTED GEOLOGIC SLIP RATE INFORMATION FOR STRIKE-SLIP FAULTS
IN CALIFORNIA AND SIMILAR TECTONIC REGIONS (Sheet 11)

Fault Reference Number	Fault Name/ Locality	Reference	Displacement Data from Reference					Slip-Rate Evaluations		Comments
			Offset Feature	Age of Feature	Amount of Offset	Age of Offset	Slip Rate (mm/yr)	Assumptions	Slip Rate (mm/yr)	
17	Awatere/ New Zealand	Lensen, 1973	River terraces	35000 to 40000 yr	330-350 ft (100-107m)	-	2.9	-	-	Age based on correlation of glacial deposits with C^{14} age deposits elsewhere. Author's rate from slip rate summary chart.
			River terraces	20,000	220-240 ft (67-73 m)	-	-	Author's age and 18000 yr for age of last glacial after Suggate and Lensen, 1973	3.4-4	Measured offsets may be low because of lateral erosion prior to downcutting. Highest rate estimate appears most reasonable.
18	West Wairarapa/ New Zealand	Lensen, 1973	Waiohine aggradation surface	20000 or 35000 yr	329-390 ft (100-120 m)	20000 or 35000 yr	2.8-3.1	Author's age and offset ranges; extending lower age to 18000 yr Suggate and Lenson, 1978)	2.9-6.6	Question as to which glacial advance created the aggradation surfaces. In cited reference, author prefers lower rate.
19	North Anatolian/ Middle East	Wellman, 1969	Lithologic units	unstated	350 km	Miocene	20	-	-	Offset from Pavoni, 1961, Cretaceous rocks, shown to be incorrect by later studies (Sengor, 1979). Not used.
		Canitez, 1976	Boundary between ancient crustal plates	Middle Miocene	85-95 km	15 m.y.	5-6	-	-	Data and rates from Seyman, 1968, based on reconstruction of depositional and metamorphic environments.
			unstated	unstated	unstated	.5 m.y.	>7	-	-	Data and "minimum rate" from Arpat and Saroglu, 1975
		Sengor, 1979	Pontide-Anatolide Suture	Budigalian	80-90 km	Budigalian to Pliocene	-	Author's offset and 5-15 m.y.	5.3-18	Age is poorly constrained but provides constraint to slip-rate range.
			unstated	unstated	50-100 km	unstated	-	-	-	Insufficient data, not used.

Table 2.5S-2
SELECTED GEOLOGIC SLIP RATE INFORMATION FOR STRIKE-SLIP FAULTS
IN CALIFORNIA AND SIMILAR TECTONIC REGIONS (Sheet 12)

Fault Reference Number	Fault Name/ Locality	Reference	Displacement Data from Reference					Slip-Rate Evaluations		Comments
			Offset Feature	Age of Feature	Amount of Offset	Age of Offset	Slip Rate (mm/yr)	Assumptions	Slip Rate (mm/yr)	
20	Sumatra/ Indonesia	Posavec and others, 1973	Streams	unstated	1 km	-	-	-	-	Other offsets such as lahars, lake terraces. No age data. Not used.
			Volcanic centers sources	unstated	130 km	-	-	-	-	Age reference is vague and undefined. Data not used.
		Tjia, 1970	unstated	unstated	unstated	4-5 m.y.	5-7	-	-	Substantiation of data is not presented.
		Tjia, 1973	Toba Ignimbrite	Less than 300,000 yrs	20 km	Less than 300,000 yrs	70	Author's age and offset	66.7	Only Quaternary data available.
21	Jordan-Dead Sea/ Middle East	Quennel, 1958	Geologic units dikes, faults	Pre Early Miocene	62 km	During Miocene and early Pliocene	-	-	-	Timing poorly defined; does not relate to present tectonic regime. Not used.
			Lisan "Delta"	Late Pleistocene	45 km	Late Pleistocene	-	-	-	Offset delta deposits have been disproven (Zak and Freund, 1966).
		Zak and Freund, 1966	Geologic features	Precambrian to Upper Cretaceous	100 km	Post-Cretaceous	-	-	-	Data from other authors; time spans older tectonic regime; not used.
			Alluvial fans, Lisan Marl	20000 yr	150 m	20000 yr	-	Author's age and offset	7.5	Age revised in Freund and others, 1970; other offsets in undated alluvium to 600 m. Not used.
		Freund and others, 1970	Lisan Marl	older than 23,000 yr	150 m	older than 23000 yr	6.5	-	-	Absolute age from Neev and Emery, 1967.
			Rock bodies	Miocene, Early Pliocene	40-45 km	7-12 m.y.	3.5-6	-	-	Offset feature not clearly defined; age limits speculative.
		Ben-Menahem and others 1976	-	-	-	-	6.5	-	-	Quotes Freund and others, 1970.
			-	-	-	3-4 m.y.	10	-	-	Quotes Girdler, 1958. No slip rate discussion in that reference.

Table 2.5S-2
SELECTED GEOLOGIC SLIP RATE INFORMATION FOR STRIKE-SLIP FAULTS IN CALIFORNIA AND SIMILAR TECTONIC REGIONS (Sheet 13)

Fault Reference Number	Fault Name/ Locality	Reference	Displacement Data from Reference					Slip-Rate Evaluations		Comments
			Offset Feature	Age of Feature	Amount of Offset	Age of Offset	Slip Rate (mm/yr)	Assumptions	Slip Rate (mm/yr)	
22	Kopet-Dagh/ Middle East	Krymus and Lykov, 1969	unstated	Middle Pliocene	20 km	Middle to Late Pliocene	-	Author's offset data and 2.5 - 4 m.y.	5-8	Older age is probably most appropriate.
				Middle Pleistocene	55-60 m	Middle Pleistocene	-	-	-	Age data are unconstrained. Data not used.
		Trifonov, V. G., 1971	unstated	500 yr recurrence intervals	1.78 m	1948 Ashkhabad earthquake	-	Assume 1.78 m per 500 year recurrence	3.6	Trifonov says the rate derived is comparable to geologic data.
			Kyarizes (water tunnels)	Holocene	3-8 m	1000 - 2000 yrs	-	1000 to 2000 yrs for largest offset during that time, 8 m.y.	4-8	Lesser offsets are the younger kyarizes.
			Streams	Holocene	6-10 m	Holocene	-	-	-	Could be any time in Holocene, poor data. Data not used.
			Streams	Middle Pleistocene	55-60 m	Middle Pleistocene	-	-	-	Age data are unconstrained. Data not used.
		Trifonov, 1978	Walls of Palace in Nissa	unstated	0.3 m	-	-	-	-	Age not known. Data not used.
			Wall of Chugundor Fortress	Middle ages	2.5 m	-	-	-	-	Age not known. Data not used.
			Kyarizes (water tunnels)	5th Century B.C. (2500 yr)	9 m	2500 yr	-	Author's age and offset	3.6	Appears to be best age and offset control.
			Streams	Holocene	8 m ±	Holocene	-	-	-	Age not known.
			Streams	Holocene Late Pleistocene	55-60 m	Holocene	-	Author's offset; Holocene-Pleistocene boundary, 10000 yr	5.5-6.0	Offset streams may be older than 10000 yr.

Table 2.5S-2
SELECTED GEOLOGIC SLIP RATE INFORMATION FOR STRIKE-SLIP FAULTS
IN CALIFORNIA AND SIMILAR TECTONIC REGIONS (Sheet 14 of 14)

Fault Reference Number	Fault Name/ Locality	Reference	Displacement Data from Reference					Slip-Rate Evaluations		Comments
			Offset Feature	Age of Feature	Amount of Offset	Age of Offset	Slip Rate (mm/yr)	Assumptions	Slip Rate (mm/yr)	
23	Dasht-e Bayaz	Tchalenko and Berberian, 1975	Black limestone	Cretaceous	4 km	-	-	-	-	Offset unconstrained; initiation of faulting age not known.
			Volcanics	Eocene	400 m	-	-	-	-	Same as above
			Stream channels	Holocene	8-24 m	-	-	Maximum age of Holocene of 10,000 yr; 24 m offset probably oldest	2.4	Rate is minimum based on assumption.

Notes: Absolute ages cited under "Assumptions" are from Van Eysinga, 1975, unless otherwise noted.

Table 2.5S-3
SUMMARY OF SELECTED GEOLOGIC SLIP RATES AND MAXIMUM EARTHQUAKES FOR STRIKE-SLIP FAULTS (Sheet 1)

Reference Number	Faults	Maximum Earthquake (M_s)	Reasonable Data Range Slip Rate (mm/yr)	References	Selected Values Slip Rate (mm/yr)	Comments on Geologic Slip Rates (b)
1	San Andreas (Northern)	8.3, 1906	20	Herd, 1978	20	Generally accepted in northern California; selected value from Herd, 1978. Criterion 1.
2	San Andreas (Central)	8.25+, 1857(a)	34-41	Sieh, 1978	37	Based on C^{14} dates and trenching at Wallace Creek. Criterion 1.
3	San Andreas (Southern)	6.5, 1948	20-25	Walden, 1979 Sieh, 1979	25	Based on C^{14} dates on displaced Holocene deposits, Lost Lake area. Criterion 1.
4	San Jacinto fault zone	7.1, 1940	4.4-12	Sharp, 1967, 1978, 1980 Morton, 1979	8.0	Based on offsets across main single trace of fault (Casa Loma Clark fault). Criterion 1.
4	Coyote Creek fault segment	6.7, 1968	1.8-5.0	Sharp, 1980	2	Based on offsets of Coyote Creek segment only. Criterion 1.
5	Elsinore	5.5-6, 1910(a)	1.8-7.1	Weber, 1977 Kennedy, 1977	2.3	Selected value based on the best documented offsets of 9-11 km. Criteria 2 and 3.
6	Whittier	4.2, 1976	.6-1.6	Heath, 1954 Yerkes, 1972 Lamar and others, 1973	1.2	Both offset and age data are not well controlled. Criterion 2.
7	Newport-Inglewood	6.3, 1933	.3-.68	Castle and Yerkes, 1976 Woodward-Clyde, 1979 Hill, 1971	.5	Offset and age data cited in literature, confirmed by CC Special Investigation (Appendix B). Criterion 3.

a. Pre-instrumental earthquake estimates.

b. Criteria described in section 2.5S.5.

Table 2.5S-3
SUMMARY OF SELECTED GEOLOGIC SLIP RATES AND MAXIMUM EARTHQUAKES FOR STRIKE-SLIP FAULTS (Sheet 2)

Reference Number	Faults	Maximum Earthquake (M_s)	Reasonable Data Range Slip Rate (mm/yr)	References	Selected Values Slip Rate (mm/yr)	Comments on Geologic Slip Rates (b)
8	Calaveras-Paicines (south of Hayward branch)	5.9, 1979 6.6, 1911(a)	5-15	Herd, 1978 Prowell, 1974	12	Based on difference in slip rates between north and central portions of San Andreas, and limited geologic data. Criterion 2.
9	Calaveras-Sunol (north of Hayward branch)	5.3, 1861(a) 5.3, 1864(a)	6-8	Herd, 1978 Prowell, 1974	6	Herd apportions 50% of Calaveras-Pacines slip rate to Calaveras-Sunol and Hayward faults respectively. Criterion 2.
10	Hayward	6.7, 1868(a)	5-7.5	Herd, 1978 Prowell, 1974	6	Herd apportions 50% of Calaveras-Pacines slip rate to Calaveras-Sunol and Hayward faults respectively. Criterion 2.
11	Antioch (and Vaca)	4.9, 1965	.022-.29	Kneupfer, 1977, 1979 Burke and Helley, 1973	1	Data gives wide range because of limited data for ages of offsets. Criterion 2.
12	San Gregorio	5.5, 1969 6.1, 1926(a)	9-16	Weber and LaJoie (1979)	16	Weber and LaJoie state 16 mm/yr is best estimate. Criterion 1.
13	Fairweather	7.9, 1958	38-58	Plafker, and others	58	Of the two rates determined from C^{14} ages, Plafker indicates 58 mm/yr is most accurate value. Criterion 1.
14	Motagua Guatemala	7.5, 1976	6	Schwartz and others, 1979 Schwartz, 1979 (personal communication)	6	Authors state that selected value is only reliable estimate. Criterion 1.

Table 2.5S-3
SUMMARY OF SELECTED GEOLOGIC SLIP RATES AND MAXIMUM EARTHQUAKES FOR STRIKE-SLIP FAULTS (Sheet 3 of 3)

Reference Number	Faults	Maximum Earthquake (M_s)	Reasonable Data Range Slip Rate (mm/yr)	References	Selected Values Slip Rate (mm/yr)	Comments on Geologic Slip Rates (b)
15	Bocono Venezuela	8, 1812(a)	8-10	Rod, 1956 Dewey, 1972 Woodward, Clyde and Associates, 1969	9.75	Best data from Cluff and Hansen, 1969. Criterion 1.
16	Hope New Zealand	6.7, 1888(a)	4	Scholz, and others, 1973	4	Author does not present data to check. Criterion 1.
17	Awatere New Zealand	7.1, 1848(a)	2.9-4	Lensen, 1964 Lensen, 1958	4	Offset river terraces and aggredation surfaces. Criterion 3.
18	West Wairarapa New Zealand	7.6, 1855(a)	2.9-6.6	Lensen, 1973	4.8	Offset Waiohine aggredation surface. Criterion 3.
19	North Anatolian Turkey	7.9, 1939	5-18	Canitez, 1977	7	Based on total offset and various times of initiation of faulting. Criterion 1.
20	Sumatra	7.6, 1943	66.7-70	Tjia, 1973	67	Based on dated ignimbrite deposit. Criterion 1.
21	Jordan-Dead Sea	6.5, 1927	3.5-6.5	Ben Menahem and others, 1976	6.5	Selected value is based on dated Quaternary offset. Criterion 1.
22	Kopet-Dagh Iran-USSR	7.3, 1948	3.6-8	Krymus, and Lykov, 1969 Trifonov, 1971 Trifonov, 1978	3.6	Best age and offset data in Quaternary results in 3.6 mm/yr. Criterion 2.
23	Dasht-E-Bayaz	7.2, 1968	2.4	Tohalenko and Berberian, 1975	2.4	Minimum rate based on maximum age for Holocene offset. Criterion 3.

A. The selected ranges are primarily based on the value cited by most workers and are from the current and most credible workers' data. For example, Kerry Sieh's work on the San Andreas fault is most widely accepted, and Robert Sharp is accepted as the primary authority of Quaternary slip rate values along the San Jacinto fault. Preference is always given to the slip rate values based on Quaternary data because they best represent the current tectonic environment and activity of the faults. The selected value is based on the referenced author's preferred slip rate value.

B. For some faults that have no slip rate assignments, but for which data are presented and can be used to calculate slip rate values, the Applicants have selected the range and single values based on the most precise age and displacement data. Quaternary data are selected whenever possible.

C. If a range of values is cited in the literature, or if several slip rate values can be calculated from the data presented and no single value is explicitly presented, the Applicants have selected the mean value of the range of values to represent a particular fault.

The range of data and the selected slip rate values for each fault along with the rationale and appropriate criteria used to choose each selected value are presented in table 2.5S-3. The data from table 2.5S-3 and historical earthquake magnitudes are plotted on the revised slip rate versus magnitude graphs (figures 2.5S-1 and 2.5S-2).

Magnitudes of earthquakes are presented as surface wave magnitudes (M_s). The values of earthquakes shown in table 2.5S-3 are taken from the various publications which discuss the seismology or geology of the faults. Pre-instrumental estimates are also taken from the various literature sources. The Applicant has made no detailed efforts to determine independent M_s values from instrumental recordings or from pre-instrumental data. Generally, M_s values or their equivalent are available in the literature (for example, Gutenberg and Richter, 1954).

The surface wave magnitude for the 1933 Long Beach earthquake is of particular interest. It was reported by Gutenberg and Richter (1949a) as M_s 6.25; review of the unpublished worksheets prepared by Gutenberg and Richter (1949b) shows that 17 station readings were used and that the computed average is 6.2 ± .2 with a mode of 6.3. Thus, the M_s 6.3 value is a conservatively accurate value.

Application of Conservatism

Selection of the slip rate value which best represent the fault was based on data presented by the various researchers and authors and assumes no specific conservatism other than to best represent the faults degree of activity. The degree of conservatism in the selected values depends on

each author's interpretation of this data. In order to further evaluate these data, a line can be drawn bounding these empirical observations as shown in figure 2.5S-3. This line suggests that there is a consistent limit to the size of an earthquake associated with the geologic slip rate of a strike-slip fault. This assumes that some of the strike-slip faults in the world have had maximum or close-to-maximum earthquakes and that when these maximum data points are enveloped they form a maximum historic earthquake limit (HEL) related to slip rate. Several procedures are used to assess the conservatism and the significance of this observational limit.

The conservatism of the slip rate versus magnitude data set is evaluated by considering the ranges of slip rate and magnitude data obtained from published and unpublished sources. The data presented in tables 2.5S-3 and 2.5S-4 provide for this assessment of uncertainty in the data interpretation.

To account for possible uncertainty in earthquake magnitude values and to provide another degree of conservatism, a magnitude range is assigned to each earthquake. The earliest surface wave magnitude estimates were considered to be dependable to one quarter of a unit (Richter, 1958, p 347). Modern estimates, based on a larger and better distributed set of stations, are dependable to one tenth of a unit at a confidence level of 95% (e.g., Shimazaki and Somerville, 1979, pp 1373-1374). The Applicants therefore conclude that a value of two tenths of a unit plus or minus is a conservative estimate of the uncertainty associated with surface wave magnitude estimates.

Another method of adding cnservatism is to extend the possible ranges of slip rates for each of the faults. The ranges shown in figure 2.5S-4 have been extended to the widest reasonable extent as discussed in available literature. Confidence in these ranges, presented in the literature, varies widely and is dependent upon how current and detailed the particular study is.

The widest reasonable ranges can be used in conjunction with the magnitude ranges to establish a maximum earthquake limit line (MEL) (figure 2.5S-4). The MEL is interpreted most conservatively by enveloping the lowest slip rate ranges and the maximum-magnitude ranges of all the data points. The most conservative use of the line is to estimate a maximum earthquake by reading the MEL value based on the maximum slip rate value provided for each fault. The Applicants believe that the MEL line represents an outer bound for maximum magnitude which will not be exceeded by future earthquakes on these faults. This line does not mean that each of these faults is capable of the MEL earthquake, but only that this line will not be exceeded by future earthquakes.

On the basis of the most conservative interpretation of the MEL line, the maximum magnitude for the NIZD associated with the highest slip rate of 0.68 mm/yr results in M_s 7.0. The physical conservatism of both the M_s 6.5 and M_s 7.0 as maximum values are discussed in sections 2.5S.3 and 2.5S.4.

APPENDIX 2.5S

Table 2.5S-4
ESTIMATED SLIP RATES FOR STRIKE-SLIP FAULTS WHICH DO NOT HAVE ESTIMATES FOR LARGE HISTORICAL EARTHQUAKES

Reference Number	Name (Location)	Geologic Slip Rate Range (mm/year)*	Selected Slip Rate Value (mm/year)	Reference(s) Selection Criteria**
24	Big Pine (California)	2.1 - 2.7	2.4	Crowell, 1962; Kahle, 1966. Criterion 3
25	Blue Cut (California)	1 - 2.5	1.8	Hope, 1969, Garfunkel, 1974. Criterion 3
26	Calico (California)	1.8 - 5	3.4	Garfunkel, 1974. Criterion 3
27	Collayami (California)	1	1	Hearn and others, 1976 Criterion 1
28	Garlock (California)	3.4 - 12.9	8	Dibblee, 1967, Carter, 1971 Criterion 1
29	Helendale (California)	2 - 4	3	Garfunkel, 1974. Criterion 3
30	Pinto Mountain (California)	2 - 4	3	Dibblee, 1967a, b, c Criterion 3
31	Sheep Hole - Ludlow (California)	3 - 3.75	3.4	Garfunkel, 1974. Criterion 3
32	Darvaz (Asia)	3.3 - 14	13	Trifonov, 1978 Criteria 1 and 3
33	Denali (Alaska)	11 - 35	35	Richter and Matson, 1971 Criteria 1 and 2
34	Lembang (W. Java)	13 - 83	30	Tjia, 1968, 1970. Criterion 1
35	Talemazar (Asia)	2.5	2.5	Wellman, 1965. Criterion 3
36	Totschunda (Alaska)	5 - 33	33	Richter and Matson, 1971 Criteria 1 and 2

* Includes faults with poor control of displacements and age of displacement but included for statistical analyses.

** Criteria described in section 2.5S.5.

APPENDIX 2.5S

2.5S.6

It is natural that the best known faults should be those with high slip rates. This leads to a bias towards high slip rates in the distribution of faults whose slip rates are known. For example, in California it is likely that all faults with high slip rates have been included in the data set, while there may be many low slip rate faults that are not included because the slip rate is unknown or because the fault has not even been identified yet. A search for larger earthquakes, particularly in California, that might be associated with previously excluded strike-slip faults did not result in added data points for figure 2.5S-4. The inclusion of all of the possible low slip rate faults would clearly increase the confidence in the slip rate/maximum-magnitude relation at low slip rates; their omission (due to the lack of data) constitutes a conservative bias.

As illustrated in table 2.5R-1, the number of faults in the median slip rate group (3.5 to 17.5 mm/yr) is almost identical to the number of faults in the lower slip rate group (0.7 to 3.5 mm/yr). The data base has been expanded, particularly for low slip rate faults, as discussed in section 2.5S.5. These added data provide substantial statistical support to the validity of the data base. The slip rate relation has not been altered by the expanded base, thus confidence in its significance is increased.

2.5S.7

Two geologic time scales were used in analysis of published displacements and in preparation of the data base presented in Table G-1 of the WCC (June 1979) report and in its revision, table 2.5S-2. For general use on a worldwide basis, geologic ages, periods, and epochs were correlated with absolute geologic time using the Geologic Time Table of Van Eysinga (1975). In the Los Angeles Basin, where detailed stratigraphic analysis of displaced facies relationships along the Newport-Inglewood Zone of Deformation (NIZD) was required, the absolute geologic ages of the Tertiary and Quaternary epochs were estimated from the upper Cenozoic Geologic Time and Stratigraphic Column for the Los Angeles Basin by Nardin and Henyey (1978). Stratigraphic correlations along the NIZD were based on the Summary of Operations volumes of the various oil fields by the California Division of Oil and Gas (referenced in Appendix B of the WCC June 1979 Report) and the Cenozoic Correlation Section Across the Los Angeles Basin, published by the American Association of Petroleum Geologists (Knapp and others, 1962).

In the study of the NIZD, absolute ages were assigned to the particular facies being correlated on the basis of their relative positions within the time-stratigraphic section (e.g., beginning of Upper Pliocene). To accommodate possible errors in this judgmental assignment of absolute ages, a ±10% error factor was added to the estimate and included in Table 1, Appendix B, of the WCC June 1979 Report. This 10% error factor is

considered reasonable because: (1) the stratigraphic units and their relative geologic ages are well defined and (2) the absolute age span of the sediments involved covers a relatively short and well-defined geologic time span. The error and uncertainty factors for each age determination are presented graphically in Figures B-7 and B-8 of Appendix B of the WCC (June 1979) Report.

For review of geologic slip rates for strike-slip faults presented in section 2.5S.5, the ranges of possible ages are given in table 2.5S-2. Those ages and ranges of age are based on historic or radiometric dating techniques wherever reported in the literature. Other offsets are assigned ranges of ages to encompass the ages of offset features or the timing of commencement of faulting according to the literature. The range of possible ages was incorporated in estimating the range of geologic slip rates applicable to any one fault. These ranges are presented in tables 2.5S-2 and 2.5S-3 and were used in preparation of the slip rate/ maximum-magnitude relationship graph, figure 2.5S-2.

REFERENCES

1. Addicott, W. O., 1968, Mid-Teritiary zoogeographic and paleogeographic discontinuities across the San Andreas fault, California: Conference on Geologic Problems of San Andreas Fault System, Stanford University, September 14-16, 1967, Proceedings, Stanford University Publications, v. 11, page 144-165.

2. Arpat, E. and Saroglu, F., 1975, Some recent tectonic events in Turkey: Geological Society of Turkey Bulletin, v. 18, p. 91-101 (in Turkish).

3. Barrows, A. G., Beeby, D. J., and Kahle, J. E., 1979, Earthquake hazards geologic mapping of the San Andreas fault zone, Los Angeles County, California, near Valyermo, Lake Hughes, Three Points and Quail Lake: U.S. Geological Survey, National Earthquake Hazards Reduction Program, Summaries of Technical Reports, v. VIII, June.

4. Ben-Menahem, A., Nur, A., and Vered, M., 1976, Tectonics, seismicity and structure of the Afro-Eurasian junction--The breaking of an incoherent plate: Physics of the Earth and Planetary Interiors, v. 12, p. 1-50.

5. Burke, D. B., and Helley, E. J., Map showing evidence of recent fault activity in the vicinity of Antioch, Contra Costa County, California: U.S. Geological Survey Miscellaneous Field Studies Map MF-533, scale 1:24,000.

6. Canitez, N., 1976, Dynamics of the North Anatolian fault: Cento Seminar on Earthquake Hazard Minimization, Teheran, Proceedings, p. 353-366.

7. Castle, R. O., and Yerkes, R. F., 1976, Recent surface movements in the Baldwin Hills, Los Angeles County, California: U.S. Geological Survey Professional Paper 882, 125 p.

8. Clark, M. M., Grantz, A., and Rubin, M., 1972, Holocene activity of the Coyote Creek fault as recorded in sediments of Lake Cahuilla, in the Borrego Mountain Earthquake of April 9, 1968: U.S. Geological Survey Professional Paper 787, p. 112-130.

9. Clark, S. H., Jr., and Nilsen, T. H., 1973, Displacement of Eocene strata and implications for the history of offset along the San Andreas fault, central and northern California: Conference on Tectonic Problems of the San Andreas fault system, Stanford University, June 20-23, 1973, Proceedings, Stanford University Publications, v. 13, p. 358-367.

10. Clayton, L., 1966, Tectonic depressions along the Hope fault, a transcurrent fault in North Canterbury, New Zealand: New Zealand Journal of Geology and Geophysics, v. 9, p. 95-104.

REFERENCES

11. Crittenden, M. D., Jr., 1951, Geology of the San Jose-Mount Hamiton area, California: California Division of Mines and Geology Bulletin 157, 74 p.

12. Crowell, J. C., 1973, Problems concerning the San Andreas fault system in southern California: Conference on Tectonic Problems of the San Andreas Fault System, Stanford University, June 20-23, 1973, Proceedings, Stanford University Publications, v. 13, p. 125-135.

13. Cummings, J. C., 1968, The Santa Clara formation and possible post-Pliocene slip on the San Andreas fault in central California: Conference on Geologic Problems of San Andreas Fault System, Stanford University, September 14-16, 1967, Proceedings, Stanford University Publications, v. 11, p. 191-207.

14. Dewey, J. W., 1972, Seismicity and tectonics of Western Venezuela: Seismological Society of America Bulletin, v. 62, no. 6, p. 1711-1751.

15. Dudley, P. H., 1954, Geology of the Long Beach oil field, Los Angeles County: California Division of Mines and Geology Bulletin 170, May, Sheet 34.

16. Durham, D. L., and Yerkes, R. F., 1964, Geology and oil resources of the eastern Puente Hills area, southern California: U.S. Geological Survey Professional Paper 420-B, 62 p.

17. Ehlig, P. L., Ehlert, K. W., and Crowe, B. M., 1975, Offset of the upper Miocene Caliente and Mint Canyon formations along the San Gabriel and San Andreas faults, in San Andreas fault in southern California: California Division of Mines and Geology Special Report 118, p. 83-92.

18. Freund, R., 1971, The Hope fault: A strike-slip fault in New Zealand: New Zealand Geological Survey Bulletin, n. 5, 86, 49 p.

19. Freund, R., Garfunkel, Z., Zak, I., Goldberg, M., Weissbrod, T., and Derin, B., 1970, The shear along the Dead Sea rift: Philosophical Transactions, Royal Society of London, Series A, v. 267, p. 107-130.

20. Girdler, R. W., 1958, The relationship of the Red Sea to the East Africa rift system: Quarterly Journal of the Geological Society of London, v. 114, p. 79-115.

21. Graham, S. A. and Dickinson, W. R., 1977, Apparent offsets of on-land geologic features across the San Gregorio-Hosgri fault trend: Geological Society of America Abstracts with Programs, 73rd annual meeting, v. 9, no. 4, p. 424.

REFERENCES

22. Greene, H. G., 1977, Slivering of the Salinian block along the Palo Colorado-San Gregorio and associated fault zones: Geological Society of America Abstracts with Programs, 73rd annual meeting, v. 9, no. 4, p. 425.

23. Gutenberg, B., and Richter, C. F., 1949a, Seismicity of the earth and associated phenomena: Princeton University Press, Princeton, 273 p.

24. Gutenberg, B., and Richter, C., F., 1949b, Unpublished worksheets for Seismicity of the Earth: California Institute of Technology, Milikan Library Archives, Pasadena.

25. Gutenberg, B., and Richter, C. F., 1954, Seismicity of the earth and associated phenomena: Hafna Publishing Company, New York, 310 p.

26. Hamilton, D. H. and Willingham, C. R., 1978, Evidence for a maximum of 20 km of Neogene right-slip along the San Gregorio fault zone of central California: EOS Transactions, American Geophysical Union, v. 59, no. 12, p. 1210.

27. Heath, E. G., 1954, Geology along the Whittier fault north of Horseshoe Bend, Santa Ana Canyon, California: Master's thesis, Claremont Graduate School, 84 p.

28. Herd, D. G., 1978, Neotectonic framework of central coastal California and its implications to microzonation of the San Francisco Bay region, in Second International Conference on Microzonation for Safer Construction - research and application, Proceedings, v. 1, p. 231-240.

29. Hill, L., 1971, Newport-Inglewood zone and Mesozoic subduction, California: Geological Society of America Bulletin, v. 82, p. 2957-2962.

30. Huffman, O. F., 1972, Lateral displacement of upper Miocene rocks and the Neogene history of offset along the San Andreas fault in central California: Geological Society of America Bulletin, v. 83, n. 10, p. 2913-2946.

31. Huffman, O. F., Turner, D. L, and Jack, R. N., 1973, Offset of late Oliogocene-early Miocene volcanic rocks along the San Andreas fault in central California: Conference on Tectonic Problems of the San Andreas fault System, Stanford University, June 20-23, 1973, Proceedings, Stanford University Publications, v. 13, p. 368-373.

32. Kanamori, H. and Jennings, P. C., 1978, Determination of local magnitude, M_L, from strong-motion accelerograms: Seismological Society of America Bulletin, v. 68, n. 2, p. 471-485.

REFERENCES

33. Kennedy, M. P., 1977, Recency and character of faulting along the Elsinore fault zone in southern Riverside County, California: California Division of Mines and Geology Special Report 131, 12 p.

34. Knapp, R. R., Traxler, J. D., Newbill, T. J., Laughlin, D. J., Stewart, R. D., Heath, E. G., Stark, H. E., Wissler, S. G., and Holman, W. H., 1962, Cenozoic correlation section across Los Angeles basin from Beverly Hills to Newport, California: American Association of Petroleum Geologists, Pacific Section.

35. Knuepfer, P. L., 1977, Geomorphic investigations of the Vaca and Antioch fault systems, Solano and Contra Costa Counties, California: Master's thesis, Stanford University, 53 p.

36. Krymus, V. N., and Lykov, V. I., 1969, The character of the junction of the Epi-Hercynian platform and the Alpine folded belt, south Turkmenia: Geotectonics, Academy of Science, U.S.S.R., translated by the American Geophysical Union, v. 6, p. 391-396.

37. Lamar, D. L., Merifield, P. M., and Proctor, R. J., 1973, Earthquake recurrence intervals on major faults in southern California, in Moran, D. E., Slosson, J. E., Stone, R. O., and Yelverton, C. A., eds., Geology, Seismicity, and Environmental Impact: Association of Engineering Geologists Special Publication, p. 265-276.

38. Lensen, G. J., 1958, The Wellington fault from Cook Strait to Manawatu Gorge: New Zealand Journal of Geology and Geophysics, v. 1, n. 1, p. 364-374.

39. Lensen, G. J., 1973, Guidebook for excursion A-10, Tour Guide for International Association of Quaternary Research Christchurch, New Zealand, 76 p.

40. Lensen, G. J., 1975, Earth-deformation studies in New Zealand: Tectonophysics, v. 29, p. 541-551.

41. Lensen, G. J., and Vella, P., 1971, The Waiohine faulted terrace sequence--recent crustal movements: Royal Society of New Zealand, Bulletin 9, p. 117-119.

42. Morton, D. M., 1979, Earthquake hazard studies, upper Santa Ana Valley and adjacent areas: U.S. Geological Survey National Earthquake Hazards Reduction Program, Summaries of Technical Reports, v. 8, June.

43. Nardin, T. R. and Henyey, T. L., 1978, Pliocene-Pleistocene diastrophism of Santa Monica and San Pedro shelves, California continental borderland: American Association of Petroleum Geologists Bulletin, v. 62, n. 2, p. 247-272.

REFERENCES

44. Neev, D. and Emery, K. O., 1967, The Dead Sea, depositional processes and environments of evaporites: Geological Survey of Israel Bulletin, v. 41, p. 147.

45. Norris, R. M., Keller, E. A., and Meyer, G. L., 1979, Geomorphology of the Salton Basin, selected observations in Abbott, P. L., ed., Geologic Excursions in the Southern California Area: Department of Geological Science, San Diego tate University, p. 19-46.

46. Page, R. A., 1969, Late Cenozoic movement on the Fairweather fault in southeastern Alaska: Geological Society of America Bulletin, v. 80, p. 1873-1877.

47. Peterson, M. S., 1975, Geology of the Coachella fanglomerate, in San Andreas fault in southern California: California Division of Mines and Geology Special Report 118, p. 119-126.

48. Plafker, G., Hudson, T., and Bruns, T., 1978, Late Quaternary offsets along the Fairweather fault and crustal plate interactions in southern Alaska: Canadian Journal of Earth Science, v. 15, p. 805-816.

49. Posavec, M., Taylor, D., Van Leeuwen, T., and Spector, A., 1973, Tectonic controls of volcanism and complex movements along the Sumatran fault system: Geological Society of Malaysia Bulletin, n. 6, p. 43-60.

50. Prowell, D. C., 1974, Geology of selected Tertiary volcanics in the central coast range mountains of California and their bearing on the Calaveras and Hayward fault problems: University of California Santa Cruz, unpublished Ph.D. thesis, 182 p.

51. Quennell, A. M., 1958, The structure and geomorphic evolution of the Dead Sea rift: Quarterly Journal of the Geological Society of London, v. 114, pt. 1, p. 1-24.

52. Richter, C. F., 1958, Elementary Seismology: W. B. Freeman and Company, San Francisco.

53. Rod, E., 1956, Strike-slip faults of northern Venezuela: American Association of Petroleum Geologists, v. 40, n. 3, p. 457-476.

54. Sage, O., 1973, Paleocene geography of the Los Angeles region, in Kovach, R. L., and Nur, A., eds., Conference on Tectonic Problems of the San Andreas fault system, Proceedings: Stanford University Publication in Geological Sciences, v. 13, p. 348-357.

55. Sengor, A. M. C., 1979, North Anatolian transform fault - its age, offset and tectonic significance: Journal of the Geological Society of London, v. 136, p. 269-282.

REFERENCES

56. Scholz, C. H., Rynn, J. M., Weed, R. W., Frohlich, C., 1973, Detailed seismicity of the Alpine fault zone and Fiordland region, New Zealand: Geological Society of America Bulletin, v. 84, n. 10, p. 3279-3316.

57. Schubert, C., and Sifontes, R. S., 1970, Bocona fault, Venezuelan Andes, evidence of postglacial movement: Science, v. 170, p. 66-69.

58. Schwartz, D., Cluff, L. S., and Donnelly, T., 1979, Quaternary faulting along the Caribbean and North American plate boundary: Tectonophysics, v. 52 (in press).

59. Sharp, R. V., 1967, San Jacinto fault zone in the Peninsular Ranges of southern California: Geological Society of America Bulletin, v. 78, n. 6, p. 705-730.

60. Sharp, R. V., 1978, Salton Trough tectonics: U.S. Geological Society, National Earthquake Hazards Reduction Program, Summaries of Technical Reports, v. 7, p. 34-35.

61. Sharp, R. V., 1980, Salton Trough tectonics: U.S. Geological Society, National Earthquake Hazards Reduction Program, Summaries of Technical Reports, Open-File Report 80-6, v. 9.

62. Shimazaki, D., and Somerville, P., 1979, Static and Dynamic Parameters of the Izu-Oshima, Japan Earthquake of January 14, 1978: Seismological Society of American Bulletin, v. 69, p. 1343-1378.

63. Shor, G. G., 1955, Deep reflections from southern California blasts: Transactions of the American Geophysical Union, v. 36, p. 133-138.

64. Sieh, K. E., 1977, A study of Holocene displacement history along the south-central reach of the San Andreas fault: Ph.D. thesis, Stanford University, 219 p.

65. Sieh, K. E., 1978, Prehistoric large earthquakes produced by slip on the San Andreas fault at Pallett Creek, California: Journal of Geophysical Research, v. 83, n. B8, p. 3907-3939.

66. Silver, E., 1977, Are the San Gregorio and Hosgri fault zones a single fault system?: Geological Society of America, Abstracts with Programs, 73rd annual meeting, v. 9, n. 4, p. 500.

67. Slemmons, D. B., 1977, State-of-the-art for assessing earthquake hazards in the United States, Report 6, Faults and Earthquake Magnitude: U.S. Army Corps of Engineers Waterways Experiment Station, Soils and Pavement Laboratory, Miscellaneous Paper S-73-1, 129 p.

68. Suggate, R. P., 1960, The interpretation of progressive fault displacement of flights of terraces: New Zealand Journal of Geology and Geophysics, v. 3.

REFERENCES

69. Suggate, R. P., and Lensen, G. J., 1973, Rate of horizontal fault displacement in New Zealand: Nature, v. 242, p. 518.

70. Tchalenko, J. S., and Berberian, M., 1975, Dasht-e Bayaz fault, Iran-Earthquake and earlier related structures in bedrock: Geological Society of America Bulletin, v. 86, n. 5, p. 703-709.

71. Tjia, H. D., 1970, Rates of diastrophic movement during the Quaternary in Indonesia: Geologie en Mijnouw (Journal of the Royal Geological and Mining Society of the Netherlands), v. 49, n. 4, p. 335-338.

72. Trifonov, V. G., 1971, The pulse-like character of tectonic movements in regions of most recent mountain-building (Kopet Dagh and southeast Caucasus): Geotectonics, U.S.S.R. Academy of Sciences, Geological Institute, n. 1, p. 234-235.

73. Trifonov, V. G., 1978, Late Quaternary tectonic movements of western and central Asia: Geological Society of Amrica Bulletin, v. 89, n. 7, p. 1059-1072.

74. Van Eysinga, F. W. B., 1975, Geologic Time Scale: Elsevier Scientific Publishing Company, Amsterdam, 3rd Edition, 1 sheet.

75. Vedder, J. G., 1975, Juxtaposed Teritary strata along the San Andreas fault in the Temblor and Caliente Ranges, California, in San Andreas fault in southern California: California Division of Mines and Geology Special Report 118, p. 234-240.

76. Weber, G. E. and LaJoie, K. R., 1979, Late Pleistocene rates of movement along the San Gregorio fault zone determined from offset marine terrace shoreline angles in Weber and others, eds., Coastal Tectonics and Hazards in Santa Cruz and San Mateo Counties, California: Field Trip Guide, Cordilleran section of the Geological Society of America, 75th annual meeting.

77. Weber, F. H., Jr., 1977a, Total right lateral offset along the Elsinore fault zone, southern California: Geological Society of America Abstracts with Programs, v. 9, n. 4, p. 523-524.

78. Weber, F. H., Jr., 1977b, Seismic hazards related to geologic factors, Elsinore and Chino fault zones, northwestern Riverside County, California: California Division of Mines and Geology Open-File Report 77-4LA.

79. Wellman, H. W., 1969, Wrench (transcurrent) fault systems: American Geophysical Union Monograph 13.

80. Woodward, Clyde and Associates, 1969, Seismicity and seismic geology of northwestern Venezuela: Report to Shell Oil Company of Venezuela, v. 2, 77 p.

REFERENCES

81. Woodward-Clyde Consultants, 1979, Report of the evaluation of maximum earthquake and site ground motion parameters associated with the offshore zone of deformation, San Onofre Nuclear Generating Station: Report for Southern California Edison Company, June, 241 p.

82. Wright, T. L., Parker, S., Erickson, R. C., 1973, Stratigraphic evidence for the timing and nature of late Cenozoic deformation in the Los Angeles basin: Paper presented at National American Association of Petroleum Geologists convention, Anaheim, California, May 1973.

83. Yerkes, R. F., 1972, Geology and oil resources of the western Puente Hills area, southern California: U.S. Geological Survey Professional Paper 420-C, 63 p.

84. Yerkes, R. F., McCulloh, T. H., Schoellhamer, J. E., and Vedder, J. G., 1965, Geology of the Los Angeles basin - an introduction: U.S. Geological Survey Professional Paper 420-A, 57 p.

85. Zak, I., and Freund, R., 1966, Recent strike slip movements along the Dead Sea rift: Israel Journal of Earth Sciences, v. 15, p. 33-37.

Personal Communications

Knuefer, P. L., 1979, Woodward-Clyde Consultants, San Francisco, California.

Seih, K., 1979, California Institude of Technology, Pasadena, California.

Schwartz, D., 1979, Woodward-Clyde Consultants, San Francisco, California.

Welden, R., 1979, California Institute of Technology, Pasadena, California.

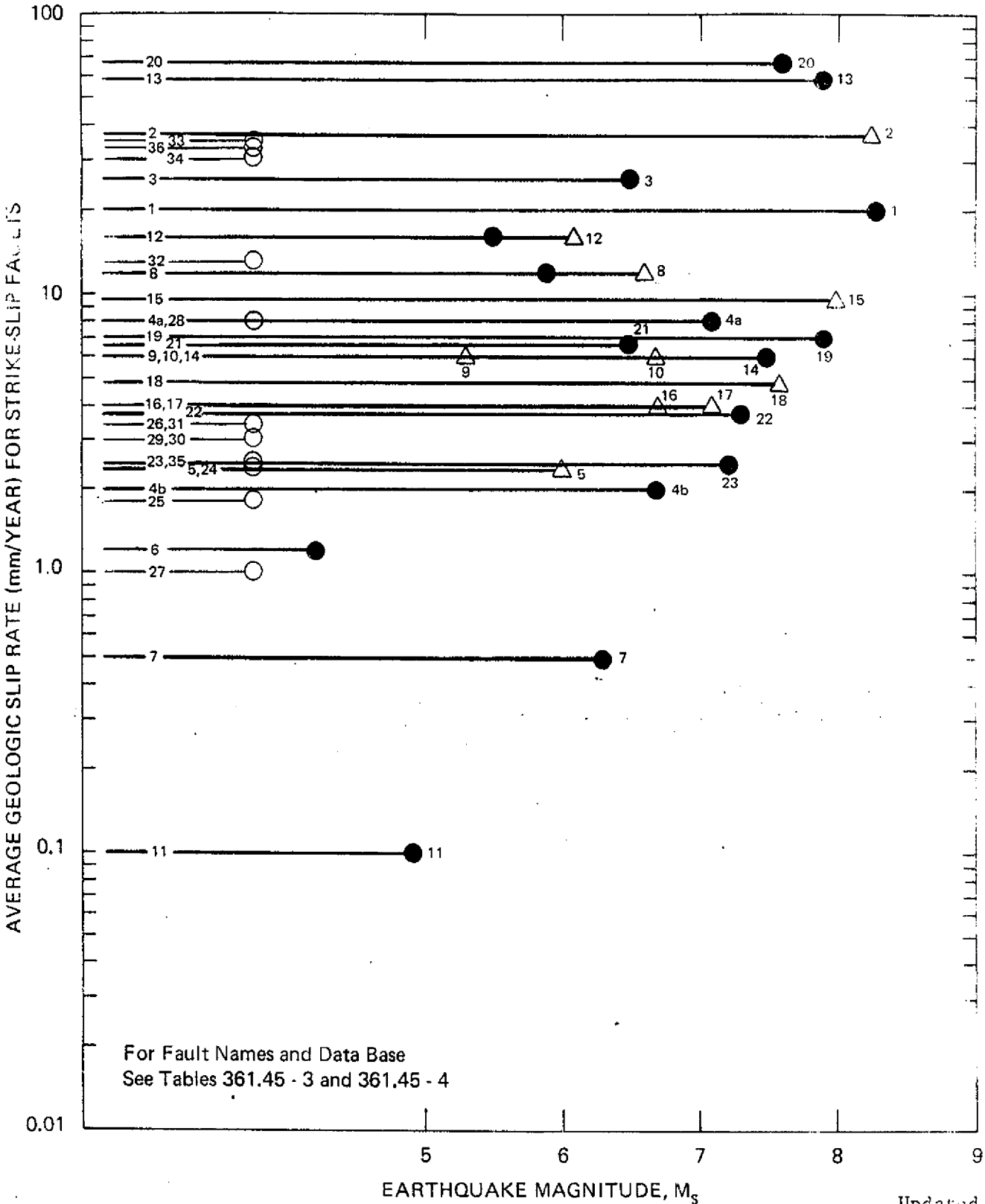

EXPLANATION

- ● Maximum instrumental recording
- △ Maximum pre-instrumental estimates
- — Range over which smaller earthquakes occur
- ○ No maximum magnitude from instrumental or pre-instrumental data.

Updated

SAN ONOFRE
NUCLEAR GENERATING STATION
Units 2 & 3

EMPIRICAL PLOT
GEOLOGIC SLIP RATE vs. HISTORICAL
MAGNITUDE FOR STRIKE-SLIP FAULTS

Figure 2.5S-1

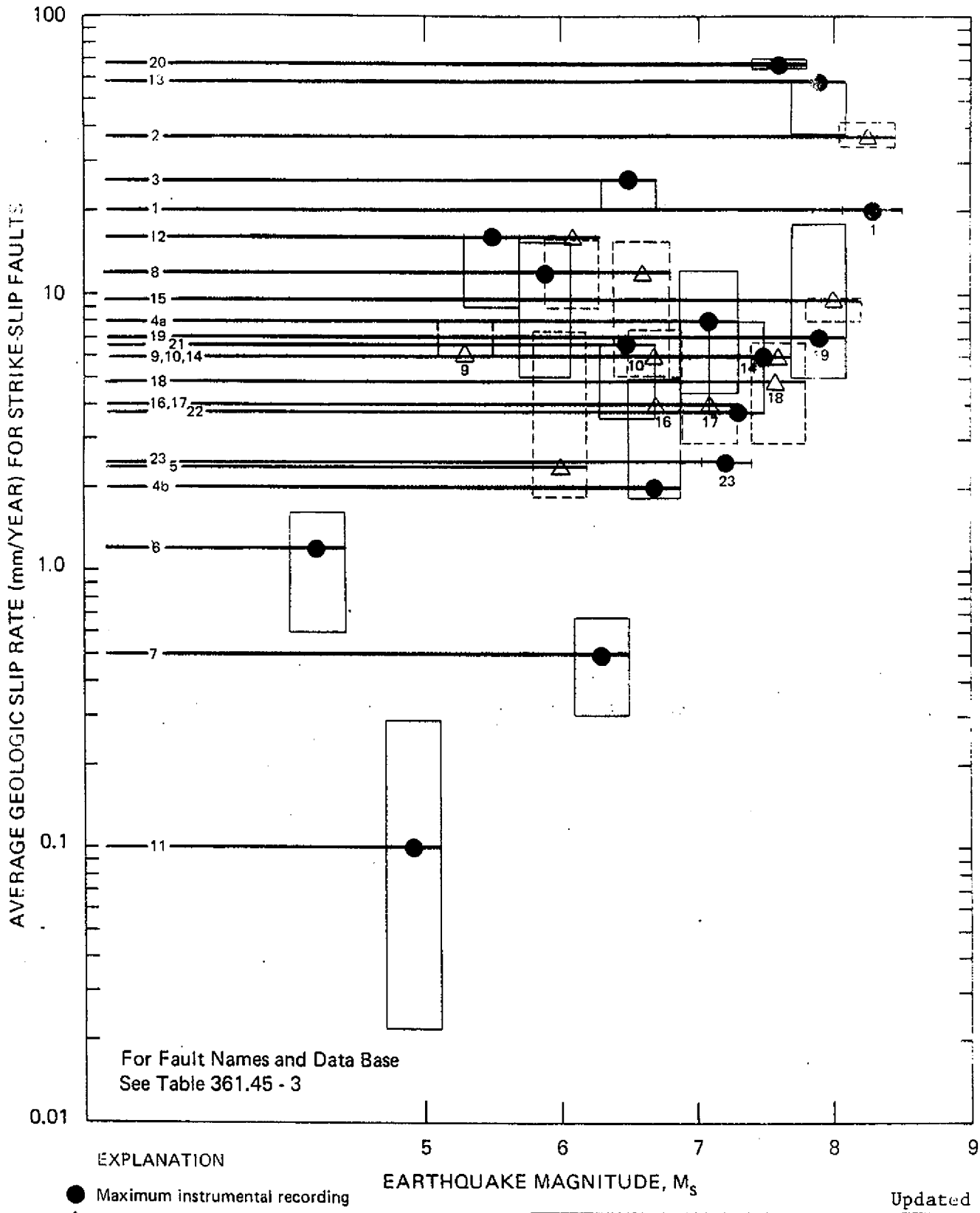

Updated

SAN ONOFRE NUCLEAR GENERATING STATION
Units 2 & 3

DATA RANGE ANALYSIS
GEOLOGIC SLIP RATE vs. HISTORICAL MAGNITUDE FOR STRIKE-SLIP FAULTS

Figure 2.5S-2

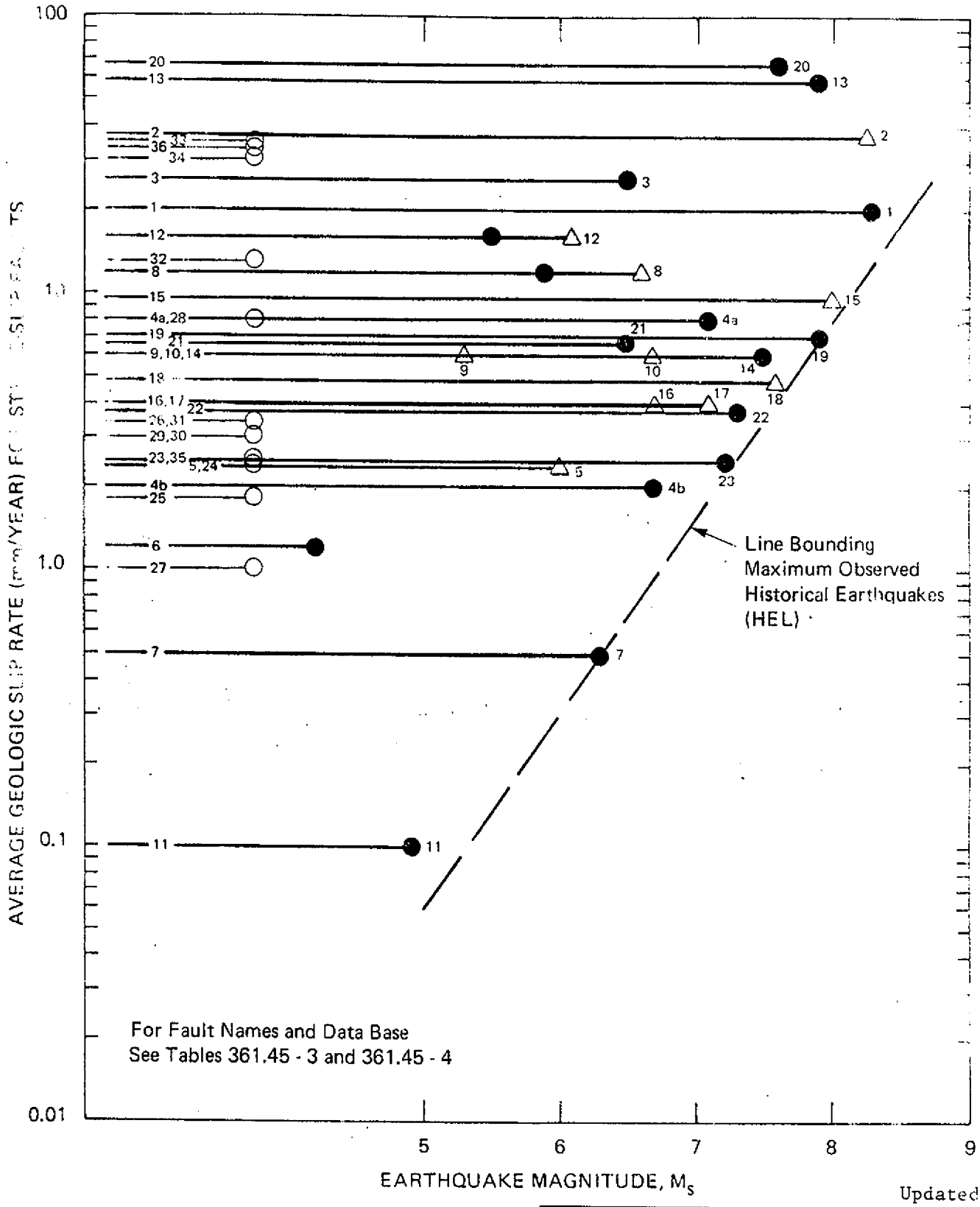

EXPLANATION

- ● Maximum instrumental recording
- △ Maximum pre-instrumental estimates
- — Range over which smaller earthquakes occur
- ○ No maximum magnitude from instrumental or pre-instrumental data.

Updated

SAN ONOFRE NUCLEAR GENERATING STATION Units 2 & 3

HISTORICAL EARTHQUAKE LIMIT GEOLOGIC SLIP RATE vs. HISTORICAL MAGNITUDE FOR STRIKE-SLIP FAULTS

Figure 2.5S-3

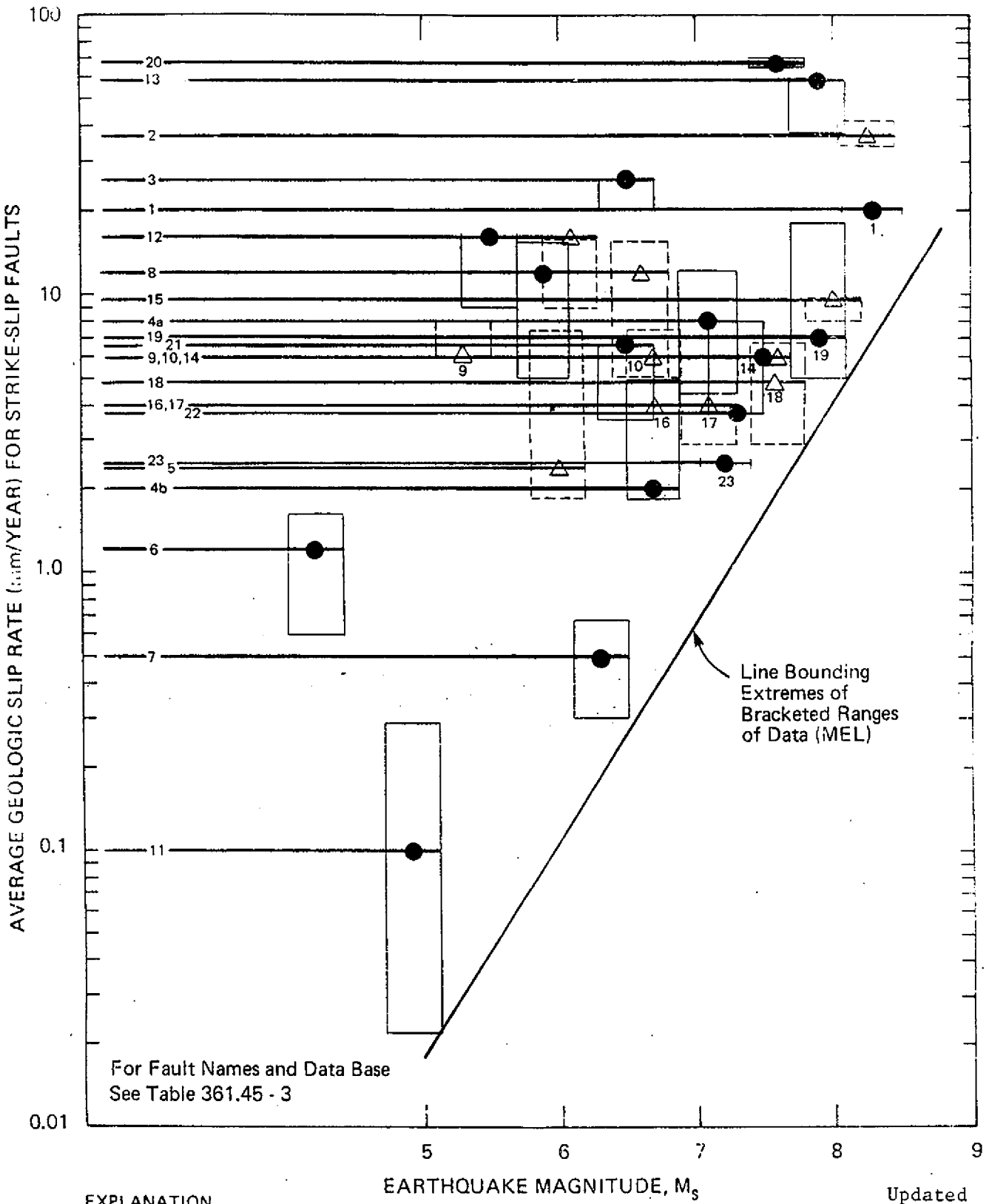

EXPLANATION

- Maximum instrumental recording
- △ Maximum pre-instrumental estimate
- — Range over which smaller earthquakes occur
- Box represents most likely range of geologic slip rate data and possible error range of ±0.2 in Magnitude calculation. Dashed box represents uncertainty of pre-instrumental estimates.

Updated

SAN ONOFRE NUCLEAR GENERATING STATION Units 2 & 3

MAXIMUM EARTHQUAKE LIMIT GEOLOGIC SLIP RATE vs. HISTORICAL MAGNITUDE FOR STRIKE-SLIP FAULTS

Figure 2.5S-4

APPENDIX 2.5T

GROUND MOTION ANALYSIS

Site File Copy

APPENDIX 2.5T

GROUND MOTION ANALYSIS

2.5T.1 REVIEW OF THE WORK BY BOORE AND OTHERS (1978) AND CROUSE (1978)

Through regression analyses of selected data from the 1971 San Fernando earthquake, Boore and others (1978) suggest that peak accelerations recorded at the base of large structures are less than peak accelerations recorded at the base of small structures. For their analyses, Boore and others (1978) used data from soil sites located in the distance range 15 to 100 km. Inspection of these data indicates that not for all distance ranges do the data points equally well represent both small and large structures as noted below:

Distance Range (km)	Number of Data Points from Small Structures	Number of Data Points from Large Structures
15 - 20	0	4
20 - 30	3	4
30 - 50	3	4
50 - 100	6	6
	12	18

These data are plotted in Figure 32 of the report by Boore and others (1978). In the distance range 15 to 20 km, no comparison is possible of the effect of structure size on peak acceleration. In the distance range 30 to 50 km, the peak accelerations vary by an unusually large amount; thus, they may not be suitable as a basis for any statistical inferences. If the data in the distance ranges 20 to 30 km and 50 to 100 km are examined, it is difficult to discern any trend for differences in peak accelerations recorded at the base of small and large structures. Boore and others (1978) observed that "the differences between the data from the large structures and the small structures are relatively small compared with the range of either data set, and we do not believe that firm conclusions are warranted solely on the basis of formal statistical tests. The differences may be due to soil-structure interaction, but more study would be required to demonstrate this." The Applicants concur with this opinion.

The work presented by Crouse (1978) is an examination of recorded ground motions in terms of spectra rather than peak acceleration; in particular, the influence of soil-structure interaction on the recorded ground motions. Based on a comparison of free-field recordings with those from the base of nearby structures for the same earthquake, Crouse (1978) concluded that "the only significant effect of soil-structure interaction that may be present in the strong-motion records is believed to be the filtering of high frequency seismic waves by the foundation of buildings in which the motions were recorded." Crouse (1978) further states that "this phenomena is probably only significant in buildings with relatively large foundations."

Amended: April 2009 TL: E048000

Crouse (1978) however, indicated that the effects of soil-structure interaction and local site conditions on spectra cannot be clearly isolated because of the types of recordings available. Most of the recordings on rock have been made in small structures, whereas most of the recordings on soil were made in larger multi-story structures and the data base for either the soil-structure interaction or local site conditions effects is not yet sufficient to draw definitive conclusions.

2.5T.2 IMPACT OF OBSERVATIONS REGARDING THE EFFECT OF STRUCTURE SIZE ON RECORDED GROUND MOTIONS

To assess the influence of the structure size on the estimated ground motion for San Onofre a review was made of the work by Boore and others (1978) and Crouse (1978). The pertinent observations from this review are described in section 2.5T.1. These observations indicate that it is not possible to distinguish differences in ground motions due to differences in structure size with the currently available data base.

2.5T.3 INFLUENCE OF NORTHWEST CALIFORNIA EARTHQUAKE DATA ON REGRESSION RESULTS

To examine the impact of including data from the northwest California earthquakes, parametric studies were made in which records from these earthquakes were excluded from the weighted regression analyses. In the first parametric analysis, records from the 1934 Eureka Earthquake, 1941 northwest California earthquake, and 1941 Eureka earthquake records were excluded. The 1954 Eureka earthquake records were included in this first analysis because this earthquake is well located based on studies by Smith (1977). In the second parametric analysis, the records from all four northwest California earthquakes were excluded. The results of both of these analyses gave lower peak accelerations at the 10 km energy center distance than the peak accelerations obtained from the analysis presented in Appendix J of the June 1979 Woodward-Clyde Consultants report.

2.5T.4 IMPACT OF THE NORTHWEST CALIFORNIA EARTHQUAKE DATA

The impact of including data from the northwest California earthquakes on the estimated ground motion for San Onofre is discussed in section 2.5T.2. Excluding these data would result in lower peak accelerations indicating no need to revise the estimated values of ground motions for San Onofre due to their inclusion in the selected data base.

2.5T.5 EXAMINATION OF RECORDINGS FROM THE AUGUST 6, 1979, COYOTE LAKE AND OCTOBER 15, 1979, IMPERIAL VALLEY EARTHQUAKES

Recordings obtained during the August 6, 1979, Coyote Lake and the October 15, 1979, Imperial Valley earthquakes have significantly increased the available strong motion data base, particularly for recordings near the fault rupture surface. The Coyote Lake Earthquake was located in the

APPENDIX 2.5T

Calaveras fault zone near Gilroy, California at a focal depth of approximately 10 kilometers. The Imperial Valley earthquake was located on the Imperial fault in southern California and northern Mexico and had a shallow focal depth (approximately 10 km). Surface rupture occurred during the 1979 Imperial Valley earthquake and very closely followed the fault rupture trace of the 1940 Imperial Valley earthquake. Magnitudes for the two earthquakes have been assigned as follows:

	m_b	M_s	M_L
1979 Coyote Lake	5.3	5.6	5.9
1979 Imperial Valley	5.6	6.8	6.6

At the location of each of these recent earthquakes, an array of strong motion stations had been positioned across the fault zone and was in operation at the time of the earthquake. These and other nearby stations provided substantial information on ground motions close to the rupture. The majority of these recording stations are instrument shelters or small buildings.

For the 1979 Coyote Lake earthquake, eight stations within 20 kilometers recorded the ground motion. Of these stations, three were within 5 kilometers and two between 10 and 20 kilometers of the rupture surface. Forty-six other stations recorded the motion at distances between 20 and 120 kilometers from the rupture surface.

For the 1979 Imperial Valley earthquake, a total of 32 stations recorded the ground motion at distances up to 160 kilometers. Six of the stations were within 5 kilometers of the rupture; eight stations were between 5 and 10 kilometers; five were between 10 and 20 kilometers; and six were between 20 and 40 kilometers of the rupture. The other seven stations were at distances greater than 40 kilometers from the rupture.

Peak horizontal accelerations recorded during these recent earthquakes are illustrated in figure 2.5T-1 versus distance to the rupture surface. All of the data for the 1979 Imperial Valley earthquake have been presented. For the smaller magnitude 1979 Coyote Lake earthquake, however, only the data within 20 kilometers of the rupture surface are presented. The corresponding response spectra available from the 1979 Imperial Valley earthquake are illustrated in figures 2.5T-2 and 2.5T-3.

A subset of these spectra from the 1979 Imperial Valley earthquake is illustrated in figure 2.5T-2. These spectra are for the distance range of 6 to 13 km from the rupture surface. The envelope and mean and 84th percentile on these 14 spectra are illustrated in figure 2.5T-3.

Amended: April 2009 TL: E048000

2.5T.6 IMPACT OF THE NEW DATA FROM THE 1979 IMPERIAL VALLEY AND THE 1979 COYOTE LAKE EARTHQUAKES

Both Imperial Valley and Coyote Lake earthquakes are well defined, well located, and produced a large number of high quality near source strong motion recordings as summarized in section 2.5T.5 above. However, the recordings obtained during the 1979 Imperial Valley earthquake are of much greater significance. The features of this earthquake and its recordings that make it particularly well-suited to developing ground motion parameters at San Onofre from the postulated events on the hypothesized Offshore Zone of Deformation (OZD) are summarized below:

A. The reported surface wave magnitude is (M_s) 6.8.

B. The earthquake was shallow (focal depth of approximately 10 km).

C. It had a vertical rupture surface and predominantly strike-slip right-lateral movement.

D. The earthquake rupture initiated near the United States-Mexican border and spread toward the network of ground motion recording stations around El Centro; consequently, the strong motion data include effects due to focusing.

E. The earthquake is well-located and occurred in the southern California tectonic environment.

F. Over 20 high quality and uniformly processed recordings are available for distances up to 40 km.

G. Essentially all recording instruments were located in small structures at ground level.

The impact of the 1979 Imperial Valley data on the estimates of peak acceleration and response spectra at the San Onofre site is discussed below.

The recorded peak accelerations for the 1979 Imperial Valley earthquake are illustrated in figure 2.5T-4 with the San Onofre attenuation curves (from Appendix J of the 1979 Woodward-Clyde Consultants report) plotted in terms of closest distance to the rupture surface. A comparison of these indicates that, in general, the San Onofre curves exceed the Imperial Valley data and that the San Onofre 84th percentile curve is essentially the upper bound of the Imperial Valley data. For a closest distance of 8 km (the distance from the OZD to San Onofre), the 1979 Imperial Valley data give mean and 84th percentile peak acceleration values of 0.32g and 0.44g, respectively. The mean and 84th percentile values estimated for San Onofre are 0.42g and 0.57g, respectively.

APPENDIX 2.5T

The mean and 84th percentile response spectral values for distances of 6 to 13 km, presented in figure 2.5T-3 for the 1979 Imperial Valley earthquake, are illustrated in figure 2.5T-5 with the DBE spectrum and the empirically derived instrumental mean and 84th percentile spectra for the 1979 Imperial Valley earthquake. The DBE spectrum exceeds both San Onofre and 1979 Imperial Valley.

On the basis of these comparisons of the 1979 Imperial Valley earthquake data with the relationships developed for San Onofre, it may be concluded that the peak accelerations and response spectra estimated for San Onofre are realistic and conservative ground motion parameters for an earthquake of magnitude 6-1/2 on the hypothesized OZD.

REFERENCES

1. Boore, D. M., Joyner, W. B., Oliver, A. A. III, and Page, R. A., 1973, Estimation of ground motion parameters: U.S. Geological Survey Circular 795, 43 pp.

2. California Division of Mines and Geology, 1979, Partial film records and preliminary data, Imperial Valley earthquake of 15 October 1979, Imperial County Services Building."

3. Crouse, C. B., 1978, Prediction of free-field earthquake ground motions: ASCE Specialty Conference on Earthquake Engineering and Soil Dynamics, Proceedings, v. 1, pp. 359-379.

4. Porcella, R. L. Matthiesen, R. B. McJunken, R. D., and Ragsdale, J. T., 1979, Compilation of strong motion records from the August 6, 1979 Coyote Lake Earthquakes: U.S. Geological Survey Open-File Report 79-385, October.

5. Porcella, R. L. and Matthiesen, R. B., 1979, Preliminary summary of the U.S. Geological Survey strong motion records from the October 15, 1979 Imperial Valley earthquake: U.S. Geological Survey Open-File Report 79-1654, 41 pp.

6. Smith, S. W., 1977, Tectonic significance of large historic earthquake in the Eureka Region: Draft Report from TERA Corporation submitted to Pacific Gas & Electric, September 9.

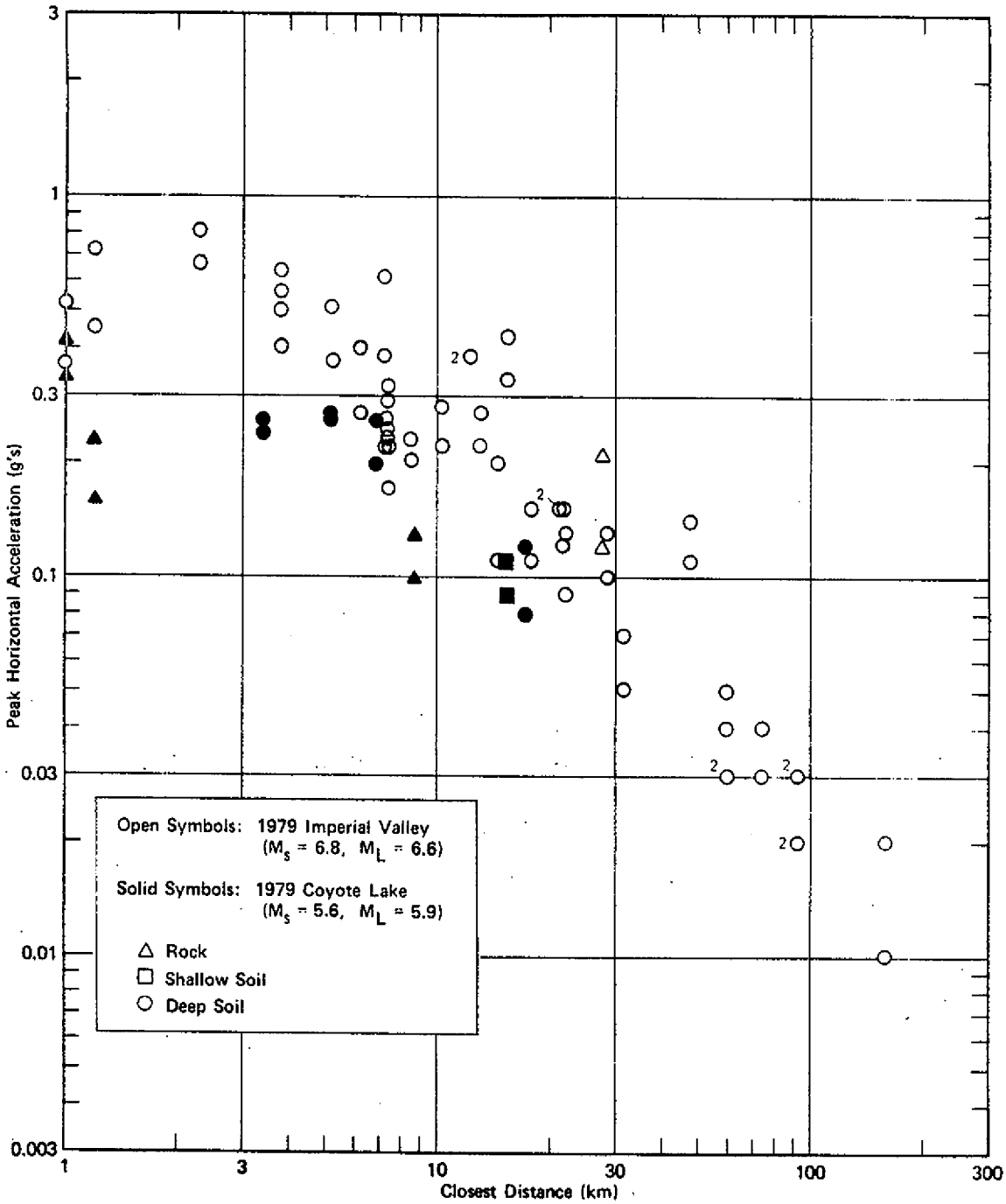

Updated

SAN ONOFRE
NUCLEAR GENERATING STATION
Units 2 & 3

PLOT OF PEAK ACCELERATION VERSUS CLOSEST DISTANCE FOR RECORDINGS OBTAINED DURING THE 1979 COYOTE LAKE AND 1979 IMPERIAL VALLEY EARTHQUAKES

Figure 2.5T-1

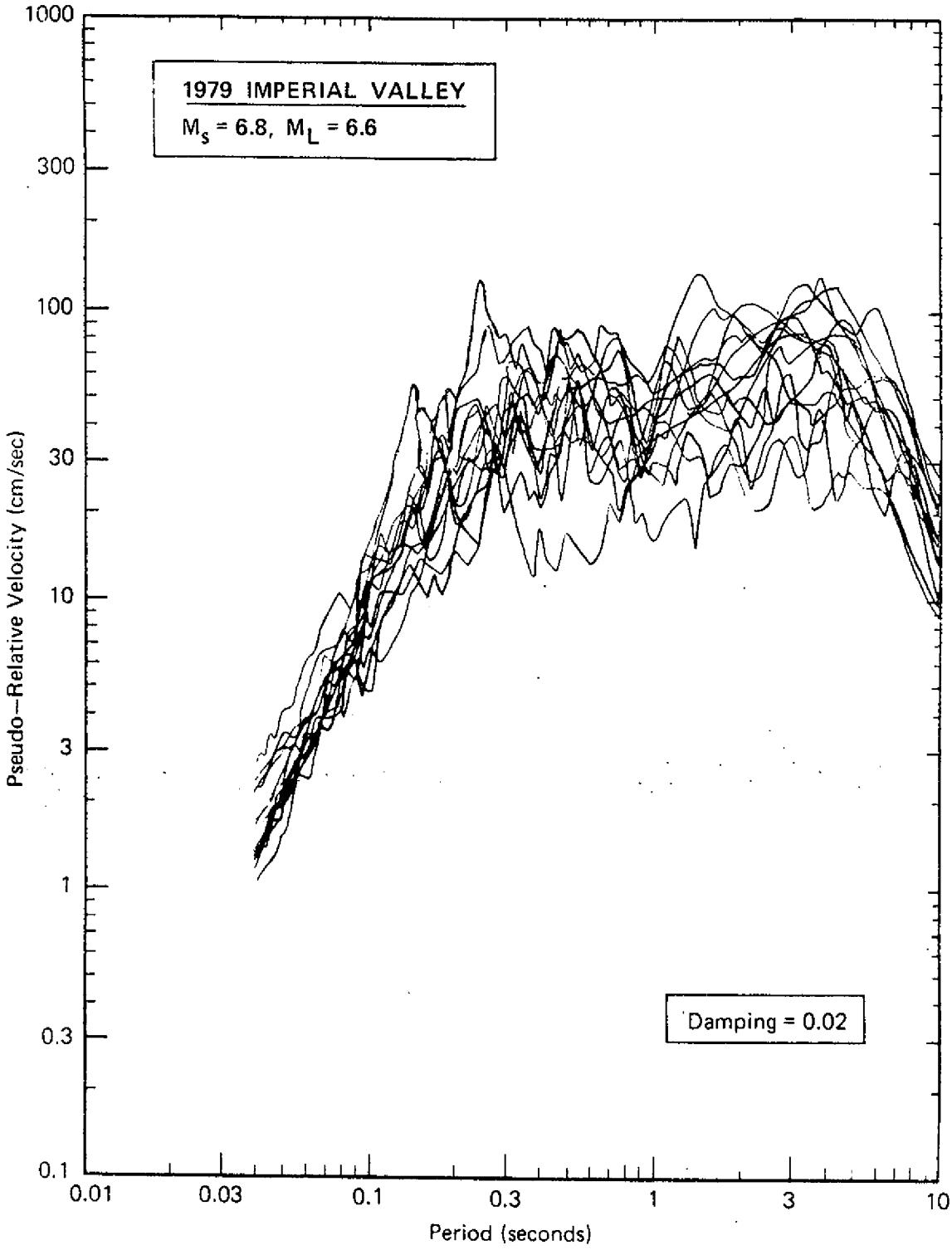

Updated

SAN ONOFRE
NUCLEAR GENERATING STATION
Units 2 & 3

RESPONSE SPECTRA FOR THE 1979 IMPERIAL VALLEY EARTHQUAKE RECORDED AT STATIONS BETWEEN 6 AND 13 KILOMETERS OF THE RUPTURE SURFACE

Figure 2.5T-2

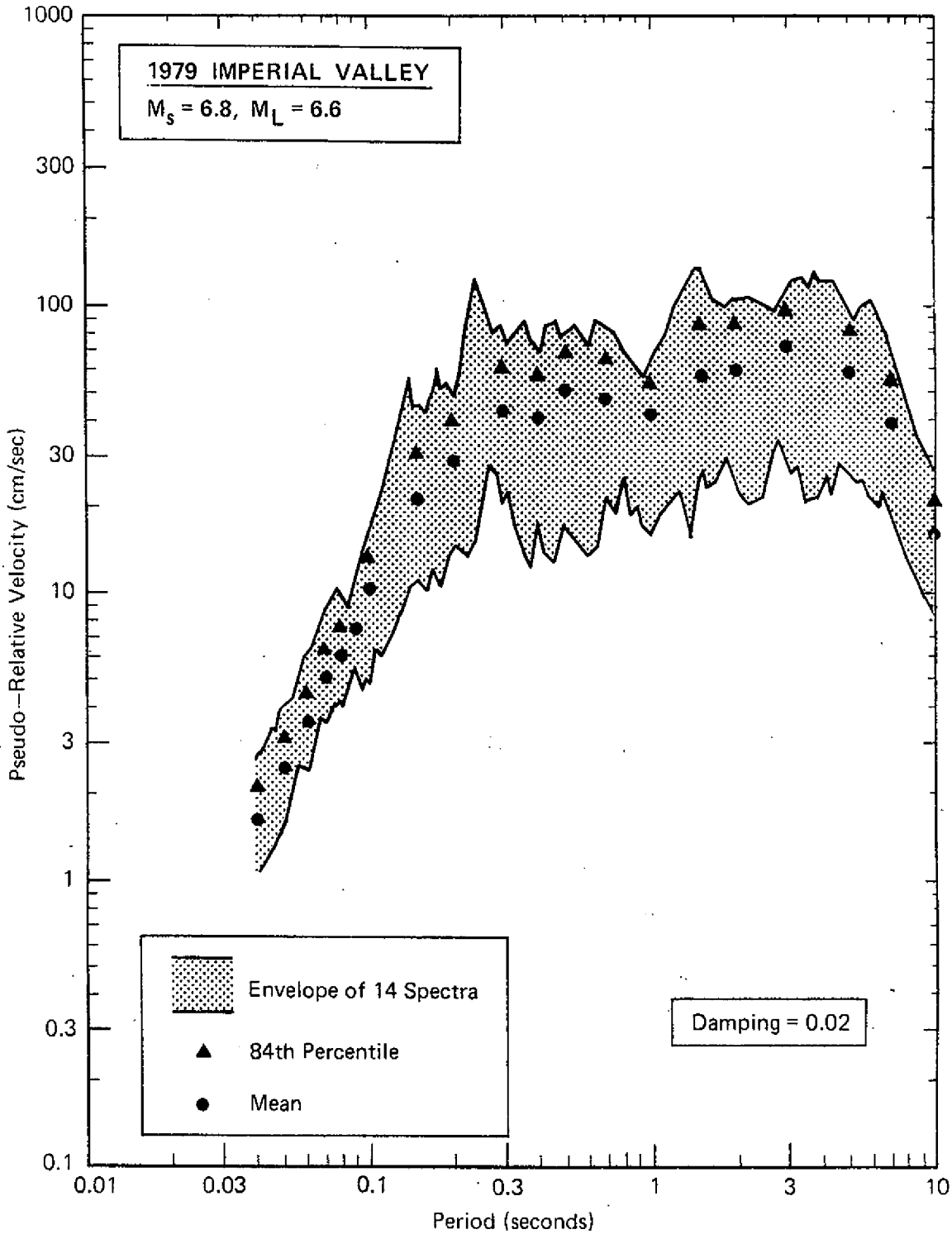

Updated

SAN ONOFRE
NUCLEAR GENERATING STATION
Units 2 & 3

ENVELOPE AND MEAN AND 84TH PERCENTILE VALUES OF THE 14 RESPONSE SPECTRA SHOWN IN FIGURE 2.5T-2

Figure 2.5T-3

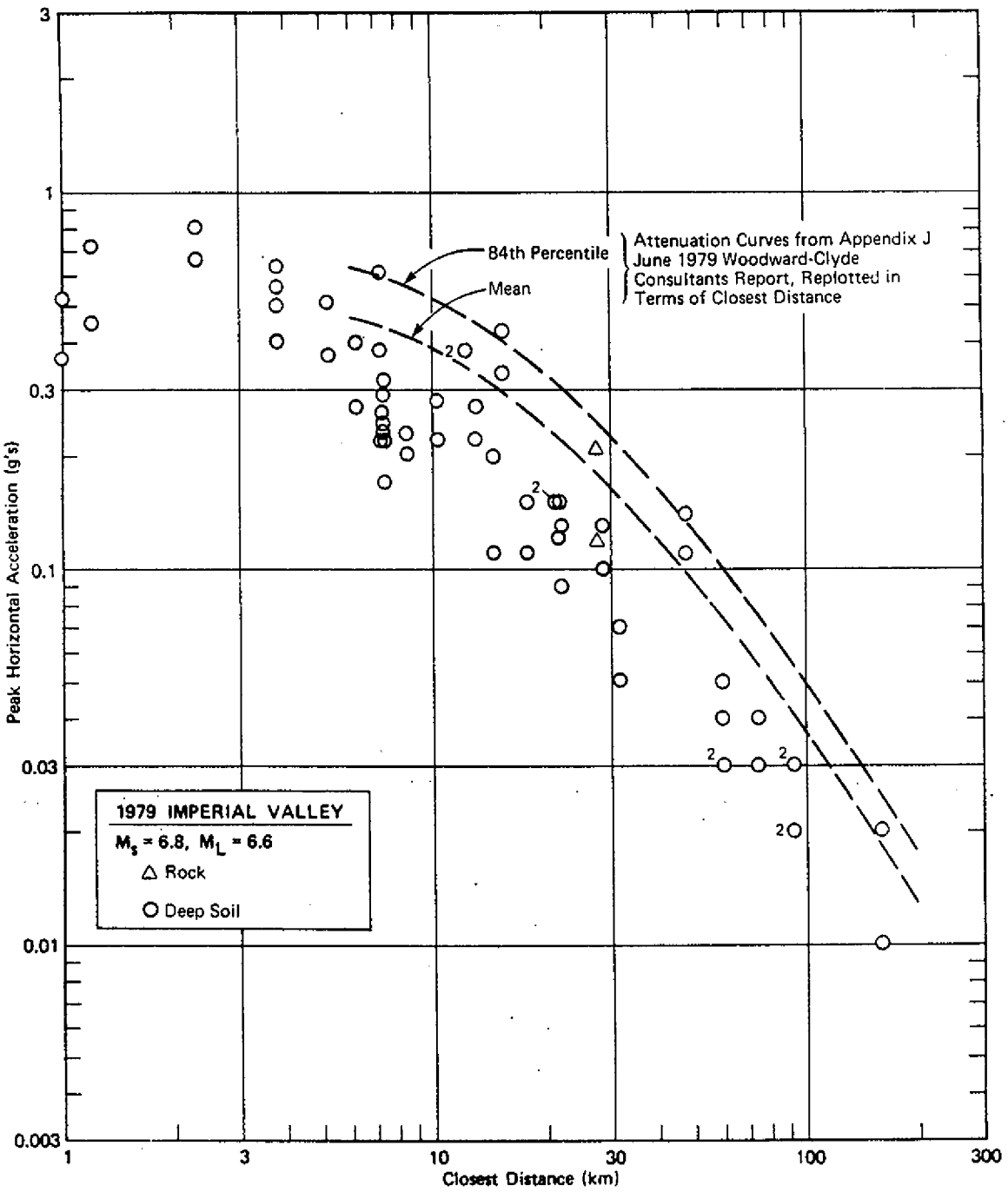

Updated

SAN ONOFRE
NUCLEAR GENERATING STATION
Units 2 & 3

COMPARISON OF PEAK ACCELERATION FOR RECORDINGS OBTAINED DURING THE 1979 IMPERIAL VALLEY EARTHQUAKE WITH THE SONGS ATTENUATION RELATIONSHIPS PLOTTED IN TERMS OF CLOSEST DISTANCE

Figure 2.5T-4

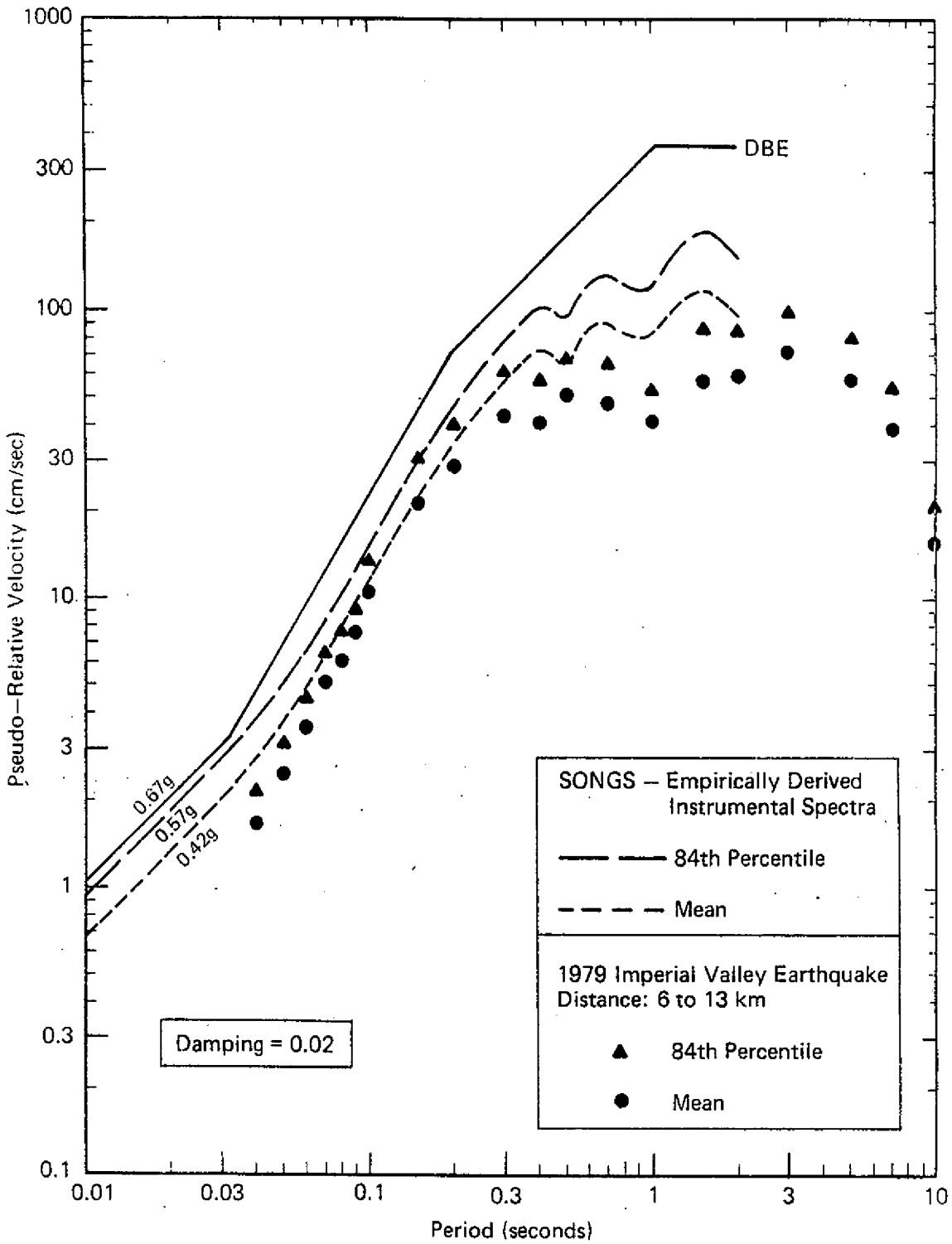

Updated

SAN ONOFRE NUCLEAR GENERATING STATION
Units 2 & 3

COMPARISON OF THE MEAN AND 84TH PERCENTILE SPECTRA SHOWN IN FIGURE 2.5T-3 FOR THE 1979 IMPERIAL VALLEY EARTHQUAKE WITH THE SONGS INSTRUMENTAL SPECTRA AND THE DBE SPECTRUM

Figure 2.5T-5